

Studies on structurally mobile regions of the varicella-zoster virus thymidylate synthase

by

Frederick John van Deursen

A thesis presented for the degree of Doctor of Philosophy

in

The Faculty of Science at The University of Glasgow

Division of Virology
Church Street
Glasgow G11 5JR

September 1997

ProQuest Number: 13815439

All rights reserved

INFORMATION TO ALL USERS

The quality of this reproduction is dependent upon the quality of the copy submitted.

In the unlikely event that the author did not send a complete manuscript and there are missing pages, these will be noted. Also, if material had to be removed, a note will indicate the deletion.



ProQuest 13815439

Published by ProQuest LLC (2018). Copyright of the Dissertation is held by the Author.

All rights reserved.

This work is protected against unauthorized copying under Title 17, United States Code
Microform Edition © ProQuest LLC.

ProQuest LLC.
789 East Eisenhower Parkway
P.O. Box 1346
Ann Arbor, MI 48106 – 1346

GLASGOW UNIVERSITY
LIBRARY

11101 (copy 1)



CONTENTS

ACKNOWLEDGEMENTS	I
SUMMARY	III
ABBREVIATIONS	V
AMINO ACIDS	VI

INTRODUCTION	1
1. The Herpesviruses.....	1
1.1 Description and classification	1
1.2 Biological properties of herpesviruses.....	2
2. Varicella Zoster virus.....	3
2.1 Genome structure	4
2.2 Transcriptional analysis	6
2.3 Gene products	8
2.4 Regulation of gene expression	12
2.5 DNA replication.....	13
2.6 Latency.....	14
2.7 VZV growth in animal models.....	19
2.8 VZV growth in vitro	19
3. Biology of varicella-zoster virus.....	20
3.1 Varicella: Pathogenesis and Disease.....	20
3.2 Zoster: Pathogenesis and Disease	21
4. Antiviral Strategies	22
4.1 VZV immune globulin and zoster immune plasma	22
4.2 Vaccination	23
4.3 Antiviral compounds and resistance	23
5. Thymidylate synthase	24
5.1 The thymidylate cycle.....	25
5.2 TS from different sources	26
6. Amino acid sequence homology	29
6.1 The conservation paradox	29
7. Catalytic mechanism of TS	30
7.1 Residues involved in catalysis	32
7.2 Ordered binding of ligands	34
7.3 Conformational changes upon ligand binding	34
8. Structural features of TS	35
8.1 X-ray crystallographic structures of bacterial TS	35
8.2 General structural features	36
8.3 Notable structural features of TS	36
8.4 Segmental accommodation	39
8.5 Structural plasticity and covariant accommodation.....	41

8.6	VZV TS model.....	43
8.7	Human thymidylate synthase.....	44
8.8	The C-terminus of VZV is unique.....	45
8.9	The DRTG loop of VZV.....	47
9.	Thymidylate synthase inhibitors.....	47
9.1	Cofactor analogues.....	48
9.2	Nucleoside analogues.....	49
9.3	Bisubstrate analogues.....	51
9.4	Oligopeptide inhibitors.....	52
9.5	Anti-sense oligonucleotides.....	52
10.	Disruption of protein-protein interactions.....	52
10.1	HSV ribonucleotide reductase.....	53
10.2	F1 protein of Paramyxoviridae.....	53
10.3	The α -TIF-Oct-1 transcription complex.....	54
10.4	Influenza virus haemagglutinin.....	55
10.5	VZV thymidylate synthase.....	55
11.	Aims of the project.....	56

MATERIALS.....57

1.	Bacteria and bacteriophage strains.....	57
2.	Bacterial growth media.....	57
3.	Plasmids.....	58
4.	Chemicals and reagents.....	58
5.	Sequencing solutions.....	59
6.	Radiochemicals.....	60
7.	Enzymes.....	60
8.	Miscellaneous materials.....	61
9.	Buffers and solutions.....	61

METHODS.....64

1.	Growth and maintenance of bacteria and bacteriophage.....	64
1.1	Overnight cultures.....	64
1.2	Bacterial glycerol stocks.....	64
1.3	Antibiotics.....	64
1.4	Titration of helper phage R408.....	64
1.5	Growth of helper phage.....	65
2.	Bacterial manipulation.....	65
2.1	Transformation.....	65
3.	DNA isolation.....	65
3.1	Mini-prep plasmid DNA preparation.....	65
3.2	STET lysis plasmid DNA preparation.....	66
3.3	Qiagen™ plasmid preparation.....	66
3.4	Plasmid DNA sequencing preparation.....	66
3.5	ssDNA sequencing preparation.....	67
3.6	Uracil-ssDNA preparation.....	67
4.	DNA manipulations.....	68
4.1	Restriction enzyme digests.....	68
4.2	Isolation of DNA from agarose gels.....	68

4.3	DNA ligations	69
5.	Oligonucleotides	69
5.1	Synthesis and purification.....	69
5.2	Spiked oligonucleotides.....	70
5.3	Oligonucleotide sequences.....	70
5.4	Sequencing oligonucleotides.....	72
6.	Mutagenesis	72
6.1	Oligonucleotide site directed mutagenesis.....	72
6.2	Region directed mutagenesis	73
6.3	Temperature sensitive mutations	73
7	Mutant screening.....	73
7.1	Restriction digests.....	73
7.2	Growth complementation assays	74
7.3	DNA sequencing.....	74
8.	Mutant characterisation.....	75
8.1	Crude TS extracts.....	75
8.2	Protein concentration determination	75
8.3	Tritium release assay.....	76
8.4	Debromination assay.....	76
9.	Peptide inhibition of TS	77
10.	Purification of mutants.....	77
10.1	T7 expression vector	77
10.2	Growth and extraction of TS.....	78
10.3	Protein mini-gel electrophoresis	78
10.4	Hydroxylapatite chromatography	79
10.5	Ammonium sulphate precipitation and dialysis.....	80
10.6	S-sepharose chromatography	80
11.	Kinetic characterisation of mutants.....	81
11.1	Kinetic parameter determination.....	81
12.	Computing and molecular modelling.....	81

RESULTS AND DISCUSSION

1.	The DRTG surface loop of VZV TS.....	82
1.1	DRTG loop mutant construction.....	83
1.2	Enzymatic properties of the DRTG mutants.....	87
1.3	Kinetics	90
1.4	Molecular modelling of the DRTG loop mutants.....	95
1.5	Second-site revertants of the DRTG loop mutants	103
1.6	Summary	107
2.	The C-terminus of VZV TS	108
2.1	Mutants.....	108
2.2	Molecular modelling of the VZV C-terminal mutants.....	111
2.3	Folate Inhibitors and phenolphthalein.....	111
2.4	Peptide Inhibition.....	117
2.5	Human thymidylate synthase C-terminal mutants.....	119
2.4	Phenolphthalein inhibition of human TS	120
2.4	Summary	121

3.	Temperature sensitive mutants.....	123
3.1	Construction and screening of temperature-sensitive mutants.....	123
3.2	Molecular modelling of temperature-sensitive mutants.....	126
3.3	Summary of temperature-sensitive mutants.....	137
4.	Final discussion and future work	138
4.1	Is a highly conserved surface loop important?.....	138
4.2	Can covariant accommodation restore the DRTG loop mutants activity?	139
4.3	Is the VZV TS unique in its C-terminal interactions?	140
4.4	Future work.....	141

REFERENCES	142
-------------------------	-----

ACKNOWLEDGEMENTS

Many thanks to Professor John H. Subak-Sharpe for providing me with the opportunity to work in and make use of the facilities at the Institute of Virology. I would also like to thank Dr Russell Thompson for his enthusiastic supervision of this project and helping me through some of the difficult times. I am also grateful for his assistance in proof-reading this thesis.

I also thank Professor Neil Issacs for allowing me to use the computer facilities in the Chemistry Department of the University of Glasgow, and to Dr Ben Luisi and James Beauchamp for their advice and help in using those facilities. Many thanks go to Dr Robert Stroud and Dr Celia schiffer for generating the model structure of VZV TS and providing the co-ordinates of the *E. coli* and *L. casei* TS.

Very special thanks go to Jim Scott for his invaluable help, advice and ridicule without which this project would not have been possible.

I would like to acknowledge and thank for their friendship and encouragement, all members of Lab 201, past and present, particularly Jane Woods and Joe Hutchinson.

I am also grateful to the friends I have been fortunate to make during my time in Glasgow, particularly Carole Robertson, Gillian McVey, Lesley Wallace and Winnie Boner.

To Ewan Dunn, Ross Reid and Russell Thompson for being the best friends anyone could wish for. Finally, I would like to 'thank' Ross and Russell for *making* me sing *Flower of Scotland* on New Years Eve!

I am indebted to my parents Joep and Joan for their unselfish and unrelinquishing encouragement, patience and support both financially and morally. I would also like to thank my brother Michael and my sister Yvette for their support.

This thesis is dedicated to my parents

The author was the recipient of a Medical Research Council award and unless otherwise stated the results presented in this thesis represent my own work.

In memory of my Father

You'll Never Walk Alone

SUMMARY

Thymidylate synthase (EC 2.1.1.45) is one of the most highly conserved enzymes. It is the sole *de novo* source of 2'-deoxythymidylate (dTMP) in a diverse range of organisms. Thymidylate synthase (TS) catalyses the conversion of 2'-deoxyuridylate (dUMP) and N⁵, N¹⁰-methylene-tetrahydrofolate to dTMP and dihydrofolate. To date, sequences are known from 36 different species of TS. These include the human enzyme which is a drug target for anti-cancer agents, thymidylate synthases from protozoa, which are generally bifunctional with TS and dihydrofolate reductase present in a single protein, and TS from bacterial and viral species. TS is an essential enzyme to almost all living species and is encoded by several large DNA viruses, presumably to support an increased need for DNA synthesis during the viral life cycle. There are only a few organisms that adequately scavenge thymidine from their environment and do not require TS. The essential requirement for TS activity makes TS an important drug target for the development of anti-parasitic and possibly antiviral agents.

The work presented in this thesis identifies a mobile surface loop region of TS (the DRTG loop) and shows that it is important for substrate turnover. It is implicated in packing against the C-terminus of VZV TS facilitating efficient closing of the active site upon ligand binding. This loop is highly conserved throughout the TS family with the phage Φ 3T and *L.lactis* being the most divergent species. Site-directed mutagenesis was used to substitute the VZV residues in the DRTG loop for their *L.lactis* counterparts. The resultant variant proteins were dysfunctional in their ability to complete the catalytic reaction. With the exception of G40M they could still bind the substrate, dUMP.

The development of a region-directed mutagenesis protocol is also described. Such an approach was used to select for covariant residues of the DRTG loop mutants that might restore activity. In this study, no covariant residues were identified. The validity of the protocol was however, shown by generation of several temperature sensitive mutants.

The C-terminal region of TS is also mobile and plays a significant role in catalysis by closing down the active site upon binding of ligands. Previous studies proposed a

unique interaction at the C-terminus of VZV TS and this has been investigated further. Mutations of the C-terminus of both VZV and human TS suggest that VZV is not unique in this respect.

Temperature sensitive mutants allow the role of amino acid residues in protein stability to be investigated. Several temperature sensitive mutants were generated to different regions of VZV TS and showed that the enzyme can tolerate many changes even within residues that are fully conserved within the TS family.

ABBREVIATIONS

Å	angstrom
A ₆₀₀	Absorbance at wavelength 600nm
Amp	ampicillin
BrdUMP	5-bromo-2'-deoxyuridine 5'-monophosphate
BSA	bovine serum albumin
C-	carboxy-
CB3717	N ¹⁰ -propargyl-5, 8-dideazafolate
Ci	Curie
CIP	calf intestinal phosphatase
dATP	2'-deoxyadenosine 5'-phosphate
dCTP	2'-deoxyadenosine 5'-phosphate
dGTP	2'-deoxyadenosine 5'-phosphate
dH ₂ O	deionised water
DMSO	dimethyl sulphoxide
dsDNA	double-stranded deoxyribonucleic acid
DTT	dithiothreitol
dTTP	2'-deoxyadenosine 5'-phosphate
dUMP	2'-deoxyuridine 5'-monophosphate
EDTA	sodium ethylenediamine tetra-acetic acid
FdUMP	5-fluoro-2'-deoxyuridine 5'-monophosphate
HSV	herpes simplex virus
IE	immediate early
IPTG	isopropyl-D-thiogalactoside
K _m	Michaelis-Menten constant
N-	amino-
Ø	phenol
Ø/CHCl ₃	phenol/chloroform 1:1 (v/v)
OD	optical density
PEG	polyethylene glycol
ssDNA	single-stranded deoxyribonucleic acid
Tris	tris(hydroxymethyl)aminomethane
V _{max}	initial enzyme rate at saturating substrate concentration
VZV	varicella-zoster virus

AMINO ACIDS

Amino Acid	Three letter code	One letter code
Alanine	Ala	A
Arginine	Arg	R
Asparagine	Asn	N
Aspartate	Asp	D
Cysteine	Cys	C
Glutamate	Glu	E
Glutamine	Gln	Q
Glycine	Gly	G
Histidine	His	H
Isoleucine	Ile	I
Leucine	Leu	L
Lysine	Lys	K
Methionine	Met	M
Phenylalanine	Phe	F
Proline	Pro	P
Serine	Ser	S
Threonine	Thr	T
Tryptophan	Trp	W
Tyrosine	Tyr	Y
Valine	Val	V

INTRODUCTION

The research presented in this thesis concerns the structural flexibility of the thymidylate synthase of varicella zoster virus. This introduction aims to overview briefly the biology and molecular biology of herpesviruses and in particular varicella zoster virus. The latter sections of this introduction will review the structural and enzymatic properties of thymidylate synthase.

1. The Herpesviruses

1.1 Description and classification

Herpesviruses are found in a wide variety of host species, ranging from fish to humans (reviewed by Roizman, 1993 and 1996). Nearly 100 herpesviruses have been characterised and seven have been isolated from humans [herpes simplex virus 1 (HSV-1), herpes simplex virus 2 (HSV-2), varicella-zoster virus (VZV), human cytomegalovirus (HCMV), Epstein-Barr virus (EBV) and human herpesvirus 6 and 7 (HHV6 and HHV7)]. Herpes virus-like sequences have been found in over 90% of AIDS-related Kaposi's sarcoma tissue, indicating that an eighth human herpes virus (Kaposi's sarcoma herpes virus; KSHV) may exist (Chang *et al* 1994). Membership of the family Herpesviridae is based primarily, though not exclusively, on virion structure. A typical herpes virion consists of a core containing a linear double-stranded DNA, an icosahedral capsid approximately 100 to 110 nm in diameter containing 162 capsomeres, which is surrounded by an amorphous proteinaceous layer of tegument which in turn is enveloped in a lipid membrane containing glycoprotein spikes.

Members of the family Herpesviridae are divided into three sub-families, the Alphaherpesvirinae, the Betaherpesvirinae, and the Gammaherpesvirinae.

Alphaherpesvirinae are neurotrophic viruses which establish latent infections primarily in sensory ganglia. They have a variable host range and relatively short reproductive cycle (less than 24 hours). Members of this sub-family include herpes

simplex virus type 1 and type 2 (HSV-1, HSV-2), varicella-zoster virus (VZV), equine herpesvirus type 1 (EHV-1) and pseudorabies virus (PRV).

Betaherpesvirinae have a restricted host range and long reproductive cycle (greater than 24 hours). Infected cells frequently fuse and become enlarged forming giant cells or *cytomegalia*. They can establish latency in secretory glands, lymphoreticular cells, kidneys and other tissues. Members of this sub-family include human cytomegalovirus (HCMV) and murine cytomegalovirus (MCMV).

Gammaherpesvirinae have a very restricted host range, infecting only the family or order to which the natural host belongs. They infect and establish latency specifically in T or B lymphocytes. Members of this sub-family include Epstein-Barr virus (EBV), herpesvirus ateles (HVA) and herpesvirus saimiri (HVS).

1.2 Biological properties of herpesviruses

Seven herpesviruses which infect humans have been identified to date (see section 1.1). They appear to be ubiquitous and transmission is usually by contact between moist mucosal surfaces. Serological studies show that a large proportion of the world's population have been exposed to and may be latently infected with one or more herpesviruses.

HSV-1 and HSV-2 usually cause cold sores and genital lesions respectively (reviewed by Whitley and Gnann Jr 1993). Primary infection can be asymptomatic or result in virus replicating at the site of infection to form a localised lesion. Virions are transported via the axons to the sensory ganglia that innervate that site of infection. Latency is established in the ganglia and the virus remains latent until reactivation. Reactivation can occur spontaneously to produce recurrent infection. The frequency of reactivation is increased by exposure to sunlight or UV light, tissue damage, immune suppression and physical or emotional stress. HSV-2 has long been suspected of an association with cervical carcinoma but its role as a causative agent of transformation is not clear. The virus can occasionally cause encephalitis or disseminated disease in newborn infants.

VZV infection has two distinct clinical manifestations: chickenpox (varicella) and shingles (herpes zoster). Varicella represents the primary infection, usually in

childhood and zoster is caused by reactivation later in life of latent virus from sensory ganglia (see section 3.1 and 3.2).

HCMV infections are most often asymptomatic and latency is established in the absence of any associated disease (reviewed by Alford and Britt 1993). Virulence is seen only in the absence of a competent immune system and is a threat *in utero*, since it has the ability to cross the placenta and cause congenital infection which can lead to birth defects. It is frequently reactivated after organ transplants and is a common opportunistic infection associated with acquired immunodeficiency disease (AIDS).

EBV infects B lymphocytes in the peripheral blood and lymphoid organs causing infectious mononucleosis or 'glandular fever' (reviewed by Miller 1990). EBV is also associated with two specific cancers: Burkitt's lymphoma and nasopharyngeal carcinoma.

HHV-6 is a lymphotropic virus acquired by most individuals during their first two years of life (reviewed by Lopez and Honess 1990). It can cause exanthem subitum, a mild fever and rash, but in most cases seroconversion is asymptomatic.

HHV-7 was recently isolated from the T lymphocytes of a healthy individual (Frenkel *et al* 1990). The virus has not yet been associated with any disease but like HHV-6 linked with rosola in infants (Burns *et al* 1994, Hidaka *et al* 1994, Tanaka *et al* 1994, Ueda *et al* 1994, Ablashi *et al* 1995).

KSHV (Kaposi's sarcoma herpes virus) has recently been speculated to be involved in the pathogenesis of the Kaposi's tumour (Schalling *et al* 1995) because these herpes virus-like sequences have also been found in Kaposi's sarcoma of HIV negative individuals.

2. Varicella Zoster virus

As its name implies, varicella-zoster virus (VZV) produces two distinct clinical syndromes: chickenpox and shingles. Chickenpox (varicella) is a ubiquitous, highly contagious, generalised exanthem that spreads rapidly in a susceptible population and displays marked seasonality. Shingles (herpes zoster), in contrast, is a less common endemic disease that occurs usually in older or immunocompromised individuals and

is characterised by a painful vesicular eruption generally limited to a single dermatome (reviewed by Arvin 1996, Cohen and Straus 1996).

Like other members of the α -Herpesviridae, VZV is an enveloped icosahedral virus that contains a double-stranded DNA genome (Almeida *et al* 1962). The complete enveloped virion measures 180 to 200 nm in diameter, while the naked capsid measures ~95 nm in diameter. The nucleocapsid consists of 162 hexagonal capsomers organised in an icosahedron and is surrounded by tegument and finally by a bilayer membrane containing radially oriented glycoprotein projections about 8 nm long on its outer surface.

VZV is extremely cell-associated and is usually passaged *in vitro* by seeding infected fibroblasts, rather than cell-free virus, onto fresh monolayers. Under these conditions it grows relatively rapidly, yet a method for preparing high titre cell-free virus with reasonable infectivity still eludes us today. This problem and the lack of a suitable animal model for infection has resulted in an almost complete lack of VZV genetics and little understanding of VZV gene expression.

2.1 Genome structure

Electron microscopy (Dumas *et al* 1980) and restriction endonuclease cleavage profiles (Dumas *et al* 1981, Mishra *et al* 1984, Straus *et al* 1981, 1982) suggest that the VZV genome is approximately $80\text{-}87 \times 10^6$ Daltons and thus is one of the smallest herpesvirus genomes. It has a G+C content of 46%, which is less than that of most herpesviruses. Restriction endonuclease mapping (Dumas *et al* 1981) showed that the genome is composed of two unique regions, U_L (~100 kbp) and U_S (5.4 kbp). The U_S region is flanked by an inverted repeat sequence R_L and R_S , and the location of each repeat is defined by I (internal) or T (terminal) called TR_S/IR_S which is 6.8 kbp (Figure 4). Restriction endonuclease profiles showed that virion DNA molecules contain predominately two genome isomers in approximately equal amount which differ in the orientation of U_S (Dumas *et al* 1981, Straus *et al* 1981, Ecker and Hymen 1982). However, more recently it has been shown that a minor proportion (~5%) of genomes exist with U_L inverted (Davison 1984, Kinchington *et al* 1985, Hayakawa and Hyman 1987). Thus, VZV virions contain four genome isomers: two major and two minor (Figure. 4). Much of the size differences between the VZV and HSV-1 genomes may be explained in terms of smaller TR_L/IR_L and U_S regions in VZV.

Upon entering the cell it is thought that the genome circularizes and that subsequent DNA synthesis occurs by a rolling circle mechanism which produces head-to-tail concatamers (Davison 1984). Cleavage of unit length molecules is intimately linked to their packaging into capsids.

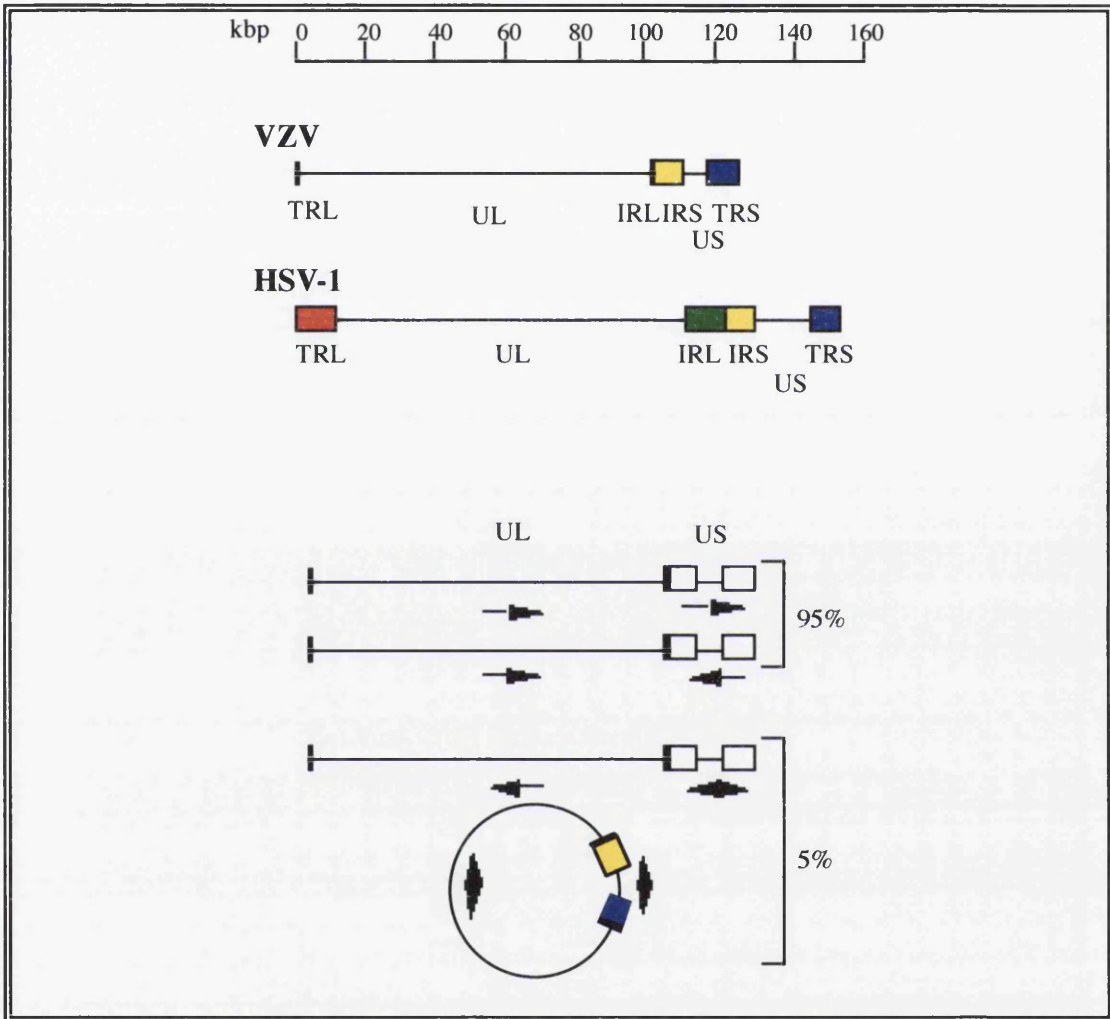


Figure 4. Comparison of VZV and HSV-1 genomes

The top panel shows schematics of the VZV (125kbp) and HSV-1 (152kbp) genomes and a scale in kbp is shown above. Inverted repeats (TRL/IRL and TRS/IRS) are shown as coloured boxes. The bottom panel shows the different isomers of the VZV genome; the two predominant forms contain the long segment in a single orientation, while the short segment is detected in an equimolar ratio in either of the two possible orientations, as indicated by the arrows. A small percentage of the VZV DNA molecules exist either in a circular form or with the long segment inverted. Data taken from Dumas *et al* 1981, McGeoch *et al* 1988)

A major step in improving the understanding of VZV molecular biology was the sequencing of the complete genome by Davison and Scott (1986). The DNA sequence of the Dumas strain of VZV (Dumas *et al* 1981) contains 124,884 bp (Davison and Scott 1986) and originally 71 ATG initiated open reading frames (ORFs) likely to encode proteins were identified. However, a further two ORFs have been identified, namely ORF 9A (Barnett *et al.*, 1992) and ORF 33.5 which encodes an N-terminal truncated form of ORF 33 (Telford *et al.*, 1992). The arrangement in the genome of the 73 ORFs in VZV is shown in Figure 5. Three are present twice, being duplicated in IR_S and TR_S and two (42 and 45) are probably expressed as spliced mRNA. Thus, there are 68 distinct genes that are arranged compactly on both strands and with little extensive overlap.

2.2 Transcriptional analysis

The first transcription maps of the VZV genome came from Ostrove *et al* 1985 using overlapping cloned restriction fragments as probes in Northern blot analysis. Subsequently, cytoplasmic polyadenylated transcripts have also been mapped (Maguire and Hyman 1986) and using ssDNA probes the direction of each RNA species was determined (Reinhold *et al* 1988). In total 77 RNAs were detected and these studies indicated that the size and map locations of many of the VZV transcripts were consistent with the open reading frames predicted within the genome sequence (Davison and Scott 1986).

The mapping of individual open reading frames to specific genes is also being refined as the function of individual genes is identified (Ellis *et al* 1985, Keller *et al* 1986, Davison *et al* 1985, Ling *et al* 1991, 1992).

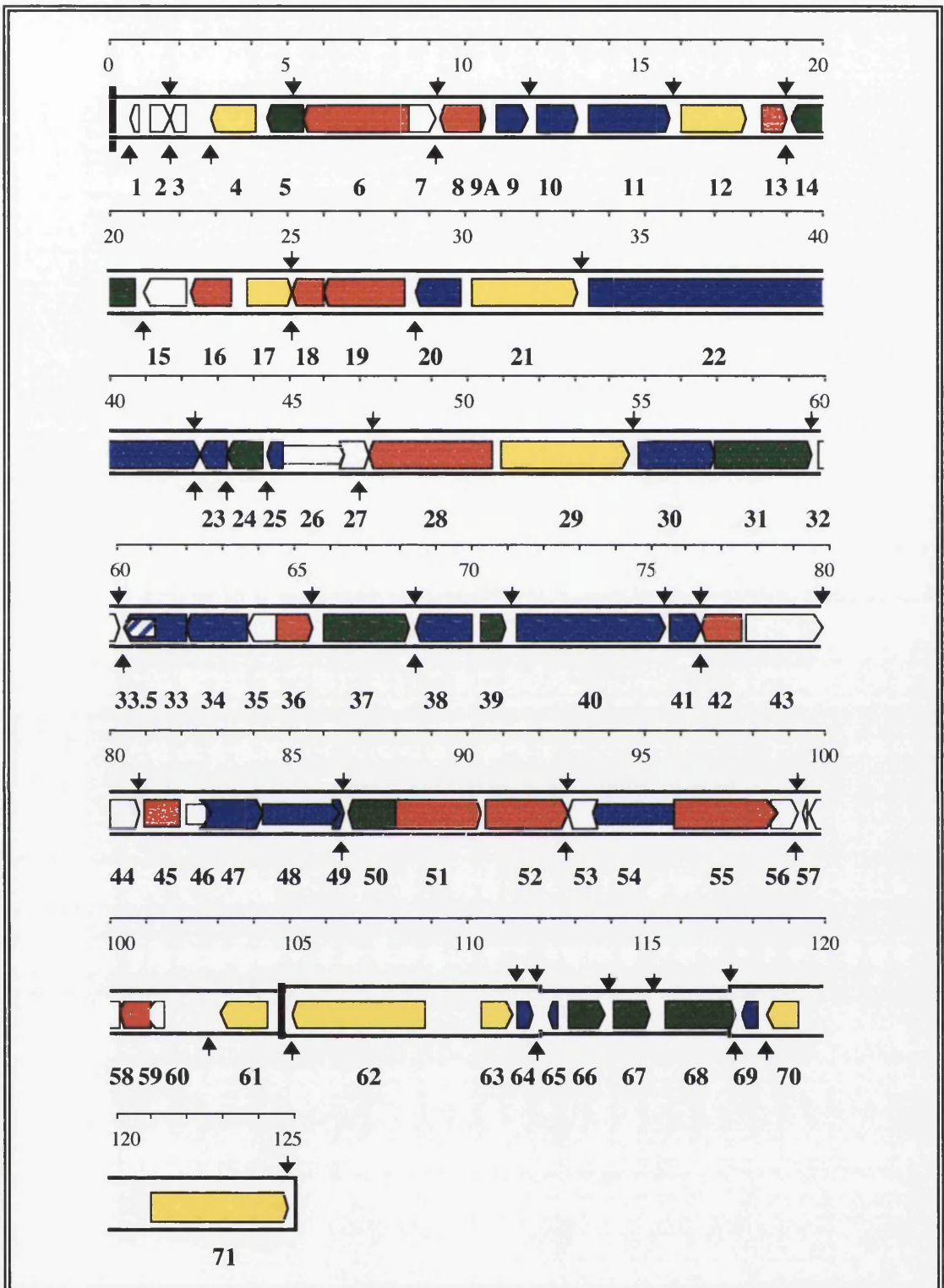


Figure 5. The arrangement of the 73 ORFs in the genome of VZV

Polyadenylation sites are indicated by vertical arrows. The colour scheme is as follows: red indicates enzymes, blue proteins in the capsid, tegument or those involved in capsid maturation/DNA packaging, yellow shows proteins involved in transcription or translational control, green membrane proteins, and finally white indicates unknown function.

Data taken from Davison 1991, 1993; Ostrove 1990; McGeoch *et al* 1993.

2.3 Gene products

Studies of VZV-specific proteins has also been hampered by the difficulties associated with purification of VZV virions. Analysis of virus-specific proteins is further compounded by the high background rate of host cell protein synthesis in the relatively asynchronous VZV infection. Most studies of VZV proteins have employed polyacrylamide gel electrophoresis of solubilized proteins derived either from purified virions or infected cells. Virus specificity has been confirmed by immunoprecipitation. With the publishing of the VZV DNA sequence (Davison and Scott 1986), comparison of the predicted VZV ORFs with those of the more fully characterised HSV-1 proteins permitted many gene functions to be assigned. Additional information as to the likely function of the predicted VZV genes has also been gained from either sequence comparison with non-herpesvirus proteins or from experimental work (reviewed by Davison 1991). The genetic relationship between VZV and HSV-1 forms the major basis for the properties or functions assigned to the VZV genes in table 2.

Four of the five HSV-1 immediate early genes (i.e. those expressed in the absence of host protein synthesis) have VZV counterparts (genes 4, 61, 62 and 63) and these are likely to play roles in the regulation of VZV gene expression of similar importance to their HSV-1 counterparts.

Five membrane glycoproteins (gpI-gpV) were proposed from the VZV DNA sequence and in addition four genes (5, 13, 32 and 50) are likely to be associated with membranes since they are multiply hydrophobic.

VZV (like HSV-1, and a characteristic of herpesviruses not shared with other animal nuclear DNA viruses) specifies a large number of enzymes involved in DNA synthesis. The VZV pyrimidine deoxyribonucleoside kinase (dPyK) was identified on its homology to the HSV-1 thymidine kinase (TK). In addition to specifying a dPyK (gene 36) which is involved in the salvage pathway for thymidine metabolism, VZV is unique among the alphaherpesviruses in that it also encodes a gene for thymidylate synthase (TS). VZV gene 13 was predicted to encode a TS enzyme by its homology to non-herpesvirus TS enzymes (Davison and Scott 1986) and the ability of the VZV TS to compliment *E.coli* Thy⁻ strains (Thompson *et al* 1987). Thus VZV supplements both pathways for providing thymidylate and it is possible that dPyK and TS are required at different stages of viral pathogenesis.

VZV Gene	HSV-1 Counterpart	Protein/function
1	—	Function Unknown
2	—	Function Unknown
3	UL55	Function Unknown
4	UL54	IE protein; Post-translational regulator of gene expression
5	UL53	Possible membrane protein
6	UL52	Component of DNA-helicase-primase
7	UL51	Function Unknown
8	UL50	Deoxyuridine triphosphatase
9	UL49	Tegument protein
9A	UL49A	Possible membrane protein
10	UL48	Tegument protein; transactivates IE genes
11	UL47	Tegument protein
12	UL46	Modulates IE gene transactivation by UL48 protein
13	—	Thymidylate Synthase
14	UL44	Membrane glycoprotein (gpV) -role in cell entry
15	UL43	Function Unknown, probable integral membrane protein
16	UL42	Subunit of DNA polymerase
17	UL41	Virion host shutoff protein
18	UL40	Ribonucleotide reductase small subunit (R2)
19	UL39	Ribonucleotide reductase large subunit (R1)
20	UL38	Capsid protein
21	UL37	Possible DNA binding function
22	UL36	Tegument protein
23	UL35	Capsid protein
24	UL34	Membrane-associated phosphoprotein
25	UL33	Role in capsid maturation/DNA packaging
26	UL32	Function Unknown

VZV Gene	HSV-1 Counterpart	Protein/function
27	UL31	Function Unknown
28	UL30	Catalytic subunit of DNA polymerase
29	UL29	Single-stranded DNA binding protein
30	UL28	Role in capsid maturation/DNA packaging
31	UL27	Membrane glycoprotein (gpII) -role in cell entry
32	—	Function Unknown
33	UL26	Protease involved in virion maturation
33.5	UL26.5	Internal protein of immature capsids (processed by UL26 in HSV-1)
34	UL25	Virion protein
35	UL24	Function Unknown
36	UL23	Thymidine kinase
37	UL22	Membrane glycoprotein (gpIII) -role in cell entry
38	UL21	Role in virion morphogenesis
39	UL20	Integral membrane protein; role in virion egress
40	UL19	Major capsid protein
41	UL18	capsid protein
42+45	UL15	Possible terminase
43	UL17	Function Unknown
44	UL16	Function Unknown
46	UL14	Function Unknown
47	UL13	Tegument protein; probable protein kinase
48	UL12	DNase- role in maturation and packaging of DNA
49	UL11	Myristylated tegument protein- role in envelopment and virion transport
50	UL10	Probable integral membrane protein
51	UL9	<i>Ori</i> -binding protein; DNA helicase
52	UL8	Component of DNA helicase-primase complex

VZV Gene	HSV-1 Counterpart	Protein/function
53	UL7	Function Unknown
54	UL6	Role in virion morphogenesis
55	UL5	Component of DNA helicase-primase complex
56	UL4	Function Unknown
57	—	Function Unknown
58	UL3	Function Unknown
59	UL2	Uracil-DNA glycosylase
60	UL1	Function Unknown
61/71	RL2	IE protein; transcriptional regulator
62	RS1	IE protein; transcriptional regulator
63/70	US1	IE protein; transcriptional regulator
64/69	US2	Virion protein
65	US9	Tegument protein
66	US3	Protein kinase
67	US7	Membrane glycoprotein (gpIV)
68	US8	Membrane glycoprotein (gpI)

Table 2. Functions or putative properties of VZV proteins

Data taken from Davison 1991, 1993; Ostrove 1990; McGeoch *et al* 1993.

One important feature of gene 13 is that it is one of the five VZV genes (1, 2, 13, 32 and 57) with no HSV-1 counterpart. The only other herpesviruses possessing a TS gene are members of the subgroup gammaherpesviruses typified by herpesvirus saimiri (Honest *et al* 1986). In the same way that the TS gene was identified by its homology to non-herpesvirus proteins, the products of two VZV genes 47 and 66, encode proteins with homology to serine-threonine protein kinases (McGeoch and Davison 1986, Smith and Smith 1989). VZV also encodes a ribonucleotide reductase (genes 18 and 19) which catalyses the conversion of ribonucleoside diphosphates to their corresponding deoxyribonucleotides. Furthermore VZV encodes a deoxyuridine triphosphatase (dUTPase) an enzyme that catalyses the conversion of deoxyuridine triphosphate (dUTP) to its corresponding monophosphate (dUMP) with the concomitant release of pyrophosphate.

2.4 Regulation of gene expression

Understanding of the temporal expression of VZV genes is still in its infancy and like many of the experiments with VZV has been hampered by the difficulty of inducing co-ordinate infections and in obtaining cell-free virus of sufficiently high titre. It is still not clear whether VZV follows a distinct cascade pattern during which the three classes of genes (immediate early, early and late) are sequentially expressed as found in other herpesviruses such as HSV-1.

Four of the five immediate early HSV-1 genes have VZV counterparts, they are genes 4, 61, 62 and 63.

The product of VZV gene 4 is the sequence homologue of HSV-1 Vmw63 sharing 29% amino acid homology (McGeoch *et al* 1988). However, VZV gene 4 only partially complements an HSV-1 virus with a *ts* lesion in Vmw63 when supplied by co-infection with VZV or from a transformed cell line (Felser *et al* 1987, Moriuchi *et al* 1994). Furthermore, the cell line expressing VZV gene 4 fails to complement an HSV-1 virus carrying a Vmw63 deletion mutation (Moriuchi *et al* 1994). VZV gene 4 was found by transient transfection analysis to activate expression of a variety of VZV and cellular genes both alone and in synergy with the product of VZV gene 62. This transactivation by gene 4 shows a degree of selectivity, as only IE gene 62 and a selection of putative early VZV genes were activated (Inchauspe *et al* 1989, Inchauspe and Ostrove 1989, Perera *et al* 1992, Defechereux *et al* 1993, Moriuchi *et al* 1994). The regulatory functions of gene 4 appeared to influence both transcriptional and post-transcriptional events, as the increase in reporter mRNA levels following transfection of a plasmid expressing gene 4 could not alone account for the high levels of reporter enzyme activity (Defechereux *et al* 1993). Therefore, in common both VZV gene 4 and its HSV-1 counterpart appear to influence pre-mRNA processing. Thus despite the functional similarities of these transcriptional activator proteins, their precise mechanisms of action differ.

The VZV gene 61 product shows limited sequence homology to HSV-1 Vmw110 (encoded by the HSV-1 IE1 gene) but in contrast to IE1, gene 61 is only represented once in the viral genome. The gene 61 protein has recently been characterised as a nuclear, phosphorylated heterogeneous species of 62-65 kD (Stevenson *et al* 1992). Even though sequence similarities between HSV-1 Vmw110 and VZV gene 61 are confined to the N-terminus, to sequences spanning the Vmw110 zinc-finger, a stable cell line expressing gene 61 is able to complement a Vmw110 deletion mutant HSV-1

virus (Moriuchi *et al* 1992). Transient assays have demonstrated VZV gene 61 to be a potent *trans*-repressor or activator of gene 4 and gene 62 mediated activation, depending on the cell type used (Nagpal and Ostrove 1991, Perera *et al* 1992a). The evidence so far suggests that VZV gene 61 may be important for up-regulating VZV gene expression at an early stage in the viral life cycle.

The product of VZV gene 62 is the sequence homologue and functional counterpart of the product of HSV-1 gene IE3, Vmw175. Transient transfection assays have been used to demonstrate that VZV gene 62 is a potent transactivator of all classes of VZV promoters and also heterologous promoters at the transcriptional level (Everett 1984, Inchauspe *et al* 1989, Cabirac *et al* 1990, Inchauspe and Ostrove 1989, Perera *et al* 1992a, 1992b). Like its HSV-1 counterpart protein VZV gene 62 negatively autoregulates its own expression in transient transfection assays, although this appears to occur in a cell type dependent manner (Disney *et al* 1990, Perera *et al* 1992b). The high abundance of VZV gene 62 within the virion tegument (Kinchington *et al* 1992) may have implications for VZV gene regulation, following release from the tegument, gene 62 may activate the other IE promoters in advance of *de novo* viral protein synthesis, playing a role analogous to HSV-1 Vmw65.

The product of VZV gene 63 shows partial sequence homology to HSV-1 Vmw68 (encoded by HSV-1 gene IE4), although VZV gene 63 is diploid in contrast to HSV-1. As is the case with HSV-1 Vmw68, the functions of the VZV protein are poorly understood. A transient transfection study of gene 63 function reports that VZV gene 63 inhibits expression of VZV gene 62, activates early but has no effect on putative late VZV promoters (Jackers *et al* 1992). However, a more recent study (Kost *et al* 1995) demonstrated that gene 63 exerts only minimal effects on immediate early and early promoters and in contrast to the work of Jackers *et al* it did not directly inhibit the expression of gene 62. A study of the functional interplay between gene 63 and the other VZV IE proteins is required before speculation as to its likely role in infection.

2.5 DNA replication

VZV is genetically related to other alphaherpesvirinae such as the two serotypes of herpes simplex virus (HSV-1 and HSV-2) and pseudorabies virus (PRV). A model for VZV DNA replication has been proposed by Davison (1984) based upon the structural features of the viral genome and experimentally supported views of PRV and HSV-1 DNA replication.

Linear VZV DNA in one of its four isomeric forms (Figure 4) circularizes, probably by direct ligation of the termini to produce a novel L-S joint identical in sequence to the normal L-S joint in the linear genome. After circularization limited replication of circular molecules occurs, and segment inversion takes place by intramolecular recombination between inverted repeats. DNA replication proceeds by the generation of head-to-tail concatamers, perhaps by a rolling circle mechanism, as has been shown for PRV and HSV-1 (Ben-Porat and Rixon 1979, Jacob *et al* 1979). Finally the concatamers are cleaved specifically to generate unit length genomes for encapsidation. Cleavage usually occurs at the novel L-S joint but occasionally at the normal L-S joint, generating the major and minor genome arrangements.

The biochemical processes of viral DNA replication are unlikely to differ markedly between VZV and HSV-1 because each of the seven HSV-1 genes that are essential for HSV-1 DNA replication (Wu *et al* 1988) have VZV sequence homologues; VZV genes 6, 16, 28, 29, 51, 52 and 55 (Davison and Scott 1986). Only one of these, the product of gene 51, has been extensively characterized in any detail (Stow *et al* 1990). This protein, the counterpart of HSV-1 gene UL9, has been shown to bind to VZV origin of replication, (Stow *et al* 1990). A VZV origin of replication has been identified within each copy of the genome short repeat, in a position analogous to that occupied by one of the HSV-1 replication origins (ORIs) (Stow and Davison, 1986). No VZV counterpart of the HSV-1 ORIL origin of replication has been identified to date, perhaps because its putative location in the long unique segment of the VZV genome is highly unstable on cloning (Davison and Scott, 1986) and it is therefore possible that such an element may have become deleted.

2.6 Latency

Both HSV and VZV have a propensity to establish long term latency as a consequence of primary infection and to emerge from latency and again cause clinically important disease. In addition, each virus can produce vesicular mucocutaneous eruptions during both primary and reactivation disease. Despite these shared properties, important differences remain between HSV and VZV. The clinical characteristics (reviewed by Meier and Straus, 1992) that distinguish the reactivation infection caused by these viruses highlight their many unique biological properties. Table 3 illustrates some of these clinical characteristics and they imply that each virus has evolved a unique strategy to ensure the establishment, maintenance, and reactivation of latency.

Feature	VZV	HSV
Frequency of recurrences in lifetime	Usually once	To several hundred
Likelihood of recurrence	Increases with age	Decreases over time
Distribution	Dermatome	Focal lesion
Associated pain	Severe pain	Mild dysesthesia

Table 3. Features of VZV and HSV reactivation infections (adapted from Croen and Straus 1991)

Animal models and neuronal cell culture systems have permitted a detailed analysis of the pathway to HSV latency and subsequent reactivation. Initial mucocutaneous infection with HSV-1 entails viral multiplication in epithelial cells that extends locally to involve the distal sensory nerves. Upon entering the nerve the nucleocapsid is transported to the neuronal cell body residing in the sensory ganglia. Once in the ganglia the pattern of gene expression changes dramatically. All genes responsible for viral reproduction are shut off except for one duplicated region of the genome that remains transcriptionally active, producing a family of RNAs referred to as the latency-associated transcripts (LATs) which are anti-sense, relative to the Vmw110 mRNA.

The cellular location of HSV latency has been determined by in situ hybridisation analyses using nucleic acid probes that specifically detect the LATs (Stevens *et al* 1987, Dealty *et al* 1988, Croen *et al* 1987, 1991, and Stroope *et al* 1984) and revealed that HSV-1 and HSV-2 LATs persist at high levels in neuronal nuclei. When reactivation occurs, the virus resumes widespread transcriptional activity to produce progeny virus that is then transported centrifugally via the axon to the epithelial surface where it multiplies and spreads.

Little is known about the mechanism by which VZV establishes latency in sensory ganglia. By analogy to HSV, it is thought that VZV travels by route of sensory nerves using axonal transport. Detailed analysis of ganglia latently infected with VZV (Croen *et al* 1988) has shown that many regions of the genome appear not to be expressed during latency. Using unidirectional probes five regions of the genome appear to be

transcribed during latency. Potential transcripts contained in these regions include gene 3 (unknown function), gene 4 (transcriptional activator homologue of HSV-1 Vmw63), gene 5 (Possible membrane protein), gene 6 (DNA helicase-primase complex) and gene 8 (deoxyuridine triphosphatase) or gene 29 (major DNA binding protein), gene 30 (role in capsid maturation/DNA packaging), gene 31 (gpII), gene 32 (unknown function) and gene 62 (transcriptional activator, homologue of HSV-1 Vmw175) assuming that transcription in the ganglion cell is in the same direction as that which occurs during a productive virus infection. Further work involving explantation and *in vitro* cultivation (Vafai *et al* 1988) detected, by immunoprecipitation, seven "VZV specific" polypeptides of 35, 36, 45, 100, 140, 170 and 200 kDa. VZV genes 62 and 63 are predicted to encode proteins of 140 kDa and 30 kDa respectively and thus the polypeptides of similar size detected in these experiments may be related to the products of genes 62 and 63.

Interestingly, studies to date confirm that VZV lacks a transcript comparable to the LATs of HSV-1 and HSV-2 (Croen *et al* 1988, Vafai *et al* 1988, Croen and Straus 1991). The latency transcripts of bovine herpesvirus (BHV) and pseudorabies virus (PRV) are antisense to another immediate early gene, in each case one equivalent to the Vmw175 of HSV. VZV possesses a Vmw175 homologue (gene 62), but transcripts to this gene have not been detected during latent VZV infections (Croen and Strauss 1991).

Clearly VZV has a unique pattern of gene activity that sets it apart from the other neurotrophic herpesvirus.

The cellular location of VZV latency has been analysed by *in situ* hybridisation and found to be the neuronal cell (Hyman *et al* 1983, Gilden *et al* 1987) and more recently in non-neuronal cells immediately surrounding the neuron (Croen *et al* 1988). The phenotype of the non-neuronal cell latently infected with VZV has not been determined with certainty, but its morphology and proximity to neuronal cells suggest it is a satellite cell. These cells structurally resemble Schwann cells and indeed may be the ganglion equivalent of the Schwann cell.

In summary comparative analysis of epidemiology, clinical presentation, pathogenesis, and molecular biology of HSV and VZV latency reveals striking differences. Data suggest that clinicoepidemiologic features that distinguish these viruses are attributable to their different cellular sites of viral persistence and molecular strategies used to modulate latency. Central to this is the presumed cellular sites of latency (Figure 6a and 6b). A neuronal cell latently infected with HSV is subject to repeated provocations

from variety of stimuli acting centrally or peripherally upon the neuron so as to trigger viral reactivation. This reactivation process remains confined to the immediate area of the involved neuron thus causing minimal neuralgia and localised mucocutaneous eruptions (Figure 6a).

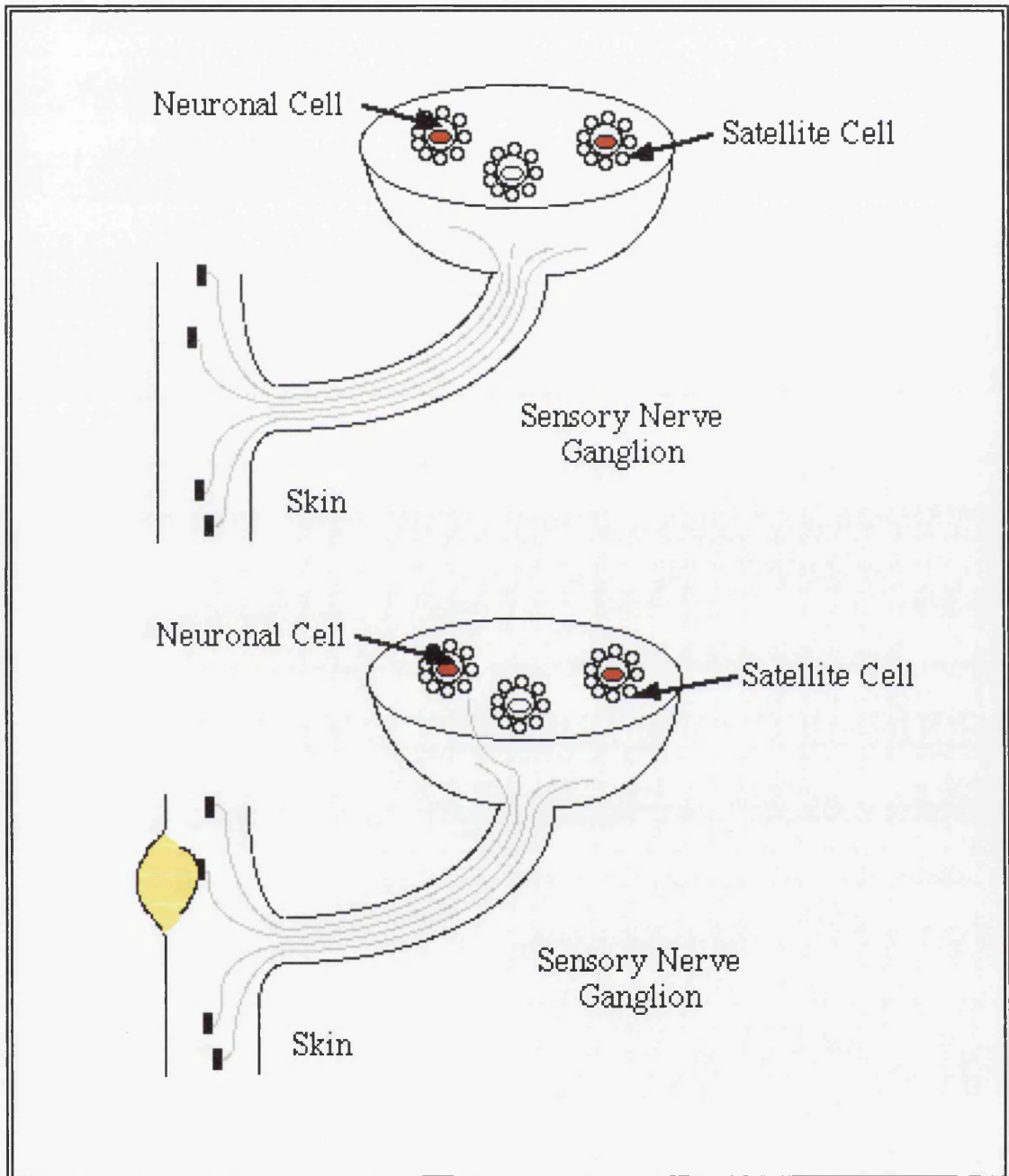


Figure 6a Schematic of hypothetical model of HSV latency and reactivation

The top panel shows latent HSV infection of neuronal cells and the bottom panel shows reactivation of HSV and axonal transport to a small area of the skin. Depicted in red is the presence of virus and in yellow areas of productive viral replication. Adapted from Meier and Straus 1992.

In contrast, latent VZV appears to reside in the satellite cell, which may be less readily influenced by stimuli that perturb neurons. Nevertheless, viral reactivation may occur eventually, yielding extensive viral proliferation and cell-to-cell spread.

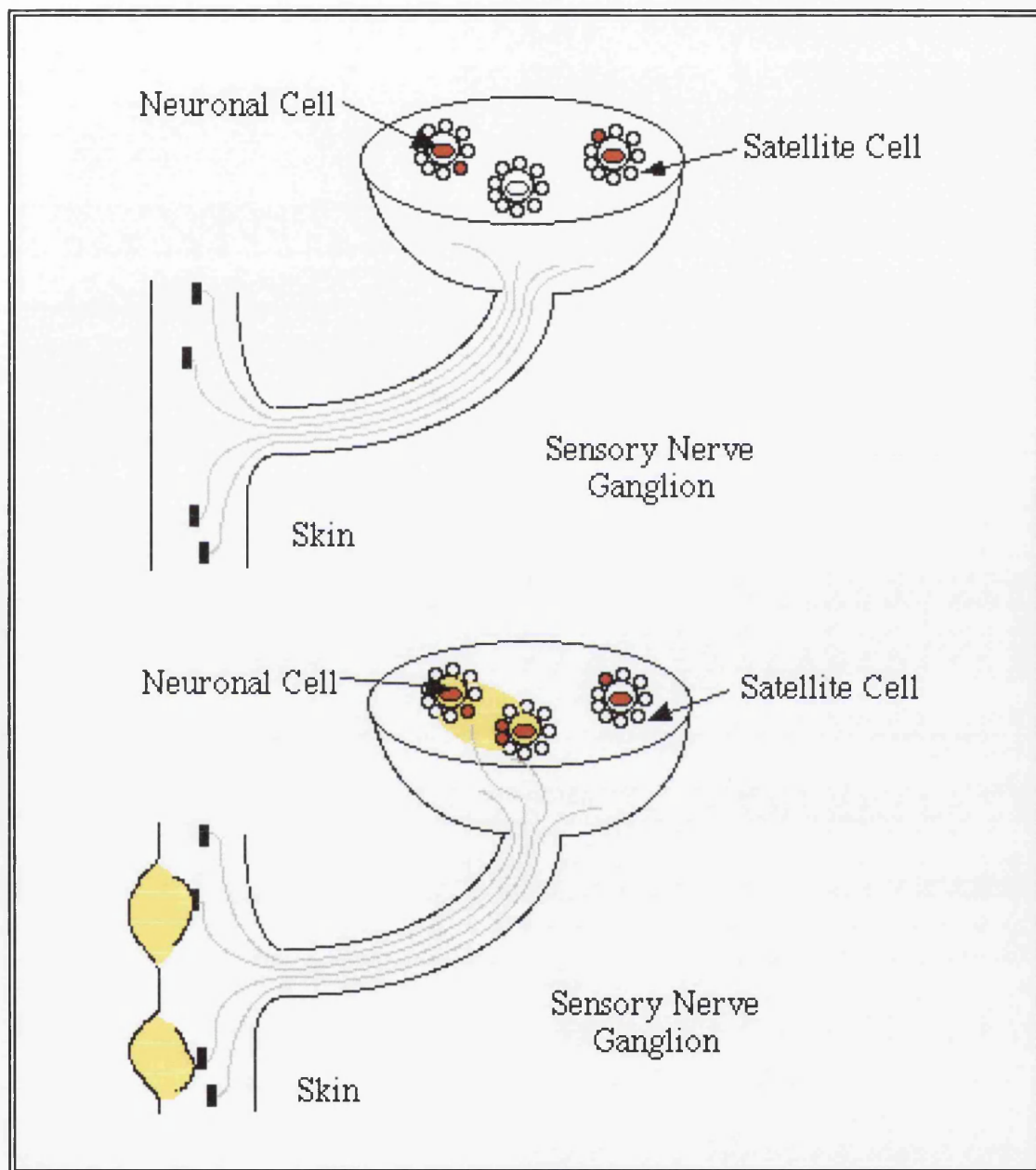


Figure 6b Schematic of hypothetical model of VZV latency and reactivation

The top panel shows latent VZV infection of non-neuronal cells (satellite cells) and the bottom panel shows reactivation of VZV, spread to non-neuronal and neuronal cells, and transport via axons to a large part of the dermatome. Depicted in red is the presence of virus and in yellow areas of productive viral replication. Adapted from Meier and Straus 1992.

In the process, numerous neurons are infected, leading to dermatomal vesicular eruptions (Figure 6b). The cumulative damage to the ganglion and its neural projections is substantial, potentially causing troublesome neuralgia.

2.7 VZV growth in animal models

Varicella-zoster virus is highly species-specific and has been demonstrated to naturally infect only humans and great apes. Simian varicella, a group of antigenically related agents distinct from VZV, infects cercopithecoids producing severe varicella-like disease but does not infect humanoids. Seroconversion following inoculation of VZV in small laboratory animals has been demonstrated in the rat, rabbit, and guinea pig (reviewed by Myers and Connelly 1992); however, animal-to-animal spread, viremia, and exanthem have been demonstrated only in guinea pigs. Both humoral and cellular immune responses to VZV infection have also been examined in the guinea pig and rabbit. Animal models of VZV persistence have been elusive although persistence may be established in the rat. Naturally occurring varicella of a gorilla has been documented with virus recovered from vesicular lesions (Myers *et al* 1987). This model was predictably too unfriendly to pursue further.

2.8 VZV growth *in vitro*

VZV has been propagated in a variety of primary cell lines, usually of human or simian origin, although continuous cell lines such as Vero or human melanoma cells have also been employed with equal success. However, even cultured cells derived from the natural host are considered to be only partially permissive for VZV growth as they do not readily support the production of cell-free infectious virus (Weller and Witton, 1958). The investigation of all aspects of VZV biology and structure have been significantly impaired by the inability to isolate stable, high titre stocks of cell-free virus. Consequently VZV growth in tissue culture is very poorly characterised.

3. Biology of varicella-zoster virus

3.1 Varicella: Pathogenesis and Disease

Knowledge of the pathogenesis of varicella comes primarily from analogy with other viral exanthems because the clinical disease is quite benign and no suitable experimental models are available.

The virus apparently enters through the mucosa of the upper respiratory tract and oropharynx or via the conjunctiva. Viral replication begins at the primary inoculation site, and subsequently virus disseminates via the bloodstream and lymphatics. After this primary viraemia the virus is then taken up by cells of the reticuloendothelial system, where it undergoes multiple cycles of replication, and in most cases, overwhelms the immune system to develop extensive secondary viraemia. This secondary viremia is associated with prodromal symptoms, which are then followed by cutaneous and mucosal lesions (Gelb 1993). These lesions appear in successive crops, probably reflecting cyclic viremia. The viremic phase is terminated in about three days by specific humoral and cellular responses, after which no new lesions appear but existing vesicles may continue to enlarge.

The rash of varicella is the most typical feature of the disease which usually begins after an incubation of 14 or 15 days. These lesions dry and the crusts fall off in one to three weeks. Successive crops of lesions appear over two to four days with lesions tending to appear first on the scalp and trunk spreading to the extremities. The distribution is predominately central, with the greatest density of lesions found on the trunk, which correlates with later presentation of herpes zoster. The illness is generally benign and while new lesions continue to appear is accompanied by a mild fever (Broughton 1966). The most marked symptom is pruritus, which lasts throughout the vesicular stage. Increased severity of the disease is more common in adults and in the immunocompromised.

The most common complication of varicella (in the normal host) is bacterial superinfection of the skin lesions, which can lead to scarring and rarely septicaemia or metastatic infections elsewhere (Bullowa and Wishik 1935) but it usually responds to antibiotics. Increased severity of disease is more common in adults and in the immunocompromised. Varicella pneumonia is the most common serious complication

in adults with mortality in the range 10% to 40% (Guess 1986). Pregnant women are at greater risk of varicella pneumonia than other adults, with a reported incidence of symptomatic pneumonia of almost 10% (Paryani and Arvin 1986). The severity and complications of varicella are significantly increased in immunocompromised patients, particularly leukaemics, those receiving immunosuppressive chemotherapy or with acquired immunological deficiencies (Feldman *et al* 1975, Krugman *et al* 1977). Fatal cases have widespread visceral dissemination, varicella pneumonia, and often encephalitis which is responsible for 20% of hospitalizations with varicella (Fleisher *et al* 1981, Feldman *et al* 1975).

3.2 Zoster: Pathogenesis and Disease

The pathogenesis of herpes zoster is also not well understood. The current model of zoster pathogenesis is based primarily on clinical and epidemiological data as well as on analogy with recurrent HSV infections (Hope-Simpson 1965). Once in the ganglion, the virus sets up a latent infection or is actually a persistent infection in which some VZV is constantly being produced. In either case, the infection remains quiescent until reactivation in the form of herpes zoster. These reversions are sporadic and infrequent. There is no temporal or spatial relationship to clinical varicella, and all evidence points to endogenous reactivation of virus in a previously infected host. When herpes zoster does appear, it occurs with the greatest frequency in those dermatomes in which the rash of varicella is most dense. The mechanism of reactivation is unclear and many conditions have been associated with the appearance of herpes zoster such as Hodgkin's disease and other lymphomas, immunosuppressive drugs and trauma to the spinal cord and adjacent structures (Gelb 1993). Since many of these precipitating conditions are associated with immunosuppression, it led to the proposal (Hope-Simpson 1965) that it is the deterioration of host defences below the level of containment that allows VZV to begin active replication in the sensory ganglia. The tiny dose of infectious virus that results is immediately contained by circulating antibody or cell-mediated immunity. When host defences deteriorate to the point that VZV replication can no longer be contained, extensive viral multiplication occurs in the ganglion, producing severe neuronal necrosis and intense inflammation, often with associated neuralgia. Infectious virus then spreads antidromically down the sensory nerve and infects the skin, where it produces the characteristic clustered vesicles of herpes zoster. Occasionally, the immune response is able to abort the cutaneous lesions, but not the necrosis and inflammatory response in the ganglion. This results in radicular pain and associated skin lesions

The rash of herpes zoster is usually preceded by pain and paresthesias in the involved dermatome. This begins several days before the eruption and ranges from mild itching or tingling to severe pain. The eruption of herpes zoster is characteristically unilateral, does not cross the midline, and is limited to the cutaneous innervation of a single sensory ganglion. The lesions are typically varicelliform and may be scattered in patches within the involved dermatome or so numerous as to form an almost confluent plaque. Crusts may take a week to form and persist an additional two to three weeks. Dermal involvement is more common in zoster and there is a greater propensity for scarring (Gelb 1993).

The most common complication of herpes zoster is post-herpetic neuralgia, which occurs in 50% of patients older than 60 years of age, but rarely in those under 40 years. It is especially common with ophthalmic zoster (de Morgas and Kierland 1957) and is often difficult to treat. The incidence of true post-herpetic neuralgia (pain lasting more than one month) is estimated to be between 9 and 14%. It resolves within two months in about 50% of patients and within one year in 70-80%. The pain can last a decade or more in a small fraction of patients. As in varicella, there may be superficial gangrene with delayed healing or secondary bacterial infection. Severe eye involvement may lead to corneal opacification or secondary bacterial panophthalmitis. Most other complications of herpes zoster are related to virus spread. As with varicella, herpes zoster tends to be much more severe (as well as more common) in immunocompromised individuals or those with malignancies.

4. Antiviral Strategies

There has always been considerable interest in specific anti-VZV therapy because varicella, particularly in the immunocompromised, can cause significant morbidity and even mortality. The current approach to the management of varicella-zoster virus infections involves choices among various therapeutic and preventive strategies (the most simplest being isolation of infectious individuals).

4.1 VZV immune globulin and zoster immune plasma

Initial attempts at passive immunization employed large doses of standard immune serum globulin (ISG). This could attenuate but not prevent varicella in normal children if given within three days of exposure (Ross 1962). Administration of varicella-zoster

immune globulin (VZIG), a high titre VZV antibody preparation, was able to prevent varicella in normal children under similar circumstances (Brunell *et al* 1969), as well as modify disease in immunosuppressed children (Gershon *et al* 1974, Zaia *et al* 1983). Zoster-immune plasma (ZIP), VZV convalescent plasma, will also modify or prevent varicella in susceptible high-risk children (Geiser *et al* 1975). Unfortunately VZIG does not modify zoster infections.

4.2 Vaccination

An alternative approach to post-exposure prophylaxis is the use of the live (Oka strain) attenuated varicella vaccine (Takahashi *et al* 1974, 1975). If administered within 72 hours of exposure this vaccine is able to prevent clinical varicella in normal susceptible children (reviewed by Gershon *et al* 1993). Although questions have been raised about persistence of immunity, degree of attenuation, risk of secondary spread, possible oncogenicity, and potential for reactivation as herpes zoster, the vaccine appears both safe and effective even in immunocompromised patients (Gelb 1993).

4.3 Antiviral compounds and resistance

Compared to the remarkable progress made in the treatment of bacterial infections over the past four decades, advances in the chemotherapy of viral diseases have occurred at a slower pace. Only a few antiviral agents of proven clinical value for a limited number of indications are available (reviewed by Whitley and Gnann Jr 1993).

Three antiviral compounds have been proven efficacious in varicella: leukocyte interferon, vidarabine and acyclovir. Human leukocyte or alpha-interferon has favourably altered varicella in children with cancer (Arvin *et al* 1982). However, it must be given parenterally and has several associated toxicities. Consequently, most studies have employed either of the two nucleoside analogues. Vidarabine (adenosine arabinoside) has proven efficacy in both varicella and zoster and also has some toxicity (Whitley *et al* 1982, Whitley and Alford 1981). Acyclovir (a guanosine derivative with an acyclic side chain) has largely superseded vidarabine for most applications. It has been shown to prevent the development of pneumonitis and systemic infection in immunosuppressed children with varicella (Prober *et al* 1982). Several nucleoside analogues (such as bromovinyl arabinosyl uracil [BV-araU], fluroiodoarabinosyl cytosine and its analogues and phosphonate methyl derivatives) have been shown to have antiviral activity *in vitro* and many are undergoing further investigation or are in

clinical trials (Whitley and Gnann Jr 1993, Cameron 1993). Antiviral compounds are not always beneficial, cytosine arabinoside and iododeoxyuridine, for example, have proven too toxic for systemic use in VZV infections and may actually worsen the disease (Gelb 1993).

The use and possible overuse of VZV-specific antivirals raises the question of antiviral drug resistance. As with herpes simplex virus, acyclovir-resistant varicella-zoster viruses can be readily selected in the laboratory by growth in the presence of acyclovir, and the first observation of a clinical isolate resistant to acyclovir has been reported (Averett *et al* 1987). The mechanisms by which the virus becomes resistant are the same as with herpes simplex virus, namely, mutation of the viral thymidine kinase or polymerase genes. Unlike herpes simplex virus, however, varicella-zoster virus disseminates readily, and the spread of resistant virus in immunosuppressed patients could result in increased visceral disease.

5. Thymidylate synthase

Thymidylate synthase (EC 2.1.1.45) is one of the most highly conserved enzymes with a evolutionary period of ~23 million years – the meantime it took to accept a single amino acid change during the divergent evolution of TS (Stroud and Finer-Moore 1993). Thymidylate synthase (TS) is the sole *de novo* source of 2'-deoxythymidylate (dTMP) in a diverse range of organisms. TS catalyses the conversion of 2'-deoxyuridylate (dUMP) and N⁵, N¹⁰-methylene-tetrahydrofolate to dTMP and dihydrofolate (reviewed by Carreras and Santi 1995). To date, sequences are known from 36 different species of TS. These include the human enzyme; which is a drug target for anti-cancer agents; thymidylate synthases from protozoa, which are generally bifunctional (Ivanetich and Santi 1990), with TS and dihydrofolate reductase present in a single protein, and TS from bacterial and viral species. TS is an essential enzyme to almost all living species and is coded for within several large DNA viruses, presumably to support an increased need for DNA synthesis during the viral life cycle. There are only a few organisms that adequately scavenge thymidine from their environment and do not require TS (Stroud and Finer-Moore 1993). The essential requirement for TS activity makes TS an important drug target for the development of anti-parasitic, anti-fungal, and possibly antiviral agents.

5.1 The thymidylate cycle

Efficient DNA synthesis requires the presence of adequate pools of the four 2'-deoxyribonucleotides, dATP, dCTP, dGTP and dTTP. The first three of these are synthesised by direct reduction of their corresponding ribonucleotides in a reaction catalysed by ribonucleotide reductase (Figure 7). In eukaryotes and certain prokaryotes, reduction occurs at the diphosphate level and is followed by phosphorylation of the dNDPs to dNTPs by the enzyme nucleoside diphosphate kinase. In other prokaryotic organisms reduction occurs at the triphosphate level. Ribonucleotide reductase also mediates the synthesis of the 2'-deoxyribonucleotide dUTP. As dTTP has no ribonucleotide counterpart, it cannot be synthesised in the same way. Instead, it is synthesised *de novo*, commencing with the formation of thymidylate (dTMP) from deoxyuridylate (dUMP) in a reaction catalysed by thymidylate synthase (Figure 8).

Deoxyuridylate is provided by the hydrolysis of dUTP, catalysed by deoxyuridylate triphosphate diphosphohydrolase (dUTPase) or by the deamination of deoxycytidylate (dCMP). dTMP can also be formed by a salvage pathway where thymidine kinase catalyses the phosphorylation of thymidine. The phosphorylation of dTMP to dTDP is catalysed by thymidylate kinase and nucleoside diphosphate kinase catalyses the phosphorylation of dTDP to form dTTP.

The thymidylate cycle involves three enzymes, thymidylate synthase, dihydrofolate reductase and serine trans-hydroxymethylase (Figure 7). Thymidylate synthase (methylenetetrahydrofolate: deoxyuridine-5'-monophosphate C-methyltransferase) catalyses the *de novo* synthesis of thymidylate via the reductive methylation of deoxyuridylate with the concomitant conversion of the cofactor N⁵, N¹⁰-methylene-tetrahydrofolate to dihydrofolate. This reaction is the only one in nature that results in the production of dihydrofolate, an oxidised form of folate that cannot be used in any biological process. To regenerate the reduced folate pools, dihydrofolate is converted to tetrahydrofolate by dihydrofolate reductase (DHFR), a reaction essential for the maintenance of these pools and thus cell viability. The enzyme serine trans-hydroxymethylase completes the thymidylate cycle by catalysing the formation of N⁵, N¹⁰-methylene-tetrahydrofolate. The pivotal roles played both by TS and DHFR in DNA precursor synthesis has led to their wide recognition as target enzymes for drugs aimed at the treatment of both infectious and proliferative diseases.

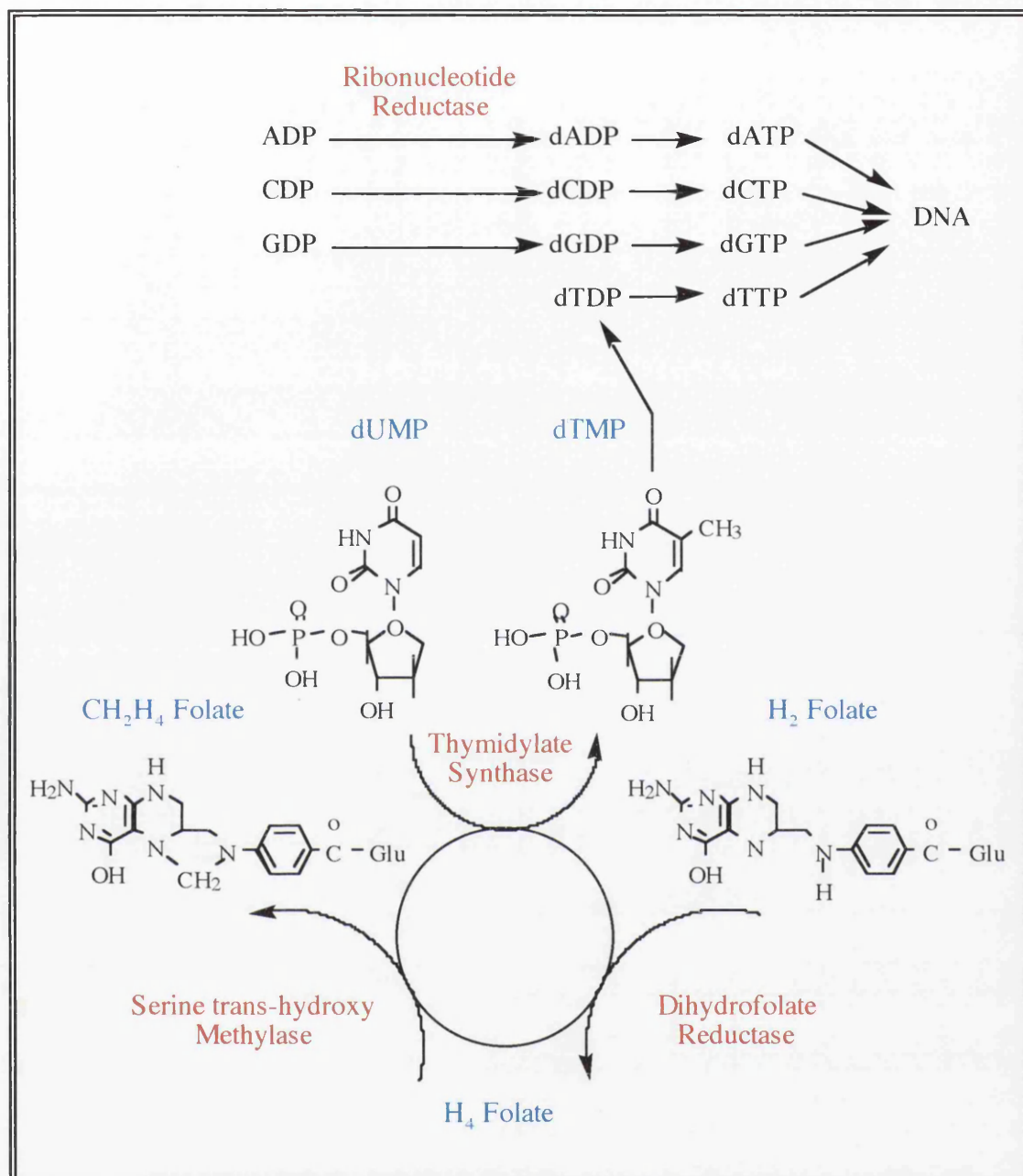


Figure 7. The Thymidylate cycle

The following abbreviations are used: H₂ Folate- dihydrofolate; H₄ Folate- tetrahydrofolate; CH₂H₄ Folate- N⁵N¹⁰-methylene-tetrahydrofolate. Standard abbreviations are used for nucleotides. Adapted from Lewis and Dunlap 1981.

5.2 TS from different sources

Thymidylate synthase is a ubiquitous enzyme found in all cellular organisms and coded by some large DNA viruses. The first studies of TS were performed on the enzyme isolated from the **bacterium** *Lactobacillus casei* (Friedkin *et al* 1962, Blakley 1963).

enzyme isolated from the **bacterium** *Lactobacillus casei* (Friedkin *et al* 1962, Blakley 1963). The isolation of a methoxotrexate resistant *L.casei* strain, that over-produced TS and DHFR, meant that large amounts of highly purified enzyme were available for study (Crusberg *et al* 1970) and has resulted in the *L.casei* enzyme becoming the most extensively studied TS from all sources (Santi and Danenberg 1984). The over-production of both TS and DHFR suggests that the genes encoding these two enzymes are closely linked. The genes encoding TS and DHFR are also closely linked in *Bacillus subtilis* and *Staphylococcus aureus*. (Piggot and Hoch 1985, Burdeska *et al* 1990). In contrast the genes for TS (*thyA*) and DHFR (*frd*) are widely separated on the *E.coli* chromosome (Bachmann 1983). However, the two enzymes have been proposed to form part of a multi-enzyme complex that is responsible for channelling newly synthesised dNTPs into replicating DNA (Mathews *et al* 1978, 1988). The gene coding for TS in *Lactococcus lactis* can complement the growth of an *E.coli thyA* strain, and its predicted amino acid sequence is the most widely diverged TS sequence known (Ross *et al* 1990).

TS and DHFR from **bacteriophage** T4 form part of a multi-enzyme aggregate, comprising both T4 and *E.coli* proteins and termed the dNTP synthetase complex (Mathews *et al* 1978, 1988, Moen *et al* 1988). This complex produces dNTPs in a manner tightly co-ordinated with DNA replication (Allen *et al* 1980, Chiu *et al* 1982, Mathews *et al* 1988, Moen *et al* 1988). In addition to their catalytic roles, the two enzymes act as structural components of the T4 virion base plate (Capco *et al* 1973), an example of an enzyme with a stable protein fold being recruited into a structural role. Φ 3T is a phage of *B.subtilis* and can complement *Thy⁻* auxotrophs upon lysogeny because it encodes a thymidylate synthase. It is a product of the *thyP3* gene (Tucker *et al* 1969) and is functional when cloned in *E.coli* (Duncan *et al* 1977, Ehrlich *et al* 1976).

TS gene expression in **mammalian** cells is tightly regulated with respect to the proliferative state of the cell (Conrad 1971, Navalgund *et al* 1980). In human, mouse and Chinese hamster, TS enzyme and mRNA levels are low in quiescent cells but increase approximately 20-fold on stimulation to re-enter the cell cycle. In human and mouse cells, the increase in mRNA levels alone is not sufficient to explain the increase seen in TS activity, thus implying some form of post-transcriptional control mechanism (Ayusawa *et al* 1986, Jenh *et al* 1985). Studies by Chu and co-workers using a cell-free rabbit reticulocyte model system and *in vitro* gel retardation assays demonstrated that the translation of human TS mRNA is controlled by its own protein product through an autoregulatory feedback mechanism (Chu *et al* 1991, 1993). This

negative autoregulatory mechanism has recently been demonstrated in *Escherichia coli* (Voeller *et al* 1995).

Thymidylate synthase has so far been found in five **herpesviruses**, HVS (Honess *et al* 1986), VZV (Thompson *et al* 1987), HVA (Richter *et al* 1988) and herpesvirus eotus 2 (Bob Honess, personal communication) and equine herpesvirus 2 (Telford *et al* 1995). All of these viruses have A+T rich genomes and this observation coupled with the fact that TS has not been found in any of the G+C rich viruses studied to date, led to speculation that TS may form part of a virus specific replication complex. This could influence the supply of thymidylate directed towards DNA replication and contribute to the non selected bias in base substitutions that have produced the A+T rich coding sequences of some subgroups of herpesviruses (Honess 1984, Honess *et al* 1986). However, a virally encoded TS gene is not a prerequisite for an A+T rich genome, as several other herpesviruses with such a genome composition lack TS (Lawrence *et al* 1990, Neipel *et al* 1991). Interestingly, the TS from VZV is highly homologous to eukaryotic and prokaryotic thymidylate synthases. The origins of the VZV TS gene (and those of the other herpesviruses) remains uncertain as there is no methodology to determine unambiguously whether the TS gene is an ancestral feature lost during divergence to herpesvirus families, or whether it has since been acquired after divergence. Incidentally, it is also unclear as to whether TS is essential for growth of VZV in normal tissue culture since VZV also encodes a thymidine kinase (TK). TK is involved in the thymidine salvage pathway perhaps negating the dependence on a virally encoded thymidylate synthase. However, TK mutants of VZV and HSV-1 are viable in tissue culture (Dubbs and Kitt 1974, Shiraki *et al* 1983) indicating that TS may also be dispensable.

In **protozoa**, TS exists on the same polypeptide as DHFR. The DHFR domain forms the amino terminus, TS the carboxy terminus and a junction peptide links the two domains to form a single protein, whose size is species dependent, usually falling in the range 110 to 140kDa (Ivanetich and Santi 1990). One immediately apparent biological advantage of a bifunctional DHFR/TS is metabolic channelling of dihydrofolate as is seen with the *Leishmania tropica* enzyme. Dihydrofolate produced by the TS component of the bifunctional enzyme is channelled to DHFR faster than it is released into the medium, thus the net rate of the sequential reactions is governed by the rate of TS (Meek *et al* 1985). This arrangement also results in both activities being co-ordinately regulated, resulting in optimal dTMP synthesis when required.

Yeast cells lack thymidine kinase and are impermeable to thymine derivatives including thymidylate, thus their only source of thymine nucleotides is from

thymidylate produced *de novo* by TS (Bisson and Thorner 1977). TS specific mRNA production peaks in *Saccharomyces cerevisiae* at the time during the cell cycle when TS levels are at their highest, a point that immediately precedes maximal rates of DNA synthesis during S-phase (Storms *et al* 1984). TS is thought to be a component of a multi-enzyme complex found in yeast, similar to those involved in dNTP synthesis seen in other organisms, although only some of its components have been identified (Jazwinski and Edelman 1984, Mathews *et al* 1988).

Early analysis of TS and DHFR in higher **plants** was limited to a handful of investigations that described the preliminary measurements of TS activity and the purification of DHFR from carrot and soybean cells (Ohyama 1976). More recently, two groups have produced conflicting reports concerning the nature of TS and DHFR expressed in carrot cells. Nielson and Cella (1988) reported the proposal that TS and DHFR from domesticated carrot cells (*Daucas carota*) may exist as a bifunctional enzyme, similar to, albeit larger than, those found in protozoa. In contrast, Goodman and co-workers have described TS activity (in wild carrots) assigned to a different polypeptide to that of DHFR (Toth *et al* 1987). A DHFR-TS gene has recently been cloned from *Arabidopsis thaliana* (Lazar *et al* 1993) and immunochemical analysis reveals the presence of a bifunctional DHFR-TS in *nicotiana plumbaginifolia* and *Oryza sativa* (Balestrazzi *et al* 1995). Bachmann and Follmann (1987) have also copurified a bifunctional DHFR-TS enzyme from the algae *Scenedesmus obliquus* indicating that a bifunctional protein is ubiquitous in plant cells.

6. Amino acid sequence homology

The amino acid sequences of TS have been determined from organisms as diverse as humans, bacteriophage and, more recently plants (see Appendix I).

6.1 The conservation paradox

A particularly striking feature of thymidylate synthase is its high degree of amino acid sequence conservation, approximately 10% (27 out of a core of 275 residues) are absolutely conserved in the 36 known TS sequences, with a further 165 residues (60%) being greater than 80% conserved. If the two most divergent TS sequences, those of *L.lactis* and bacteriophage Φ 3T are excluded, the degree of conservation rises to 24% (61 out of a core of 275 residues). Such a degree of amino acid homology

places TS amongst the most highly conserved enzymes, a group that includes proteins such as the cytochromes. This contrasts with dihydrofolate reductase, the enzyme which regenerates the folate cofactor oxidised by TS, although amino acid sequences have been reported from a much smaller group of organisms; only 6% of residues (11 residues from a core of approximately 170) are completely conserved, a further 41 residues (24%) being greater than 80% conserved (Lagosky *et al* 1987). The high degree of conservation in TS, at the level of the primary structure, is also evident at the tertiary-structure level, A comparison of the three-dimensional structure of the native enzymes from *E.coli* and *L.casei* showed that they are 89% conserved in terms of corresponding atom types (3824 common atoms out of 4300; *E.coli* TS), despite sharing only 60% amino acid identity (Perry *et al* 1990). It has been suggested that some reasons why TS is so highly conserved are related to the chemical reaction catalysed and the conformational dynamics that occur during catalysis (Finer-Moore *et al* 1990). Conservation may also be due to the need to maintain interactions with other enzymes such as DHFR.

Mutagenesis studies (Maley and Maley 1988, Dev *et al* 1988, Michaels *et al* 1990, Climie *et al* 1990, LaPat-Polasko 1990) on the TS of several organisms particularly from *L.casei* and *E.coli* have revealed a conservation paradox, such that, almost all the conserved residues (except at least 8 critical residues including the catalytic cysteine residue-C183 in VZV TS) can be substituted without severe disruption to the activity of the enzyme. Why these residues have been conserved throughout evolution, yet are not essential to the function of the enzyme, is not fully understood.

7. Catalytic mechanism of TS

Thymidylate synthase catalyses the conversion of 2'-deoxyuridylate (dUMP) and N⁵, N¹⁰-methylene-tetrahydrofolate (CH₂H₄ folate) to 2'-deoxythymidylate (dTMP) and dihydrofolate (Figure 8). The source of the methyl group for transfer to dUMP, the cofactor CH₂H₄ folate, plays a dual role. First, it is a one-carbon donor, and then reductant of the transferred methylene at different steps in the reaction. The major chemical steps in the methylation reaction have been deduced using chemical models as well as by studying the structures and kinetics of the formation of reaction intermediates (Santi and Danenberg 1984).

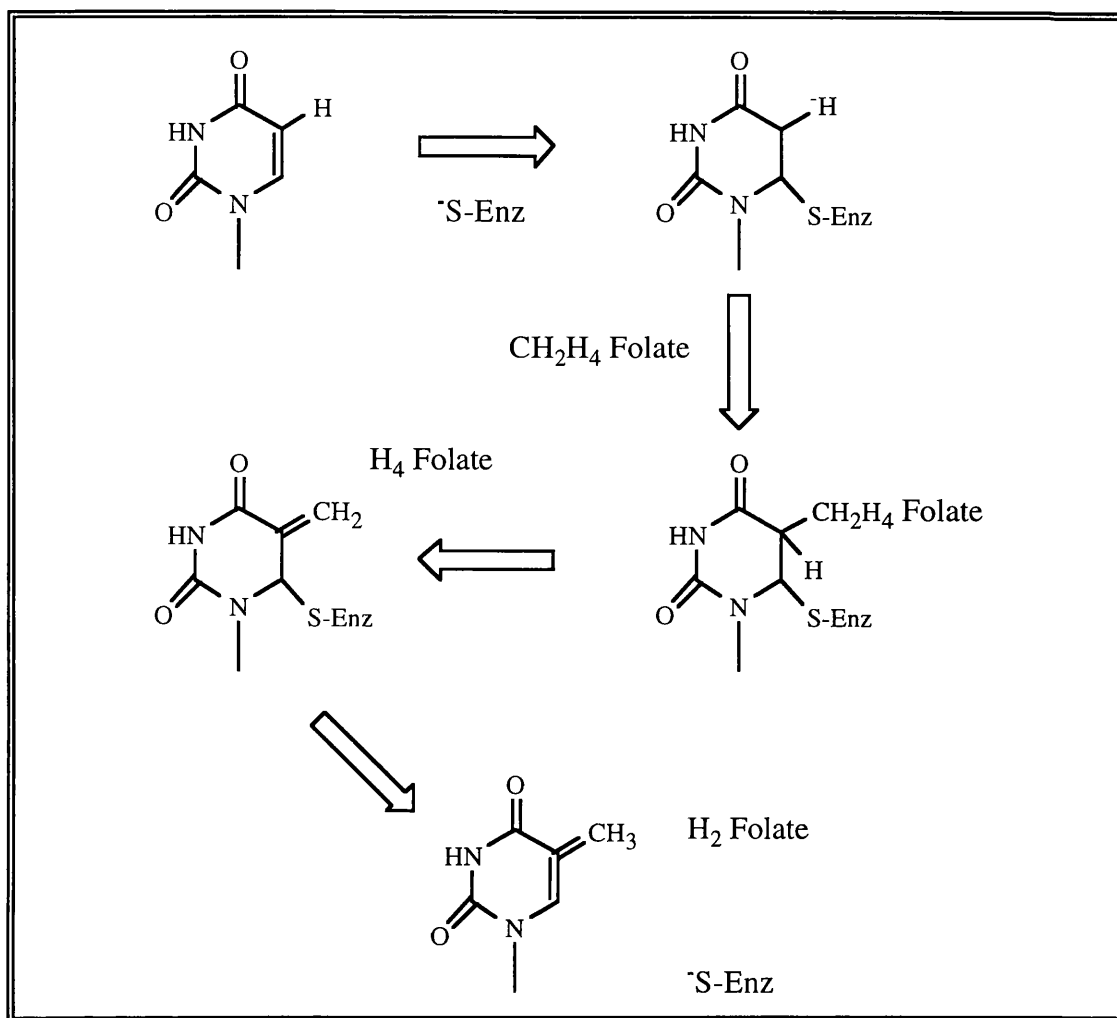


Figure 8 The catalytic mechanism of Thymidylate synthase (adapted from Hardy *et al* 1987). R= deoxyribose-5'-phosphate.

A more detailed reaction mechanism is given in Stroud and Finer-Moore 1993

The catalytic mechanism of TS involves the initial formation of a covalent bond between the 6-position of dUMP and a catalytic thiol (Cysteine 183 in VZV TS) of the enzyme (Figure 8). Formation of this binary complex serves to activate the 5-position of dUMP. After the CH₂H₄ folate binds, its imidazolidine ring opens, giving a reactive iminium ion that condenses with the activated C-5 of dUMP. Subsequent to formation of the ternary covalent complex, β elimination and hydride-transfer reactions occur to generate the methylated pyrimidine, the oxidised cofactor, and the catalytically active enzyme.

TS is an obligate dimer of identical subunits that are related by a twofold axis of rotation (Figure 9). The structure of TS shows why it is an obligate dimer, as components of each monomer contribute to each of two active sites. There is no

conclusive evidence for cooperativity between the monomers in the dimer (Stroud and Finer-Moore 1993). However, as ligand binding induces large conformational changes (see section 7.3) that extend throughout the protein, the ligand affinities will depend on the liganded state at both active sites.



Figure 9 Thymidylate synthase dimer

The view is directly down the dimer interface between the 2 monomers. β -strands are coloured yellow, α -helices are red, connecting loops white and both the substrate and cofactor are depicted as space filling models.

7.1 Residues involved in catalysis

The first crystal structure of TS, that of the *L.casei* enzyme, revealed structural details of the ligand binding site. Subsequent crystallographic studies of complexes of TS that are analogues of reaction intermediates or ligands have provided useful information on residues involved in catalysis (for a full review see Stroud and Finer-Moore 1993, Carreras and Santi 1995). A summary of specific contacts between ligands and protein in the covalent ternary complex is outlined below. All residue numbers are for the

L.casei enzyme with the VZV residue number in brackets, primed numbers indicate residues from the other monomer of the dimeric protein (see Appendix I).

Four highly conserved arginines, two from each monomer, provide a favourable, positively charged binding surface for the phosphate anion. These four arginines, Arg-23 [38], Arg-218 [207], Arg-178' [163'] and Arg-179' [164'], as well as Ser-219 [208] are involved in an extensive hydrogen bonding network around the phosphate. Each arginine forms at least one hydrogen bond to the phosphate oxygens.

Arginine-23 [38] is also hydrogen bonded to the COOH terminus of the protein.

Arginine-218 [207] is hydrogen bonded to the carbonyls of residues Pro-196 [181] and Arg-178' [163]. Arginine-178' [163] is hydrogen bonded to the hydroxyl of Tyr-261 [246].

Invariant Tyr-261 [246] and His-259 [244] are the primary contacts to the ribose ring of dUMP, they are hydrogen bonded to O-3' on the ribose ring. Hydrogen bonds between the pyrimidine of dUMP and invariant Asn-229 [214] and the main chain amide of Asp-221 [206] are the only other hydrogen bonded contacts between dUMP and the protein. Asparagine-229 [214] is hydrogen bonded to both O-4 and N-3 of dUMP. Cys-198 [183] (the active-site sulfhydryl) forms a covalent bond to C-5 of dUMP linking it to the methylene group and N-5 of the cofactor.

The only protein side chain to hydrogen bond to the folate cofactor is that of invariant Asp-221 [206]. Other hydrogen bonds involving the cofactor are made either with water or backbone atoms. The exocyclic amino group on the pterin ring is hydrogen bonded to the terminal carbonyl residue (315 [301]) in the protein.

The PABA ring lies in a hydrophobic pocket surrounded by the side chains of the highly conserved residues Ile-81 [96], Leu-224 [209], Phe-228 [213] and Val-314 [Met 299; only the bacteria, phage Φ 3T and *Tn*4003 do not have methionine at this position]. The pocket is formed in part by movement of the carboxy terminus on ligand binding. Phe-228 [213] and Leu-224 [209] are within van der Waals contact of the PABA ring. Trp-82 [97] and Trp-85 [Tyr 100] are just below the PABA ring, stacked against the pterin ring.

The cofactor is normally linked to a linear sequence of as many as seven glutamate residues that are γ -linked or α -linked to the PABA ring and to each other. The crystal structure of the *E.coli* enzyme reveals that interactions between protein and polyglutamyl moiety are primarily electrostatic (Kamb *et al* 1992b). The only three

clearly discernable hydrogen bonds between the tetraglutamyl group and the protein are mediated by ordered water.

7.2 Ordered binding of ligands

Initial experimental investigation using monoglutamylated cofactor provided evidence that the ligands bind in an ordered fashion in which dUMP binds first, followed by cofactor, and that cofactor leaves before dTMP in bi-bi reaction sequence (Lorenson *et al* 1967, Danenberg and Danenberg 1978). These results may be explained in part by the fact that dUMP is an important binding surface for the pterin ring.

However, the intracellular pool of folates consists mainly of polyglutamylated molecules. Polyglutamyl folates have affinities for TS that are in some cases more than 400-fold greater than that of the monoglutamyl form (Lu *et al* 1984). Under certain reaction conditions, the increased binding affinity of polyglutamyl folates for TS results in random binding order of ligands (Ghose *et al* 1990). Crystal structures of the enzyme are consistent with the observation of random binding of ligands under certain reaction conditions (Kamb *et al* 1992a).

7.3 Conformational changes upon ligand binding

Conformational changes of a protein in response to the binding of ligands is now a well-established phenomenon and is often necessary to account for effects such as cooperativity and allosteric control of enzyme reactions.

A series of conformational changes have been associated with the catalytic reaction performed by thymidylate synthase. Early evidence for a conformational change upon ligation with both substrate and cofactor came from a number of groups (Galivin *et al* 1975, Leary *et al* 1975, Donato *et al* 1976). On complexation, aromatic groups on the protein (tyrosine and tryptophan residues) and of the folate chromophore were perturbed, as detected by Raman spectroscopy, circular dichroism, ultraviolet spectroscopy and fluorescent spectroscopy. In both human and *L.casei* TS, the stokes radius decreased by 3.5% upon formation of the TS•FdUMP•CH₂H₄ folate complex (Lockshin and Danenberg 1980). The structures of native, unliganded TS from *L.casei*, *E.coli* phage T4 and human present large cavernous openings that close down progressively as ligands bind. In the binary complex formed as the substrate dUMP binds, the active sites remain open and very close to the unliganded state (Finer-Moore

et al 1993). On the other hand, the binding of a folate analogue (CB3717) by itself serves to sequester the reactants from solution (Kamb *et al* 1992a). These results demonstrate that structure change during catalysis is triggered mainly by the binding of cofactor, and not by dUMP.

The dramatic changes in the spectra and hydrodynamic behaviour of *L.casei* TS on formation of ternary complexes suggest large conformational differences between unliganded TS and TS in ternary complex with substrate and cofactor analogues. In fact, the differences between P_i-bound *E.coli* TS and TS•dUMP•CB3717, although quite extensive, are not particularly large (Montfort *et al* 1990). Segments of helices, β-sheet and loops move toward the active site, usually less than 1 Å, to accommodate ligand binding. The ligand binding side chains do not themselves change conformation as the active site closes. The greatest segmental shift is in residues 312-316 (*L.casei* TS) at the carboxy terminus and the surface loop containing arginine-21 (the DRTG loop). These residues become more ordered in the ternary complex and move more than 4 Å into the active site, forming an important binding determinant for the cofactor (see section 8.4).

8. Structural features of TS

Prior to X-ray crystallographic studies, the structure of TS was mainly predicted using the technique of circular dichroism (Manavalan *et al* 1986). The understanding of many facets of TS function and dynamic behaviour during catalysis have been significantly enhanced by X-ray crystallographic studies.

8.1 X-ray crystallographic structures of bacterial TS

In the past 6 years, the 3-dimensional structures of TS from various sources in several forms have been solved. Refined TS crystal structures include unliganded (Pi-bound) TS from *L.casei* (Hardy *et al* 1987, Finer-Moore *et al* 1993), *E.coli* (Perry *et al* 1990, Mathews *et al* 1990), Phage T4 (Finer-Moore *et al* 1994), *Leishmania major* (Knighton *et al* 1994), human species (Schiffer *et al* 1991, Robert Stroud, personal communication), and *pneumocystis carinii* (Perry and Stroud personal communication); binary complexes of TS with dUMP (Finer-Moore *et al* 1993) and with a polyglutamylated cofactor analogue (Kamb *et al* 1992a), ternary complexes that are analogues of the steady-state intermediate (Mathews *et al* 1990a; 1990b, Montfort

et al 1990, Kamb 1992b), and a product complex of TS with dTMP and dihydrofolate (Fauman *et al* 1994). Crystallisation of human TS (Schiffer *et al* 1991) is the first example of TS crystallisation from phosphate and/or substrate free medium, thus representing true native enzyme. Indeed, the addition of phosphate to the suspension cracks the crystals, suggesting that a possible induced conformational change takes place. Sequence similarity would suggest that all TS structures will be similar.

8.2 General structural features

Structural studies of TS have revealed several novel and interesting features. TS is an obligate dimer of identical subunits that are related by a two-fold axis of rotation. The structure of TS shows why it is an obligate dimer (Figure 10), as components of each monomer contribute to each of two active sites. The dimer interface is formed by a back-to-back apposition of two five-stranded (or six) β -sheets with a unique right-handed twist of one sheet relative to the other (Hardy *et al* 1987). Three contiguous β -strands bend sharply away from the remainder of the sheet in a β -kink and form one wall of the large active site cavity. The cavity is lined by many conserved side chains, including the active site cysteine. Two layers of helices and loops pack on top of the central β -sheet.

Several species of TS contain insertions and there are six sites where these inserts are found around the TS core. They are all present in surface loops or in a smaller 'variable' domain. For example, *L.casei* contains a 50 amino acid insertion which is arranged as three short α -helices within the variable domain (Hardy *et al* 1987). As these insertions are not present in all species (and found in non core regions) they cannot be relevant to fundamental aspects of structure or function. Perhaps they serve roles specific to individual organisms (such as DHFR binding) or have become redundant features during evolution.

8.3 Notable structural features of TS

β -sheet interfaces have previously only been described with a left-handed twist. One consequence of this unique right-handed twist is the formation of a β -kink that facilitates the close packing of the two β -sheets. Hardy and co-workers (1987) described an aligned discontinuity in β -strands i, ii and iii of the *L.casei* enzyme at residues Gly-33, Ala-258, and Gln-217 twisting the bottom left corner of the sheet outward. Although distorted, hydrogen bonding between the three anomalous residues

is preserved through the bend. The β -kink structure also serves as one of the major hinge points around which segments of secondary structure move during catalysis (Perry *et al* 1990; see section 7.3).

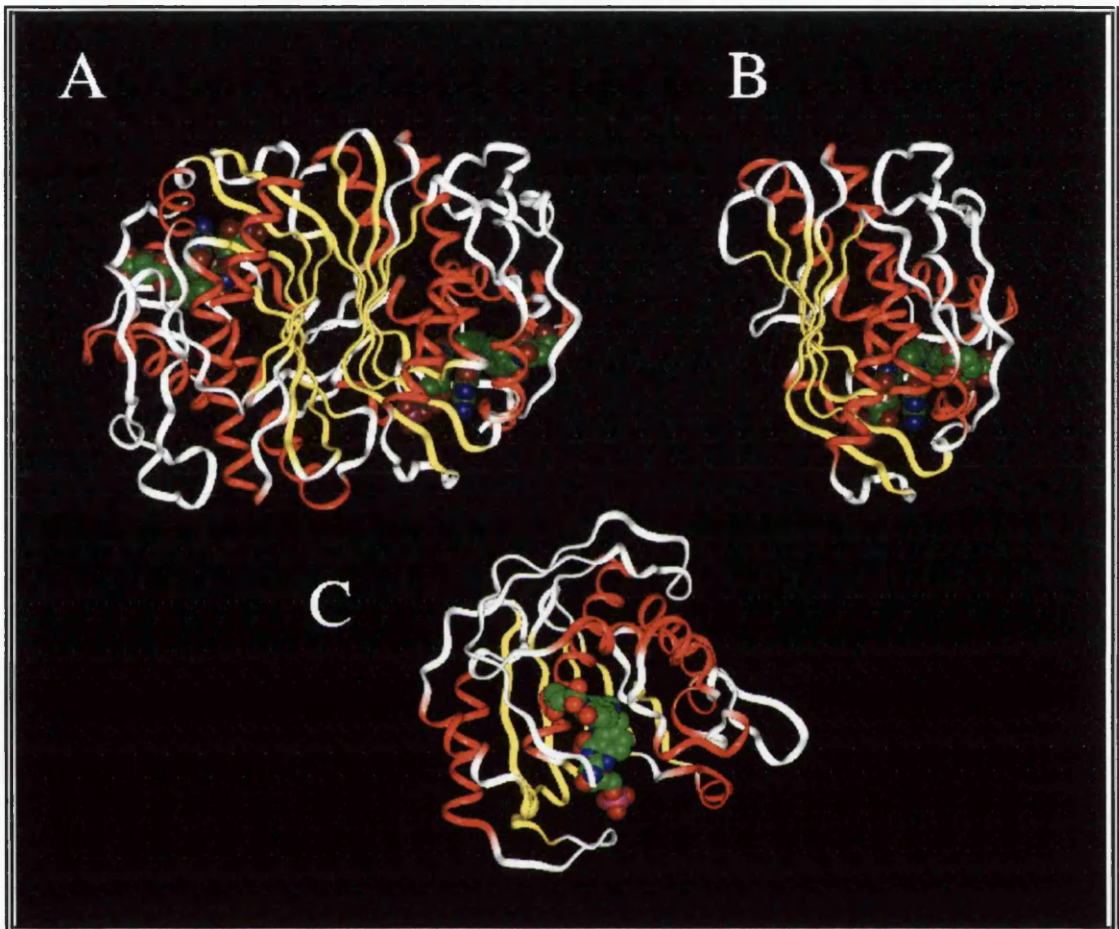


Figure 10. Different views of thymidylate synthase

The dimer (A), a monomer of TS (B) and the same monomer rotated through 90° (C) to give our standard view of a TS monomer.

β -strands are coloured yellow, α -helices are red, connecting loops white and both substrate and cofactor depicted as space filling models.

A core structural element around which the protein is folded is the **J-helix** (Figure 11a, 11b). This is a six-turn unusually hydrophobic α -helix, even more so than some membrane spanning helices, and is almost inaccessible to solvent. It sits on top of the β -sheet, is flanked by the amphiphatic α -helices A and H, and is capped by helix B.

The **active site** is a shallow cavity which contains the catalytic cysteine residue. The left wall of the cavity is formed by the sharply turning part of β -strands ii and iii, and

the loop connecting α -helix A and β -strand i. The ceiling is composed of residues from the solvent exposed N-terminus of the J-helix and the right-hand wall by the end of β -strand iv. The back of the cavity is formed by four residues of the β -sheet of the other monomer, one of which Arg-179' (*L.casei* enzyme) protrudes directly into the cavity, explaining why TS is an obligate dimer.



Figure 11a. A monomer of thymidylate synthase

β -strands are coloured yellow, α -helices are red, connecting loops white. The central J helix is green, and the active site cysteine is blue. The C-terminal residue and the DRTG loop are coloured cyan. substrate and cofactor are not shown for clarity.



Figure 11b. A dimer of *E. coli* thymidylate synthase

One monomer is shown in light purple the other light blue. The β -strands and α -helices are numbered.

Image kindly provided by RM Stroud.

8.4 Segmental accommodation

The conformational changes associated with the catalytic reaction performed by thymidylate synthase have attempted to be understood by comparing the differences between the structures of the unliganded and ligand bound forms of *E. coli* TS (Finer-Moore *et al* 1990, Mathews *et al* 1990a; 1990b, Montfort *et al* 1990, Perry *et al* 1990). To quantitate conformational change, a core of α -carbon residues whose mutual disposition remains unchanged ($\pm 0.5\text{\AA}$) between liganded and unliganded enzyme was identified. This core of 155 α -carbon atoms differs from most non-core residues

in that they have shifted between 0.5 to 1.25Å (Figure 12). In contrast to the domain shifts seen in proteins such as hexokinase (Anderson *et al* 1978) or citrate synthase (Remington *et al* 1982), the changes in TS are due to **segmental accommodation**, where α -helices, β -strands and connecting loops undergo concerted movement towards the active centre (Mathews *et al* 1990b, Montfort *et al* 1990).



Figure 12. Segmental accommodation by TS

A single monomer of *E. coli* TS is illustrated in the same orientation as in figure 11. Residues shown in yellow deviate from their original position by less than 0.5Å upon ligand binding, whereas residues shown in blue undergo substantial movement. Reproduced from Finer-Moore *et al* 1990.

The β -kink acts as one of several hinge points around which other segments of secondary structure move. The central J-helix pivots around a central point such that

the N-terminal end moves approximately 0.5Å towards the active centre. This in turn, causes the region of β -strands i, ii and iii below the β -kink to move towards the same location. The region containing the active site residue (Cys-183 in VZV TS) moves inward while the loop containing the two arginine residues (Arg-163' and Arg-164', VZV TS) also moves inwards. The two largest shifts involve the loop (the DRTG loop) containing Arg-38 and Thr-39 (VZV TS) that moves up to interact with the C-terminus, and the movement of the four C-terminal residues. In the unliganded structure, these four residues point out into the solvent, suggesting they are disordered (Mathews *et al* 1990a). However, on binding of ligands, this region moves approximately 4.0Å, sequestering several water molecules, to anchor the cofactor in place. This directs the exact alignment of substrate and cofactor to allow the formation of the observed H-bonds in this region of the crystal structure (Finer-Moore *et al* 1990, Mathews *et al* 1990a; 1990b, Montfort *et al* 1990)

8.5 Structural plasticity and covariant accommodation

The introduction of amino acid substitutions by site-directed mutagenesis affects protein function in an, as yet, poorly understood manner. The variations are often tolerated by adjustment of neighbouring residues and can result in unexpected properties. The accommodation of substitutions is due to the **structural plasticity** of the protein, the ability of a protein to adopt to changes in its primary structure, whilst maintaining the integrity of its tertiary structure. Several hundred site-directed mutations have been made in TS (Maley and Maley 1988, Dev *et al* 1988, Michaels *et al* 1990, Climie *et al* 1990, LaPat-Polasko 1990). Highly conserved active-site residues have been replaced by several other amino acids, though generally the protein remains active for several of the substitutions made at any position. Thus there is plasticity of function as well as structure

Structural plasticity, in response to substitutions, could feasibly be quantitatively described by two approaches. The first is comparison of structures of many site-directed mutations of a single protein, while the second approach is to compare two structures that differ at many positions in an attempt to generalise the effects of substitutions. The first approach suffers because each mutation at a single locus is a special case; substitutions at a particular site may produce no change elsewhere, or large and distant changes. This approach also requires the determination of many structures.

The second approach using the structures of the unliganded TS from *L.casei* and *E.coli* has proved more fruitful (Perry *et al* 1990). This species comparison of thymidylate synthase has served to map the tolerance of this protein toward mutation. A detailed study of the buried region of TS from both structures demonstrate three mechanisms by which mutations are accommodated (Perry *et al* 1990).

The first is the occurrence of local change, whereby large effects observed close to the site of mutation dissipate as a function of distance. This is usually achieved by a mechanism that involves local rearrangements, often the repacking of adjacent residues, with only minimal effects on the overall architecture of the protein. This local flexibility permits relief of strain at the protein surface (Perry *et al* 1990).

The second mechanism by which plastic adaptation can occur is by systematic shifts in individual elements of secondary structure, particularly in helices, where clusters of tightly packed, nonpolar residues change position in a concerted fashion. Several of the helical regions of TS, which contain the largest structural differences between the enzyme from *L.casei* and *E.coli*, have been accommodated in this way. The 'ensemble' movement of helices B, C and G is the most prominent example of this process, where these structures have shifted together as a unit in the *L.casei* structure, relative to *E.coli*. This movement has occurred to accommodate the interactions between the three-helix unit and helix-D of *L.casei*, a helix that is absent from *E.coli* TS (Perry *et al* 1990).

The final mechanism is **covariant accommodation** where multiple sequence changes combine to minimise the distortion of the main chain atoms and simultaneously preserve the volume of the packed side-chains. An example of covariant accommodation in TS is found the β -sheet, structurally the most conserved region of the TS protein. At the centre of β -strand ii, Phe-255 of *L.casei* is substituted by glycine in *E.coli*. The 'space' produced by mutation of the larger Phe residue to glycine is 'filled' by the concomitant mutation of His-253 to tryptophan and Ala-258 to threonine. This corresponds to net difference of only a single atom in these three residues. The position of the main chain α -carbon atoms are essentially unchanged. Generally, it has been found that when a substitution introduces three or more heavy atoms (carbon, oxygen, sulphur or nitrogen), this nearly always results in a second, or covariant change nearby (Perry *et al* 1990). Experimental data obtained from mutagenesis studies of the hydrophobic core of bacteriophage lambda repressor protein demonstrate that where a mutation increases the volume of the core in excess of the permitted level, second site mutations that can reduce the net volume of the core can restore activity (Lim and Sauer 1991).

For thymidylate synthase this suggests that in evolution, a certain degree of variation in sequence can be tolerated by plastic adaptation in structure, but the larger substitutions are generally compensated by covariant changes.

8.6 VZV TS model

Two models of the VZV thymidylate synthase, one of the ternary complex and the other of the native enzyme with bound phosphate (figure 12), have been constructed by Celia Schiffer and Robert Stroud (personal communication). The models are based upon the coordinates of the ternary complex of *E.coli* TS with CB3717 and dUMP (Montfort *et al* 1990) and the coordinates of the *E.coli* TS structure with bound phosphate respectively (Perry *et al* 1990). All residues from the *E.coli* sequence that differed from the equivalent residue of the VZV sequence were substituted by the latter using the graphics programme INSIGHT (Dayringer *et al* 1986). The substituted residues were positioned in a conformation which overlapped as much as possible with that of the residue existing in the *E.coli* structure. Where a VZV residue was larger than one it replaced, it was placed in a conformation which corresponds to that most frequently found for that amino acid in protein structures. The model lacks the first 19 amino acids from the VZV sequence, and the two short insertion sequences common to all eukaryotic thymidylate synthases (residues 105-116 and 134-141; VZV numbering), that are not found in the *E.coli* enzyme. At the time the model was generated, these regions of the human TS being studied by this group (Schiffer *et al* 1991) were unresolved. The model of the VZV native TS was refined by 200 cycles of conjugate gradient minimization with the refinement package of XPLOR (Brünger *et al* 1987), clearing up the bad contacts generated by the amino acid substitutions. The minimization resulted in a root mean square (RMS) shift of 0.38Å of the α -carbons. The model of the VZV ternary complex was refined with 150 cycles of XPLOR. Due to difficulties in the initial stage of energy minimization, the α -carbon atoms were constrained to stay fixed, thus allowing only movement of side chains to remove any energetically unfavourable contacts.

8.7 Human thymidylate synthase

Recently the crystal structure of unliganded human TS was resolved (Schiffer *et al* 1995) providing the first three-dimensional view of a mammalian TS. The structure follows those of the bacterial systems which is as expected due to the high degree of sequence identity.

As described for other thymidylate synthases human TS has 2 insertions, and they are present as α -helices and lie close together on the outside of the protein. No homologous insertions are present in prokaryotes suggesting they are eukaryotic specific insertions and have a eukaryotic specific function (Hardy *et al* 1987, Perry *et al* 1990). Human TS also has a unique amino terminal sequence which is 27 residues longer than *L.casei* (see Appendix I). It consists of 8 proline and 7 charged residues and is predicted to have a randomly coiled structure suggesting a unique function to the human TS. This may well enable human TS to interact with other proteins in the cell, some of which are involved in DNA synthesis. Perhaps the charged nature of this region allows it to interact with its own mRNA and negatively autoregulate its translation.

Although human TS has a similar overall fold to the bacterial enzymes it has a major divergence in the structure of the active site. Despite the high sequence homology between the *L.casei* and the human sequence in this region the human thymidylate synthase's entire active site is twisted 180° relative to the *L.casei* enzyme. This 180° twist buries the active site cysteine residue in the β -sheet dimer interface and upon ligand binding this catalytically crucial residue must 'untwist' 180°. It appears that in addition to the normal conformational changes that occur (as in all species of thymidylate synthase), which sequester solvent, orientate the substrate and cofactor, the human TS must also reorientate the active site cysteine. It has been suggested that one possible function for such an orientation of the active site may be to protect the catalytic cysteine from being modified in the cell (Schiffer *et al* 1995). However, such a reorientation may be energetically unfavourable and the highly conserved nature of the thymidylate synthases lends strength to the notion that all the structures would have a similar (if not identical) core structure. As to why the human TS thus has a different active site orientation to all other crystal structures of TS remains open to question.

Indeed, since its publication the human TS structural coordinates have been withdrawn, indicating a problem with the solved structure, perhaps with the active site cysteine.

8.8 The C-terminus of VZV is unique

Carboxypeptidase cleavage of the *L.casei* C-terminal valine from a single subunit of TS completely inactivates the enzyme and decreases its affinity for CH₂H₄ folate (Aull *et al* 1974). Subsequent mutagenesis of this residue confirms that the *L.casei* C-terminal residue is crucial for catalysis (Climie *et al* 1990).

In contrast to such bacterial enzymes removal of the C-terminal residue from VZV TS (L301Δ) does not inactivate the enzyme. This mutant retains a significant amount (3%) of wild-type activity, and in addition has normal debromination activity (Harrison *et al* 1995). This suggests a different mechanism of interaction at the C-terminus.

In *L.casei* TS the carboxylate group of the C-terminal residue makes four hydrogen bond contacts (Figure 13). They are to arginine 23, threonine 24, tryptophan 85 and one to the PABA ring of the folate cofactor. In VZV TS arginine 38 and threonine 39 (equivalent to R23 and T24 in *L.casei*) form virtually identical H-bonds to the carboxylate group of the C-terminal residue. However, a H-bond equivalent to the one between the C-terminal residue of *L.casei* and W85 is not found in the VZV TS model. This is because the equivalent to W85 from *L.casei* TS is tyrosine 100 in VZV TS (Figure 13). The hydroxyl group of Y100 can act as a H-bond donor and acceptor, however, it could not be positioned such that its hydroxyl group was able to form a H-bond with the carboxylate group of the C-terminal amino acid of VZV TS, without significant disruption to the rest of the protein.

A comparison of all the TS sequences at the position equivalent to Y100 reveals the presence of asparagine in phage T4 and all the eukaryotic thymidylate synthases, whilst tryptophan is found at this position in TS from all other organisms. Modelling of this asparagine residue in the *E.coli* structure (replacement of W83, equivalent to W85 in *L.casei*) has shown that asparagine allows the formation of an H-bond to the C-terminal carboxylate of similar length to that of wild-type. This suggests that asparagine could form a H-bond to the carboxylate group of the C-terminal residue in all other TS enzymes. Asparagine at this position may play an analogous role to the conserved tryptophan in TS from prokaryotes.

Removal of the C-terminal residue of *E.coli* (I264Δ) and *L.casei* (V316Δ) inactivate the enzyme by destroying the H-bonds occurring in this region and presumably prevent the tight closing down of the active site. The VZV model suggests retention of activity in the mutant L301Δ must be due to another interaction at the C-terminus which can

still close down the active site, if only partially. The candidate residue for such an interaction is tyrosine 100, since it is not found in other thymidylate synthases.

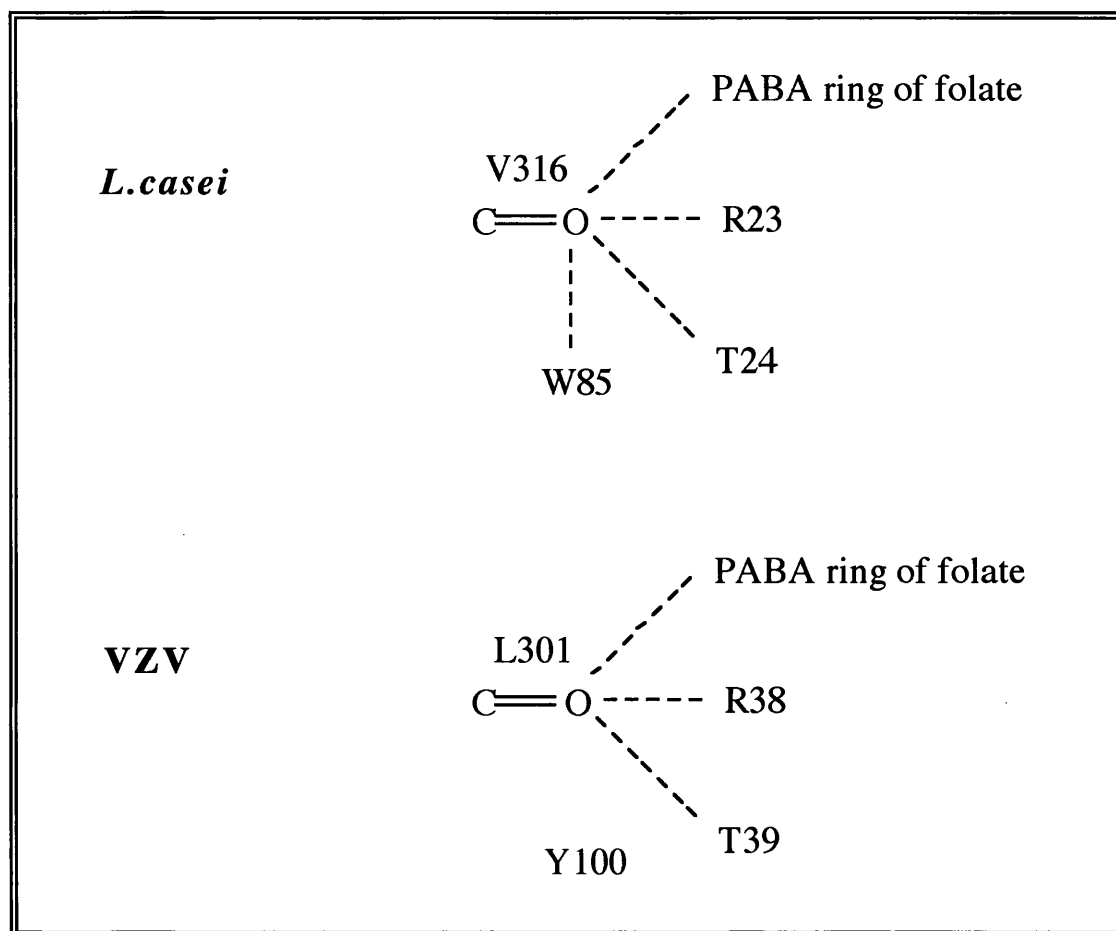


Figure 13 Interactions at the C-terminus of *L.casei* and VZV thymidylate synthase

Hydrophobic interactions could be important in C-terminus of VZV TS as they may occur between the side chains of isoleucine 99 and tyrosine 100 and the side chains of the C-terminal residues methionine 299 and leucine 301. Removal of the C-terminal residue does not inactivate the enzyme because presumably the remaining three residues (I99, Y100 and M299) can still interact, and this hydrophobic packing holds the two sides of the active site together. Additionally, the aromatic ring structure of Y100 may also help stabilise binding of the cofactor in an analogous manner to that seen by tryptophan. Further support for the observation that hydrophobic packing is important (more so, perhaps, than H-bonds) in the C-terminus of VZV TS is that *E.coli* and *L.casei* TS both have a valine residue as the position equivalent to M299 in VZV. They also have a hydrophilic glutamate residue at the position equivalent to I99. These

residues may be sufficient to prevent significant hydrophobic interactions in the bacterial enzymes. So in part the tyrosine at position 100 is responsible for the residual activity in the VZV TS mutant V313Δ.

This has led to the proposal that hydrophobic interactions are more important for the stabilisation of the VZV ternary complex (Harrison *et al* 1995).

Contrastingly, this tyrosine 100 residue is either a tryptophan in almost all prokaryotes or an asparagine in eukaryotes (and phage T4) suggesting that removal of their C-terminal residue will result in inactive proteins. Indeed VZV TS appears unique in this respect.

8.9 The DRTG loop of VZV

Below the C-terminal region of TS is a highly mobile loop. This loop consists of aspartic acid 37, arginine 38, threonine 49 and glycine 40 and as such has been named the DRTG loop. The D37 residue is fully conserved, while the remaining residues are almost completely conserved, the few exceptions being *L.lactis* and phage Φ3T. The loop moves along with the C-terminus upon binding of substrate and cofactor helping to sequester solvent forming the closed ternary form of the enzyme. Arginine 38 has also been implicated (by virtue of its equivalent residue; R23; in *L.casei*) in coordinating the phosphate of the substrate. Threonine 39 and arginine 38 make hydrogen contacts to the COOH terminus of the protein. Little is known in detail about this loop region of TS.

9. Thymidylate synthase inhibitors

Because of its central position in the pathway of DNA biosynthesis, thymidylate synthase is an important target enzyme in cancer chemotherapy, anti-parasitic, anti-fungal and possibly anti-viral therapies. Analogues of either substrate or cofactor are potential inhibitors of this enzyme, and as such, a large number of dUMP and N⁵, N¹⁰-methylene-tetrahydrofolate analogues have been synthesised and evaluated as candidate inhibitors. Some of these inhibitors, for example, FdUMP and CB3717 (10-propargyl-5, 8-dideazafolic acid), have been of great value in elucidating certain aspects of the mechanism of action and structure of this enzyme.

9.1 Cofactor analogues

Folate analogues have several advantages over nucleoside analogues for chemotherapeutic use. These include a better specificity; in that the analogue pteroyl-hexaglutamate could inhibit bacteriophage T2 thymidylate synthase at a concentration 100-fold lower than that required to inhibit *E.coli* TS (Maley *et al* 1979); a decreased susceptibility to metabolic degradation and they appear to pose no significant risk of mutagenicity or carcinogenicity as they are not incorporated into RNA or DNA (Keyomarsi and Moran 1990). Moreover, the high levels of dUMP found in many tumours (that would reduce the effects of nucleotide analogues such as FdUMP) would potentiate binding of folate analogues (Danenbergs and Lockshin 1982, Myers *et al* 1974, Keyomarsi and Moran 1988, 1990, Pogolotti *et al* 1986). Conversely, the existence of low levels of N⁵, N¹⁰-methylene-tetrahydrofolate in many tumours would result in little competition for exogenous anti-folate analogues binding to TS (Houghton *et al* 1981, Evans *et al* 1981, Jackson *et al* 1983).

Several folate analogues have been shown to inhibit TS. The first were the 2-amino-4-hydroquinazolines (Bird *et al* 1970) and folylpolyglutamates (Kisliuk *et al* 1974). 10-propargyl-5, 8-dideazafolate (CB3717) is one of the most studied compounds to emerge from the investigation of folate analogue inhibitors of TS (Figure 14). CB3717 has a K_i value of 1x10⁻⁹ M for TS isolated from murine leukemia L1210 cells (Jones *et al* 1981). Phase I and II clinical trials have shown that CB3717 has demonstrable clinical activity against ovarian, breast and liver cancers, but the occurrence of renal toxicity in a sporadic, unpredictable and life-threatening manner, has precluded its further development as an anti-cancer drug (Harrap *et al* 1989). Inhibition of thymidylate synthase is not due to CB3717 itself, but potentiated by intracellular polyglutamation. However, CB3717 has been used as a parent compound to identify derivatives which retain the useful therapeutic properties but which are devoid of its major toxicity. Indeed several derivatives with such properties have been synthesised and include C²-desamino, C²-methyl and C²-methoxy derivatives (Harrap *et al* 1989).

Dihydrofolate can inhibit thymidylate synthase directly when it accumulates at high levels due to inhibition of dihydrofolate reductase (Bunni *et al* 1988, Seither *et al* 1991). Direct inhibition of thymidylate synthase due to build up of dihydrofolate is a major cause of growth inhibition, depletion of tetrahydrofolate also plays a role (Chu *et al* 1990). This has led to the suggestion that inhibition of *de novo* thymidylate synthase is a multifactorial process (Chu *et al* 1990).

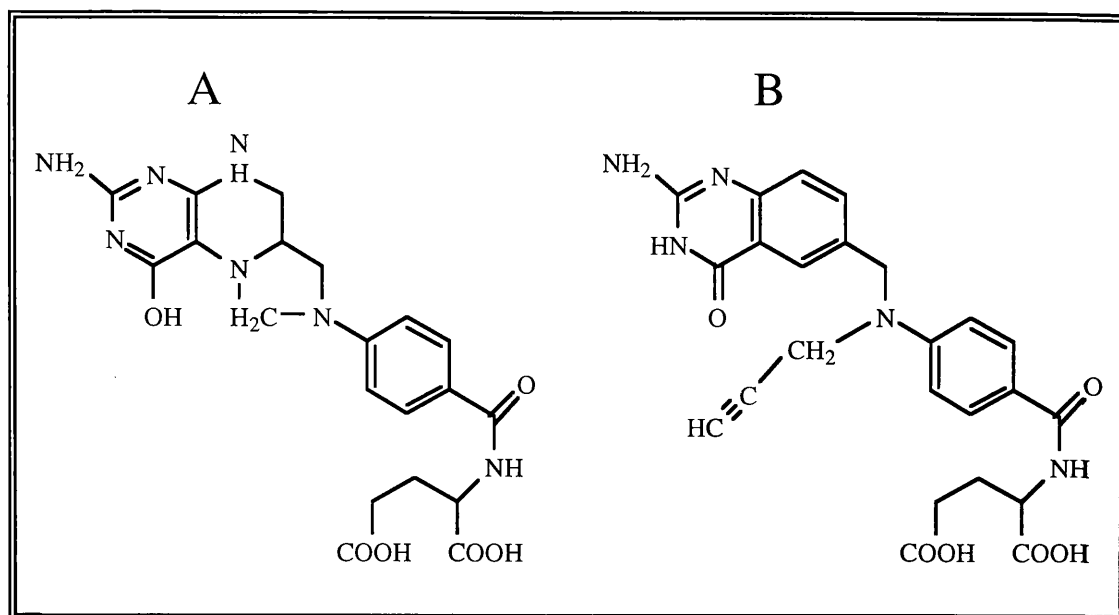


Figure 14. Methylene tetrahydrofolate (A), and 10-propargyl-5,8-dideazafolate (CB3717), a folate analogue inhibitor of thymidylate synthase (B).

9.2 Nucleoside analogues

As with the folate cofactor thymidylate synthase can also be inhibited by analogues of the substrate dUMP. Most of the nucleoside compounds studied are 5-substituted-2'-deoxyuridine analogues (Figure 15). For these analogues to exert their inhibitory effect *in vivo*, they must first be enzymatically activated by thymidine kinase.

The requirement for phosphorylation has been shown *in vivo* by the fact that mutations in the activation step lead to resistance to these analogues, and deoxyuridine itself is not a substrate for the purified enzyme (Reyes and Heidelberger 1965). 5-fluoro-2'-deoxyuridine (FUdR), 5-(trifluoro-methyl)-2'-deoxyuridine (CF₃UdR), trifluorothymidine (TFT), 5-nitro-2'-deoxyuridine (NO₂-UdR) and 5-ethynyl-2'-deoxyuridine (EYUdR) have consistently emerged as the most potent thymidylate synthase inhibitors in both *in vitro* and *in vivo* experiments with nucleoside analogues (Balzarini *et al* 1982, Lewis and Dunlap 1981). The mode of action of these compounds is now reasonably well understood. FdUMP, the active form of FUdR, forms a covalent ternary complex with thymidylate synthase in the presence of the cofactor N⁵, N¹⁰-methylene-tetrahydrofolate, which is similar to the catalytic intermediate (Lewis and Dunlap 1981). This complex is stable and terminates the reaction because the fluorine atom cannot be abstracted, as normally occurs with the C-5 hydrogen in the native reaction. This is presumably due to the strength of the

C⁵-F bond (Santi and Danenberg 1984). In contrast to FdUMP, CF₃-dUMP and NO₂-dUMP can inhibit thymidylate synthase in the absence of the folate cofactor, and this ability is thought to be the basis of their tight binding to, and inhibition of, TS (Danenberg *et al* 1974, Wayata *et al* 1980). EYUdR is a potent inhibitor of S-49 murine lymphoma cells and like FUdR, inhibits thymidylate synthase only in the presence of the folate cofactor (Barr *et al* 1981).

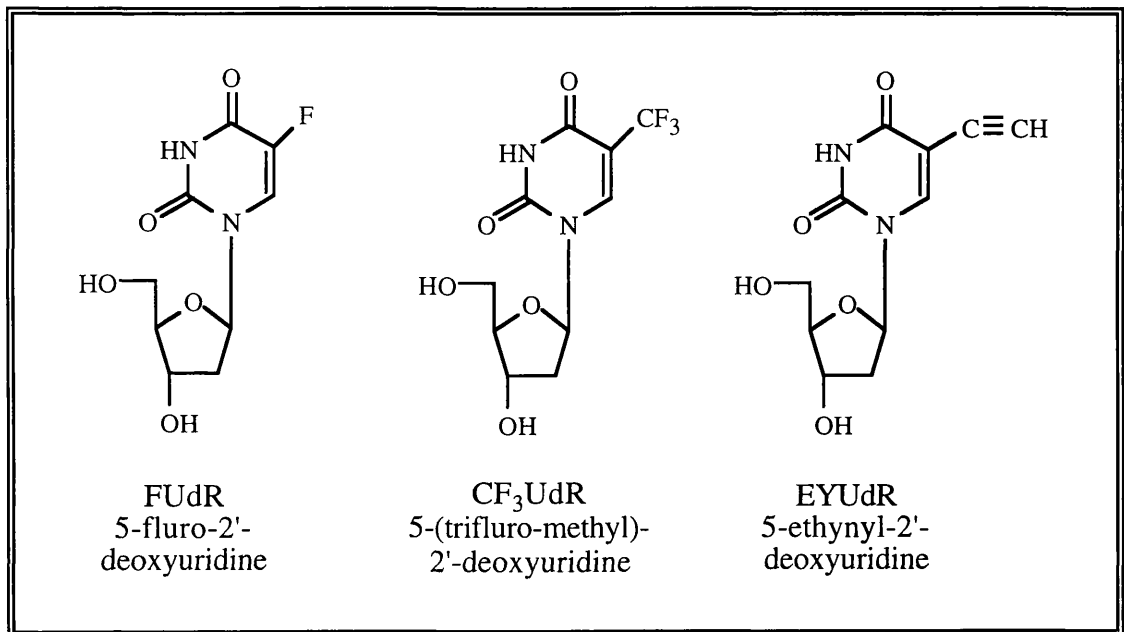


Figure 15. 5-substituted deoxyuridine analogue inhibitors of TS

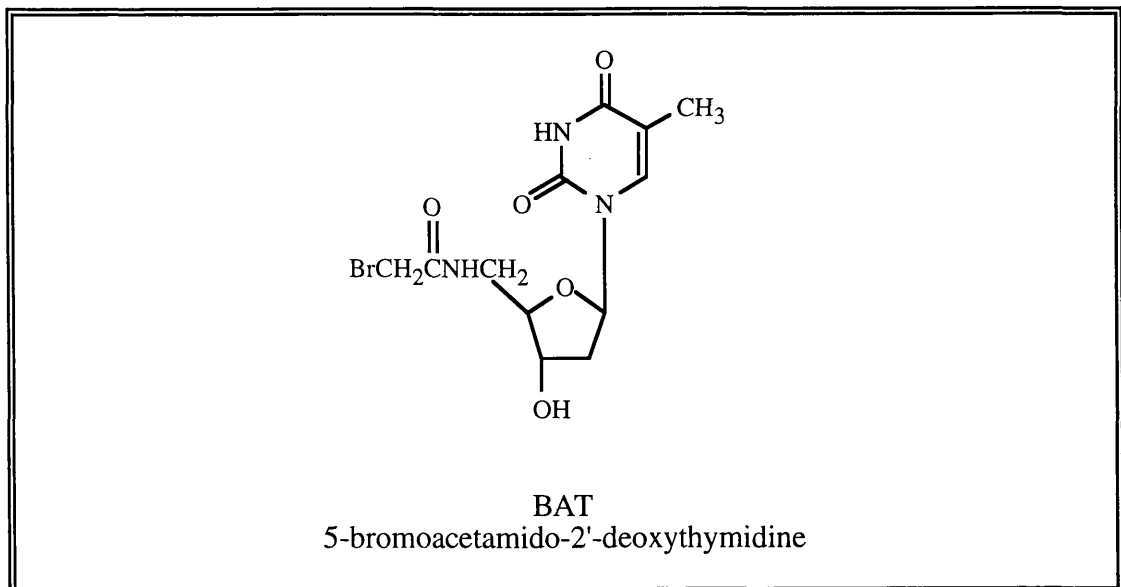


Figure 16. 5'-haloacetamido-2'-deoxyuridine analogue inhibitors of TS

A novel group of nucleoside analogues, the 5'-haloacetamido-2'-deoxythymidines (Figure 16), do not require phosphorylation or the cofactor to inhibit thymidylate synthase (Santi *et al* 1986). Three compounds 5'-bromo-, 5'-chloro-, 5'-iodoacetamido-2'-deoxythymidines (BAT, CAT and IAT respectively) inhibit TS from L1210 cells (Sani *et al* 1986). Kinetic studies with BAT suggest that it acted as a competitive inhibitor with dUMP

9.3 Bisubstrate analogues

In addition to folate and nucleoside only analogues a class of thymidylate synthase inhibitors are available which consist of a folate molecule covalently linked to a nucleoside analogue. These so-called bisubstrate analogues are designed to mimic the non-enzymic portion of the catalytic intermediate of the TS reaction, and have been shown to inhibit thymidylate synthase (Park *et al* 1979, Amarnath *et al* 1984). N⁵-dUMP-8-deazatetrahydrofolate (Figure 17) inhibits purified TS from murine leukemic L1210 cells as does N⁵-dUMP-N¹⁰-propargyl-deazatetrahydrofolate its analogue. Both these compounds inhibit TS in a competitive manner with respect to dUMP (Veda *et al* 1986). These workers have also shown that rather than entering into the active site of the enzyme to produce an inhibitory ternary complex, these compounds inhibit TS by blocking the nucleotide and folate binding sites.

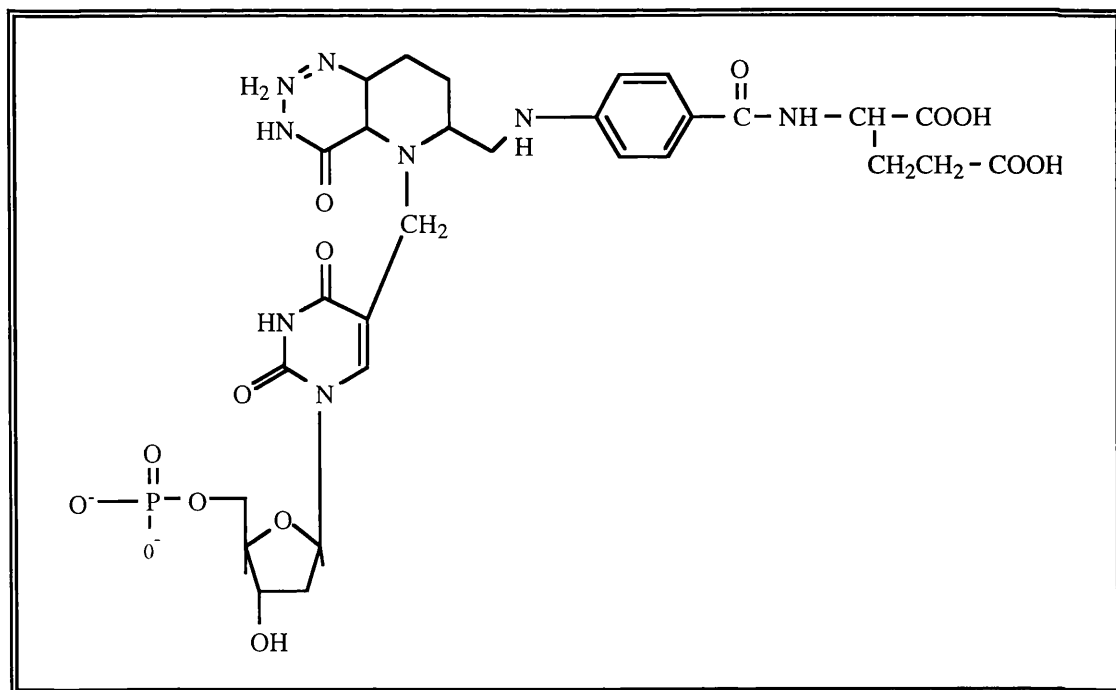


Figure 17. N⁵-dUMP-8-deazatetrahydrofolate, a bisubstrate inhibitor of TS

9.4 Oligopeptide inhibitors

Recently, oligopeptides have been shown to inhibit several enzymes and the mode of inhibition is discussed more fully in section 10.

9.5 Anti-sense oligonucleotides

An alternative approach to the inhibition of enzyme function other than the use of drugs is to specifically inhibit enzyme synthesis. The use of anti-sense oligodeoxynucleotides (oligos) to arrest translation of specific mRNA molecules (Hélène and Toulmé 1990) has recently been directed to the DHFR-TS mRNA of the parasite *Plasmodium falciparum*. A 49mer targetted to the conserved region of thymidylate synthase gave 50% inhibition at 6 μ M and 90% inhibition at 45 μ M (Sartorius and Franklin 1991a). Such a oligo is very specific to the DHFR-TS mRNA of *P. falciparum*. It also differs considerably from the human TS mRNA, sharing 59% (29 out of 49) nucleotide sequence identity (Ayusawa *et al* 1986). However, the fact that certain useful modifications such as the use of methylphosphonates or poly (L-lysine) conjugates cannot be used for long oligos, may delay their development as anti-malarial drugs (Sartorius and Franklin 1991b).

10. Disruption of protein-protein interactions

Many biological processes rely on the specific interactions between two macromolecules and could, in principle, be inhibited by interfering with that interaction. Recognition sites on proteins are specific, and there are various examples of peptides, derived from the recognition site on one of the ligands, which retain sufficient structure to compete with the whole protein for a binding site.

Essential interactions between viral protein subunits are potential targets for antiviral agents. Interactions involving virus proteins that can be specifically inhibited have been reviewed by Marsden (1992). Described below are some examples of disruption of viral protein interactions.

10.1 HSV ribonucleotide reductase

The best studied examples of protein complexes which can be disrupted by a peptide from one of the subunits are the ribonucleotide reductases from HSV and *Escherichia coli*. These enzymes catalyse the reduction of all four ribonucleotides to deoxyribonucleotides utilizing nucleoside diphosphates as substrates. The deoxyribonucleotides are phosphorylated and incorporated into DNA. Both the *E.coli* and HSV enzymes are heterodimers containing two molecules of a large subunit (R1) and two molecules of a small subunit (R2).

A nonapeptide (YAGAVVNDL) corresponding to the carboxy-terminus of HSV R2 specifically inhibits the viral enzyme and not the cellular ribonucleotide reductase (Dutia *et al* 1986, Cohen *et al* 1986). The peptide acts by competing for the R2 binding site on the R1 protein, and thus inhibits the normal association of the two subunits. The mammalian and *E.coli* enzymes can be similarly inhibited by their corresponding C-terminal peptides (Yang *et al* 1990, Cosentino *et al* 1991).

Although effective at inhibiting HSV ribonucleotide reductase enzyme activity *in vitro*, the YAGAVVNDL peptide does not inhibit virus growth in tissue culture, probably because it is too large to cross the cell membrane (Dutia *et al* 1986). However, it does provide a starting point from which therapeutically useful compounds could be developed.

10.2 F1 protein of Paramyxoviridae

Membrane fusion by *Paramyxoviridae* is an example of a virus-host cell interaction that can be disrupted by a peptide fragment of the virus component. *Paramyxoviridae* — the family to which measles and mumps viruses belong — have two surface glycoproteins: an attachment protein and a fusion (F) protein. The F protein is made fusogenic by proteolytic cleavage of an inactive precursor (F₀) to give two disulphide-linked polypeptides, F₁ and F₂. The newly generated N-terminus of F₁ is very hydrophobic and can insert into cell membranes (reviewd by Kingsbury 1990). Short peptides with amino acid sequences similar to the N-terminal region of F₁ specifically inhibit virus-induced cell fusion and virus infection (Nicolaides *et al* 1968, Miller *et al* 1968, Richardson *et al* 1980, Richardson and Choppin 1983). The cell membrane components of this interaction are as yet undetermined.

10.3 The α -TIF-Oct-1 transcription complex

The HSV-1 virion protein α -TIF (Vmw65, VP16) plays a central role in the assembly of a virus-specific transcription complex responsible for the expression of IE genes. The complex (Figure 18) is composed of α -TIF and at least two cellular proteins: the cellular transcription factor Oct-1 (OTF-1, NFIII, TRF) and the complex forming factor CCF (HCF, VCAF-1, C1)

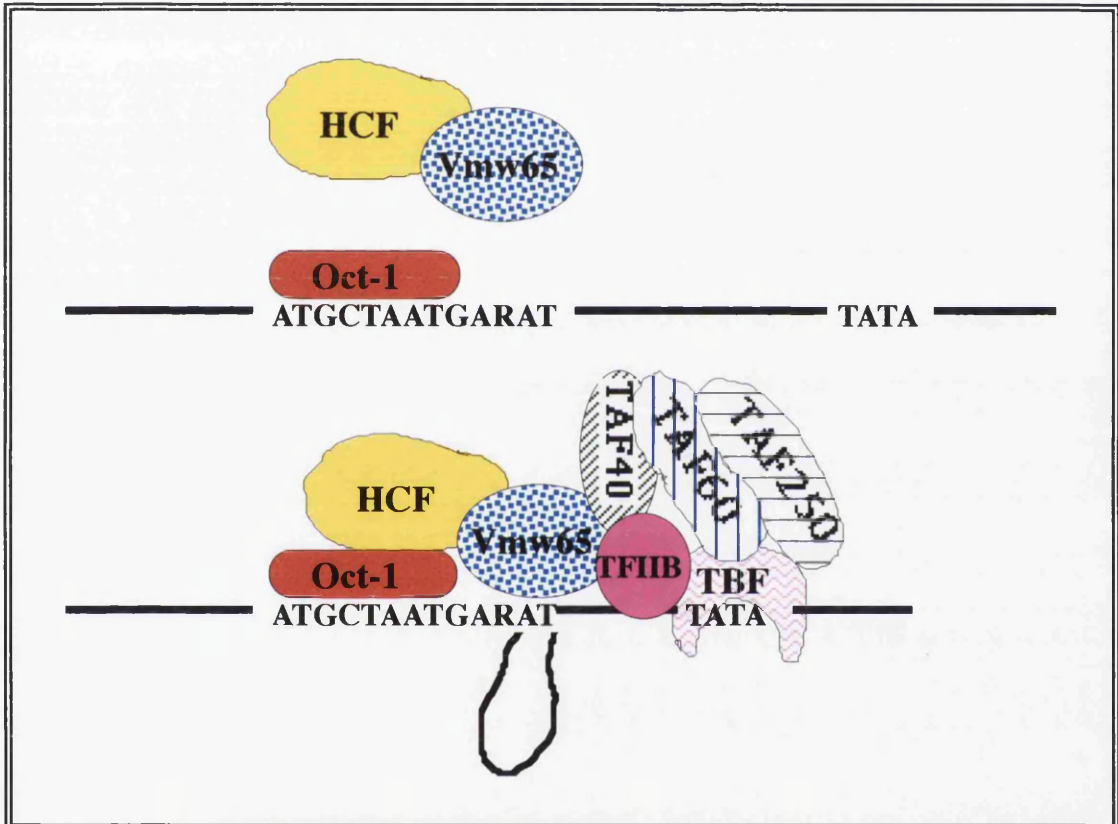


Figure 18 A model for the α -TIF-Oct-1 transcription complex formation and transcriptional activation

This schematic diagram depicts interactions that have been experimentally observed between the various protein components of the immediate early complex and the basal transcription machinery. Following release of the viral DNA from the capsid, the octamer sites of the IE promoters become occupied by Oct-1. Independently, Vmw65 complexes to HCF, and this heterocomplex then recognises Oct-1 in the context of the flanking GARAT signal to form the immediate-early complex. The Vmw65 acidic activation region is now positioned to activate transcription by promoting assembly of the transcription complex at the TATA box, through interactions with the basal transcription factors. Figure compiled and adapted from O'Hare 1993, and Goodrich *et al* 1993

Formation of the complex can be inhibited by peptides corresponding to a region of α -TIF involved in the interaction (Haigh *et al* 1990, Hayes and O'Hare 1993). The region of α -TIF encompassing amino acids residues 360-388 was found by mutational analysis, to be critical for complex assembly (Greaves and O'Hare 1990). A peptide corresponding to amino acids 360-373 was found to inhibit complex assembly without affecting the DNA-binding property of Oct-1 (Haigh *et al* 1990). The peptide, proposed to act by competing with α -TIF for binding to the cellular components of the complex, inhibited complex formation when added to nuclear extracts prior to the addition of α -TIF, but was not able to disrupt pre-formed complex (Haigh *et al* 1990). By using overlapping peptides, the inhibitory sequence has been narrowed down to eight amino acids, REHAYSRA, corresponding to residues 360-367 (Hayes and O'Hare 1993). It remains to be tested whether the presence of this peptide in a cell prevents the expression of IE genes upon HSV-1 infection.

10.4 Influenza virus haemagglutinin

Influenza A, an orthomyxovirus, contains two membrane glycoproteins, haemagglutinin (HA) and neuraminidase (N). HA consists of two disulphide-linked chains, HA₁ and HA₂. The protein is anchored in the cell membrane close to the C-terminus of HA₂, with a short (11 amino acid residue) region on the internal side of the membrane. Virion assembly is poorly characterised, but appears to involve interactions between viral matrix proteins, the nucleocapsid and the cytoplasmic domains of the viral glycoproteins at the plasma membrane.

A 10 amino acid peptide (NGSLQCRICI), corresponding to the cytoplasmic domain of HA₂, was shown to inhibit the release of infectious virions when added to the culture medium during infection (Collier *et al* 1991). The peptide acted specifically on influenza virus and had no other effect on two other enveloped RNA viruses, Sindbis and vesicular stomatitis virus. It was postulated to cross the plasma membrane and act by competing with the haemagglutinin for sites recognised by nucleocapsids or matrix protein.

10.5 VZV thymidylate synthase

Recently, oligopeptides have been shown to inhibit VZV thymidylate synthase activity. A linear pentadecapeptide corresponding to the amino acid sequence of β -strand i (LPPCHTLCQFYVANG) inhibits TS *in vitro* (IC₅₀ = 50 μ M). Amino and carboxy

terminal deletions of this peptide have defined the active core as CHTLCQFY, which corresponds precisely to those amino acids at the interface of the two monomers (HS Marsden and R Thompson, personal communication). These oligopeptides are thought to disrupt activity by preventing the correct formation of the dimer.

11. Aims of the project

The aim of this project was to investigate the role of structurally mobile regions of VZV thymidylate synthase using site-directed and region-directed mutagenesis. The regions chosen were the DRTG loop and the C-terminus. The loop, along with the C-terminus shows a dramatic movement upon ligand binding and is highly conserved within members of the TS family. The *L. lactis* enzyme displays significant variation in this region. Our aim was to substitute VZV residues in the DRTG loop for their *L. lactis* counterparts. It was anticipated that such mutants would be inactive and then they would allow selection for covariant residues that might restore enzyme activity.

The C-terminal region places a significant role in catalysis by closing the active site and sequestering ligands from solvent. Previous studies had suggested that the VZV enzyme might be unique among the TS family in terms of the interactions at the C-terminus (Harrison 1992, Harrison *et al* 1995). We aimed to extend these studies and to include the human TS with a view to probing the species specific differences.

A variety of folate analogues and a substrate-folate mimic were tested to examine the effect of amino acid substitutions on the enzyme's sensitivity to such inhibitors. The potential for peptide inhibition of the C-terminal interactions will be explored.

MATERIALS

1. Bacteria and bacteriophage strains

Strain	Genotype
BW313	<i>relA1, spoT1, dut-1, ung-1, thi-1</i> , Hfr KL16(PO45)
NM522	<i>supE, thi</i> , Δ (Lac-proAB), <i>DhssdI5</i> (r, m ⁻) [F', <i>proAB, lacI^q</i> ZDM15]
χ 2913	<i>thyA</i> Δ 752
BL21 (DE3)	F ⁻ , <i>ompT, hsdSB, gal, dcm</i> , (DE3)
TG1	<i>supE44, hsd5, thi1</i> , Δ (Lac-proAB)/ F' [<i>traD36, proAB⁺, lacI^q, lacZ</i> M15]

thyA derivatives were made of strains NM522 and BL21 (DE3)

Bacteriophage M13 R408 and M13 K07 were laboratory stocks.

2. Bacterial growth media

Liquid media (all per litre unless stated otherwise):

Luria-Bertani Medium (LB)

NaCl	10g
Bactopeptone	10g
Yeast extract	5g
Adjusted to pH 7.0 prior to sterilisation	

2xYT Medium (2YT)

Bactotryptone	16g
Yeast extract	10g
NaCl	5g
Adjusted to pH 7.0 prior to sterilisation	

All LB media (both liquid and solid) was supplemented with 100 μ g/ml thymidine unless otherwise stated.

Minimal Medium (M9) per 400ml

dH ₂ O	300ml
M9[x4] salts	100ml
15% casamino acids	20ml
20% glucose	4ml
1M mgCl ₂	500μl
0.8mg/ml thiamine	100μl

M9[x4] salts per 1000ml

Na ₂ HPO ₄ .7H ₂ O	24g
KH ₂ PO ₄	12g
NH ₄ Cl	4g
NaCl ₂	2g

Solid media:

LB

As above except supplemented with 15g Bacto-agar

M9

As above except 300ml dH₂O replaced by 300ml 2% Bacto-agar

3. Plasmids

pAD768 VZV TS containing BamHI/HindIII fragment cloned into pBS⁻
constructed by Harrison 1992

pAD876 Human TS containing SacI/HindIII fragment of pHTS-pUC19
cloned into pBS⁻
Plasmids constructed by Harrison 1992

4. Chemicals and reagents

Unless specifically stated below, all chemicals were purchased from BDH chemicals Ltd, Poole, Dorset, or from Sigma (London) Ltd.

Ammonium persulphate (APS) Bio-Rad Laboratories, Richmond,
California, USA.

N,N,N',N'-tetramethylethylenediamine
(TEMED) Bio-Rad Laboratories, Richmond,
California, USA.

Ampicillin Smithkline and Beecham.

Bactopeptone	Difco.
Bio-Rad protein assay reagent	Bio-Rad Laboratories, Richmond, California, USA.
Casamino acids	Difco.
Deoxynucleoside triphosphates	Pharmacia LKB, Uppsala, Sweden.
Ecoscint A	National Diagnostics, Manville, New Jersey, USA.
Kanamycin	Sigma.
Organic solvents	May and Baker.
Replicote™	BDH.
Wacker solution	Wacker Chemical company.

5. Sequencing solutions

Labelling mix	1.5 μ M dGTP, 1.5 μ M dTTP, 1.5 μ M dCTP
Termination mix:	G contained 8 μ M ddGTP, 80 μ M dGTP, 80 μ M dATP, 80 μ M dTTP, 80 μ M dCTP, 50mM NaCl
	A contained 8 μ M ddATP, 80 μ M dGTP, 80 μ M dATP, 80 μ M dTTP, 80 μ M dCTP, 50mM NaCl
	T contained 8 μ M ddTTP, 80 μ M dGTP, 80 μ M dATP, 80 μ M dTTP, 80 μ M dCTP, 50mM NaCl
	C contained 8 μ M ddCTP, 80 μ M dGTP, 80 μ M dATP, 80 μ M dTTP, 80 μ M dCTP, 50mM NaCl
Annealing buffer (5x™)	0.1M tris pH 8.0, 0.1M MgCl ₂

Stop solution	95% deionised formamide, 20mM EDTA pH 7.5, 0.05% Xylene cyanol FF, 0.05% bromophenol blue
Wacker solution (5ml)	25µl Wacker silane GF38, 150µl 10% acetic acid, 5ml ethanol

6. Radiochemicals

All radiochemicals were purchased from Amersham International Ltd, Maidstone, UK.

<u>Nucleotide</u>	<u>Activity</u>	<u>Concentration</u>	<u>Code</u>
[$\alpha^{35}\text{S}$]dATP	37TBq/mmol	1mCi/mmol	SJ1304
5-[^3H]dUMP	622GBq/mmol	16.8Ci/mmol	TRK287

7. Enzymes

Restriction enzymes	Boehringer Mannheim, Lewes, E. Sussex, UK. New England Biolabs, Bishops Stortford, UK.
T4 polynucleotide kinase	New England Biolabs, Bishops Stortford, UK.
T4 gene 32 protein	Pharmacia LKB, Uppsala, Sweden.
Klenow fragment of DNA polymerase I	Purified in house by Moira Watson from <i>E.coli</i> cells expressing a plasmid construct (Joyce & Grindley, 1983).
Sequenase™	United States Biochemicals.

8. Miscellaneous materials

Kodak X-Omat Film	Kodak Ltd, UK.
Whatman Paper	Whatman International Ltd, Maidstone, UK.
S-Sepharose	Pharmacia LKB, Uppsala, Sweden.
Hydroxylapatite	BDH

9. Buffers and solutions

5x Electrode buffer	4.5g tris base, 21.6g glycine, 1.5g SDS made to 300ml with dH ₂ O
Boiling mix	80mM Tris pH 6.8, 2% SDS, 0.1M DTT, 20% glycerol, Bromophenol blue
Coomasie blue stain	1.25g Coomasie blue, 228ml methanol, 45ml acetic acid, made to 500ml with dH ₂ O
Destain solution	50% dH ₂ O, 40% methanol, 10% acetic acid
Enzyme dilution buffer	130mM Tris pH 7.5, 0.125mM DTT, 0.15% BSA
Ligase buffer (BM)	66mM tris pH 7.5, 1mM DTT, 5mM MgCl ₂ , 1mM ATP
Ligase buffer (BRL)	50mM tris pH 7.6, 1mM DTT, 10mM MgCl ₂ , 1mM ATP, 5% (w/v) PEG 8000 (or 6000)
Loading buffer	15% ficoll, Bromophenol blue in 1xTBE

Lysozyme solution	0.4% egg white lysozyme, 50mM glucose, 25mM tris pH 8.0, 10mM EDTA
Ø/CHCl ₃	Phenol/chloroform 1:1 (v/v)
Oligo elution buffer	500mM ammonium acetate, 10mM MgCl ₂ , 1mM EDTA, 0.1% SDS
Oligo loading buffer	90% (v/v) deionised formamide in 1xTBE
Potassium acetate solution	60ml 5M potassium acetate, 11.5ml glacial acetic acid, 28.5ml dH ₂ O
Reaction buffer (debromination assay)	200mM N-methylmorpholine hydrochloride pH 7.4, 25mM MgCl ₂ , 1mM EDTA, 75mM β-mercaptoethanol
Sonication buffer	50mM tris pH 7.4, 10mM DTT, 0.1% (v/v) Triton X-100
Spectrophotometric assay buffer	50mM TES, 25mM MgCl ₂ , 6.5mM HCHO, 1mM EDTA, 75mM β-mercaptoethanol
STET buffer	8% sucrose, 50mM tris pH 8.0, 40mM EDTA, 1% Triton X-100
Stop solution (tritium release)	3 volumes 33% TCA, 1 volume 5mg/ml dUMP
TBE	90mM Tris, 90mM boric acid. 1mM EDTA
TE	10mM Tris-Cl pH 8.0, 1mM EDTA
TES buffer	50mM tris pH 7.4, 5mM EDTA, 50mM NaCl ₂
TM buffer	0.1M tris pH 8.0, 0.1M MgCl ₂

TSB	7.4ml LB, 2ml 50% PEG 4000, 100 μ l 1M MgSO ₄ /1M MgCl ₂ , 500 μ l DMSO
[2x] assay mix (tritium release assay)	128mM NaF, 260mM Tris-HCl pH 7.5, 64mM sucrose, 0.3% (w/v) BSA, 0.25mM DTT, 38mM HCHO, 2mM tetrahydrofolate

METHODS

1. Growth and maintenance of bacteria and bacteriophage

1.1 Overnight cultures

An isolated single colony was inoculated into 5ml LB, supplemented with the appropriate antibiotics and thymidine. The culture was incubated with vigorous shaking at 37°C overnight.

1.2 Bacterial glycerol stocks

A 15ml overnight culture of the appropriate clone was set up in a universal. Cells were harvested by centrifugation at 7000rpm for 5 minutes in a Beckman centrifuge. The cell pellet was resuspended in 5ml of 2% bactopectone. To this 5ml 80% glycerol and 40µl 25mg/ml thymidine were added, mixed and stored at -70°C.

1.3 Antibiotics

Antibiotics were used at the following final concentrations, unless otherwise stated. Ampicillin (Amp) 100µg/ml; Kanamycin (Km) 75µg/ml

1.4 Titration of helper phage R408

10ml of 2YT broth was inoculated with 1ml of an overnight culture of TG1 cells and incubated at 37°C with vigorous shaking for 1 hour. 3ml aliquots of molten top agar were equilibrated to 45°C in a waterbath. A series of 1 in 10 dilutions of the helper phage was made in T2 buffer. To the equilibrated top agar was added 200µl of NM522 Thy⁻ cells and 100µl of the diluted helper phage (in the range 10⁸ to 10¹²). The top agar was mixed together and immediately poured on to LB plates. After the top agar layer had solidified the plates were incubated overnight at 37°C. Helper phage plaques were counted the next day and the titre calculated.

1.5 Growth of helper phage

Four individual plaque plugs of helper phage were inoculated into 100ml 2YT broth containing exponentially growing *E.coli* NM522 Thy⁻ cells. This was incubated with vigorous shaking at 37°C overnight. The overnight culture was cleared of bacteria by centrifugation at 9K at 4°C for 10 minutes. The supernatant was decanted to a fresh tube and recleared by a further centrifugation step. This supernatant was heat-inactivated at 55°C for 20 minutes, allowed to cool to room temperature and stored at 4°C. The titre of the helper phage was determined as described above.

2. Bacterial manipulation

2.1 Transformation (Chung and Miller, 1988)

20ml of LB was inoculated with 1ml of an overnight of the appropriate bacterial strain and incubated at 37°C with vigorous shaking until A₆₀₀ was ~ 0.5. Cells were pelleted by centrifugation at 7K/10 minutes at 4°C and resuspended in 2ml transformation storage buffer (TSB). The resuspended cells were made competent by incubation on ice for 15 minutes.

10 to 100ng of DNA was added to 100µl competent cells and incubated on ice for 30 minutes. 900µl of LB (supplemented with thymidine) was added to the cells and incubated at 37°C for 1 to 1½ hours. 100µl was spread on to LB plates supplemented with ampicillin and thymidine and incubated at 37°C overnight. Both a positive (~10ng plasmid DNA) and a negative (no DNA) control was always included in a transformation experiment.

3. DNA isolation

3.1 Mini-prep plasmid DNA preparation (Hattori *et al*, 1986)

A fresh single colony (or 50µl of an overnight culture) harbouring the desired plasmid was picked and inoculated into 5ml LB supplemented with the appropriate antibiotics and thymidine. The culture was incubated at 37°C with vigorous shaking overnight. Cells were pelleted by centrifugation of 1½ ml in a microfuge for 2 minutes at full speed. The cell pellet was resuspended and lysed with 100µl

lysozyme solution at room temperature for 5 minutes. 200µl 0.2M NaOH/1%SDS was added and incubated on ice for 5 minutes. 150µl of potassium acetate solution was added, mixed gently and incubated for a further 5 minutes on ice. The cell debris was removed by centrifugation at 12K for 10 minutes (microfuge) and the supernatant removed to a fresh tube. The supernatant was CHCl_3 extracted and the aqueous layer removed. The DNA was precipitated with 2 volumes ethanol by incubation at room temperature for 15-30 minutes followed by centrifugation at 12K for 5 minutes. The DNA pellet was washed with 70% ethanol, dried under vacuum and resuspended in an appropriate volume of TE buffer.

3.2 STET lysis plasmid DNA preparation

1½ ml of an overnight culture was centrifuged (12K/40 seconds) to pellet the cells. The cell pellet was resuspended in 200µl STET buffer and 20µl lysozyme (25mg/ml) added. The solution was boiled for 2 minutes and centrifuged (12K/10 minutes). The supernatant was removed and to it added $\frac{1}{10}$ volume 3M sodium acetate and 2 volumes isopropanol. The DNA was precipitated by centrifugation at 12K for 10 minutes, the pellet dried under vacuum and resuspended in 20µl dH₂O.

3.3 Qiagen™ plasmid preparation

100ml of LB supplemented with ampicillin was inoculated with 10ml of an overnight culture of the appropriate plasmid containing *E.coli* strain and incubated overnight at 37°C with vigorous shaking.

The plasmid was isolated from the bacteria as described in the MIDI protocol of the Qiagen™ handbook.

3.4 Plasmid DNA sequencing preparation

DNA was extracted from cells as described in section 3.1 with the pellet being resuspended in a final volume of 50µl TE buffer. RNase was added to a final concentration of 10µg/ml and incubated at 37°C for 30 minutes. The DNA was precipitated by incubation on ice for 1 hour with 30µl 20% PEG 6000/2.5M NaCl followed by centrifugation at 12K for 5 minutes. The DNA pellet was washed with 70% ethanol, dried under vacuum and resuspended in 18µl TE buffer. The DNA was denatured by the addition of 2µl 2M NaOH and incubation for 5 minutes at room

temperature. 8µl 5M ammonium acetate, 100µl ethanol was added and incubated in a dry ice bath for 5 minutes followed by centrifugation. The pellet was washed with 70% ethanol, dried under vacuum and resuspended in 10-20µl dH₂O. 5µl was used directly for sequencing.

3.5 ssDNA sequencing preparation

A single colony was inoculated into 5ml 2YT broth containing ampicillin (75µg/ml), thymidine (100µg/ml) and M13 K07 helper phage (2×10^8 pfu/ml) and incubated at 37°C with vigorous shaking for 2 hours. Kanamycin was added to a final concentration of 70µg/ml and the culture incubated at 37°C with vigorous shaking overnight.

3x 1½ ml of the culture was centrifuged at 12K for 10 minutes in a microfuge to pellet the cells. 1ml of the supernatant was transferred to a fresh eppendorf tube and 300µl 2.5M NaCl/20% PEG added, vortexed and incubated on ice for 15 minutes. The phage was pelleted by centrifugation in a microfuge (12K for 5 minutes) and the supernatant discarded. The phage pelleted was resuspended in 400µl 0.3M sodium acetate and an equal volume of Ø/CHCl₃ added, vortexed vigorously and microfuged for 5 minutes. The top aqueous layer was transferred to a fresh eppendorf tube and 1ml ethanol added, vortexed and incubated at room temperature for 30 minutes. The ssDNA was pelleted by centrifugation at 12K for 5 minutes (microfuge) and the supernatant carefully discarded. The 3 ssDNA pellets were dried under vacuum (5 minutes in a speedivac), resuspended in 5-25µl TE buffer and stored at -20°C until needed.

3.6 Uracil-ssDNA preparation (Künkel, 1985; Künkel *et al.*, 1987)

10ml of 2YT broth supplemented with the appropriate antibiotics and uridine (100µg/ml) was inoculated with 50µl glycerol stock of *E.coli* strain BW313 Dut⁻Ung⁻ harbouring the required plasmid. The culture was incubated at 37°C with vigorous shaking overnight. The overnight culture was added to 200ml of 2YT supplemented with the appropriate antibiotics and uridine (100µg/ml) in a 2L baffled flask and incubated at 37°C with vigorous shaking until A₆₀₀ was 0.5. At this point M13 R408 helper phage was added to a final pfu/ml of 5×10^9 and the culture incubated at 37°C with vigorous shaking for a further 8 hours. The cells were pelleted by centrifugation at 7K for 20 minutes using a Sorvall GS3 rotor and the

supernatant kept. The supernatant was centrifuged one final time. To the supernatant $\frac{1}{4}$ volume of 3.75M ammonium acetate/20% PEG 6000 was added, mixed, split in two and incubated on ice for $\frac{1}{2}$ hour. Phage was precipitated by centrifugation at 9K for 30 minutes using a Sorvall GS3 rotor. The phage pellet was allowed to air dry for ten minutes and then resuspended in TE buffer (400 μ l per pellet). The protein was removed by chloroform extracting twice and CHCl_3 extracting 3 to 6 times or until the interface became clear. The aqueous phase was chloroform extracted one final time and to it added 0.36 volumes 7.5M ammonium acetate and 2.5 volumes ethanol followed by incubation on ice for 20 minutes. The ssDNA was pelleted by centrifugation at 12K for 20 minutes, washed with 70% ethanol and dried under vacuum. The lyophilised pellet was resuspended in 50 μ l dH₂O. This ssDNA template was checked to ensure it was enriched with uracil by transforming it into a Dut^+ Ung^+ host and a Dut^- Ung^- host (see section 2.1). Uracil-enriched DNA gave no colonies in the Dut^+ Ung^+ host. The concentration of ssDNA produced was estimated spectrophotometrically*.

* 1 A_{260} unit \equiv 40 μ g/ml ssDNA

4. DNA manipulations

4.1 Restriction enzyme digests

Restriction enzyme digests were usually carried out in 10 to 50 μ l reaction volumes. Restriction enzyme buffers are available commercially at 10x concentration and were diluted accordingly. Enzymes were added at 1 to 10 units (U) per μ g DNA and incubations performed at 37°C for 3 hours or overnight.

When mini or STET prep DNA was digested, RNase was added to a final concentration of 100mg/ml for the last hour of the incubation. Digested DNA to be used in cloning experiments was always CHCl_3 extracted (to remove the restriction enzymes) and ethanol precipitated prior to use.

4.2 Isolation of DNA from agarose gels

DNA was isolated from agarose using a Pharmacia Sephaglass™ kit as per the manufacturers instructions

4.3 DNA ligations

Ligations were usually performed in a total volume of 10 μ l. 100ng of vector and 17ng insert DNA were mixed with 2 μ l 5x ligation buffer (BRL) or 1 μ l 10x LB (Boehringer-Mannheim), 1 unit T4 DNA ligase and the volume made up to 10 μ l with dH₂O. The ligation mix was incubated at 16°C overnight. 1-5 μ l of the ligated DNA was used for transformation of *E.coli*.

5. Oligonucleotides

5.1 Synthesis and purification

Oligonucleotides were synthesised on a Biosearch 8600 DNA synthesiser by Dr John McLaughlin or on a Cruachem PS250 DNA synthesiser by myself.

Oligonucleotides were provided still attached to the column upon which they were synthesised. Oligonucleotides were removed from the column by flushing the column with one column volume (~0.25ml) of concentrated ammonia solution, and incubating at room temperature for 20 minutes. This process was repeated until 1.5ml of concentrated ammonia had been flushed through the column. Oligonucleotides from the Biosearch machine were already provided in 1ml of ammonia solution.

The oligonucleotide containing ammonia solution was heated at 55°C for 5 hours and subsequently lyophilised overnight. The lyophilised pellet was resuspended in 50 μ l dH₂O and this crude preparation stored at -20°C until needed.

10 to 25 μ l of the crude preparation was mixed with an equal volume of loading buffer without any dyes (1xTBE, 90% deionised formamide) and boiled for 2 minutes. The sample was loaded on to a 15% polyacrylamide gel along with 5 to 10 μ l formamide dyes (in a separate well) as a marker track. Electrophoresis was performed at 250V in 1xTBE buffer. For oligonucleotides of length 15 to 30 bases the bromophenol blue band was allowed to migrate approximately 7cm down the gel (~1 hour). For oligonucleotides 30 to 60 bases in length the bromophenol blue band was allowed to migrate to approximately the end of the gel (~2-3 hours).

To isolate the oligonucleotide the gel was removed from the glass plates and wrapped in cling film. The DNA was visualised using the shadow casting technique, which involved illumination of the gel whilst on a thin layer chromatography (TLC) plate using a short-wave UV lamp. The DNA appears as a dark band against a uniform green fluorescent background. The largest moving band at the top of the gel was excised and cut into several smaller pieces prior to being eluted in 1/2ml oligo elution buffer by overnight incubation at 37°C. The eluted oligonucleotide was centrifuged at full speed in a microfuge for 5 minutes to remove any acrylamide. The supernatant was carefully removed to another eppendorf tube and ethanol precipitated. The DNA pellet was resuspended in 50µl of dH₂O, its concentration determined spectrophotometrically* and stored at -20°C prior to use.

* 1 A₂₆₀ unit ≡ 20µg/ml oligonucleotide

5.2 Spiked oligonucleotides

Spiked oligonucleotides were synthesised on the Biosearch 8600 DNA synthesiser using phosphoramidite mixes containing 96% of the normal nucleotide and 1.33% each of the other three nucleotides.

5.3 Oligonucleotide sequences

A complete list and sequences of all the oligonucleotides used in this project are shown below.

VZV TS Site-directed mutagenesis oligonucleotides

Sequence	Mutation
CCT-GTT-CCA-TCG-CGT	R38G
CGT-TCC-GAT-TCC-TTG-TCG-ATC-GCG-TTT	T39Q
TAA-CGT-TCC-GAT-CAT-TGT-TCG-ATC-GCG	G40M
AGA-TAA-CGT-TCC-GGC-GAT-TCC-TGT-TCG	41A42

AGA-TAA-CGT-TCC-GGC-TCC-TGT-TCG	I41A
AAT-CCA-TTA-AGC-AAG-AGC-CAT	A302
AAT-CCA-TTA-TCC-AAG-AGC-CAT	G302

Human TS Site-directed mutagenesis oligonucleotides

Sequence	Mutation
G-GAA-ATG-GCT-TAA-TAG-GGT-GC	V313Δ

The numbering system refers to the VZV (or Human) TS gene, with nucleotide +1 referring to the A in the ATG codon specifying the first methionine residue.

Spiked oligonucleotides

Number	Sequence targeted	Size
RO1	CAA-ATT-GTA-TCG-AGC-TTG-CAT-TCC-AAA-TAA-AGA-TAA-CGT-TCC-GAT-TCC-TGT-TCG-ATC	57mer
RO5	ATT-CCA-AGA-CGA-TAT-AAT-CAT-TCG-TCG-GCT-TTC-TGG-GTT-TGT-TTT-AAT	48mer
RO7	GTT-TGC-AAC-GTA-AAA-CTG-ACA-TAA-CGT-GTC-ACA-TGG-AGG-TAG-TAC	45mer
RO8	CAT-ATC-CCC-CGA-TCT-CTG-GTA-TAC-TTG-GCA-GGA-TAA-TTC-ACC-GTT-TGC	48mer

RO10 TAA-ATC-TCC-GGT-TTT-AAG-TCC-TGT-AAC- 54mer
 ATG-CGC-TAC-TAT-GTA-GGT-AAG-AAG-TGC

5.4 Sequencing oligonucleotides

Sequence	Number
GTC-TGT-GTA-TAT-CAT	59
CCA-TTG-TAT-GAA-TTA	60
TTT-AAT-TGT-ATC-TAT	61
CCA-CGA-CGG-CCC-TCC	62
GGA-CCA-CTT-GGC-CTG	HP1
GTA-CCT-GGG-GCA-GAT	HP2
AAG-AGC-TGT-CTT-CCA	HP3
GAC-ACC-ATC-AAA-ACC	HP4
GCT-CAC-GTA-CAT-GAT	HP5
CTC-AGG-ATT-CTT-CGA	HP6
AAG-GGT-ACA-ATC-CGC	HP7
TTC-ATC-TCT-CAG-GCT	HP8
GCC-GCA-GCG-GAG-GAT	HP9
CTG-CTG-ACA-ACC-AAA	HP10

6. Mutagenesis

6.1 Oligonucleotide site directed mutagenesis

Oligonucleotides were used to introduce specific mutations at defined sites within a TS gene. The strand selection scheme of Kunkel was employed using a uracil-enriched template strand which is degraded in a Ung⁺ host strain.

500pmole oligonucleotide was phosphorylated in 20 μ l ligation buffer containing 10 units of T4 polynucleotide kinase at 37°C for 30 minutes. The T4 kinase was inactivated by incubation at 65°C for 15 minutes. The phosphorylated oligonucleotide was diluted with dH₂O to a final concentration of 5pmole/ μ l. 1 μ l

phosphorylated oligonucleotide was annealed to 0.1pmole U-ssDNA in 10µl TM buffer at 37°C for 30 minutes. The annealed oligo was filled in by the addition of 1µl 5mM dNTP (a 5mM solution of all four dNTP's), 5 units Klenow fragment of DNA polymerase I, 1 unit of T4 polynucleotide kinase, 2.0µg gene 32 protein in 20µl ligation buffer.

6.2 Region directed mutagenesis

Spiked oligonucleotides were designed to have on average two base changes per oligonucleotide. They were used to introduce random mutations to a targeted region of the TS gene. As for site-directed mutagenesis the strand selection scheme of Kunkel was employed using a uracil-enriched template strand which is degraded in a Ung⁺ host strain.

Mutagenesis was performed as outlined for site-directed mutagenesis (see section 6.1).

6.3 Temperature sensitive mutations

Spiked oligonucleotides were used to probe for residues involved in protein stability. Mutagenesis was performed as outlined for site-directed mutagenesis. Colonies were patched on to minimal media (M9) with or without thymidine and grown at 30°C, 37°C and 42°C.

7. Mutant screening

7.1 Restriction digests

Potential mutations were screened by restriction digest analysis prior to sequencing to remove those clones that did not give the correct restriction pattern and thus did not contain the plasmid of interest.

Restriction analysis was performed as described in section 4.1.

7.2 Growth complementation assays

1 to 5 μ l mutagenised DNA was used to transform a suitable *E.coli thyA* strain. Transformants were picked, using sterile tooth picks, and patched onto M9 plates and M9 plates supplemented with thymine 50 μ g/ml and incubated overnight. Appropriate clones were used to set up overnight cultures and mini-prep (or STET prep) DNA prepared for restriction digest analysis. Both Thy+ and Thy- clones with the correct restriction pattern were sequenced. In all cases the entire TS coding region was sequenced for each clone.

7.3 DNA sequencing

All DNA sequencing was performed in a 96 well micro-titre plate using a Sequenase™ kit. 3 μ l (~10-30ng) sequencing primer, was annealed to 0.1-1.0 μ g of DNA (ssDNA or dsDNA) in 10 μ l 1x reaction buffer by incubating at 37°C for 30 minutes in an eppendorf tube. The annealed reaction mix was transferred to a micro-titre plate and 1 μ l DTT, 2 μ l label mix (previously diluted 1 in 3), 1-2 μ l [α^{35} S]dATP, and 2 μ l Sequenase enzyme (previously diluted 1 in 8) added. The plate was spun in a centrifuge 1K for 30 seconds to mix the reagents and incubated at room temperature for 1 minute. 3.5 μ l of this mix was transferred to a separate well containing 2.5 μ l of ddGTP. This was repeated for the other three dideoxy termination mixes (ddATP, ddTTP, ddCTP) and the plate sealed with a plate sealer (Flow Laboratories Ltd or Corning) and incubated for at 37°C 15 minutes. To the sequencing reaction 2 μ l of stop solution was added and the plate boiled for 2 minutes prior to loading 3 μ l on to a polyacrylamide gel.

Sequencing reactions were resolved on a 4% acrylamide, 7.7M urea, 1/2x TBE gel. Prior to use both plates were washed in 100% ethanol. If the gel was to be oven dried then the front plate was coated in Replicote™ then washed once with 100% ethanol. The back plate was coated with ~5ml Wacker solution and then washed 5 times with 100% ethanol prior to the gel being poured. If the gel was to be transferred to 3M paper then both plates were coated with Replicote™ and washed once with 100% ethanol before the plate was poured. Electrophoresis was performed at 40W in 1xTBE. For normal runs the bromophenol blue was used as a marker to terminate electrophoresis. For longer runs the gel was run for a further 1-2 hours.

8. Mutant characterisation

8.1 Crude TS extracts

300ml LB supplemented with the appropriate antibiotics and thymidine was inoculated with 10ml of an overnight culture of the appropriate clone and incubated at 37°C with vigorous shaking until A600 ~ 0.3. A small volume of culture was removed and kept on ice for a phenotype check (see later). The cells were pelleted by centrifugation at 7K/10 minutes (Sorvall GS3 rotor) at 4°C. The pellets were drained resuspended in 10ml TES buffer, and vortexed to disrupt any lumps. The cells were pelleted once more (MSE bench top centrifuge) by centrifugation at 3K for 10 minutes at 4°C. The pellet was resuspended in 2 volumes of sonication buffer and sonicated (Branson Sonifier with the microprobe setting on 3). Sonication was performed in 10 second bursts three times with 30 seconds cooling between each burst. The sonicated extract was transferred to an eppendorf tube(s) and spun at 10K for 10 minutes in a pre-cooled (4°C) Beckman SS34 rotor. The supernatant was removed to fresh tubes and its protein concentration determined prior to being snap frozen in a dry ice/ethanol bath. and stored at -70°C.

To check the phenotype of the extract a drained loop full of the culture was streaked to single colonies on a LB agar plate (supplemented with thymidine only) and incubated at 37°C overnight. Single colonies were then patched on to M9, M9 plus thymidine and LB (supplemented with ampicillin and thymidine) agar plates and incubated at 37°C overnight.

8.2 Protein concentration determination

A modified version of the Bradford assay was used to determine the protein concentration of crude and purified protein extracts. Assays were performed in micro-titre plates using an Anthos HTII plate reader at wavelength 620nm.

To a series of wells 400µl of Bradford reagent was added and to these 10µl BSA protein standard was mixed. 1-10µl of the test protein was added to a well and mixed prior to reading the plate. The plate reader read the plate and determined the protein concentration of the test protein from the standard curve it plotted.

8.3 Tritium release assay

This assay follows the release of radioactivity from 5-[³H] dUMP to the solvent. Unreacted substrate is absorbed to charcoal, removed by centrifugation and the radioactivity in the supernatant determined by scintillation counting.

TS extract was mixed with 20µl [2x] assay mix, 0.4µCi 5-[³H] dUMP and dH₂O in a total volume of 40µl and incubated at 30°C for 15 minutes. The reaction was terminated by addition of stop solution and 180µl 2% charcoal suspension. The sample was vortexed and centrifuged for 2 minutes following which 500µl supernatant was removed and added to 5ml Ecoscint A prior to liquid scintillation counting in a Beckman LS5000CE scintillation counter. A total counts control was included using 5µl sonication buffer instead of extract and adding 940µl dH₂O instead of charcoal suspension. A background control was also included by replacing extract with 5µl sonication buffer and this value subtracted from all experimental values. Assays were performed in duplicate on two or more independent extracts for each clone. The amount of extract used was adjusted so that less than 30-60% of the total counts are released. This ensures that assays are in the linear region of the reaction curve.

The amount of dTMP generated is directly equivalent to the amount of [³H] released during the assay. The amount of [5-³H] dUMP added to the reaction in pmol can be calculated from its specific activity. The total counts represents the equivalent amount of product (dTMP)

$$\text{dTMP produced} = \frac{\text{Sample CPM}}{\text{Total CPM}} \times \text{pmol [5-}^3\text{H] dUMP added}$$

From protein concentration, the specific activity of TS in the crude extracts can be expressed in terms of pmol dTMP produced per µg protein per minute.

8.4 Debromination assay

This assay follows the reduction in absorbance at 285nm caused by the release of bromine from 5-BrdUMP (Garret *et al* 1979). It represents the first stage of the TS

reaction and as such does not require the presence of folate cofactor. Reactions were performed in Hellma quartz microcells containing 250 μ l reaction buffer (2x strength), 5 μ l 4mM 5-BrdUMP (40 μ M final concentration), 1-5 μ l of crude extract and dH₂O to final volume of 500 μ l. Absorbance change was monitored using a Cecil CE595 double beam spectrophotometer (zeroed on the cuvettes before adding extract) and displayed on a chart recorder. Reactions were run for 15 minutes to 20 minutes at room temperature. An extract of wild-type VZV TS was included in each batch of assays and assays were performed in duplicate on two or more independent extracts for each clone. To compare extracts initial rates were calculated and expressed as mOD/min/ μ g protein.

9. Peptide inhibition of TS

Peptides that potentially inhibited VZV TS were tested essentially the same as for the tritium release assay (see section 8.3).

Peptides were preincubated with the enzyme, in a reaction mix that did not contain folate or 5-[³H]dUMP, for 15 minutes prior to their addition. The tritium release assay was then performed as section 8.3.

Peptides were tested in duplicate in a range of concentrations ranging from 0.2mM to 2.0mM and with varying preincubation and assay temperatures (30° or 42°C).

Peptides were made and purified by Gillian McVey by continuous-flow Fmoc chemistry using a Novabiochem peptide synthesiser. Purification was by reverse phase chromatography on a Beckman System Gold HPLC using a Dynamax 300Å C8 preparative column. Lyophilised pellets were stored at -20°C.

10. Purification of mutant proteins

10.1 T7 expression vector

To enable large quantities of protein to be purified from a bacterial culture system the TS gene was cloned in to the T7 vector pET8c. This vector when transformed in to the host *E.coli* strain BL21 (DE3) is inducible by IPTG allowing high levels of protein to be expressed.

Prior to transformation into BL21 (DE3) cells the TS containing pET8c vector was first transformed into *E.coli* strain NM522 Thy⁻, and a STET lysis DNA preparation

made for restriction digest analysis. This DNA was then transformed into BL21 (DE3) cells.

10.2 Growth and extraction of TS

A fresh single colony was picked into 50ml LB supplemented with the appropriate antibiotics and thymidine and incubated at 37°C with vigorous shaking overnight. 5ml of the overnight culture was used to inoculate 750ml LB supplemented with the appropriate antibiotics and thymidine in a 2L baffled flask. A total of 6L (8 flasks) was inoculated and incubated at 37°C with vigorous shaking until the A₆₃₀~ 0.5. At this point 1ml was transferred to a universal and incubated at 37°C as before. To the flasks IPTG was added to a final concentration of 0.2mM and incubation at 37°C continued for a further 3-5 hours. 1ml of the induced culture was removed to a universal and along with the previous 1ml sample processed (as described in section 10.3) to check for protein induction.

The induced culture was centrifuged at 9K for 10 minutes (4°C) and the resulting pellets were resuspended in a total of 10ml TES buffer. A further 10ml of TES buffer was added and the suspension vortexed to disrupt any lumps. The cells were once again pelleted by centrifugation at 9K for 5 minutes (4°C) and the supernatant discarded. The bacterial pellet was resuspended in 10ml 50mM potassium phosphate buffer pH 7.0 and vortexed vigorously prior to sonication. Sonication was performed (using a Branson sonifier) with the microprobe on setting 5 and entailed five 15 second bursts with 30 seconds cooling between each burst. The sonicated sample was centrifuged at 18K for 30 minutes (4°C) and the supernatant removed. The remaining cells were resuspended in a further 5ml 50mM potassium phosphate buffer pH 7.0 and re-sonicated. The two supernatants were combined and stored at 4°C prior to purification.

10.3 Protein mini-gel electrophoresis

SDS polyacrylamide gel electrophoresis was performed using a Bio-Rad MINI-PROTEAN™ II kit. Gels were cast according to the manufacturers instructions and consisted of a separating gel (12% acrylamide, 0.37M tris pH 8.8) and a stacking gel (4% acrylamide, 0.125M tris pH 6.8).

Bacterial cultures to be tested were initially pelleted by centrifugation of 1ml of the appropriate culture in a microfuge (full speed) for 1 minute. The supernatant was removed and the pellet resuspended in 50µl dH₂O and then 50µl of boiling mix

added. The sample was boiled for 2 minutes prior to loading on the gel. Purified protein samples to be tested were mixed with an equal volume of boiling mix and boiled as before. Electrophoresis was performed at 450V in 1x electrode buffer for 45 minutes or until the bromophenol blue dye front had reached the bottom of the gel. The acrylamide gel was removed from the casting plates and the top stacking layer carefully discarded. The gel was stained using a coomassie blue stain for 20 minutes. The gel was then destained for 20 minutes, the destain discarded and the process repeated.

Destained gels were air dried overnight between a sheet of porous polythene.

10.4 Hydroxylapatite chromatography

All chromatographic procedures were performed at 4°C. A 30ml column was poured by resuspending ~12g hydroxylapatite in 6x column volume of 50mM potassium phosphate buffer pH 7.0 and mixing by gentle swirling. The hydroxylapatite was allowed to settle and the buffer decanted, fresh buffer was added and the process repeated. The washed hydroxylapatite was finally resuspended in an equal volume of 50mM potassium phosphate buffer pH 7.0 and poured in to the column. Two bed volumes of 50mM potassium phosphate buffer pH 7.0 were pumped through the column at 1ml/minute to wash and equilibrate the column.

Samples were kept from all stages of the chromatography (loading, washing and eluting) for analysis on a protein mini-gel (see section 10.3). The supernatant usually appeared viscous after sonication and was thus diluted two times with 50mM potassium phosphate buffer pH 7.0 prior to loading on to the column at 1/2 ml/minute, and the flow through collected. The unbound protein was removed by washing (1ml/minute) the column with increasing phosphate concentrations. The first was 2 volumes 50mM potassium phosphate buffer pH 7.0 and the second 2 volumes 100mM potassium phosphate buffer pH 7.0. The TS protein was eluted from the hydroxylapatite by washing the column in 2 volumes 300mM potassium phosphate buffer pH 7.0 at 1ml/minute.

The partially purified TS protein was cut by ammonium sulphate precipitation to reduce its volume and then dialysed reduce the phosphate concentration to 50mM prior to purifying further on a S-sepharose column.

10.5 Ammonium sulphate precipitation and dialysis

TS protein was precipitated with 70% ammonium sulphate by adding it slowly to the protein solution while stirring on ice. The solution was then stirred on ice for a further 30 minutes. The precipitate was pelleted by centrifugation (4°C) at 18K for 30 minutes. The pellets were resuspended carefully without frothing in a minimal volume of 50mM potassium phosphate buffer pH 7.0. The protein solution was dialysed overnight against 1 litre of 50mM potassium phosphate buffer pH 7.0 using Spectra/Por (Mol Wt. cut off 10, 000) dialysis tubing. The dialysed protein solution was centrifuged (microfuge) to remove any sediment and the supernatant kept ready to load on to an S-sepharose column.

10.6 S-sepharose chromatography

All chromatographic procedures were performed at 4°C. A 10ml S-sepharose column was poured. As before samples were kept from all stages of the chromatography (loading, washing and eluting) for analysis on a protein mini-gel. The column was washed and equilibrated with 6 bed volumes of 50mM potassium phosphate buffer pH 7.0 at 1ml/minute. The dialysed protein sample was loaded directly on to the top of the column and pumped on at 1ml/minute. The unbound protein was washed from the column with 2 volumes 50mM potassium phosphate buffer pH 7.0. The TS protein was eluted from the column using a salt gradient (50mM potassium phosphate buffer pH 7.0 to 50mM potassium phosphate buffer pH 7.0 plus 400mM KCl). The gradient was applied using a mixing chamber (20ml of each buffer in a separate chamber) at $\frac{1}{2}$ ml per minute, and fractions collected every 2 minutes.

The Bradford assay was used to visualise which fractions contained the TS protein. These fractions were tested for activity (tritium release assay) and stored at -70°C until needed.

11. Kinetic characterisation of mutants

11.1 Kinetic parameter determination

Steady-state kinetic constants were determined using the spectrophotometric assay as described (Pogolotti *et al* 1986). Reactions of 200 μ l volume were set up in microplate wells at room temperature and the change in absorption at 340nm was monitored on an Anthos Labtec HTII microplate reader. When the concentration of dUMP was varied, (CH₂H₄-folate was constant at 550 μ M; when CH₂H₄-folate was varied, the dUMP concentration was 225 μ M.

12. Computing and molecular modelling

Computer analysis of DNA and protein sequences were performed on the MicroVax II computer in this institute using the software package from the University of Wisconsin Genetics Computer Group (GCG Inc., Madison, Wis.). The models of the VZV TS native enzyme and ternary complex were visualised and manipulated using INSIGHT® II (Biosym technologies) run on a Silicon Graphics Indigo Workstation and a Iris Workstation.

RESULTS AND DISCUSSION

The research presented in this thesis concerns two areas of structural flexibility in the thymidylate synthase of varicella zoster virus, namely the DRTG loop and the C-terminus. The results and discussion are divided into individual sections which detail the experiments for both the DRTG loop and C-terminus and discuss the outcome.

1. The DRTG surface loop of VZV TS

The conservation paradox that exists for members of the TS family (in that there are many residues fully conserved which can be substituted without loss of catalytic activity) remains unresolved. Previous work has centred on replacing these conserved residues one by one and observing the affect they have on catalysis, providing evidence for the role many residues have in the structure and function of TS.

Two observations prior to the start of this work showed that thymidylate synthase structurally was a highly flexible enzyme (Finer-Moore *et al* 1990) and that the *L. lactis* enzyme was the most widely diverged TS sequence known (Ross *et al* 1990). Why this enzyme is divergent is not known, one possibility is that the divergent residues of the *L. lactis* enzyme may cluster within particular structural regions of the protein. Clustering may provide insight into mutational hot-spots within a protein where the structure can tolerate some change without affecting function. Initial thoughts were that these may cluster on the surface of the protein and in particular within a region that is involved in dihydrofolate reductase (DHFR) binding, as some other species such as the protozoa, produce a bifunctional TS-DHFR enzyme. All the divergent (differing from those in VZV) amino acid residues of *L. lactis* were substituted into the VZV model. Detailed examination of this structure did not show any reasonable clustering with most of the changes seeming to be distributed throughout the enzyme. The *L. lactis* enzyme can be considered to be the result of an elegant yet 'natural' mutagenesis experiment that has shown that a large number of conserved amino acids can be substituted *en masse* without inactivating the enzyme.

The absence of obvious ‘hot-spots’ leaves the possibility of covariance where multiple sequence changes combine to minimize distortion and side-chain packing clashes on the overall structure. Using sequence data a highly conserved surface loop was identified on the VZV enzyme. This loop consists of five residues (Glu 37, Arg38, Thr39, Gly40, Ile41) and is located between alpha helix A and beta strand i (Figure 19, appendix I, and figure 11a, 11b of introduction). Figure 11a and 11b are also contained loose in the back of this thesis for easy reference. This surface loop (named the DRTG loop, because it starts with a fully conserved glutamate (D) residue) is highly mobile moving approximately 4Å upon binding of ligands. With the exception of TS from phage Φ3T and *L. lactis* the DRTG loop is fully conserved across all published TS sequences. The initial aim of this work was two fold, firstly to examine the basis for the effect whereby a conformational mobile region might affect catalysis and secondly, if this region does affect catalysis can we discover covariant residues which minimise this effect. Our approach was to “lacticise” the VZV protein by replacing residues in the DRTG loop with those from *L. lactis*.

	29 helix A		38		Beta strand i
VZV	I R Y G V R K R	D R T G	I G T L S		
<i>L.lactis</i>	L D N G V F S E N A R P K Y K D	G Q M A N S K Y			

Figure 19. Partial sequence alignment of VZV and *L. lactis* TS

The DRTG loop is shown in bold and the variant *L. lactis* residues in red.

1.1 DRTG loop mutant construction

To examine the effect upon catalysis of mutating the DRTG loop of VZV thymidylate synthase the corresponding *L. lactis* residues were substituted into the VZV protein.

Plasmid pAD768 (Harrison, 1992; see materials section 3) a pBS⁻ backbone vector containing VZV TS was used to construct all the VZV mutants during this study. This vector confers ampicillin resistance and contains the bacteriophage f1 origin of replication to allow ssDNA selection. TS is expressed from a *tac* promoter.

Site-directed mutagenesis was used (using the appropriate primers 1-5, see section 5.3 of the methods section) to construct the mutants R38G, T39Q, G40M, I41A (where the first letter represents the wild-type amino acid, followed by its position and the final letter the substituted amino acid). In addition to the four mutants outlined above, an insertion mutation was made fortuitously using an incorrectly designed oligo. This mutant, 41A42, corresponded to the insertion of alanine between residues 41 and 42.

The strand selection procedure of Kunkel (Kunkel, 1985; Kunkel *et al*, 1987) for mutant enrichment was used for both site-directed and random mutagenesis. The method uses a ssDNA template that contains a number of uracil residues instead of thymine. This uracil-enriched ssDNA (U-ssDNA) is produced in an *E.coli* *dut*⁻ *ung*⁻ strain. These strains lack the enzymes dUTPase and uracil N-glycosylase. Lack of dUTPase activity leads to raised levels of dUTP and results in increased incorporation of uracil into DNA instead of thymine. The lack of uracil N-glycosylase, which normally removes uracil from DNA, means that the uracil is stably incorporated. The resultant U-ssDNA molecule can be used as a template for *in vitro* mutagenesis reactions as the coding potential of uracil is the same as that of thymine. The completely double stranded molecule, the product of the *in vitro* mutagenesis reaction, has a parental strand that contains both uracil and thymine residues, whilst the newly synthesised mutant strand contains only thymine residues. When wild-type *E.coli* strains (i.e. *dut*⁺ *ung*⁺) are transformed with this double-stranded mutant DNA, there is a strong *in vivo* biological selection against the replication of the parental template strand that results in the production of predominately mutant dsDNA molecules. The high efficiency of mutant production (typically >70%) allows the screening of site-directed mutants by DNA sequencing or the generation of highly mutated DNA libraries by random mutagenesis.

The strand selection efficiency was confirmed in that ssDNA (normal thymine containing DNA) was capable of transforming both *E.coli* BW313 (*dut*⁻ *Ung*⁻) and NM522 (*dut*⁺ *ung*⁺), whereas U-ssDNA could transform *E.coli* BW313, but not NM522.

Our experimental system involved expressing the VZV TS gene via the *tac* promoter in *Thy*⁻ *E.coli* strains. The wild-type VZV enzyme is active and can complement the *Thy*⁻ phenotype allowing growth in the absence of exogenous thymidine or thymine.

A qualitative assay for TS activity *in vivo* involves complementation of growth of *Thy*⁻ *E.coli* in the absence of thymine. Although this method provides a rapid genetic

method for the assessment of whether or not TS is active, it is sensitive to the level and activity of the expressed enzyme and is not quantitative. The minimum level of TS that can be detected corresponds to about 1% of wild-type activity (approximately 0.002 U/mg in soluble extracts).

Because of its high degree of conservation we anticipated that the DRTG loop mutants would be inactive. Colonies that were phenotypically Thy⁻ in *E.coli* strain NM522 Thy⁻ were picked and grown overnight. DNA was isolated from each culture by either a mini-prep or STET lysis preparation and restriction digested with EcoRI. Colonies that yielded a restriction profile the same as that of wild-type (pAD768) DNA (Figure 20) were glycerol stocked and sequenced.

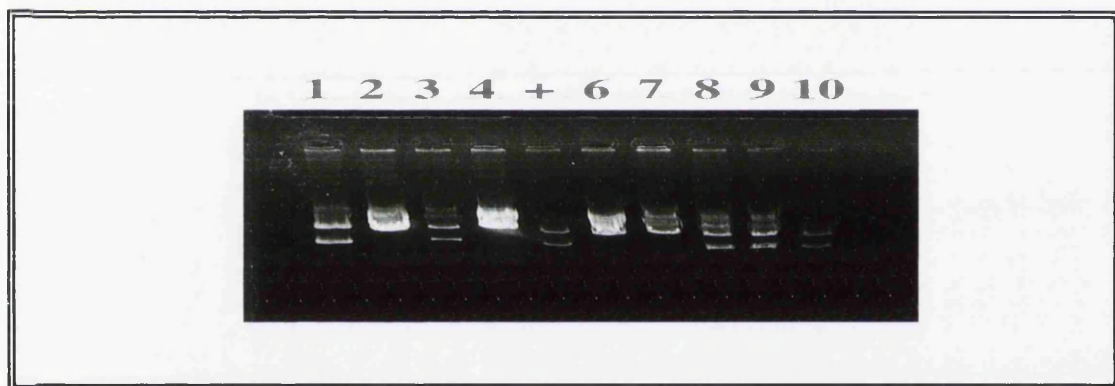


Figure 20. Restriction analysis of Thy⁻ clones after mutagenesis

DNA digested with 10U EcoRI for 3 hours. Lanes 1, 3, 8, 9 and 10 show positive restriction profiles comparable to that of the control (+). Lanes 2, 4, 6, and 7 show a negative restriction profile.

Mutations were initially identified by sequencing across the loop region using primer 62 (Figure 21). That no further changes were introduced during the mutagenesis step was confirmed by sequencing the complete TS gene with primers 59-62 (see methods section 5.4).

Phenotype was assigned on the basis of growth on minimal media (M9) in the absence of thymidine, where strong growth is Thy⁺, no growth Thy⁻ and weak growth Thy^{+/-}. *E.coli* strain NM522 Thy⁻ contains a point mutation in TS, whereas X2913 has its TS deleted. Mutants are selected initially in NM522 Thy⁻ because X2913 transform poorly. However, to exclude the possibility that the host strain TS may have reverted (by correction of its point mutation), enzyme characterisation is performed in the strain X2913.

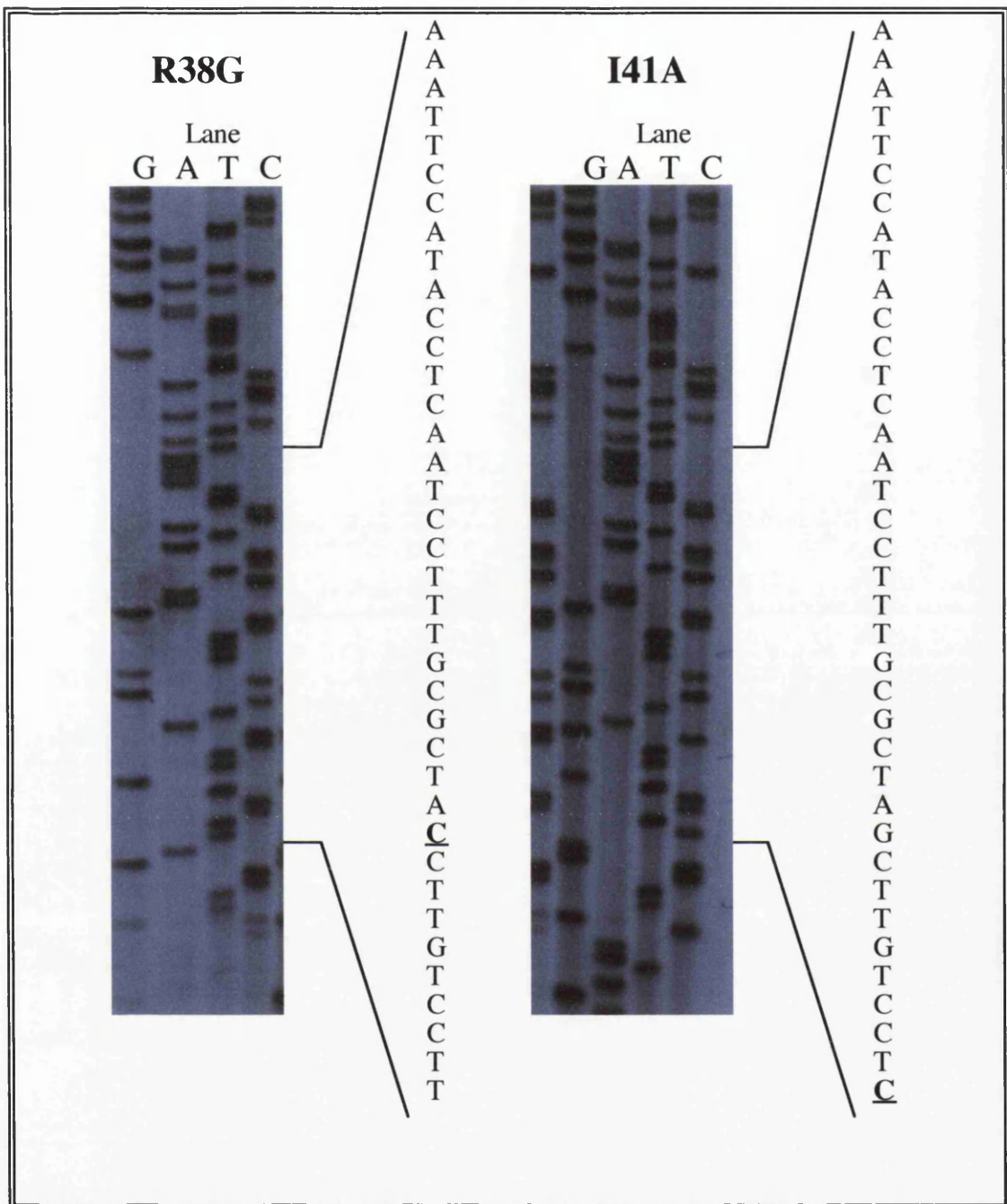


Figure 21. Sequence analysis of clones showing mutant R38G and I41A
The nucleotide change for each mutant is shown underlined and in bold.

Upon transforming the mutants into λ 2913 (to enable enzymatic characterisation—see below) some of the mutants (except G40M and 41A42) became Thy^+ (Table 4). This phenotype change is thought to be due to the differences in the level of expression of lac repressor in these two different strains. The *lacI^q* strain (NM522) producing approximately 10 times more repressor than the *lacI⁺* strain (λ 2913).

Mutant	Phenotype	
	NM522 (<i>lacI^q</i>)	χ2913 (<i>lacI⁺</i>)
R38G	Thy ⁻	Thy ⁺
T39Q	Thy ⁻	Thy ⁺
G40M	Thy ⁻	Thy ⁻
I41A	Thy ⁻	Thy ⁺
41A42	Thy ⁻	Thy ⁻

Table 4. Phenotype of VZV DRTG loop mutants in two different strains of *E. coli* cells. All variants were derivatives of pAD768 expressed in *E. coli*.

1.2 Enzymatic properties of the DRTG mutants

Transformation of the DRTG loop mutants into *E. coli* strain χ2913 (a strain deleted for *E. coli* TS) has enabled characterisation of the enzymatic properties of each mutant from a crude extract (see methods section 8.1) in the absence of any *E. coli* TS protein.

Two convenient assay systems for thymidylate synthase are available which monitor different parts of the catalytic mechanism. The partial reaction involves the binding of substrate dUMP in the **absence** of cofactor and can be monitored by following the debromination of 5-Br-dUMP. The debromination assay was used to monitor the ability of each DRTG loop mutant to participate in the partial reaction (and hence bind the substrate dUMP and activate the C-5 position for subsequent substitution). Figure 22 shows a typical debromination result. However, the reaction is slow compared to dTMP formation and the assay suffers from low sensitivity.

Two independent extracts were assayed at least in triplicate and the results for the DRTG surface loop mutants are summarised in table 5.

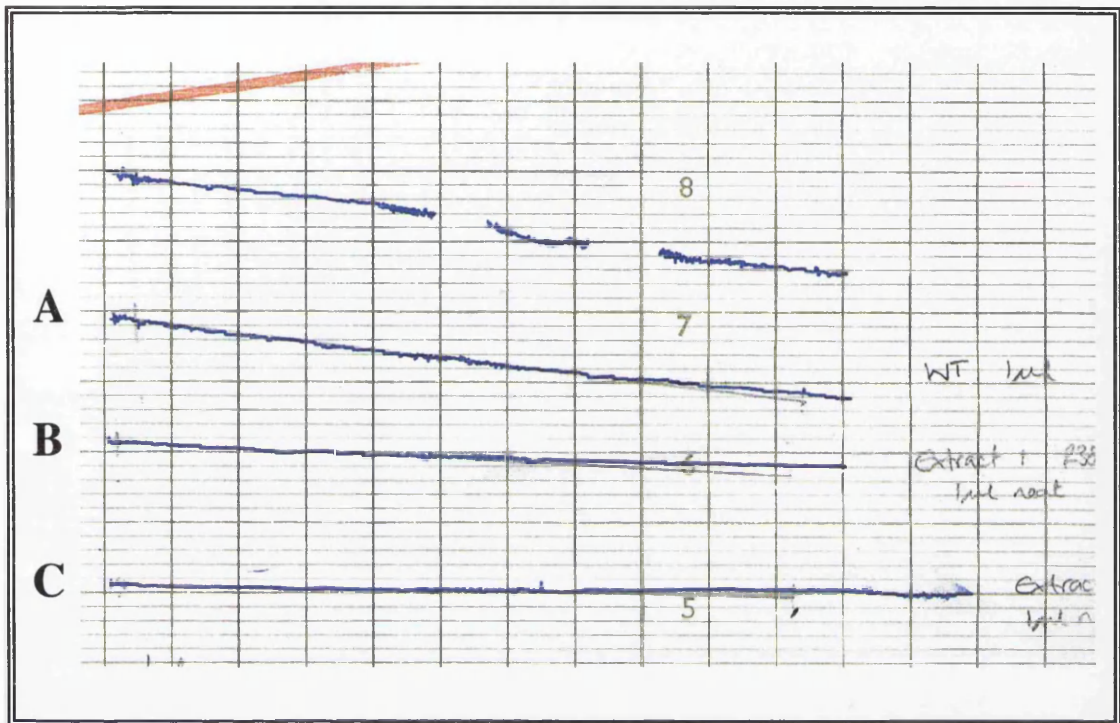


Figure 22. A typical debromination assay

Wild-type TS (A), and 2 different extracts of R38G (B and C) are shown. Chart recorder speed was 120 seconds/cm, recorder range 1. Reaction rates were obtained by determining the change in mOD units per minute (by drawing a tangent line through the linear part of the trace). Rates were divided by the amount of protein added to the reaction in μg to give mOD/min/ μg . The loss of absorbance at 285nm is due to the debromination of 5-BrdUMP.

The complete reaction of thymidylate synthase (i.e. substrate turnover) can be monitored by an assay in which ^3H is released from [5- ^3H] dUMP into solvent upon the formation of dTMP. The tritium release assay is performed in the **presence** of folate cofactor and is highly sensitive detecting as little as 10^{-8} U/mg TS activity.

The results of the two assays on the mutant proteins have provided new data about the role of the DRTG loop in the catalytic mechanism of thymidylate synthase (Table 5). The mutant protein R38G has an approximate 10-fold decrease over wild-type activity for the complete reaction (tritium release assay), T39Q has a 100-fold reduction and I41A an approximately 6-fold reduction. The mutants G40M and 41A42 have a much greater effect on catalysis with an approximately 140-fold and 125-fold reduction respectively, an almost total inhibition of the complete reaction. However when the data for the debromination assay is examined (Table 5) it can be

seen that with the exception of G40M all the mutants have a less than 3-fold reduction in their activity in the partial reaction.

Expressed enzyme	Tritium release assay pmol/min/ μ g	% Wild Type	Debromination assay mOD/min/ μ g	% Wild Type
pAD768 (WT)	160.7 \pm 9.8	100.0	0.19 \pm 0.02	100.0
R38G	21.1 \pm 1.1	13.1	0.07 \pm 0.02	36.8
T39Q	2.2 \pm 0.5	1.3	0.10 \pm 0.02	52.6
G40M	1.1 \pm 0.5	0.7	0.00 \pm 0.0	0.0
I41A	24.2 \pm 2.0	15.1	0.19 \pm 0.02	100.0
41A42	1.3 \pm 0.1	0.8	0.09 \pm 0.01	47.4

Table 5 TS assays (tritium release and debromination) from crude extracts of wild-type VZV TS and variants with mutations the DRTG loop region.

Activities are given as means \pm standard error of the mean. All variants were derivatives of pAD768 expressed in *E. coli* strain χ 2913. χ 2913 not expressing TS exhibits no activity in either assay (R. Thompson, personal communication).

The low sensitivity (approximately 5-10% of wild-type levels) of the debromination assay is highlighted by the mutant G40M. It is inactive in this assay and thus would appear not to be able to bind substrate. In contrast however, it is active (0.7%) in the tritium release assay (which is highly sensitive) and thus this mutant must be able to bind substrate for the complete reaction to take place.

These data suggests that the ability of the DRTG loop mutants to debrominate substrate is not adversely affected and thus they can bind the substrate dUMP albeit slightly less than wild-type. In contrast, the tritium release assay reveals that the DRTG loop mutants are drastically impaired in their ability to turnover substrate. Without the final step of the catalytic reaction occurring these mutant proteins are unable to produce the product dTMP with any great efficiency, leading to their Thy⁻ phenotype.

In conclusion, the DRTG loop region of VZV thymidylate synthase may not play a role in substrate binding but is important for substrate turnover. These results are complementary to those obtained by Carreras et al (1992) who found that the C-terminus of *L. casei* thymidylate synthase is not needed for debromination.

1.3 Kinetics

The above characterisation of the DRTG surface mutants of VZV thymidylate synthase were carried out using crude extracts. In order to obtain a detailed kinetic characterisation, high levels of purified protein were produced by cloning the VZV TS gene into a T7 expression vector for ease of purification.

The open reading frame (of the mutant TS proteins R38G, T39Q, G40M and wild-type) was subcloned from the pBS⁻ based vector pAD768 into the pET based vector pET8C as detailed in figure 23.

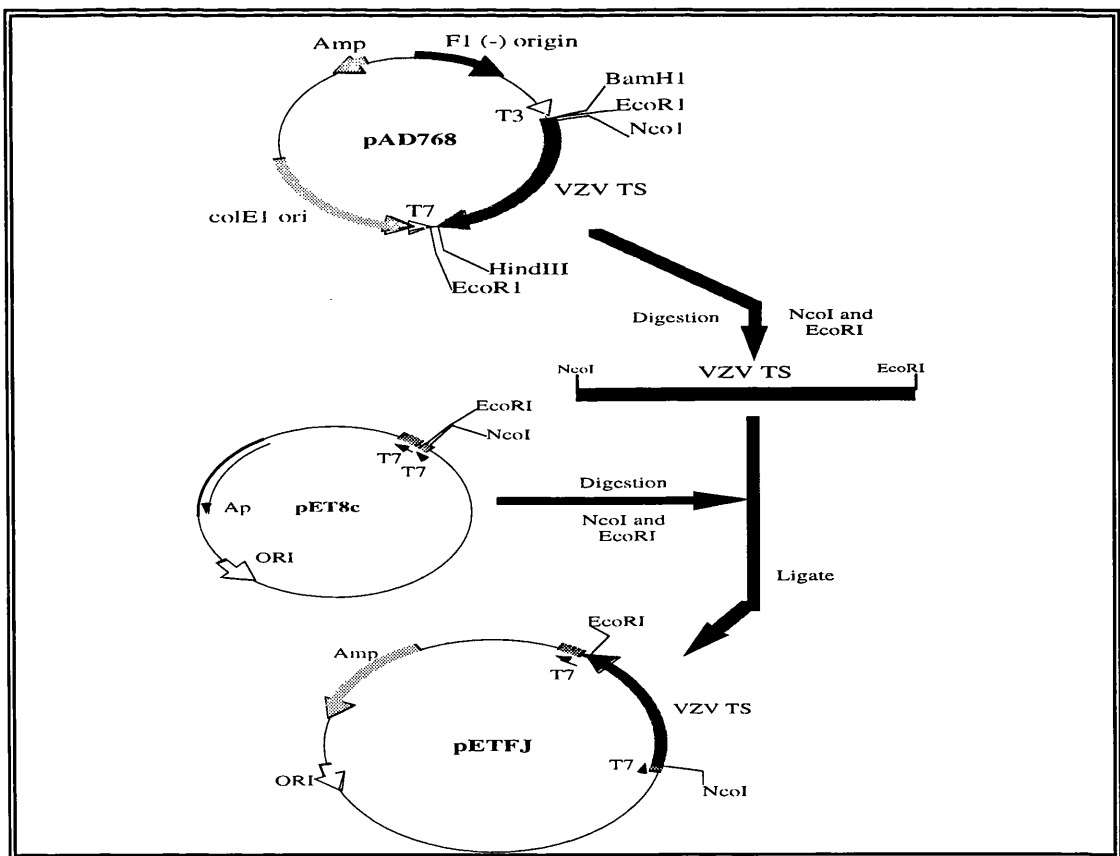


Figure 23. Strategy for construction of the pET8c based expression vectors

The TS gene was ligated into the T7 vector pET8c as described in the materials and methods (section 4.3) and transformed into *E.coli* BL21 (DE3). Clones were analysed by restriction digestion. However, transforming pET8c directly into *E.coli* strain BL21 (DE3) proved problematic in that very few colonies were recovered. Those that were gave a restriction profile different to that of the parental backbone control, indicative of the loss of an EcoRI or NcoI restriction site. To overcome this problem the ligated vector was transformed initially into *E.coli* strain NM522 Thy⁻. Clones from this strain were analysed as before and those that were correct re-transformed into *E.coli* strain BL21 (DE3). Transferring the cloned vector directly into BL21 (DE3) cells was unsuccessful probably due to the restriction status of the *E.coli* strain used to make the original vector. The small amounts of DNA from the cloning would not be sufficient to overcome the restriction difference of the two strains (NM522 cells, a K strain and BL21 (DE3), a B strain) for direct transformation, hence large amounts of DNA were produced by first transforming the clone into NM522 cells. This strategy of transforming the vector between two strains was successful. Hundreds of colonies were recovered in BL21 (DE3) and the majority had the correct restriction profile.

Analysis of clones revealing the correct restriction pattern were test-induced with IPTG. Clones that induced produced a protein of approximately 39K (Figure 24).

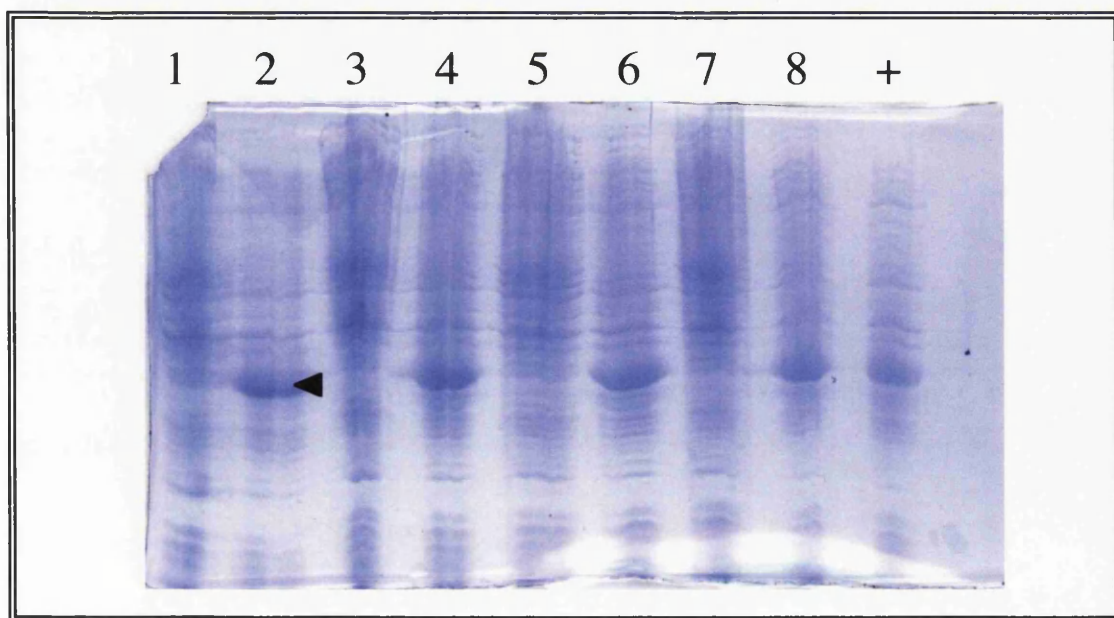


Figure 24. Test induction of R38G mutant clones of TS with IPTG

Lanes 1, 3, 5 and 7 are uninduced, lanes 2, 4, 6, and 8 are induced. An arrowhead indicates the TS band. A positive induction of wild-type TS is shown (+) as a control. Proteins were separated on a 12% acrylamide SDS gel.

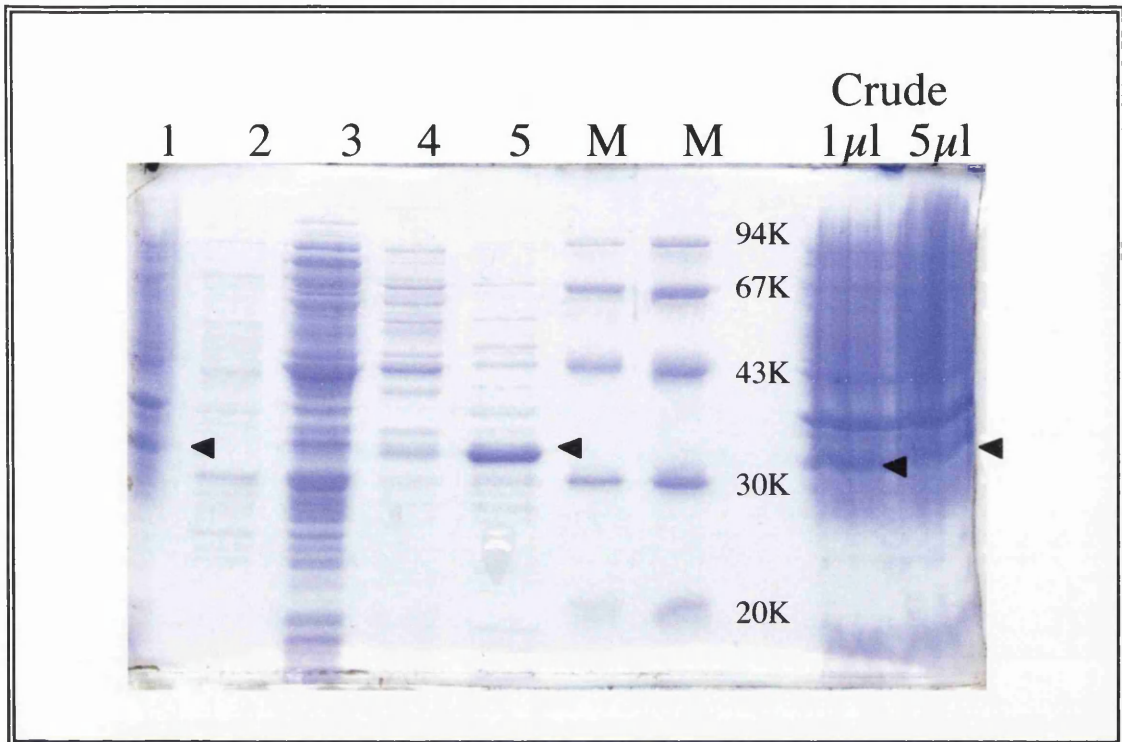


Figure 25. Purification of R38G TS by hydroxylapatite chromatography

Lane 1=crude extract, 2=column flow through, 3=50mM KPO₄ wash, 4=100mM KPO₄ wash, 5=300mM KPO₄ wash, M=molecular weight markers (from top to bottom showing, 94K, 67K, 43K, 30K, 20K). The final two lanes show different amounts of the crude extract. The thymidylate synthase band is indicated by an arrow head. Note that the load was cycled through the column several times prior to elution.

A 6000ml culture was centrifuged and sonicated prior to purification (see section 10 of methods). The first step in the purification process was hydroxylapatite chromatography. Hydroxylapatite consists of a calcium phosphate powder which can bind proteins and was chosen for the first step in the purification process for two reasons. Firstly, it does bind TS with some slight selectivity, while not binding the majority of proteins contained in the bacterial extract. TS probably binds to hydroxylapatite due to its phosphate 'binding' pocket, which co-ordinates the phosphate of dUMP in the wild-type situation. The second reason is that hydroxylapatite is relatively cheap and thus disposable. This is useful as it prevents the potential cross contamination of one mutant with another that can occur when columns are re-used. Each step of the purification was monitored by protein mini-gel analysis of the appropriate collected fractions (Figure 25). Cycling the load several

times through the column can reduce the amount of TS that elutes in the flow through.

After hydroxylapatite chromatography the TS was precipitated with ammonium sulphate and then dialysed over night against 1 litre of 50mM potassium phosphate buffer. The dialysed sample containing the TS was further purified by S-sepharose chromatography (Figure 26). The procedure followed for purification of mutant proteins was identical to that for wild-type enzyme. The purity of the mutants and wild-type was estimated at between 90-95%. Unsuccessful attempts were made to remove the high molecular weight contaminating bands (see Figure 26) by re-purifying the TS containing fractions on a second S-sepharose column. Changing the rate of the elution gradient was also unsuccessful as was further purification using a Mono-S column.

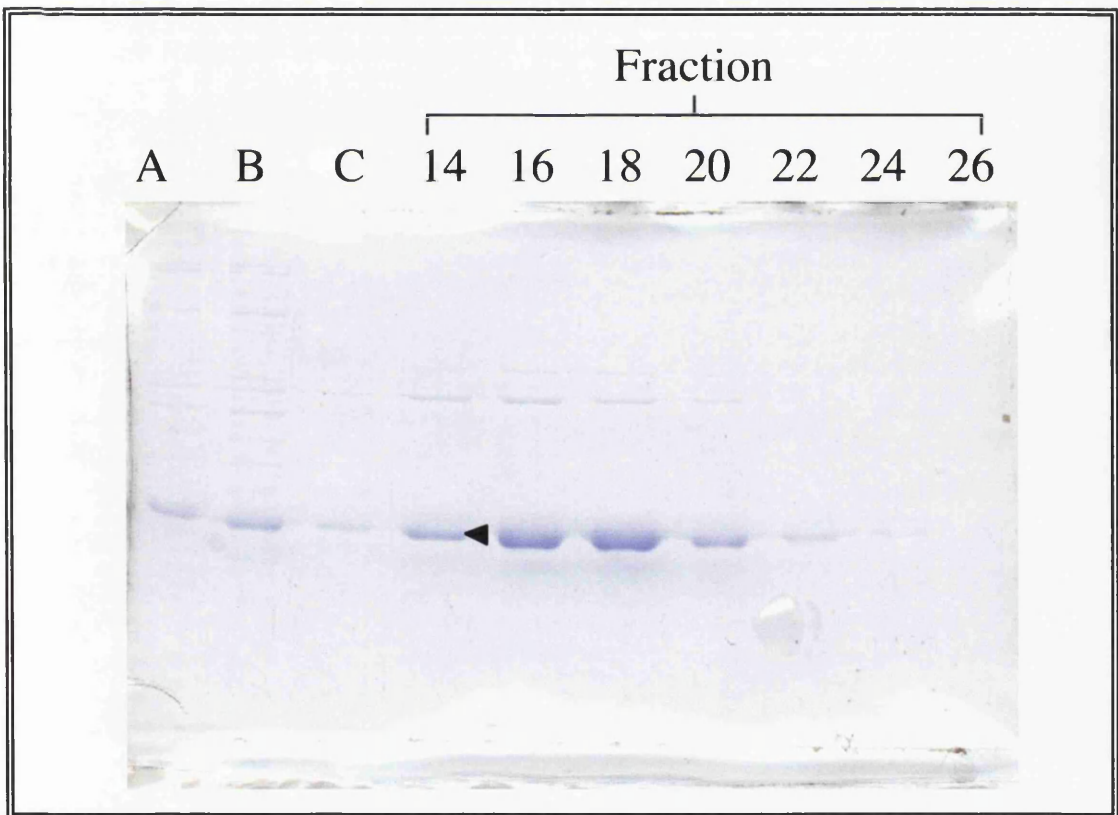


Figure 26. Visualisation of the fractions containing purified R38G TS

A= column load, B= flow through, C= 50mM KPO₄ wash. Various fractions collected during the 50-400mM KCl gradient are shown. Purified TS was eluted in fractions 14-21, and a TS band is illustrated by an arrow head.

The mutants R38G and T39Q were analysed to determine further the role of the DRTG loop in catalysis. Details of determining the kinetic parameters are given in the materials and methods. Enzyme activity as measured by the complementation assay indicated these residues were essential for catalysis (Table 4). Further analysis on crude extracts (Table 5) confirmed that both these variants were dysfunctional. This dysfunction was not in their ability to bind substrate but because they could not turnover substrate (and thus complete the catalytic reaction). Kinetic data indeed confirms this conclusion as the K_m for wild-type VZV TS is $5\mu\text{M}$ (Table 6) and variants R38G and T39Q have K_m values ($3.47\mu\text{M}$ and $4.8\mu\text{M}$ respectively; table 6) comparable to that of wild-type. Interestingly, the debromination assay indicates that these mutants are somewhat impaired in their ability to participate in the partial reaction, perhaps reflecting the low sensitivity of this assay.

Expressed enzyme	K_m for dUMP	K_m for CH_2H_4 folate
Wild-type TS	5.0 ± 0.31	25.77 ± 2.20
R38G TS	3.4 ± 0.94	300.48 ± 85.91
T39Q TS	4.8 ± 1.53	138.32 ± 26.31

Table 6. K_m values for dUMP and CH_2H_4 folate of wild-type VZV TS, and variants with mutations in the DRTG loop region corresponding to the *L. lactis* TS. Activities are expressed as mean \pm standard error of the mean.

The more sensitive ^3H release data is substantiated by the K_m values for the folate cofactor. Wild-type VZV TS has a K_m of $25.77\mu\text{M}$ whereas R38G has a K_m of $300.48\mu\text{M}$; a dramatic increase of 11-fold of that of wild-type enzyme. A less dramatic, but still significant, 5-fold increase in K_m for the mutant T39Q ($138.32\mu\text{M}$) is observed. These significant increases in the K_m values for folate must play a part in the diminished activity of these variants.

Kinetic data was not obtainable for the mutant G40M, because it was too inactive to be detected in the spectrophotometric assay.

The K_m for dUMP for both mutant proteins was comparable or slightly lower than that of wild-type suggesting a more open structure allowing better binding of dUMP. A similar situation of reduced K_m for dUMP and increased folate K_m was observed for the C-terminal truncation mutant L301 Δ , which is believed to be defective in effective closure of the active site (Harrison *et al* 1995).

1.4 Molecular modelling of the DRTG loop mutants

The models of the VZV TS native enzyme and ternary complex were visualised and manipulated using INSIGHT® II (Biosym technologies) run on a Silicon Graphics Indigo Workstation and an Iris Workstation. Mutations were introduced into the VZV model using the programme SwissModeler before manipulation with INSIGHT® II. Output files were captured using Snapshot and converted from RGB to TIFF files using XV. The TIFF images were then imported into Photoshop for fine tuning.

In the wild-type situation the DRTG loop appears to be somewhat unstructured, however, it moves up towards the C-terminus upon binding of ligands. Modelling of the VZV ternary complex in this region shows a very tight packing of residue side chains (Figure 27).

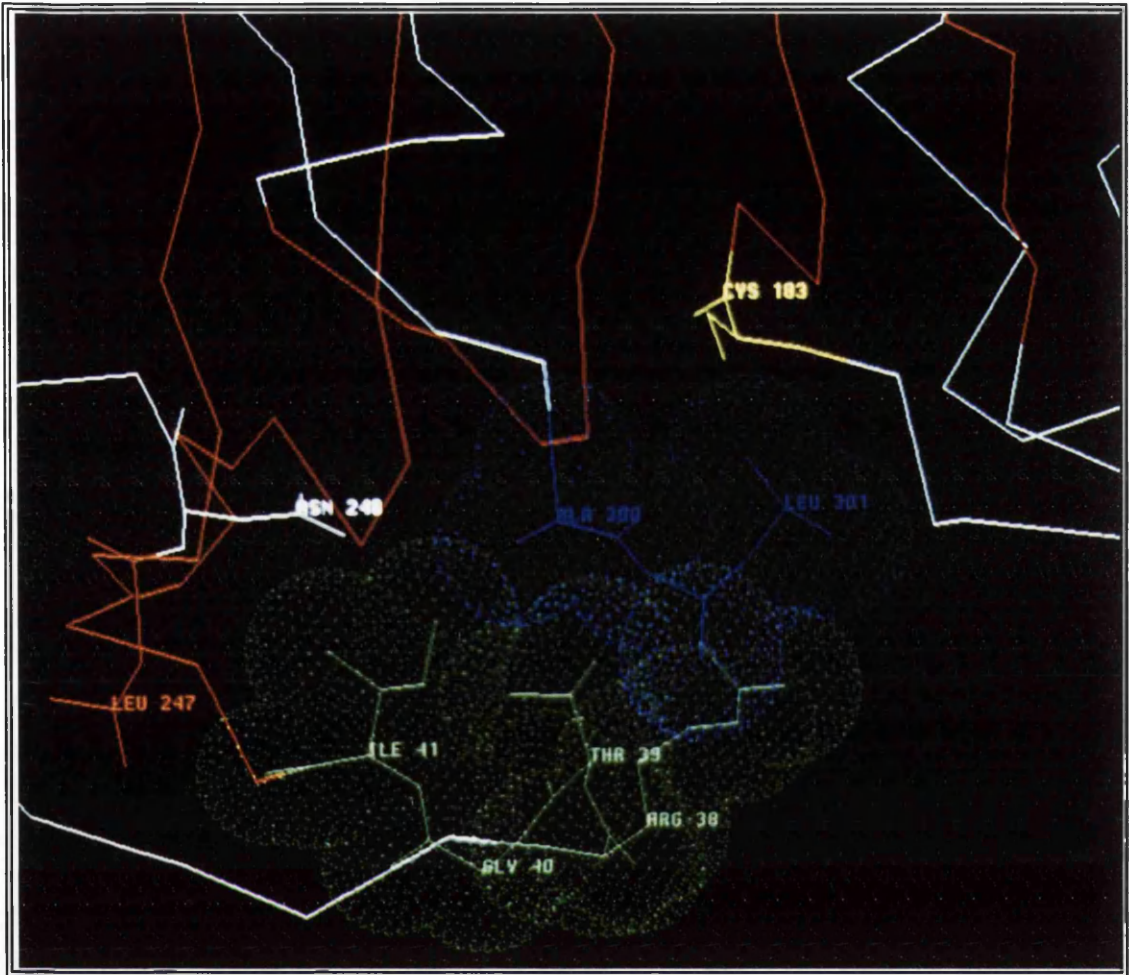
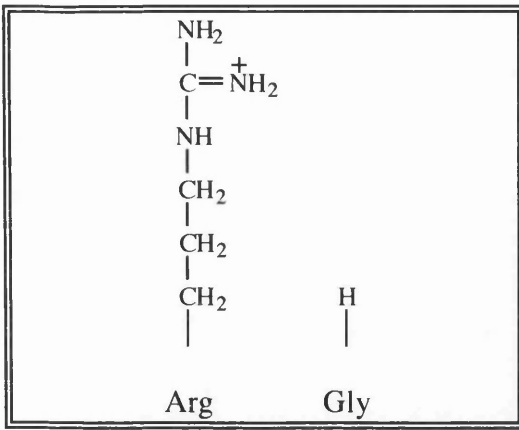


Figure 27 The DRTG loop and C-terminus of VZV thymidylate synthase ternary complex

van der Waals radii are shown for the residues Arg-38, Thr-39, Gly-40, Ile-41 (DRTG loop; green) and for Ala-300 and Leu-301 (C-terminus; blue). Also shown is the active site cysteine (yellow), leucine 247 and asparagine 248. The bottom of the β -sheets are shown in red, and connecting loops in white

That substitution of any one of the loop residues results in dramatic loss of substrate turnover is indicative of a functional role for this loop in the VZV enzyme, perhaps explaining why they have been almost fully conserved throughout the TS family. Throughout this section the amino acid side chains are shown for comparison of size and charge on the left of the page.



R38G

In the wild-type ternary complex the arginine-38 side chain makes a hydrogen bond to the carboxylate group of the C-terminal leucine (L301). This hydrogen bond helps stabilise both the packing of the loop the C-terminus after they have moved towards the active site upon ligand binding. Arginine-38 is also one of

four highly conserved arginines, two from each monomer, which provide a favourable, positively charged binding surface for the phosphate anion of dUMP. These four arginines as well as Serine-208 are involved in an extensive hydrogen bonding network around the phosphate. Each arginine forms at least one hydrogen

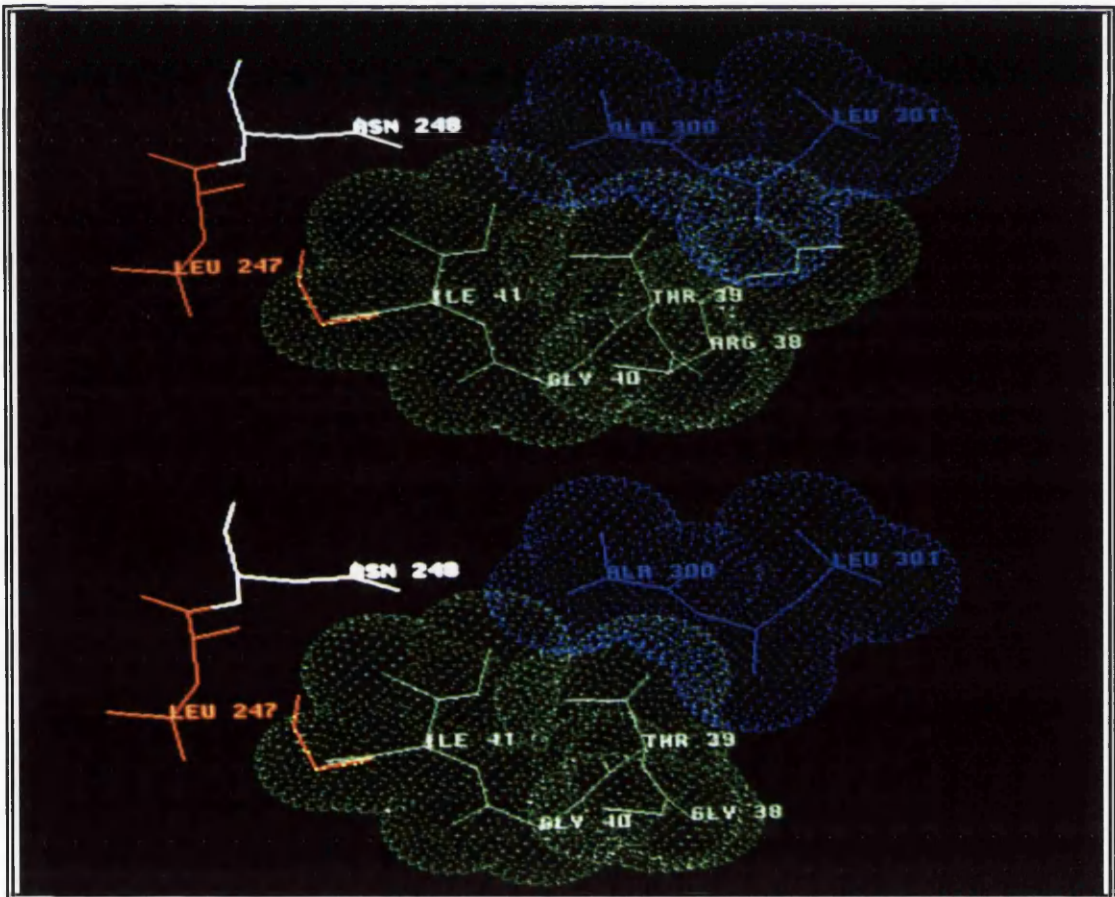


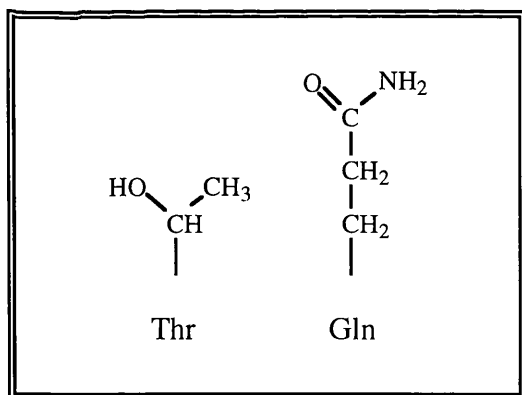
Figure 28 R38G

The wild-type structure is shown on top and the mutant below. Residues 38-41 are shown in green and residues 300-301 in blue with their van der Waals radii, several other amino acid are also shown.

bond to the phosphate oxygens. Substitution of the charged arginine residue for glycine, an uncharged and the smallest amino acid in the mutant **R38G** results in loss of this H-bond to the carboxylate group of leucine-301 (Figure 28). Without such a H-bond the loop does not pack tightly against the C-terminus. C-terminal packing is needed for tight folate binding/retention. With the exception of the mutant **G40M** this mutant is the least active in its ability to debrominate halogenated dUMP being approximately 65% less active than wild-type (Table 5). This suggests that this mutant is impaired in its ability to bind the substrate dUMP. Replacing arginine-38 with glycine removes one of the hydrogen bonds in the network that is involved in stabilising substrate binding. However loss of this one hydrogen bond from a network of H-bonds does not appear to affect dUMP binding because its K_m for substrate is very similar to that of wild-type. Thus the main driving force for loss of activity for this mutant must be the loss of the H-bond to the carboxylate group of leucine-301.

T39Q

Manipulation of the ternary model to examine the mutant T39Q (Figure 29) reveals that the methyl group of threonine in the wild-type situation packs in a hydrophobic pocket next to alanine 300 and its hydroxyl groups points out to the solvent.



Threonine also makes a H-bond to the carboxylate group of leucine-301 (as does arginine-38). Replacement of threonine by glutamine results in a side chain that points out to solvent leaving a hole in the hydrophobic pocket. This destabilises the packing of the loop against the C-terminus. It appears that the glutamine residue

points out to solvent in order to prevent any gross steric clashes with surrounding residues, particularly isoleucine-41 and alanine 300. The easiest way for a structure to accommodate changes is by orientating its side chains into empty space, however, this can best be achieved when the area containing the change (such as the DRTG loop) is on the surface of the protein.

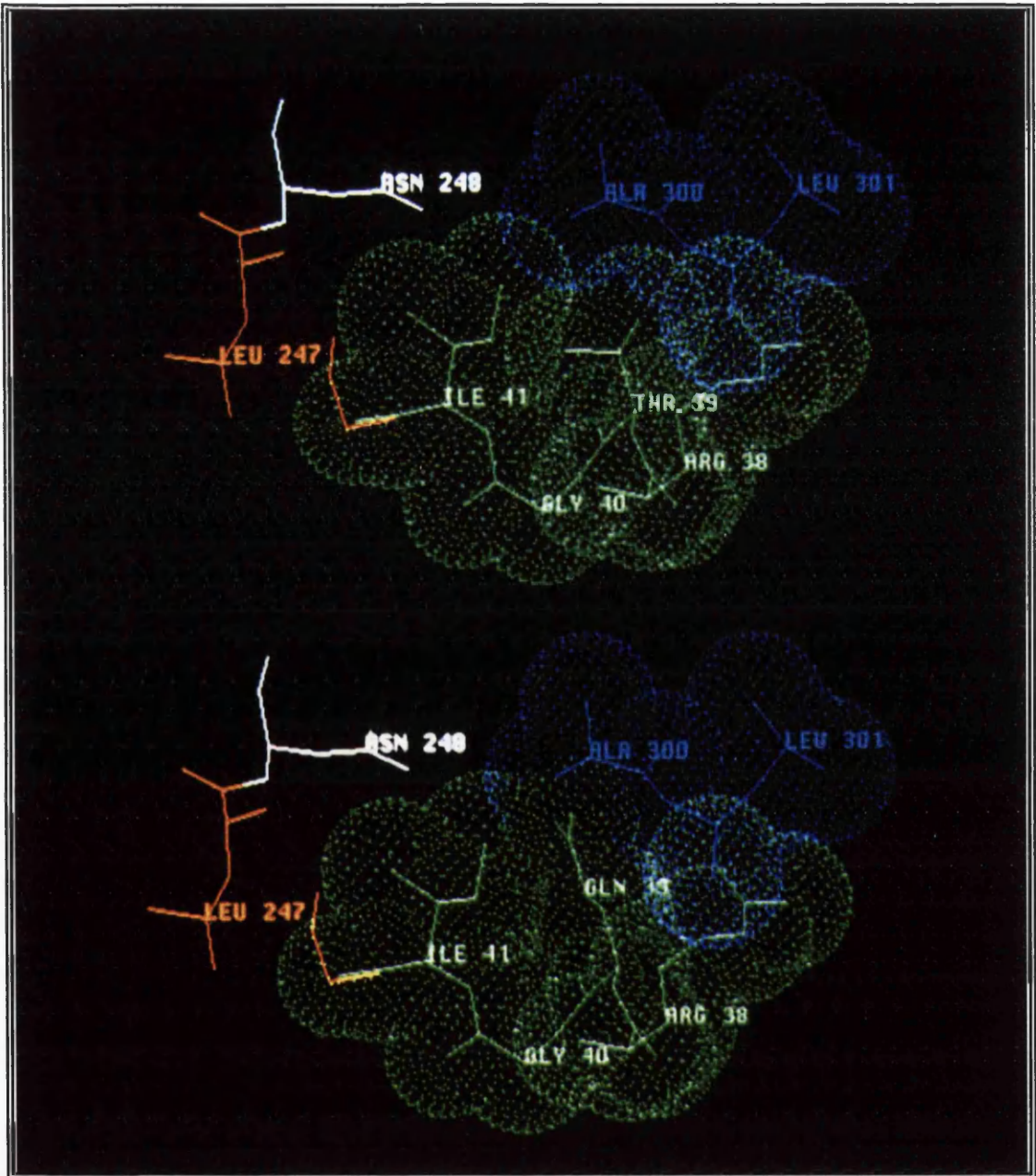


Figure 29 T39Q

The wild-type structure is shown on top and the mutant below. Residues 38-41 are shown in green and residues 300-301 in blue with their van der Waals radii, several other amino acid are also shown.

Each amino acid is associated with two conformational angles phi (Φ) and psi (Ψ) within a peptide unit, where Φ is the angle of rotation around the N-C $_{\alpha}$ bond and Ψ is the angle around the C $_{\alpha}$ -C' bond from the same C $_{\alpha}$ -atom. Most combinations of Φ and Ψ angles for an amino acid are not allowed because of steric collision between the side chains and the main chain. Glycine with only a hydrogen atom as a side

chain can adopt a much wider range of conformations than the other residues. Glycine thus plays a structurally very important role; it allows unusual main chain conformations in proteins and is one of the main reasons why a high proportion of glycine residues are conserved among homologous protein sequences.

G40M

The most dramatic reduction in enzyme activity is for the mutant G40M both substrate binding and turnover being almost totally diminished (Table 5). Its activity is so low, that its K_m was not determinable. Obviously this glycine residue is functionally or structurally important. Modelling of this glycine (Figure 30)

indicates that it is crucial structurally in that it facilitates a tight turn in the loop and

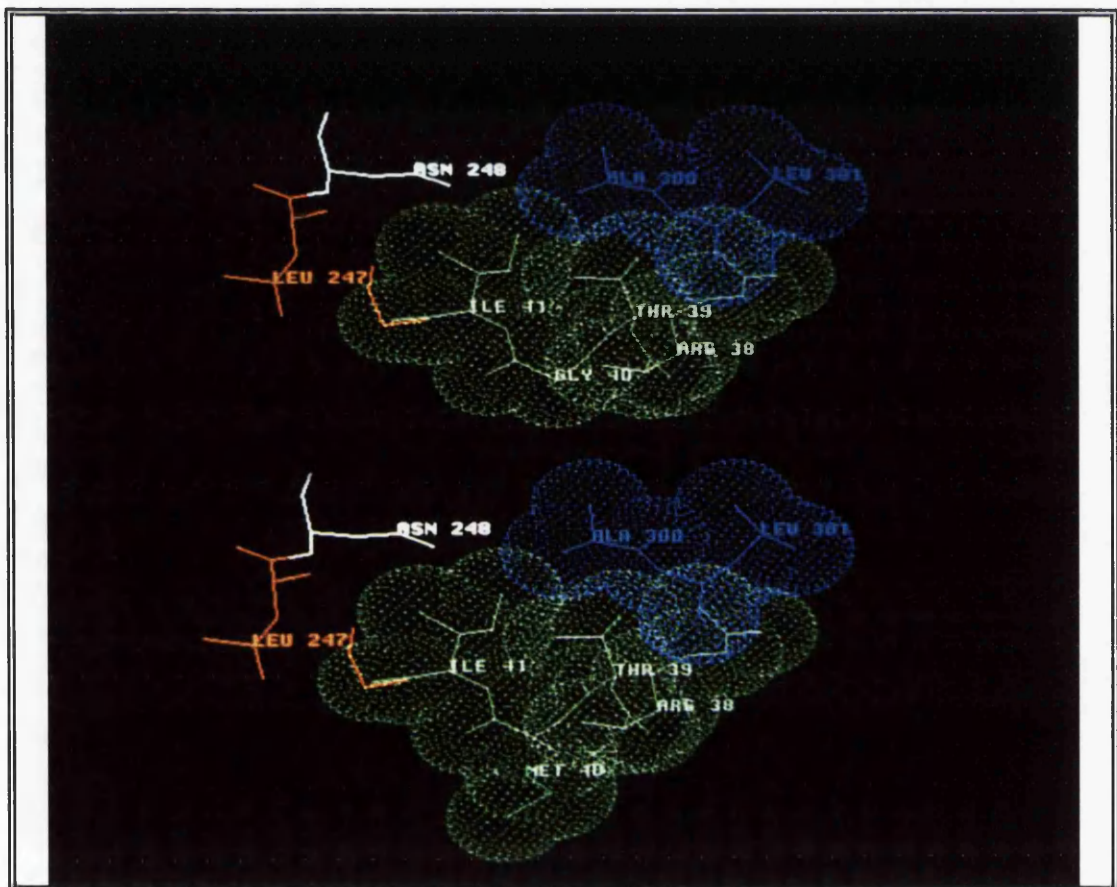
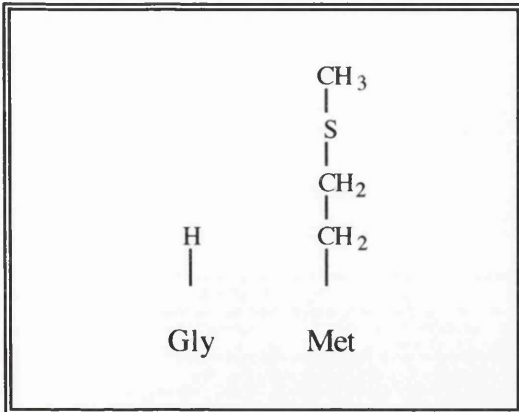


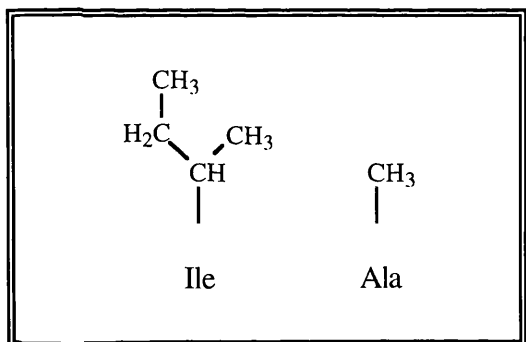
Figure 30 G40M

The wild-type structure is shown on top and the mutant below. Residues 38-41 are shown in green and residues 300-301 in blue with their van der Waals radii, several other amino acid are also shown.

keeps it in the required conformation. Mutating this residue to the *L. lactis* residue methionine, which is larger and hydrophobic, places large restrictions on the conformation it can adopt in this loop. It therefore kinks the loop destabilising it and in turn preventing correct positioning of the C-terminus.

I41A

The hydrophobic amino acid isoleucine at position 41 packs tightly against residue 300 (alanine). It also packs neatly into a cleft created by the hydrophobic side-chains of tyrosine-246 and leucine-247 to form part of a flat hydrophobic surface (Figure 31). This surface is at right angles to the orientation of the backbone carbonyl group of threonine-39 and methionine-299, and the carboxyl group of the C-terminal residue. Substitution for the much smaller, but still hydrophobic alanine in the mutant I41A (Figure 31) leaves a hole in this hydrophobic cleft. This gap may lead



to incorrect formation of this region of the protein which could disrupt the orientation of the surrounding residues. Comparison with other TS sequences at this position shows that only threonine and valine are found at this position (except for phage Φ 3T and, *L. lactis* both of which have an alanine at this position, see figure 19

and appendix I). Both threonine and valine, like isoleucine, have a branched β -carbon, one arm of which contains a lone methyl group. Both these two amino acids can be modelled in this position filling the cleft between tyrosine-247 and leucine-248, without disrupting the planar hydrophobic surface. This confirms the need for the presence of a methyl group in the cleft and although alanine contains a methyl group it is not on a branched β -carbon and cannot reach to fit into the cleft. The absence of a methyl group in this cleft is probably the major factor that contributes to reduced enzyme activity.

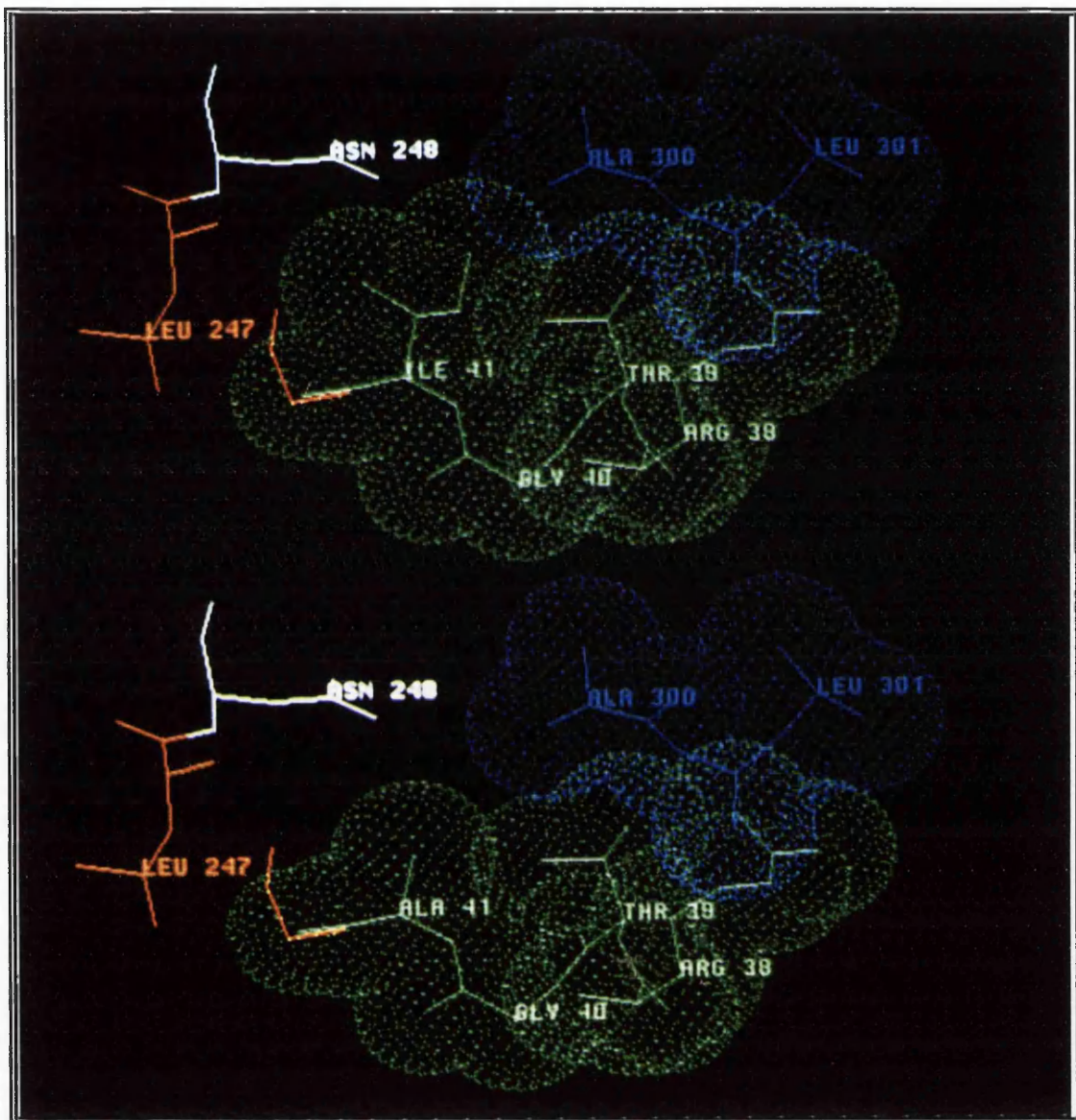


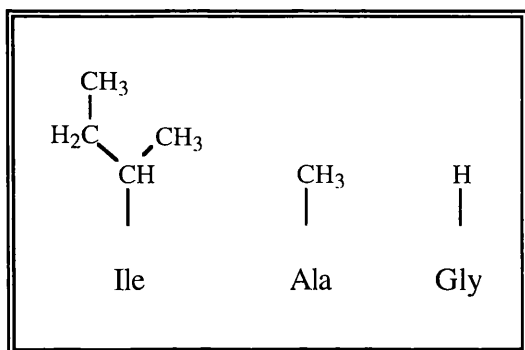
Figure 31 I41A

The wild-type structure is shown on top and the mutant below. Residues 38-41 are shown in green and residues 300-301 in blue with their van der Waals radii, several other amino acid are also shown.

Insertions within a protein can have many effects depending on the position, the size (one or more residues) and the properties of the amino acid (size, charge, hydrophobicity) inserted. The thymidylate synthase of VZV has tolerated insertions (or perhaps deletions) during evolution. Sequence alignments shows an insertion of 17 amino acids at the amino terminus which is not found in the *E. coli* structure and a further two short insertions at positions 105-116 and 134-141 both of which are between helical regions and thus presumably loops. These extra elements are not modelled in the VZV structure. So extra amino acids appear to be tolerated by VZV

TS, perhaps by being in non critical structural regions or on the surface of the protein.

If the DRTG loop was not functional (or structural) then insertions within it would most likely be tolerated as this loop would probably serve as a connection between α -helix A and β -strand i.



41A42

The insertion mutant 41A42 (an alanine between isoleucine-41 and glycine-42) allows us to further examine the role of the DRTG loop. The ability of this mutant to bind substrate, as assayed by the debromination assay, indicates that

this insertion reduces by approximately 50% the ability of the mutant protein to bind substrate. Although, substrate dUMP is still bound albeit diminished, the ability of the mutant protein to turn this substrate over is almost knocked out (0.8% of wild-type; Table 5). Modelling of this mutant was not possible using the programmes available to us. However, an insertion (even such a small one) into what appears to be a critical functional part of the structure would cause some gross steric clashes. Perhaps this results in preventing maximal packing of the loop against the C-terminus and also prevents the formation of the hydrogen bond between Arginine-38 and the carboxylate group of the C-terminal leucine by moving the arginine out of range of efficient hydrogen bond formation.

1.5 Second-site revertants of the DRTG loop mutants

As thymidylate synthase is so highly conserved it was considered that in order for the *L. lactis* enzyme to accommodate highly variant residues in the DRTG loop there may be other 'co-variant' residues within the TS structure. These 'co-variant' residues may allow accommodation of the vastly differing residues within the overall structure. In order to attempt to identify co-variant positions we screened for second-site revertants that would restore activity to the DRTG loop mutants.

Most methods of random mutagenesis can be susceptible to mutagenic 'hot spots', that is the clustering of mutations in certain regions of the gene, whilst other regions may be left unmutated (McPherson 1991). The method of 'spiked oligonucleotide'

mutagenesis avoids such hot spots and is probably the most truly random mutagenesis protocol available (Blacklow and Knowles 1991).

Isolation of second-site revertants of the DRTG loop mutants which would restore high levels of enzyme activity was attempted using 'spiked oligonucleotides'. These 'spiked oligonucleotides' are long (~55 bases) oligos synthesised using phosphoramidite mixes containing 96% of the normal oligonucleotide and 1.3% of the other three mixes (Ner *et al* 1988, McNeil and Smith 1985). These should contain an average of two base changes per oligonucleotide. These changes are essentially random but since they are restricted to the region covered by the spiked oligonucleotide we refer to the process as "region directed mutagenesis".

U-ssDNA was prepared for each DRTG loop mutant (as previously described). Each mutant uracil-enriched template was checked for efficient strand selection and templates that failed to give colonies in strain NM522 *thy*⁻ but did for BW313 *dut*⁻ *ung*⁻ were used to attempt to generate second-site revertants via region directed mutagenesis. A total of 22 spiked oligonucleotides were synthesised that were approximately 50 bases in length and covered the whole VZV TS gene (Figure 32).

Oligo	Size	Region Of TS Gene (bp)*	Amino Acid Sequence*	Secondary Structures
R01	57mer	108-165	37-55	DRTG loop, β -Strand i
R05	48mer	465-513	156-171	Helix H 156-159, Loop 160-164, β -Strand v
RO7	45mer	534-579	180-194	Helix I 179-180, loop 181-182, β -Strand iv, Loop 192-194
RO8	48mer	572-620	192-207	Loop 192-196, β -Strand iii, Helix J 208
R010	54mer	654-708	219-237	Helix-J 219-230, Loop 231-234, β -Strand ii 235-237

Table 7 Spiked oligonucleotides used in the covariant studies

* see figure 32

Region directed mutagenesis on the DRTG loop mutants (R38G, T39Q, G40M and I41A) was performed using the spiked oligonucleotides R01, R05, R07, R08, R010 (Table 7). These spiked oligonucleotides were chosen because they targeted surface areas of the structure which we thought could accommodate changes more easily than other more buried regions of TS.

Our selection criteria for a second-site revertant was the restoration of activity to the DRTG loop mutant protein. The initial mutant proteins were Thy⁻ in the *in vivo* complementation assay, thus potential second-site revertants were isolated initially on their ability to complement *E. coli* strain NM522 Thy⁻ when grown on minimal media without thymidine. Colonies that were now phenotypically Thy⁺ were selected and analysed by restriction digestion with EcoRI. Those giving the correct restriction pattern were sequenced initially across the region that was targeted by the spiked oligonucleotide.

A total of 6000 colonies from the random mutagenesis were isolated on non-selective medium and then screened for their ability to grow on minimal media in the absence of thymine by patching. Only 800 of these colonies were phenotypically Thy⁺. To increase the number of Thy⁺ colonies obtained a different transformation method was tested (calcium chloride shock instead of PEG-DMSO), however the number of colonies that were Thy⁺ did not increase. Mutagenised DNA was transformed directly into *E. coli* strain χ 2913 to test if NM522 Thy⁻ had reverted to a Thy⁺ strain (it only has a point mutation inactivating its TS gene) giving rise to false Thy⁺ colonies. This did not appear to be the case and the poor transformation efficiency of χ 2913 cells made its use of limited value for a first round screening system. Further analysis of the colonies obtained by comparison of their restriction profile reduced the numbers still further to 110 perhaps indicative of problematic filling-in reactions after primer annealing. Sequencing of these across the appropriate targeted region revealed that no amino acid substitutions had occurred. Interestingly, mutagenesis with random oligo 1 (which covers the original DRTG loop) did not generate any wild-type revertants. Why a previously Thy⁻ clone could acquire the ability to grow in the absence of exogenous thymidine after mutagenesis (indicating restoration of an active TS) may have been due to some sort of mis-priming event where the oligo has changed the promoter or copy number of the plasmid backbone. These changes could then have resulted in an overproduction of the weakly active protein which although has no second site changes can now overcome the deficiency of thymidine in the media.

Failure to find covariant residues which would compensate for the *L. lactis* residues introduced into the DRTG loop may be due to several reasons. The most compelling reason is that residue(s) in more than one region of the enzyme may need to be substituted to allow accommodation of a loop mutant. Mutagenesis was performed using a region directed oligonucleotide targeted to a specific region of VZV TS (Table 7) and although these targeted regions are reasonably large (most oligos being 50mers or bigger) they may not encompass enough of the TS gene. Perhaps the covariant residues needed were in two or more distinct parts of the enzyme which single oligos could never cover. We did not attempt to use a cocktail of non-overlapping spiked oligonucleotides, although this approach would seem to have merit.

1.6 Summary

These studies have identified a highly conserved surface loop (the DRTG loop) of VZV thymidylate synthase and shown that the loop does have some functional role in catalysis. This may be mediated by close contact with the C-terminus and other surrounding residues perhaps helping to stabilise the C-terminus after its concerted movement (along with the DRTG loop) towards the active site upon ligand binding. This stable tightly packed region of the enzyme presumably excludes bulk solvent from the active site and also helps in overall stabilising of ligand binding. This is the first indication that DRTG loop is an important functional element that may be critical for active site closure. Interference with loop movement may provide a target for novel TS inhibitors.

The combined power of modelling, phylogentic comparisons and mutagenesis provide arguments as to why some residues are highly conserved and suggestions as to why substitutions lead to inactivation of thymidylate synthase. Many of the mutants are inferred to lead to inactivation (or diminished activity) due to steric clashes or the creation of gaps in core regions of the protein. Such clashes must be overcome in order to form a stable protein structure. Inability to eliminate steric clashes leads to an unstable enzyme or one that attempts to repack and accommodate the changes but by so doing re-orientates residues that play a critical part in catalysis.

2. The C-terminus of VZV TS

The C-terminal region of thymidylate synthase closes upon ligand binding effectively forming a lid over the active site which, in concert with other movements (the DRTG loop included), results in the adoption of a tight closed conformation of the enzyme (Stroud and Finer-Moore 1993). Many of the key interactions appear to be H-bonds between the carboxylate group of the C-terminal residue (rather than contributions from its side chain) and several highly conserved residues including arginine-21 and tryptophan-83 (*E.coli* TS numbering). These interactions anchor the cofactor in place and stabilize the closed protein conformation.

Previous studies have shown that the TS of *L.casei* is totally inactivated by the removal of the C-terminal residue by carboxypeptidase (Aull *et al* 1974) and this has recently been confirmed by site-directed mutagenesis (Climie *et al* 1990). It seems that the exact position of the carboxylate group is critical. In contrast, findings by Harrison (1992) and Harrison *et al* (1995) has shown that removal of the C-terminal residue from VZV TS results in an enzyme that can still complement Thy⁻ *E. coli* . We have extended these studies to examine a variety of C-terminal modifications.

2.1 VZV C-terminus Mutants

The C-terminus of VZV TS was extended by one amino acid to examine the effect of moving the position of the carboxylate group upon catalysis. To prevent introducing gross structural constraints upon the enzyme the two smallest amino acids, glycine and alanine, were chosen.

Site-directed mutagenesis using the appropriate oligonucleotide was employed to construct the mutants A302 and G302. Colonies that yielded a restriction profile the same as that of wild-type (pAD768) DNA were glycerol stocked and sequenced. Mutations were initially identified by sequencing across the C-terminal region using primer 59. As before the absence of further changes introduced during the mutagenesis step was confirmed by sequencing the complete TS gene with primers 59-62.

C-terminal mutants	Phenotype
A302	Thy ^{+/-}
G302	Thy ⁺

Table 8 C-Terminal mutants of VZV thymidylate synthase and their phenotype

All variants were derivatives of pAD768 expressed in *E. coli* NM522 Thy⁻ cells

Complementation data reveals that both these mutants fail to inactivate VZV TS (Table 8), however, extension of the C-terminus with the larger alanine results in an enzyme that barely complements NM522 Thy⁻ cells. Analysis of crude extracts shows that addition of alanine significantly reduces the overall capacity of the enzyme to perform the catalytic reaction. The ability of this mutant protein to participate in the partial reaction (and hence bind substrate) is reduced approximately 70% and substrate turnover reduced approximately 80% when compared to wild-type VZV TS (Table 9) and almost certainly accounts for its much reduced Thy⁺ phenotype. Substrate turnover of 20% (of wild-type) for A302 is relatively high when compared with the DRTG loop mutant proteins (0.7-15%). Interestingly, the addition of glycine has a more profound affect on the enzyme. This mutant enzyme

Expressed enzyme	Tritium release assay pmol/min/μg	% Wild Type	Debromination assay mOD/min/μg	% Wild Type
pAD768 (WT)	160.7 ± 9.8	100.0	0.19 ± 0.02	100.0
A302	30.7 ± 1.2	19.1	0.06 ± 0.01	30.2
G302	74.1 ± 2.3	46.0	0.69 ± 0.13	363.2

Table 9 Site-directed mutants of the DRTG surface loop of VZV thymidylate synthase

All variants were derivatives of pAD768 expressed in *E. coli* strain X2913. Assays were performed on crude extracts.

can participate in the partial reaction with a much greater efficiency than that of wild-type enzyme with an approximate 3-fold increase (Table 9) in its debromination ability. In stark contrast this mutant cannot turnover substrate at wild-type levels being approximately 2-fold reduced in its ability to release tritium from [5-³H] dUMP (Table 9).

Purification of these two C-terminal mutant proteins as previously described for the DRTG loop variants allowed K_m values to be determined for substrate and cofactor. These data complement the crude extract studies. The mutant enzyme A302 has a K_m of 7.03 μ M for dUMP (table 10) representing a 1.4-fold increase over that of wild-type (5.0 μ M) indicative of its reduced ability to bind substrate. Its inability to complete the catalytic reaction and thus turnover substrate is also reflected in its K_m for folate (147.47 μ M) which is an almost 6-fold increase. The addition of an alanine to the C-terminus results in an enzyme that has a reduced binding capacity for both the substrate and cofactor. Extending the C-terminus with a glycine residue (G302) has a similar effect on the K_m for folate (table 10) as that of the mutant A302 in that it is increased approximately 7-fold (176 μ M). However, its ability to bind substrate is significantly increased, reflected in a much lower K_m value (1.86 μ M) representing an approximately 2.5-fold decrease. It appears that addition of a glycine results in an enzyme with a greater affinity for the substrate, but a reduced affinity for the cofactor.

Expressed enzyme	K_m for dUMP	K_m for CH ₂ H ₄ folate
Wild-type TS	5.0 \pm 0.31	25.77 \pm 2.20
A302 TS	7.03 \pm 1.51	147.47 \pm 51.2
G302 TS	1.86 \pm 0.88	176.00 \pm 22.87

Table 10 K_m values for dUMP and CH₂H₄ folate of wild-type VZV TS, and variants with mutations in the C-terminal region.

Activities are expressed as mean \pm standard error of the mean

2.2 Molecular modelling of the VZV C-terminal Mutants

Both the mutants A302 and G302 were not modelled on the VZV ternary structure. As both mutants lie at the end of the protein precise positioning of the side-chains in 3 dimensions is difficult as there are no residues immediately in close proximity with which to constrain its position .

Alanine, although a small uncharged hydrophobic amino acid does affect the catalytic reaction of TS. This extra methyl group (and peptide backbone) presumably does somehow interfere with the closing down of the active site. As both folate and dUMP binding is affected this residue may clash with either the C-terminus and/or the DRTG loop. Perhaps it may exert this effect by bringing some order to the C-terminus in the unliganded state placing it in such a position as to sterically hinder binding of ligands. The solved crystal structure of this mutant will be the way forward in assessing what is happening at the structural level.

Glycine is much smaller than alanine, but is also uncharged. Although there is little difference between the two residues they have contrasting effects on the enzyme. A glycine at this position may interfere with the H-bond between arginine 38 and leucine 301. This may 'hold' the enzyme in a more open conformation thus allowing more efficient binding of dUMP. However as the active site cannot readily close down folate binding is affected, presumably as it can leave the active site easily before catalysis has begun.

2.3 Folate inhibitors and phenolphthalein

Many folate based inhibitors of TS have been developed, the most notable one being 10-propargyl-5, 8-dideazafolate (CB3717). Although CB3717 has an inhibition constant (K_i) of 40nM (Shoichet *et al* 1993) for TS, it shows liver and kidney toxicity. This toxicity emphasises the need for more efficacious agents whether based on derivatives of the folate cofactor or not. Anti-TS drugs dissimilar to the substrate and cofactor remain attractive because they are less likely to have the side effects that are produced by the nucleotide and folate mimics.

The structure based approach to drug design couples critical protein and nucleic acid structural information with specialised computer programmes to propose novel enzyme inhibitors and other therapeutic agents. One such computer programme, DOCK (Kuntz 1992), has been developed and used on thymidylate synthase.

From an X-ray crystallographic structure of the macromolecule, DOCK first characterises the surface of a localised site (the active site in the case of thymidylate synthase) filling it with sets of overlapping spheres. This serves as the negative image of the active site. The second step in the programme's algorithm searches 3D databases (such as the fine chemical directory) for putative ligands, matches them to the negative image and ranks each candidate on the basis of the best orientations for a particular molecular confirmation. Use of DOCK on thymidylate synthase has led to the discovery of a novel TS inhibitor, namely, phenolphthalein (PTH). DOCK finds ligands that fill the entire active site cavity, rather than analogues of substrate or cofactor alone. As such PTH can be considered as a substrate-folate mimic.

Three C-terminal mutants, namely L301 Δ (Harrison *et al* 1995), A302 and G302 were assayed for activity by the tritium release assay in the presence or absence of phenolphthalein or a series of antifolates (at 30ng/ μ l). The antifolates (analogues of CB3717) were a gift from Imperial Chemical Industries plc and were called ICI-1 to ICI-8. Assays were performed in triplicate on two independent extracts.

Mutant L301Δ		
Inhibitor	% Activity	
	Wild-type	Mutant
ICI 1	0.9 \pm 0.15	7.4 \pm 2.3
ICI 2	2.8 \pm 1.1	4.4 \pm 0.4
ICI 3	7.1 \pm 1.8	4.8 \pm 1.3
ICI 4	17.4 \pm 4.2	6.9 \pm 1.6
ICI 5	23.4 \pm 2.1	3.2 \pm 0.4
ICI 6	3.3 \pm 0.6	1.3 \pm 1.0
ICI 7	3.1 \pm 1.7	1.5 \pm 1.0
ICI 8	23.8 \pm 2.7	29.3 \pm 4.9
PTH (50 μ M)	61.9 \pm 2.1	87.8 \pm 3.6
PTH (100 μ M)	47.0 \pm 5.8	79.6 \pm 7.0

Table 11 Inhibition of mutant L301 Δ by folate analogues and phenolphthalein

Activities are expressed as % of the enzyme activity in the absence of inhibitor.

Deletion of the C-terminal leucine from the VZV TS has a marked effect on the ability of the enzyme to resist inhibition by phenolphthalein (Table 11 and Figure 33). At 100 μ M concentrations of PTH the mutant protein is 59% more active than that of the wild-type enzyme. All the folate analogues inhibited both the mutant protein (Table 11) and wild-type, however, L301 Δ appears more resistant to ICI 1 than wild-type (approximately 7-fold more resistant) albeit both are significantly inhibited. It is also slightly more resistant to ICI 2 and 8. Interestingly, L301 Δ is markedly more sensitive to folate analogues ICI 4 and 5 compared to wild-type. The mutant also shows greater sensitivity for analogues ICI, 3, 6 and 7 (2-fold, 0.5-fold, 2-fold, and 2-fold respectively).

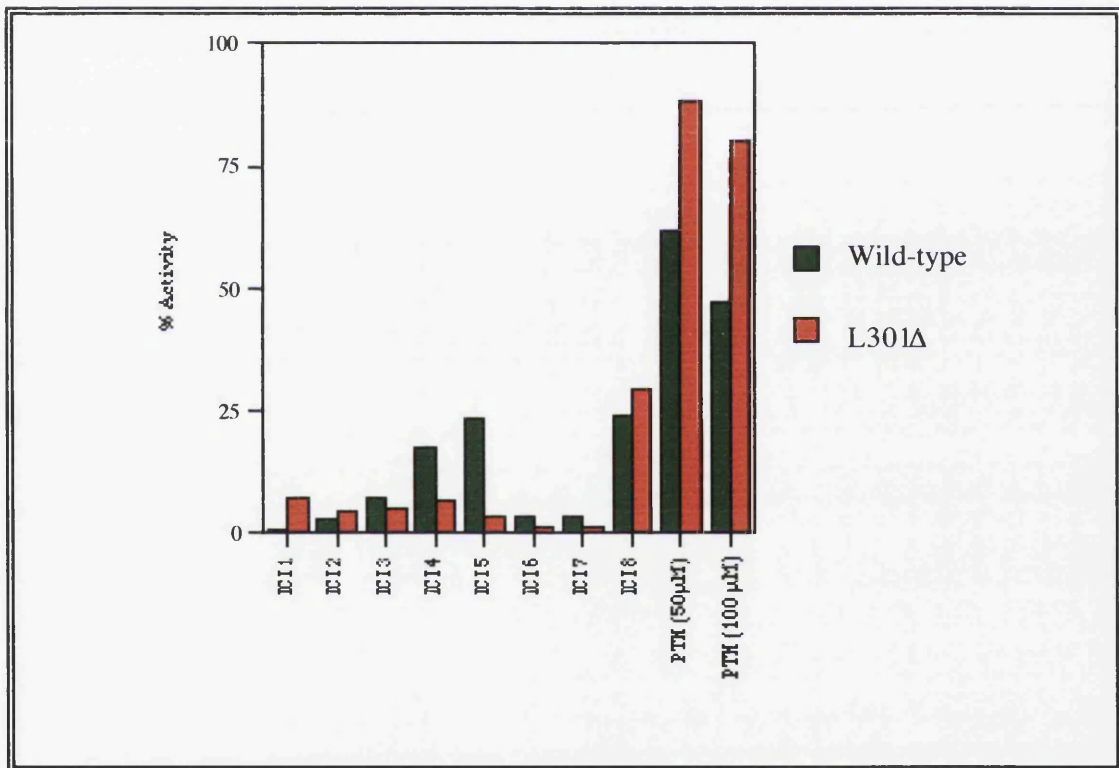


Figure 33. Inhibition of L301 Δ by folate analogues and Phenolphthalein

The mutant A302 shows a different response to the folate analogues (Table 12 and Figure 34) with no greater resistance (compared to wild-type) to the analogues. However, like L301 Δ a greater sensitivity to inhibition is shown for ICI 3, 4 and 5 indicating a similar mechanism of action on the enzyme.

Inhibitor	Mutant A302	
	% Activity	
	Wild-type	Mutant
ICI 1	1.3 ± 0.5	0.8 ± 0.6
ICI 2	1.45 ± 0.6	0.2 ± 0.2
ICI 3	6.4 ± 0.7	1.7 ± 0.8
ICI 4	15.5 ± 2.1	2.2 ± 0.25
ICI 5	23.4 ± 2.2	2.9 ± 0.6
ICI 6	3.0 ± 1.0	0.2 ± 0.2
ICI 7	1.9 ± 0.8	0.3 ± 0.25
ICI 8	23.5 ± 5.0	8.4 ± 2.1

Table 12 Inhibition of mutant A302 by folate analogues

Activities are expressed as % of the enzyme activity in the absence of inhibitor.

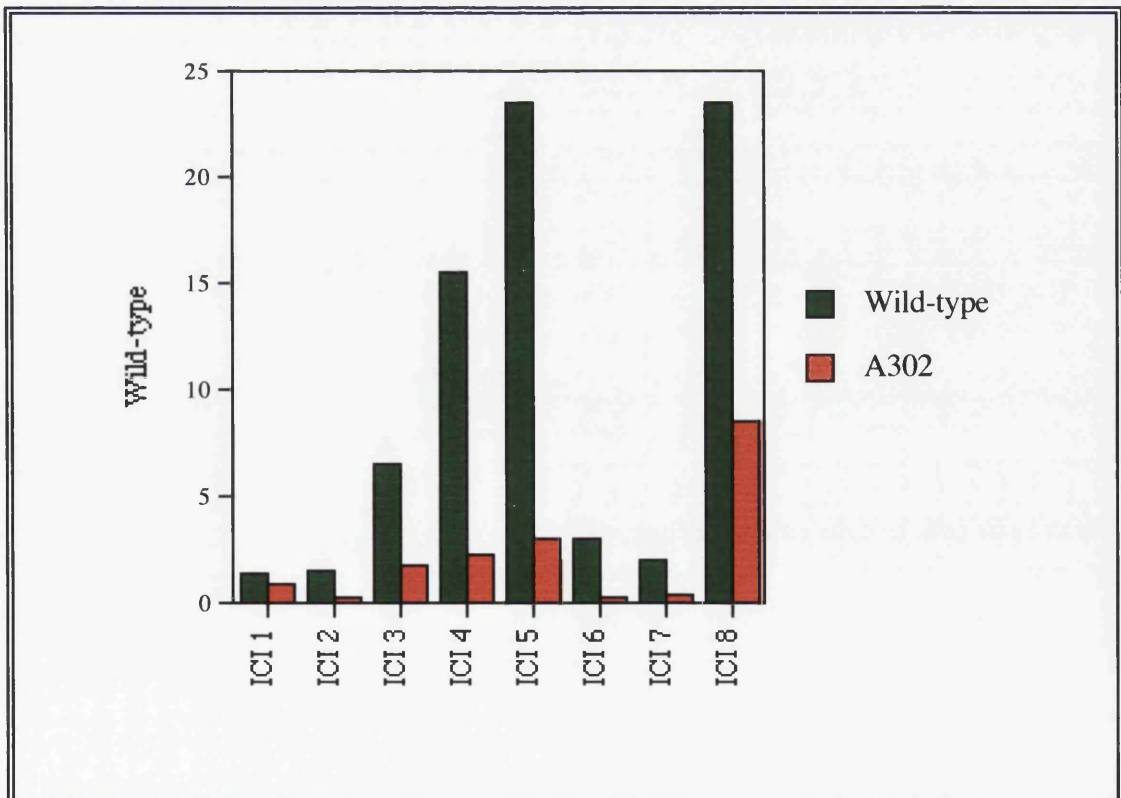


Figure 34. Inhibition of A302 by folate analogues.

G302 exhibits resistance to phenolphthalein being approximately 2-fold more resistant than wild-type at 100 μ M (Table 13 and Figure 35). Extension of this study revealed that the G302 can be inhibited by phenolphthalein (17% remaining activity at 1mM, data not shown) but still represents a resistance to inhibition by phenolphthalein. This perhaps is reflected by G302's higher affinity for the substrate dUMP, and thus its preference for this over the inhibitor phenolphthalein. In comparison, G302 is more sensitive than wild-type to inhibition by all the folate analogues with the exception of ICI 1 in which it shows a very slight resistance (Table 13). As for the other C-terminal mutant proteins, G302 shows greatest sensitivity to ICI 3, 4, and 5

Mutant G302		
Inhibitor	% Activity	
	Wild-type	Mutant
ICI 1	0.9 ± 0.05	1.7 ± 0.4
ICI 2	2.7 ± 0.2	0.8 ± 0.1
ICI 3	6.4 ± 1.0	2.1 ± 0.2
ICI 4	18.2 ± 5.0	3.7 ± 0.8
ICI 5	22.7 ± 3.5	2.7 ± 0.7
ICI 6	4.3 ± 0.1	0.9 ± 0.2
ICI 7	4.0 ± 2.1	0.5 ± 0.3
ICI 8	29.8 ± 3.0	8.3 ± 0.8
PTH (50 μ M)	65.5	74.6
PTH (100 μ M)	56.3	93.4

Table 13 Inhibition of mutant G302 by folate analogues and phenolphthalein

Activities are expressed as % of the enzyme activity in the absence of inhibitor.

Without the structures of the folate analogues it is difficult to make any rational comparisons as to the differences between the inhibition by each analogue. However, this information when coupled to the mutagenic and enzymatic data for these mutants would show that a better understanding of the interactions between the enzyme and ligands could have positive implications for rational drug design. The inhibition studies presented here clearly show that removal of the C-terminal residue of VZV TS can for some analogues (ICI 1, 2, 8 and PTH) produce an enzyme more

resistant to inhibition (Figure 35a). This leads to the speculation that these compounds are very similar in structure and mechanism of inhibition, and presumably need a tight closing down of the active site which the C-terminal leucine carboxylate provides. Extension of the C-terminus with a glycine or alanine renders the resultant protein more sensitive to the folate analogues tested (Figure 35a).

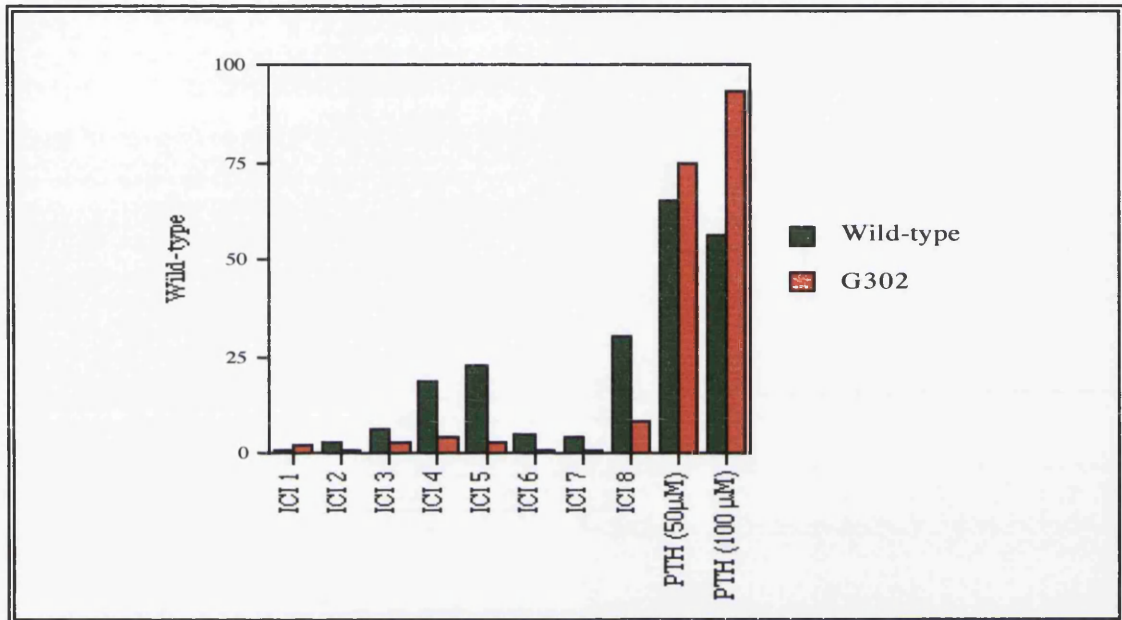


Figure 35. Inhibition of G302 by folate analogues and phenolphthalein

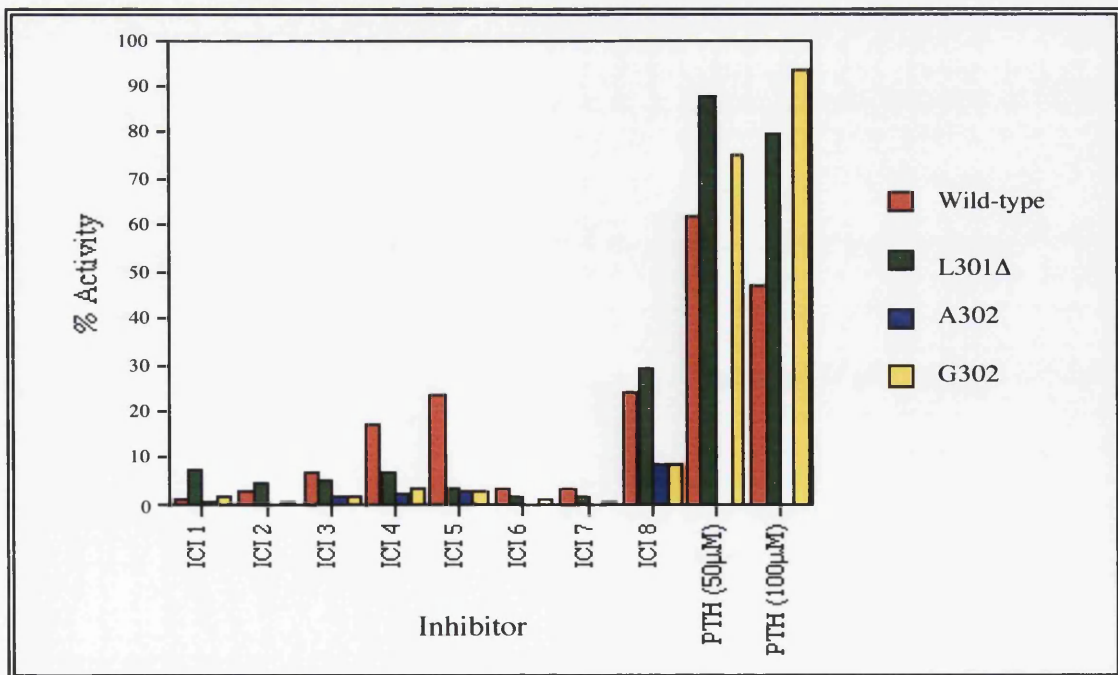


Figure 35a. Comparison of the effects of folate inhibitors and PTH on the C-terminus

2.4 Peptide Inhibition

A series of peptides corresponding to the dimer interface of VZV TS have been previously characterised and shown to inhibit the VZV enzyme (R Thompson and H Marsden, personal communication). VZV TS is speculated to have a different interaction at its C-terminus compared to that exhibited by different members of the TS family (Harrison *et al* 1995). Harrison and co-workers propose that hydrophobic packing in this region may play a more important role in stabilising the ternary complex than does a hydrogen bond network. This proposed species difference in the C-terminal interactions allowed us to probe the potential for selectively inhibiting VZV TS. Based on the proposed unique interaction at the C-terminus of VZV TS we investigated the effect of two peptides corresponding to the last 4 (EMAL) or 5 amino acids (MEMAL) of the C-terminus of VZV TS on enzymatic activity.

A slightly modified tritium release assay (see materials and methods) was used to assay peptide activity. The effect of peptide A on TS activity is given in Table 14 (and graphically in Figure 35) and that of peptide B in Table 15 and Figure 35.

Figure 35 shows the effect of pre-incubating VZV TS with both test peptides and the control peptide 386. The control peptide disrupts the interface between the 2 monomers of thymidylate synthase and its subsequent inhibition of enzyme activity is dramatic (inhibiting activity by 99.7%). However, in contrast both of the peptides to the C-terminus of VZV TS (peptide A [MEMAL] and peptide B [EMAL]) do not exhibit any inhibition of VZV thymidylate synthase. Indeed, both these peptides show a slight increase in activity. Prior to ligand binding the C-terminus is unordered, with no fixed location in space, to increase this disorder and perhaps generate a more open, accessible enzyme the peptide inhibition experiment was repeated at 42°C. This did not result in any change in the inhibition profile of the peptides.

Provision of what amounts to another C-terminal region to the reaction instead of inhibiting the interactions at the C-terminus actually enhances them. This is perhaps mediated through the peptide reducing the amount of shuffling the protein has to do to close down the active site as it does this for the enzyme. This could be more energetically stable. An analogy could be imagined, in that the peptides have an effect similar to that of someone pushing the door shut rather than it closing by itself.

Concentration (mM)	Tritium release assay pmol/min/ μ g	% Wild-type
0	2072.97	100
0.5	2397.74	115
0.6	2494.58	120
0.8	2074.86	100
1.0	1939.29	93
1.2	2173.80	103
1.5	2581.53	124
2.0	2471.29	119
Positive control	7.82	0.3

Table 14 Tritium release assay showing the effect of peptide A (MEMAL)

The positive control was peptide 386 (a peptide that disrupts the interface between the monomers of TS) at 2 μ M. VZV TS was expressed in *E. coli* strain BL21 using a pET8C vector.

Concentration (mM)	Tritium release assay pmol/min/ μ g	% Wild-type
0	2072.97	100
0.5	2065.79	99
0.6	2267.05	109
0.8	2308.62	111
1.0	2490.92	120
1.2	2427.13	117
1.5	2327.86	112
2.0	2563.79	123
Positive control	7.82	0.3

Table 15 Tritium release assay showing the effect of peptide B (EMAL)

The positive control was peptide 386 (a peptide that disrupts the interface between the monomers of TS) at 2 μ M. VZV TS was expressed in *E. coli* strain BL21 using a pET8C vector.

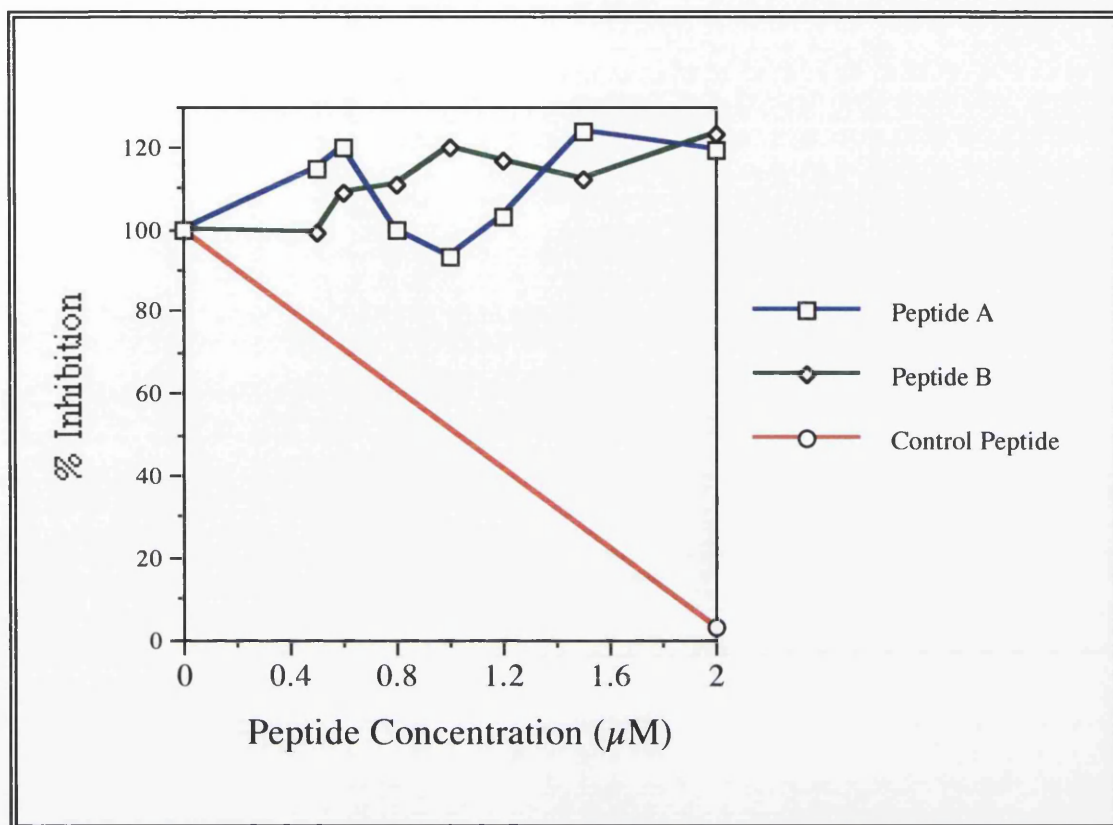


Figure 35. Inhibition of VZV TS by peptides A and B

2.5 Human thymidylate synthase C-terminus Mutants

Based on work in our lab (Harrison 1992, Harrison *et al* 1995) it was proposed that the C-terminus of human TS may well respond in a similar fashion to C-terminal deletion of the *L. casei* and *E. coli* enzyme, namely total inactivation. The human thymidylate synthase mutant V313 Δ was made to investigate this hypothesis.

Site directed mutagenesis using the appropriate oligonucleotide was employed to construct the mutant V313 Δ in NM522 Thy⁻ cells. Screening all colonies whether or not they were Thy⁻ yielded the correct mutation. Complementation data indicates a Thy⁺ phenotype for this mutant. Sequencing confirmed the desired mutation was the only change introduced.

V313 Δ , like the VZV mutant L301 Δ , can perform the partial (debromination) reaction at wild-type levels (Table 16) indicating that substrate binding is not impaired. Again, as for the VZV C-terminal truncation, V313 Δ can turnover

substrate (Table 16) which is in stark contrast to the *L. casei* and *E. coli* C-terminal deletion mutant.

Expressed enzyme	Tritium release assay pmol/min/ μ g	% Wild Type	Debromination assay mOD/min/ μ g	% Wild Type
Human WT	94.9 \pm 7.6	100.0	0.15 \pm 0.02	100.0
V313 Δ	15.2 \pm 1.6	16.0	0.14 \pm 0.02	93.0

Table 16 Site-directed mutant of the Human TS.

All variants were derivatives of pAD876 expressed in *E. coli* strain λ 2913.

A significant difference between the response of VZV and human TS to truncation of the C-terminus is worthy of comment. The human mutant retains 16% of wild-type activity compared to 3% in the VZV C-terminal truncation.

2.5 Phenolphthalein inhibition of human thymidylate synthase

The human C-terminal mutant was tested against the TS inhibitor phenolphthalein to assess its sensitivity compared to that of wild-type enzyme. Deletion of the C-terminal valine does not make the enzyme any more or less sensitive to inhibition (Table 17 and Figure 36). The VZV mutant L301 Δ and G302, in contrast, is more resistant (less sensitive) than the wild-type VZV enzyme.

Enzyme	Phenolphthalein Concentration (μ M)	% activity
WT human TS	0	100.0
	50	68.5
	100	38.1
V313 Δ	0	100.0
	50	78.9
	100	25.3

Table 17 Inhibition of human TS and V313 Δ by phenolphthalein

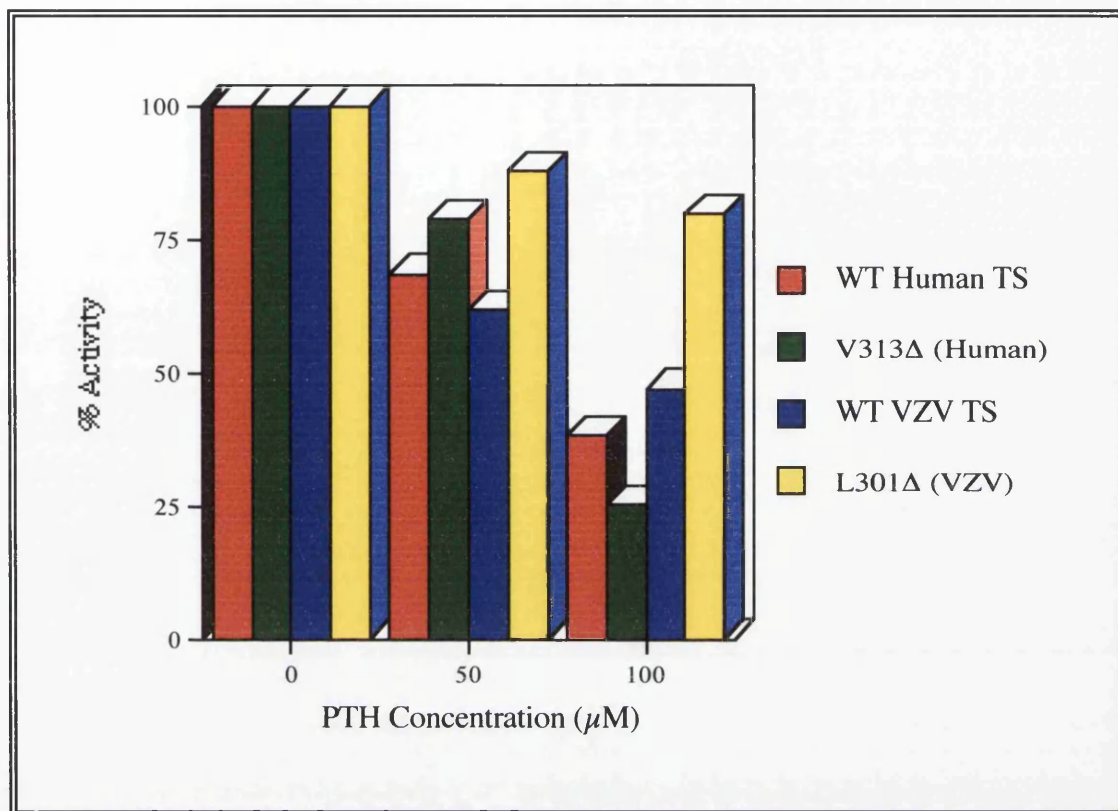


Figure 36. Inhibition of TS C-terminal truncation mutants by phenolphthalein. Wild-type VZV TS and the VZV mutant L301 Δ are also shown for comparison.

2.6 Summary

Previous studies indicated the important role the C-terminal region has upon the function of the enzyme and the mutants A302, G302, and V313 Δ complements an already interesting picture of the role of the C-terminus in both VZV and human thymidylate synthase.

The importance of the C-terminus is emphasised by all the mutants as they all effect catalysis to varying degrees. Extension of the VZV C-terminus has radically differing effects depending on what residue is added. Interestingly, due to the critical nature of this residue in the bacterial enzymes, extending this region would be expected to drastically inhibit catalysis. While this is true to some degree with the mutant A302 (a 5-fold reduction in substrate turnover), it is less adversely affected by addition of a glycine residue (a 2-fold reduction). As glycine is the smallest of the amino acids and has no charge, this perhaps is not surprising. What is unexpected is

the effect a glycine addition has on the ability of the enzyme to bind substrate (increasing its ability 3-fold). Due to the difficulties in modelling such mutants it is near impossible to speculate as to what is happening at a structural level. One may think that on a surface region of a protein any insertions would be tolerated more readily, and in particular, in one that is relatively unordered prior to ligand binding. Perhaps, the importance of the DRTG loop should not be underestimated in its role in the catalytic function of thymidylate synthase. Any addition, particularly such small residues, probably can easily be orientated in surface regions as to point out to solvent (provided they are not hydrophobic). However, as the C-terminus becomes more ordered upon ligand binding and is tightly packed against the bottom of the active site, the DRTG loop packs against it and as such may limit the orientation the additional residues can adopt. Such clashes in this region have already been shown to have dramatic effects upon catalysis.

Analysis of folate inhibitors is useful because it can help probe the role of those residues in catalysis. The importance of the C-terminus is illustrated by the effects the folate analogues have on the different mutations. Addition of glycine or alanine in general makes the enzyme more sensitive to the ICI folate analogues, as does removal of the C-terminal leucine. Conversely, all these mutants are less sensitive to phenolphthalein indicative of the different nature of interaction these compounds have with the enzyme. The human TS C-terminal deletion mutant V313 Δ is much more sensitive (3-fold) to phenolphthalein than its VZV counterpart. This adds weight to the suggestion that the human TS has a different interaction at the C-terminus than that of VZV TS.

Peptide inhibition of biologically important interactions can help in our understanding of the role of these interactions by providing data on the nature and type of interaction that occurs. It also provides a way of inhibiting such interactions such that new peptide like moieties can be used as anti-infectives against various protein-protein interactions. That VZV is an obligate dimer is elegantly illustrated by its inhibition with a peptide that disrupts the interaction between the two monomers. It binds between the dimer interface to one of the monomers thus preventing dimerisation. As the interaction at the C-terminus of VZV TS was speculated to be different to that of all the other TS enzymes (human included), it was an obvious target for a peptide inhibition experiment. Due to this speculated difference and that the C-terminus is important in catalysis it may provide a potential exploitable difference between the human and VZV enzymes for anti-viral agents. Despite that no inhibition was observed it does confirm the importance of this region. Provision

of a peptide targeted to the C-terminus enhanced the ability of the enzyme to carry out its natural catalytic function.

3. Temperature sensitive mutants

Temperature-sensitive mutants are an efficient way of identifying amino acid positions which are critical for protein stability. We have developed a highly efficient method to isolate such mutants based on the use of 'spiked oligonucleotides.

3.1 Construction and screening of temperature-sensitive mutants

Oligonucleotides targeted to buried regions in the protein structure were chosen (Table 19) for random mutagenesis as these would have more effect on the structure of the protein. Mutant dsDNA was transformed using the PEG/DMSO method into *E. coli* strain NM522 Thy⁻. Colonies that were ampicillin resistant were patched on to minimal media (M9) alone or minimal media supplemented with thymidine and incubated overnight at either 30°C, 37°C or 42°C. Temperature-sensitive isolates were selected on their ability to grow in the absence of exogenous thymidine at low but not high temperatures (Figure 37). Phenotype was assigned on the basis of growth on minimal media (M9) in the absence of thymidine, where strong growth is Thy⁺, no growth Thy⁻ and weak growth Thy^{+/-}.

Sequencing of the temperature sensitive mutants was carried out using the appropriate oligonucleotide and the mutations obtained are detailed in table 20 along with the areas of TS secondary structure they affect.

OLIGO	SIZE	REGION OF TS GENE	AMINO ACID SEQUENCE	SECONDARY STRUCTURES
R09	54mer	613-667	205-223	β -Strand iii 205, 206 Helix-J 207-222
R010	54mer	654-708	219-237	β -Strand ii 235-237 Helix-J 219-230
R011	54mer	698-752	234-252	β -Strand ii Helix-k 252
R015	57mer	339-396	114-133	Helix-G
R016	54mer	416-470	140-158	Helix-H

Table 19 Random oligonucleotides and the region of VZV TS they targeted

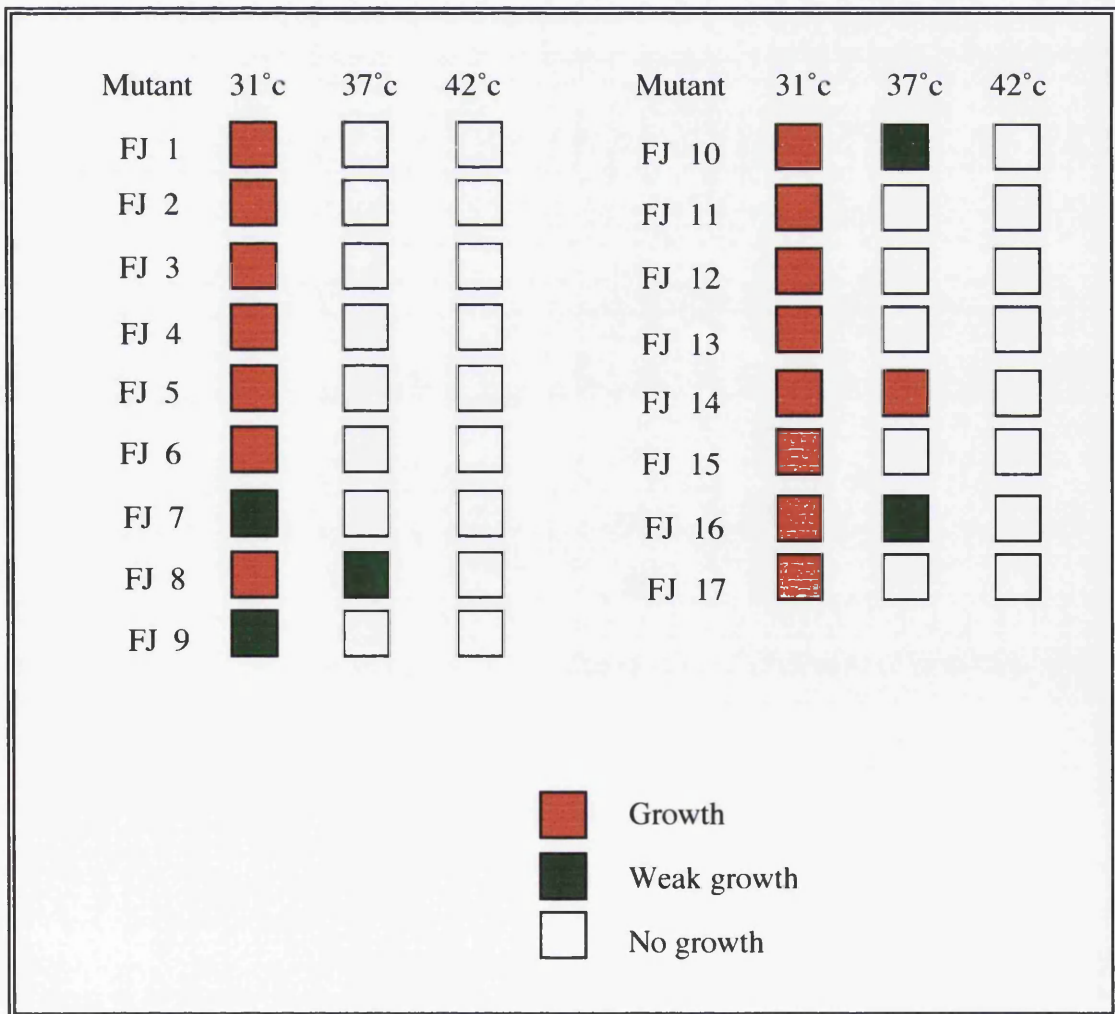


Figure 37 Phenotypes of the isolated temperature-sensitive mutants of VZV TS

Mutant	Gene position	Nucleotide change(s)	Amino acid change(s)	Secondary structure(s) affected
FJ 1 [§]	621	1 base deletion	Frame shift	
	657	GCA → GCG	Ala 219 → Ala	Helix J
FJ 2 [§]	626	1 base deletion	Frame shift	
	649	GGA → GAA	Gly 217 → Glu	Helix J
FJ 3	615	GGG → GGT	Gly 205 → Gly	β-strand iii
	625	CTT → TTT	Leu 209 → Phe	Helix J
FJ 4*	646	GCT → TCT	Ala 216 → Ser	Helix-J
FJ 5	647	GCT → GAT	Ala 216 → Asp	Helix-J
FJ 6	693	CTT → CTC	Leu 231 → Leu	Loop between Helix J and β-strand ii
FJ 7	678	GCG → GC	Ala 226 → Ala	Helix J
	687	ACA → GCA	Thr 229 → Ala	Helix J
FJ 8 [§]	653	TAT → TNT	Tyr 218 → ?	Helix J
FJ 9 [†]	753-754	70 base insertion	Frame shift	Before Helix K
FJ 10	714	CAT → CAG	His 238 → Gln	β-strand ii
FJ 11	381	TGG → TGT	Trp 127 → Cys	Helix G
	386	CAT → CCT	His 129 → Pro	Loop between Helix G and Helix H
FJ 12	350	GGG → GAG	Gly 117 → Glu	Loop between Helix D and Helix G
	354	CAG → GAG	Gln 126 → Glu	Helix G
	367	TAC → AAC	Tyr 123 → Asn	Helix G
	370	GGC → AGC	Gly 124 → Ser	Helix G
FJ 16	390	TTT → TTA	Phe 130 → Leu	Loop between Helix G and Helix H

Table 20 Sequence changes found in temperature-sensitive mutants

[§] The single base deletion results in a stop codon at position 670 (Ile 224)

* A double-priming event occurs in which the sequence loops back to position 593 (Cys 198) until position 664 (Thr 222) where it continues out of frame until a stop codon at position 670

[§] Nucleotide change undetermined

[†] A double-priming event resulting in a 70 amino acid insert (16 bases of unknown origin plus the original random oligo) and a frameshift culminating in a stop codon at position 799 (Leu 267)

FJ 13, FJ 14, FJ 15 and FJ 17 sequence data not determinable

Use of the spiked oligonucleotides towards buried regions of VZV TS was successful in that it generated several temperature sensitive proteins. However, table 20 illustrates one drawback such an approach to mutagenesis has because in addition to the temperature sensitive mutants, several unexpected variants were found. These comprised mainly of single base deletions, but one FJ 9 contained a 70 base insertion. One explanation could be that due to the degenerate nature of the spiked oligonucleotides, mis-priming events are more common than for site-directed mutagenesis. Indeed, this may explain why many of the clones examined for covariant residues of the DRTG loop exhibited a Thy⁺ phenotype but had no changes in the TS gene. Subsequent studies in our lab (J Boffey, personal communication) using spiked oligonucleotides targeted to different regions of VZV TS have produced similar findings. This does not make this approach to mutant generation invalid because overall the number of useful mutants outweighs the erroneous ones.

The generation of temperature sensitive mutants illustrates that such an approach to generate covariant residues which would revert the phenotype of the DRTG loop mutants was justified.

3.2 Molecular modelling of temperature-sensitive mutants

Molecular modelling was performed on a selection of the temperature sensitive mutants. Those that had undetermined sequence or contained frame shifts (and hence stop codons would result in truncated proteins) were not modelled due to the difficulties these would pose, as would FJ 9 with a 70 base insertion. Mutations were introduced into the VZV model using the programme SwissModler and visualised using the programme O on an Iris Indigo 2. Final output files were labelled using Showcase and saved as RGB images with Snapshot, converted to TIFF format for manipulation in Photoshop.

The temperature sensitive mutants have been illustrated with the original wild-type residue superimposed onto the new variant residue. For clarity the wild-type amino acid is shown in light blue. However, the original or mutant side chain is not always visible due to size differences or near perfect superimposition.

Mutation FJ 3 contains the substitution L209F, which is one of the highly conserved residues involved in van der Waal radii contacts with the PABA ring of folate. Phenylalanine 213 also plays a role in formation of this hydrophobic pocket for the PABA ring. L209F appears to be a direct substitution of a like residue for like (in terms

of function) as both can form the hydrophobic pocket which surrounds the PABA ring. The model indicates that there is a big space that the phenylalanine could occupy, perhaps facilitated by methionine 297 and 299 moving slightly out of the way. It may also be the case that the phenylalanine protrudes slightly more into the hydrophobic pocket reducing the cofactor binding.

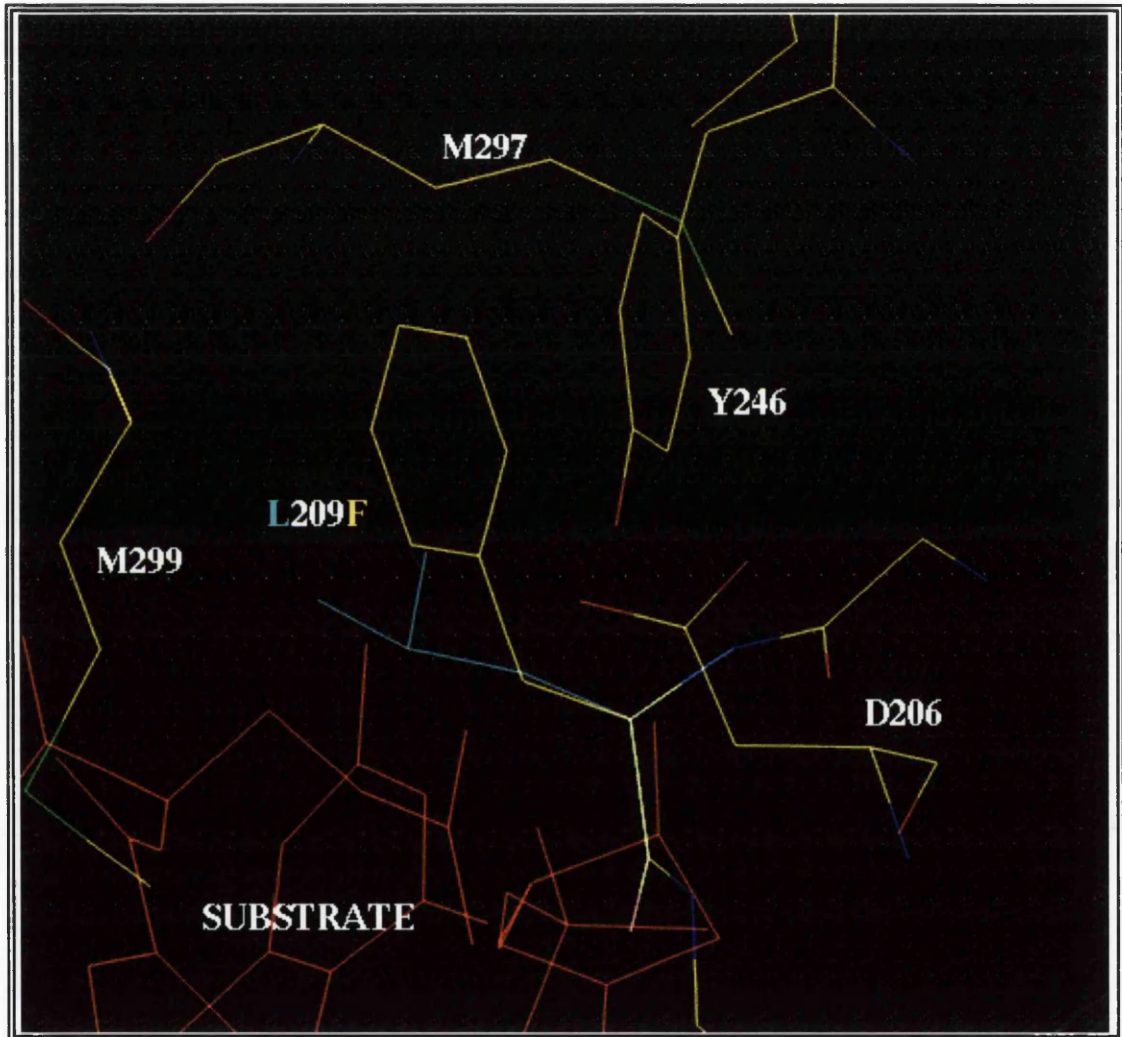


Figure 37 Temperature sensitive mutant FJ 3, showing the mutation L209F

The original wild-type residue is shown in light blue, next to the mutated residue. Several other amino acids are shown for reference.

Substitution of alanine with aspartic acid (A216D) in the mutant FJ 5 is illustrated in figure 38. The bigger, charged aspartic acid is easily accommodated by pointing out towards the surface despite this substitution occurring in the buried J-helix. This region undergoes segmental accommodation during ligand binding and thus may be

able to tolerate changes more freely because it is not a fixed structural part of the protein.

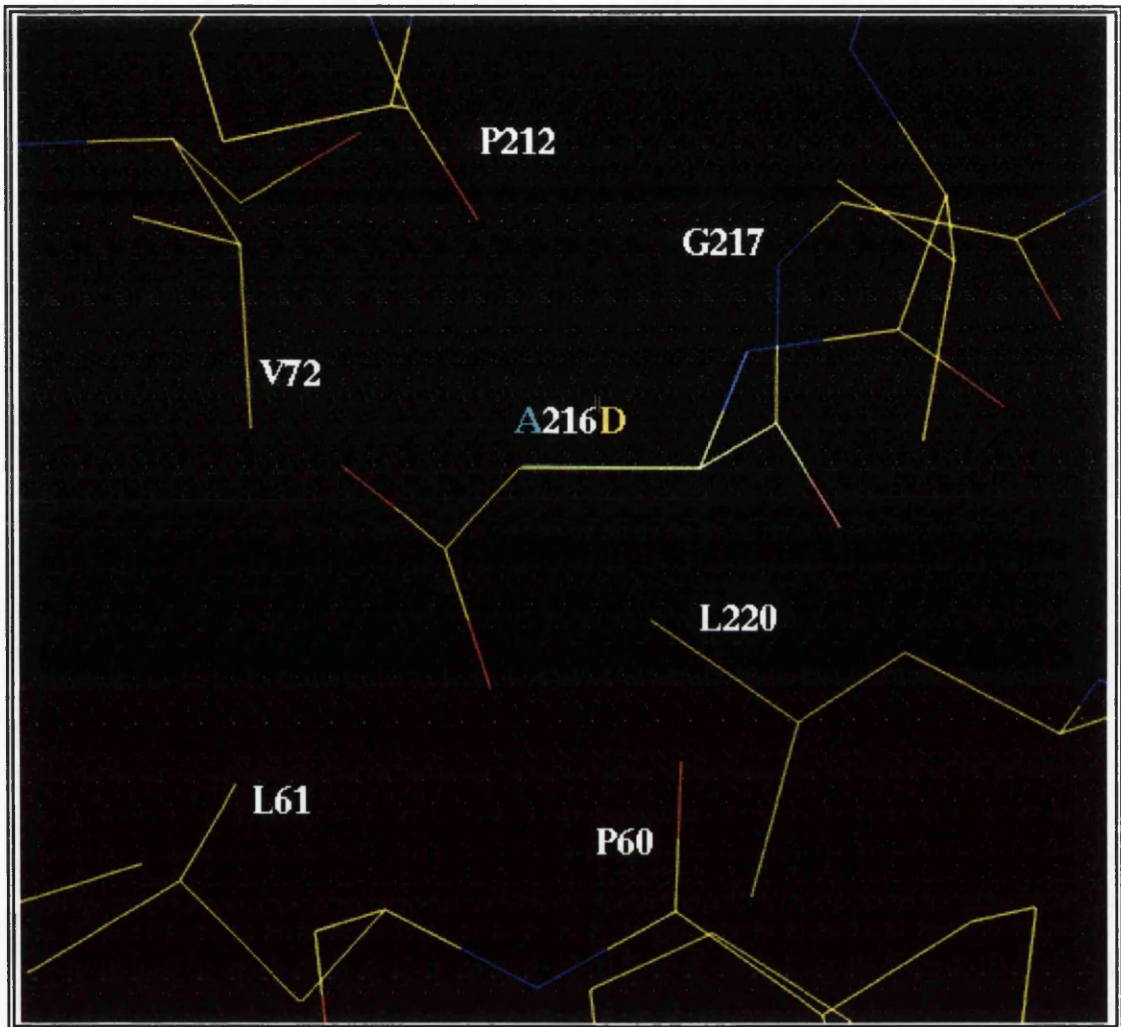


Figure 38 Temperature sensitive mutant FJ 5, showing the mutation A216D

The original wild-type residue is shown in light blue, next to the mutated residue. Several other amino acids are shown for reference.

The central J helix appears to tolerate amino acid substitutions more readily than anticipated. Due to its helical nature and the fact that its buried within the TS structure, substitutions in this region were thought to be more disruptive. However, disruption of protein stability is a consequence of such tolerance as exhibited by the temperature sensitive phenotype of mutant FJ 7 (Figure 39). The much smaller alanine can easily be accommodated, but it does not have the branched methyl or

hydroxyl groups of threonine. Presumably these are important for stabilising this region of the protein.

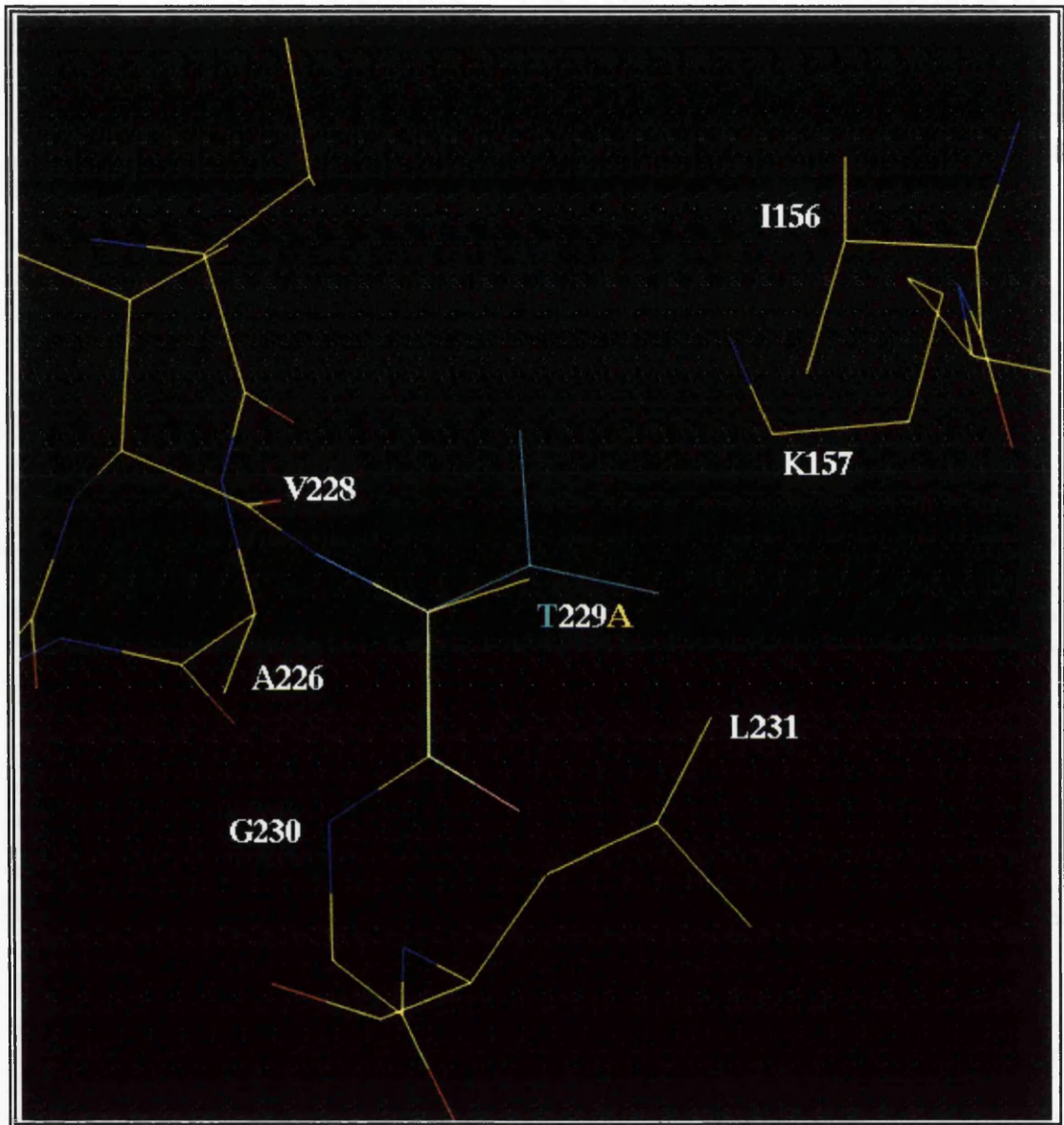


Figure 39 Temperature sensitive mutant FJ 7, showing the mutation T229A

The original wild-type residue is shown in light blue, next to the mutated residue. Several other amino acids are shown for reference.

The almost fully conserved histidine at position 238 is located at the beginning of β -strand i and can be substituted for a tryptophan (*E. coli*), a tyrosine (*L. lactis*), and a phenylalanine (phage T4 and Φ 3T). TS can also tolerate other substitutions at this position, as FJ 10 has a glutamine at this position. Its position at the beginning of the

β -strand allows it to position the variant residues such that they point out to solvent (Figure 40).

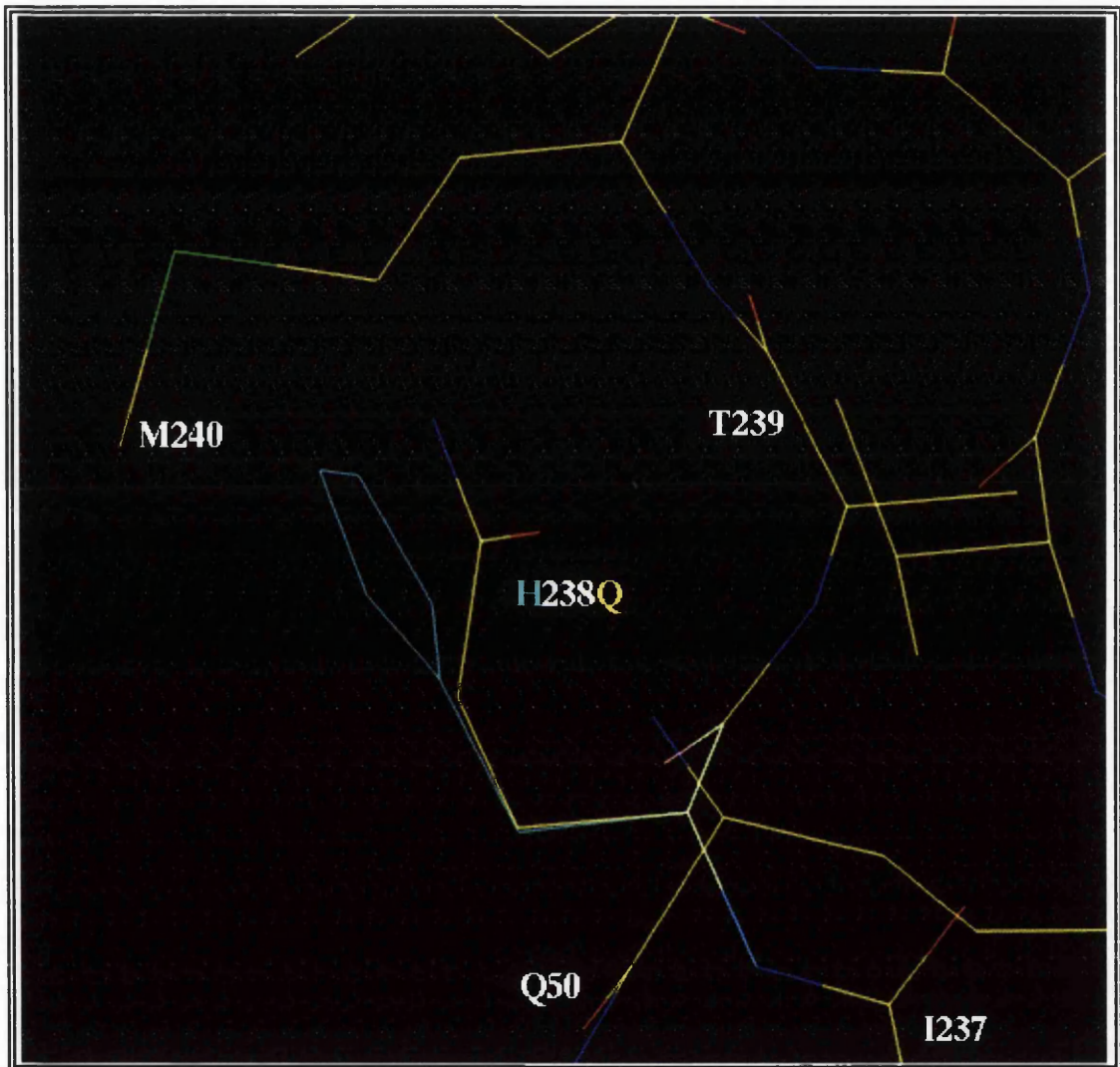


Figure 40 Temperature sensitive mutant FJ 10, showing the mutation H238Q. The original wild-type residue is shown in light blue, next to the mutated residue. Several other amino acids are shown for reference.

Mutant FJ 11 has the substitution W127C, a residue located at the end of β -strand ii, and as like FJ 10 can position any unfavourable side chains into solvent. Interestingly, Tryptophan at position 127 is over 80 % conserved throughout the TS family.

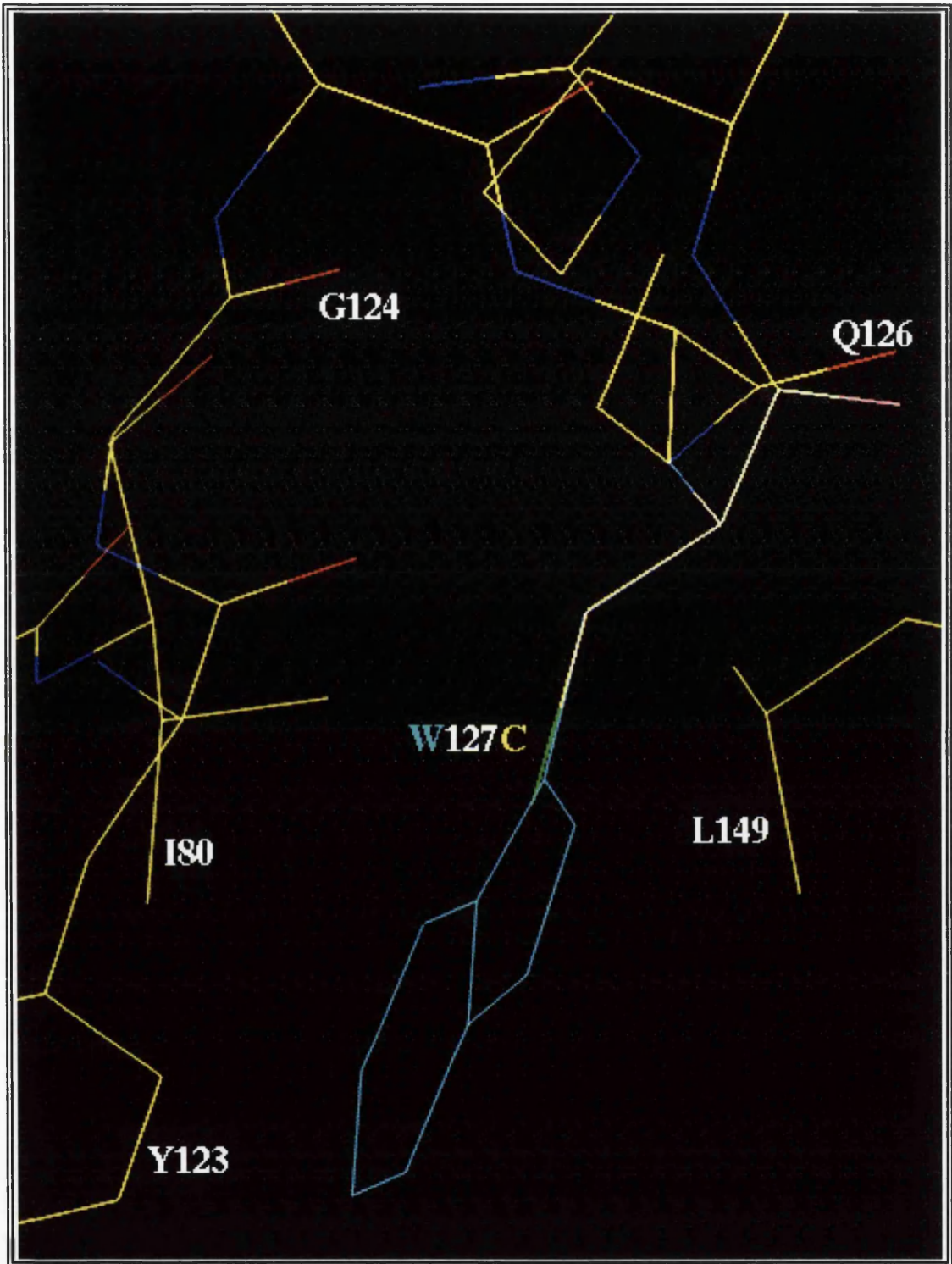


Figure 41 Temperature sensitive mutant F J11, showing the mutation W127C
The original wild-type residue is shown in light blue, next to the mutated residue. Several other amino acids are shown for reference.

The temperature sensitive mutant FJ 11 also contains the substitution H129P. This proline residue may disrupt the protein backbone at this position (Figure 42), implicating this residues role in protein stability.

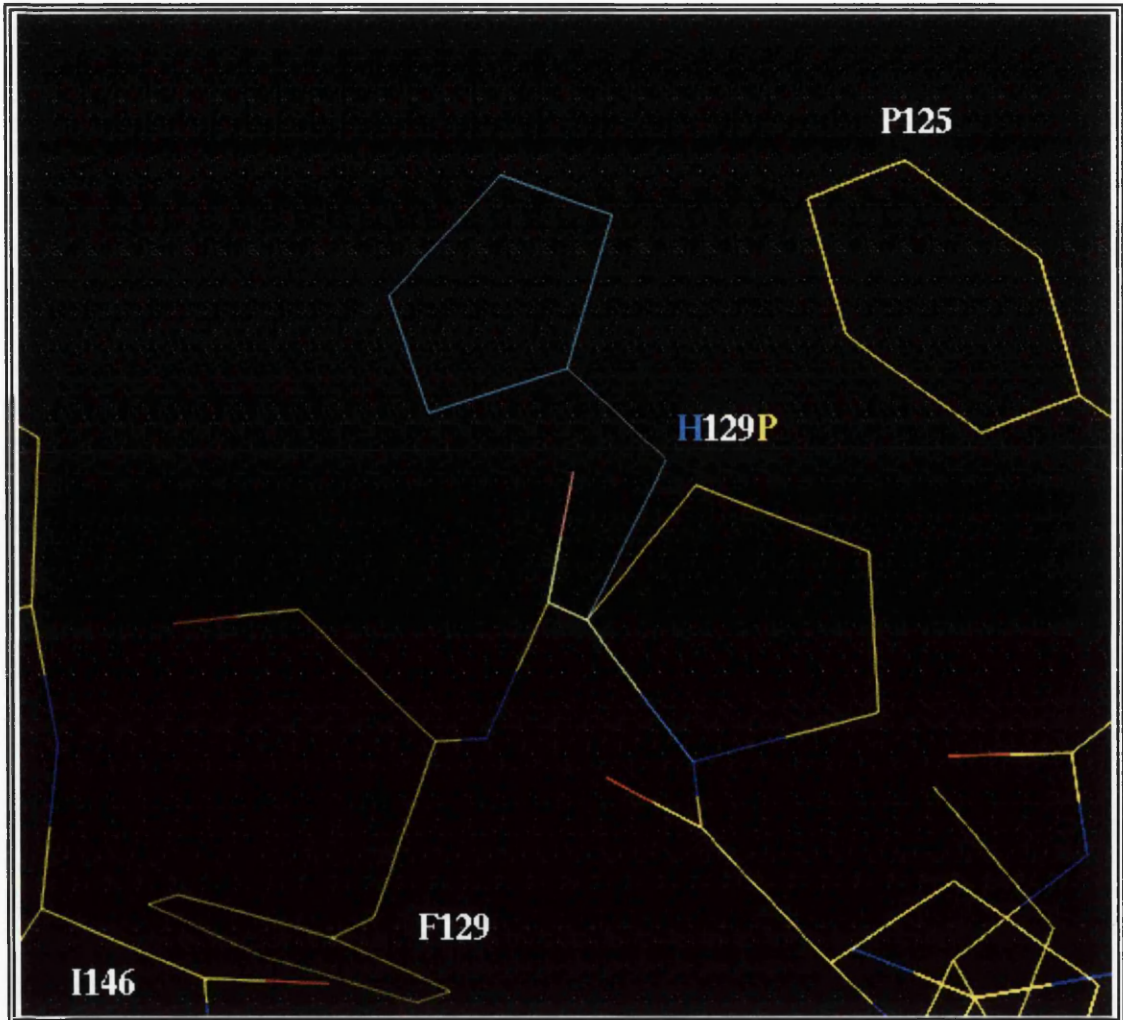


Figure 42 Temperature sensitive mutant FJ 11, showing the mutation H129P

The original wild-type residue is shown in light blue, next to the mutated residue. Several other amino acids are shown for reference.

The mutant FJ 12 contains four substitutions G117E, Q126E, Y123N, and G124S. All are located in helix G with the exception of G117E which is located in the loop before helix G. Amino acid tyrosine 123 and glycine 124 are fully conserved throughout the TS family, illustrating the conservation paradox. Clearly these fully conserved residues can be substituted for different amino acids without total loss of

function. The substitution G117E is shown in figure 43 and illustrates that in surface loop areas, variant side chains are more easily accommodated.

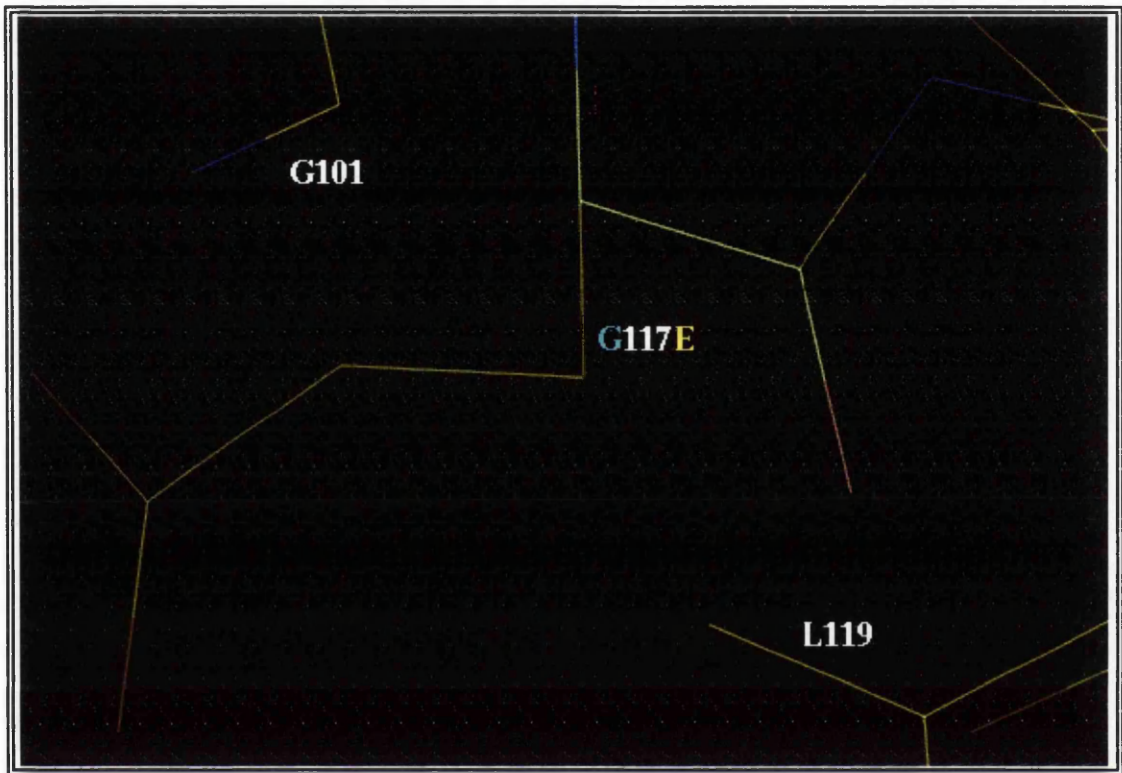


Figure 43 Temperature sensitive mutant FJ 12, showing the mutation G117E

The original wild-type residue is shown in light blue, next to the mutated residue. Several other amino acids are shown for reference.

The substitution of glutamine with the almost identical glutamic acid does not appear to perturb the local structure (Figure 44). Perhaps this mutant alone would not lead to a temperature sensitive phenotype.

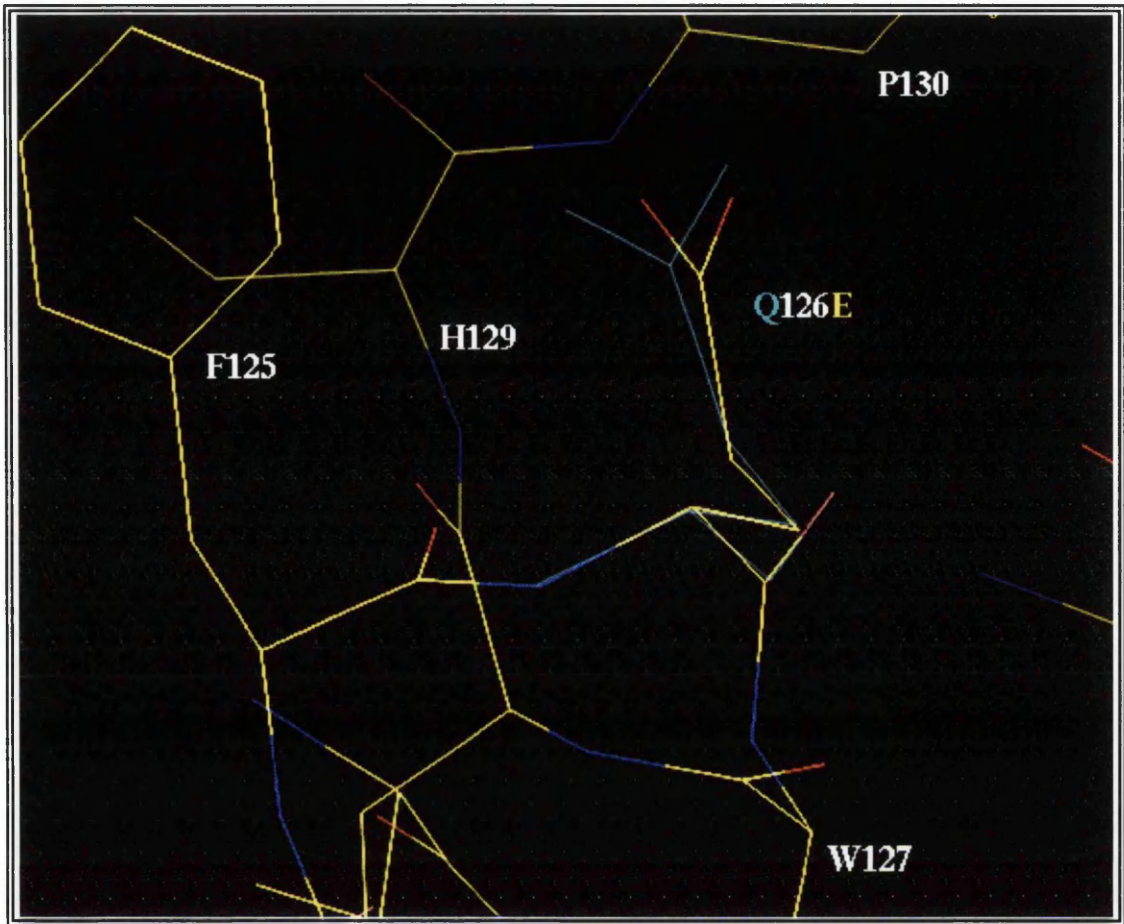


Figure 44 Temperature sensitive mutant FJ 12, showing the mutation Q126E

The original wild-type residue is shown in light blue, next to the mutated residue. Several other amino acids are shown for reference.

As for the previous mutation (Q126E) within FJ 12, replacement of tyrosine 123 with asparagine can easily be accommodated because asparagine is much smaller than tyrosine (Figure 45). However, reduction in the volume occupied by the asparagine residue may account for the phenotype of FJ12.

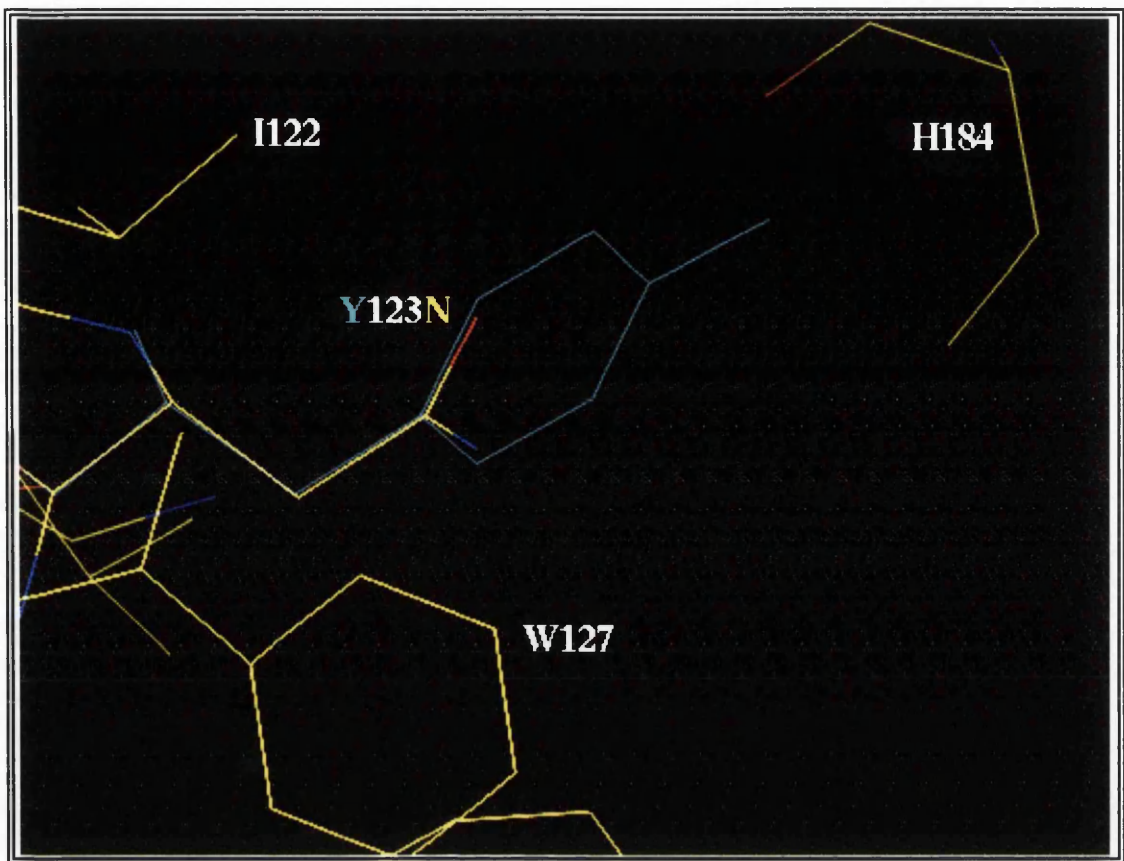


Figure 45 Temperature sensitive mutant FJ 12, showing the mutation Y123N

The original wild-type residue is shown in light blue, next to the mutated residue. Several other amino acids are shown for reference.

The last substitution in FJ 12 is G124S. Glycine 124 is fully conserved and may be important in maintaining the overall structure of the helix G. Figure 46 illustrates this mutation within VZV TS. The extra CH_2OH group that is different in serine compared to glycine may cause small distortions in this tiny helix, although it can be orientated so it points out to solvent.

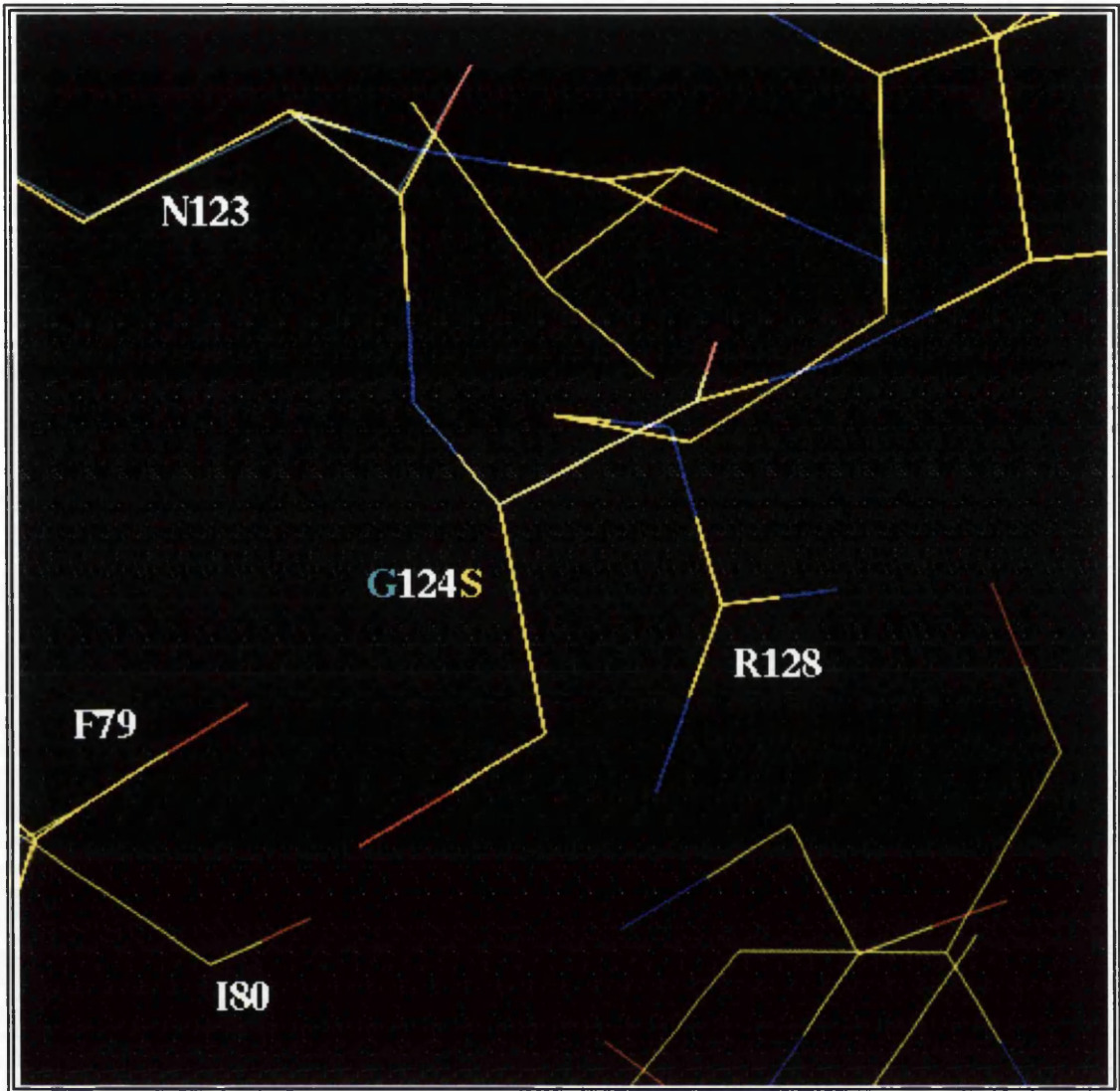


Figure 46 Temperature sensitive mutant FJ 12, showing the mutation G124S

The original wild-type residue is shown in light blue, although cannot be seen because it superimposes exactly below the mutant residue. Several other amino acids are shown for reference.

The final temperature sensitive mutant examined contains the substitution F130L (FJ 16). Leucine can easily be accommodated in this position with no gross structural changes (Figure 47). However, phenylalanine at this position is implicated in maintaining a stable TS structure by virtue of this mutants temperature sensitive phenotype.

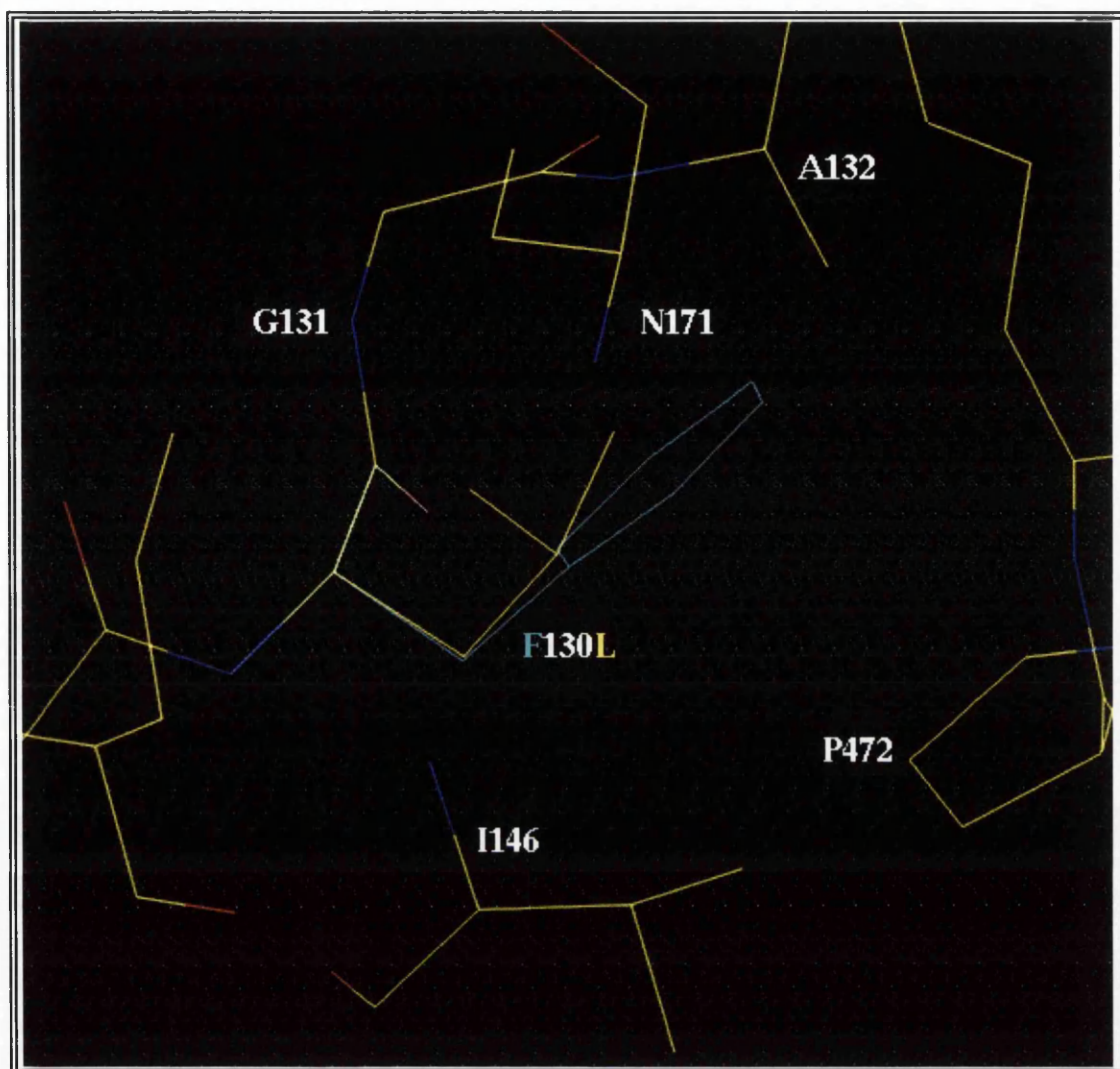


Figure 47 Temperature sensitive mutant FJ 16, showing the mutation F130L

The original wild-type residue is shown in light blue, next to the mutated residue. Several other amino acids are shown for reference.

3.3 Summary of temperature-sensitive mutants

A notable feature of the temperature sensitive mutants is that most of the substitutions have occurred in regions which appear not to be important in catalysis and can tolerate change. Perhaps these are the natural 'hot spots' of VZV which can tolerate variation. They also illustrate elegantly the conservation paradox as mutant FJ 3 has a mutation in a fully conserved leucine residue (209). Similarly FJ 12 also has conserved residue changes (Y123N and G124S), yet have produced proteins that

tolerate these substitutions. How the enzyme accommodates these substitutions at the lower temperature (30°C) and not the higher temperatures is not fully understood. Two plausible theories may explain this temperature sensitivity. Firstly, the enzyme is a more rigid less fluid structure at 30°C and at this temperature variant side chain residues may be more easily positioned such that they either point out to solvent or pack in to the structure with the least disruption. Raising the temperature to 37°C or 42°C gives rise to a much more fluid enzyme, and as such positioning of the side chains where no other residue will come into contact with it is more problematic. Secondly, such variants may be the result of two TS genes within the host bacteria, one wild-type and the other a variant. Mutant homodimers would be inactive, but heterodimers consisting of one monomer of wild-type enzyme and one monomer of variant enzyme may be sufficiently active.

The generation of many temperature sensitive mutants using the randomly 'spiked' oligonucleotides vindicates their use in a targeted mutagenesis protocol to search for covariants of the DRTG loop mutant proteins.

4. Final discussion and future work

This discussion outlines the original aims of the work and contrasts them with our findings with suggestions for some future research.

4.1 Is a highly conserved surface loop important?

The original aim of this study was to examine the role of the highly conserved surface DRTG loop and to provide a possible explanation as to why this loop was not conserved in the *L. lactis* phage Φ 3T enzyme. Mutagenesis of the DRTG loop does impair the ability of thymidylate synthase to catalyse the formation dTMP without significantly affecting substrate binding. Detailed examination of these mutants on the VZV model has provided some insight into what may be happening at the structural level. Furthermore, kinetic characterisation of the mutants does show that the DRTG loop is important for catalysis. Much work has centred on the C-terminus, because it has been implicated heavily in catalysis and closing down the active site.

This is the first study implicating the DRTG loop as an important functional element in catalysis. The DRTG loop in VZV TS may be critical for effective active site closure.

4.2 Can covariant accommodation restore the DRTG loop mutants activity?

Based on these studies, there does not appear to be any covariant residues for the *L. lactis* residues. However, it was by no means a fully exhaustive search and problems with the experimental approach hindered any real progress. The fact that region targeted random mutagenesis generates many temperature sensitive mutants shows that this approach is feasible. Mis-priming events were problematic and probably helped to mask any real covariants. Furthermore, it may be that to accommodate such drastic changes in an important loop, there needs to be more than one covariant residue. These residues are probably in different regions of the protein making a mutagenesis protocol difficult, if not unfeasible. Perhaps when a crystal structure of the VZV enzyme becomes available along with that of the *L. lactis* enzyme such residues may be more easily detected. Determination of the crystal structure of VZV TS is in progress (R. Thompson, personal communication). The *L. lactis* enzyme can be considered to be the result of an elegant yet 'natural' mutagenesis experiment that has shown that a large number of conserved amino acids can be substituted *en masse* without inactivating the enzyme. Perhaps it is this *en masse* substitution of residues that allows it to accommodate its 'novel' DRTG loop.

We have discovered novel structural plasticity in VZV TS that has not been previously reported and shown that VZV TS can tolerate amino acid substitutions (R38G, T39Q, G40M, I41A) and insertions (41A42, A302, G302). This plasticity has been extended throughout the protein with the temperature sensitive mutants (e.g. L209F, A216S, A216D, T229A, F130P, T123N, G124S) and with the VZV model we have been able to predict the manner in which these changes may have been accommodated. In summary, these observations show that VZV TS, like several other proteins possesses inherent structural plasticity. Our studies and those of others (Climie *et al* 1990, Michaels *et al* 1990) have revealed that highly conserved residues are not always resistant to substitution.

The conservation paradox that exists for TS may be explained by the fact that it is not the precise residue that is important but maintenance of the 'core structure' of the protein. It is around this core that the majority of changes are more easily

accommodated. Conservation of the core residues may be the result of fine-tuning to give the most efficient protein. Substituting one of these conserved residues does not have a catastrophic effect upon catalysis but results in a slightly less efficient variant of the protein which still has the same core structure.

4.3 Is the VZV TS unique in its C-terminal interactions?

Previous work has led to the notion that the interactions at the C-terminus of VZV were unique. This was primarily based on sequence alignment data and computer modelling. Based on this premise, it was predicted that all the other TS family members, including the human TS would interact differently in this region. It was proposed that the bacterial and human thymidylate synthase would be inactivated if their C-terminal residue was removed because this would disrupt the crucial hydrogen bond network within this region that helps maintain the closed ternary conformation.

Work presented in this thesis shows that the C-terminal mutant V313 Δ of the human TS behaves in a similar fashion to VZV TS, namely it is not inactivated by C-terminal truncation. V313 Δ exhibits 16% of wild-type activity compared to 3% for VZV L301 Δ . Since the human enzyme is not inactive as predicted the uniqueness of the VZV enzyme in this region is open to question.

Changes within the C-terminus of the VZV and human TS result in proteins that respond differently to folate inhibitors. Mutations in the C-terminus of VZV TS result in an enzyme that is more resistant to the folate-substrate mimic phenolphthalein reflecting the need of this inhibitor to have a fully closed active site. The C-terminal mutants cannot form a tight closed conformation upon ligand (or inhibitor) binding as reflected in their folate K_m values. In contrast, the C-terminal mutant proteins show a greater sensitivity to ICI inhibitors 4 and 5 compared to the wild-type protein. This is reflected in their dUMP K_m which indicates that these proteins are in a more open conformation. This allows the inhibitors better access to the active site and once there they can form irreversible ternary complexes. That these mutants do not close down the active site is not important for inhibition.

Peptides targeted against the C-terminus of VZV TS were tested for inhibition without success, perhaps reflecting an unrewarding target. Given the crucial role of

the DRTG loop presented in this thesis peptides generated against this region may meet with more success.

Generation of temperature sensitive mutants using the spiked oligonucleotides validated this approach in the search for covariant residues of the DRTG loop mutants. They also provide information about which residues are important in protein stability and help to illustrate that TS is a fluid structure only accommodating many changes at lower temperatures when there is more order to its structure.

4.4 Future work

We have shown that the DRTG loop of VZV TS is crucial for catalysis by introducing single *L. lactis* residues into this region. It would be of further interest to replace the VZV DRTG loop with combinations of the *L. lactis* residues until the whole loop was identical to that of *L. lactis*. Similarly, other covariant residues may still be needed for accommodation of the new residues which may include the 7 base insertion located immediately before the loop. Covariant residues could be identified by using cocktails of the spiked oligonucleotides, while yielding many temperature sensitive mutants along the way.

Crystallisation of the VZV TS is under way and the elucidation of its structure will be of great value to these studies.

REFERENCES

Ablashi DV, Berneman ZN, Kramarsky B, Whitman J Jr, Asano Y, Pearson JR (1995). Human herpesvirus 7 (HHV7): current status. *Clinical and Diagnostic Virol.* **4**, 1-13

Ackermann M, Braun DK, Pereira L, Roizman B (1984). Characterization of herpes simplex virus 1 α proteins 0, 4 and 27 with monoclonal antibodies. *J. Virol.* **52**, 108-118.

Alford CA and Britt WJ (1993). Cytomegalovirus. In *The Human Herpesviruses* 227-255. B Roizman, RJ Whitley and C Lopez (eds). Raven Press, New York.

Allen JR, Reddy GPV, Lasser GW, Mathews CK (1980). T4 ribonucleotide reductase. *J. Biol. Chem.* **255**, 7583-7588

Almeida JD, Howatson AF, Williams MG (1962). Morphology of varicella (chickenpox) virus. *Virology* **16**, 353-355

Arvin AM (1996). Varicella-Zoster Virus. In *Fields Virology* (3rd ed) 2, 2547-2585. BN Fields, DM Knipe *et al* (eds). Raven Press, New York

Arvin AM, Kushner JH, Feldman S, Baehner RL, Hammond D, Merigan TC (1982). Human leukocyte interferon for the treatment of varicella in children with cancer. *N. Engl. J. Med.* **306**, 761-765

Aull JL, Lyon JA, Dunlap RB (1974). Gel electrophoresis as a means of detecting ternary complex formation of thymidylate synthetase. *MicroChemistry Journal* **19**, 210-218

Averett ER, Pahwa S, Swenson P, Stanat SC Biron KK (1987). Varicella-zoster virus clinical isolate resistant to acyclovir. In *Proceedings of the 87th annual meeting of the American society of microbiology*. Abstract No. A94

Ayusawa D, Shimizu K, Koyama H, Kaneda S, Takeishi K, Seno T (1986). Cell-cycle-directed regulation of thymidylate synthase messenger RNA in human diploid fibroblasts stimulated to proliferate. *J. Mol. Biol.* **190**, 559-567

- Bachmann B** and Follmann H (1987). Deoxyribonucleotide biosynthesis in green algae-Characterisation of thymidylate synthase-dihydrofolate reductase in *Scenedesmus obliquus*. Archives Biochem. **256**, 244-252
- Bachmann BJ** (1983). Linkage map of *Escherichia coli* K-12, edition 7. Microbiological Reviews **47**, 180-230
- Balestrazzi A**, Branzoni M, Carbonera D, Parisi B, Cella R (1995). Biochemical evidence for the presence of a bifunctional dihydrofolate reductase-thymidylate synthase in plant species. J. Plant Physiol. **147**, 263-266
- Balzarini J** and DeClercq E (1982). 5-substituted-2'-deoxyuridines: correlation between inhibition of tumour cell growth and inhibition of thymidine kinase and thymidylate synthase. Biochemical Pharmacol. **31**, 3673-3682
- Barr PJ**, Nolan PA, Santi DV, Robins MJ (1981). Inhibition of thymidylate synthetase by 5-alkynyl-2'-deoxyuridylates. J. Medicinal Chem. **24**, 1385-1388
- Becker Y**, Dym H, Sarov I (1968). Herpes simplex virus DNA. Virology **36**, 184-192
- Ben-Porat T** and Rixon FJ (1979). Replication of herpesvirus DNA. IV. Analysis of concatamers. Virology **94**, 61-70
- Bird OD**, Vaitkus JW, Clark J (1970). 2-amino-4-hydroquinazolines as inhibitors of thymidylate synthetase. Mol. Pharmacol. **6**, 573-575
- Bisson L** and Thorner J (1977). Thymidine 5'-mono-phosphate-requiring mutants of *Saccharomyces cerevisiae* are deficient in thymidylate synthetase. J. Bacteriol. **132**, 44-50
- Blacklow SC** and Knowles JC (1991). In Directed Mutagenesis: A Practical Approach. 177-198. MJ McPherson (ed). Oxford University Press, New York.
- Blakely RL** (1963). The biosynthesis of thymidylic acid. IV. Further studies on thymidylate synthetase. J. Biol. Chem. **238**, 2113-2118
- Broughton CR** (1966). Varicella-zoster in Sydney. I. Varicella and its complications. Med. J. Aust **2**, 392-397

Brunell Pa, Ross A, Miller LH, Kuo B (1969). Prevention of varicella by zoster immune globulin. *N. Engl. J. Med.* **280**, 1191-1194

Brünger A, Kuriyan J, Karplus M (1987). Crystallographic *R* factor refinement by molecular dynamics. *Science* **235**, 458-460

Bullowa JGM and Wishik SM (1935). Complications of varicella. I. Their occurrence among 2,534 patients. *Am. J. Dis. Child.* **49**, 923-926

Bunni M, Doig MT, Donato H, Kesavan V, Priest DG (1988). Role of methylene-tetrahydrofolate depletion in methotrexate-mediated intracellular thymidylate synthase inhibition in cultured L1210 cells. *Cancer Res.* **48**, 3398-3404

Burdeska A, Ott M, Bannwarth W, Then RL (1990). Identical genes for trimethoprim-resistant dihydrofolate reductase from *Staphylococcus aureus* in Australia and Central Europa. *FEBS Letters* **266**, 159-162

Burns JC, Newburger JW, Sundell R, Wyatt LS, Frenkel N (1994). Seroprevalence of human herpesvirus 7 in patients with Kawasaki disease. *The Pediatric Infectious Disease J* **4**, 168-169

Cabirac GF, Mahalingam R, Wellish M, Gilden DH (1990). Trans-activation of viral tk promoters by proteins encoded by varicella zoster virus open reading frames 61 and 62. *Virus Res.* **15**, 57-68

Cameron JM (1993). New antiherpes drugs in development. *Medical Virology* **3**, 225-236

Capco Gr, Krupp TL, Mathews CK (1973). Bacteriophage-coded thymidylate synthetase: characteristics of the T4 and T5 enzymes. *Archiv. Biochem. Biophys.* **158**, 726-775

Carreras CW and Santi DV (1995). The catalytic mechanism and structure of thymidylate synthase. *Ann. Rev. Biochem.* **64**, 721-762

Carreras CW, Climie SC, Santi DV (1992) Thymidylate synthase with a C-terminal deletion catalyses partial reactions but is unable to catalyse thymidylate formation. *Biochemistry* **31**, 6038-6044

- Chang Y**, Cesarman E, Pessin M, Lee F, Culpepper, J Knowles D, Moore P (1994). Identification of herpesvirus-like DNA in AIDS-associated Kaposi's sarcoma. *Science* **266**, 1865-1869
- Chiu CS**, Cook KS, Greenberg GR (1982). Characteristics of a bacteriophage T4-induced complex synthesising deoxyribonucleotides. *J. Biol. Chem.* **257**, 15087-15097
- Chu E**, Drake JC, Boarman D, Baram J, Allegra CJ (1990). Mechanism of thymidylate synthase inhibition by methotrexate in human neoplastic cell lines and normal human myeloid progenitor cells. *J. Biol. Chem.* **265**, 8470-8478
- Chu E**, Koeller DM, Casey JL, Drake JC, Chabner BA, Elwood PC, Zinn S, Allegra CJ (1991). Autoregulation of human thymidylate synthase messenger RNA translation by thymidylate synthase. *Proc. Natl. Acad. Sci. USA.* **88**, 8977-8981
- Chu E**, Voeller D, Koeller DM, Drake JC, Takimoto CH, Maley GF, Maley F, Allegra CJ (1993). Identification of an RNA binding site for human thymidylate synthase. *Proc. Natl. Acad. Sci. USA.* **90**, 517-521
- Chung CT** and Miller RH (1988). A rapid and convenient method for the preparation and storage of competent bacterial cells. *Nucl. Acids Res.* **16**, 3580
- Clements JB**, Watson JR, Wilkie NM (1977). Temporal regulation OF herpes simplex virus type 1 transcription: location of transcripts on the vural genome. *Cell* **12**, 275-285
- Climie S**, Ruiz-Perez L, Gonzalez-Pacanowska D, Prapunwattana P, Cho SW, Stroud RM, Santi DV (1990). Saturation site-directed mutagenesis of thymidylate synthase. *J. Biol. Chem.* **265**, 18776-18779
- Cohen EA**, Gardreau P, Brazeau P, Langelier Y (1986). Specific inhibition of herpesvirus ribonucleotide reductase by a nonapeptide derived from the carboxy terminus of subunit 2. *Nature* **321**, 441-443
- Cohen JI** and Straus SE (1996). Varicella-Zoster Virus and its replication. In *Fields Virology* (3rd ed) 2, 2525-2545. BN Fields, DM Knipe *et al* (eds). Raven Press, New York

- Collier** NC, Knox K, Schlesinger MJ (1991). Inhibition of onfluenza virus formation by a peptide that corresponds to sequences in the cytoplasmic domain of the haemagglutinin. *Virology* **183**, 769-772
- Conley** AJ, Knipe DM, Jones PC, Roizman B (1981). Molecular genetics of herpes simplex virus. VII. Characterization of a temperature-sensitive mutant produced by in vitro mutagenesis and defective in DNA synthesis and accumulation of γ polypeptides. *J. Virol.* **37**, 191-206.
- Conrad** AH (1971). Thymidylate synthetase activity in cultured mammalian cells. *J. Biol. Chem.* **246**, 1318-1323
- Cosentino** G, Lavalee P, Rakhit S, Plante R, Gaudette Y, Lawetz C, Whitehead PW, Duceppe J-S, Lepine-Frenette C, Dansereau N, Guilbaut C, Langelier Y, Gaudreau P, Thelander L, Guidon Y (1991). Specific inhibition of ribonucleotide reductases by peptides corresponding to the C-terminal of their second subunit. *Biochem. Cell Biol.* **69**, 79-83
- Croen** KD and Straus SE (1991). Varicella-zoster virus latency. *Annu Rev Microbiol.* **45**, 265-282
- Croen** KD, Ostrove JM, Dragovic LJ, Smialek JE, Straus SE (1987). Latent herpes simplex virus in human trigeminal ganglia: detection of an immediate-early gene "antisense" transcript. *N. Engl. J. Med.* **317**, 1423-1432
- Croen** KD, Ostrove JM, Dragovic LJ, Straus SE (1987). Characterisation of herpes simplex virus type 2 latency associated transcription in human sacral ganglia and in cell culture. *J. Infect. Dis.* **163**, 23-28
- Croen** KD, Ostrove JM, Dragovic LJ, Straus SE (1988). Patterns of gene expression and sites of latency in human nerve ganglia are different for varicella-zoster and herpes simplex viruses. *Proc. Natl. Acad. Sci. USA* **85**, 9773-9777
- Crusberg** TC, Leary R, Kisluik RL (1970). Properties of thymidylate synthetase from dichloromethatrexate-resistant *Lactobacillus casei*. *J. Biol. Chem.* **245**, 5292-5296
- Danenberg** PV and Lockshin A (1982). Tight-binding complexes of thymidylate synthase, folate analogues and deoxyribonucleotides. *Adv. Enz. Reg.* **20**, 99-110

Danenberg PV, Langenbach RJ, Heidelberg C (1974). Structures of reversible and irreversible complexes of thymidylate synthetase and fluorinated pyrimidine nucleotides. *Biochemistry* **13**, 926-933

Danenberg PV and Danenberg KD (1978). Effect of 5, 10-methylenetetrahydrofolate on the dissociation of 5-fluoro-2'-deoxyuridylate from thymidylate synthase: evidence for an ordered mechanism. *Biochemistry* **17**, 4018-4024

Davison AJ (1984). Structure of the genome termini of varicella-zoster virus. *J. Gen. Virol.* **65**, 1969-1977

Davison AJ (1991). Varicella-zoster virus. The fourteenth Fleming Lecture. *J. Gen. Virol.* **72**, 475-486

Davison AJ and Scott JE (1986). The complete DNA sequence of varicella-zoster virus. *J. Gen. Virol.* **67**, 597-611

Davison AJ and Wilkie NM (1981). Nucleotide sequence of the joint between the L and S segments of herpes simplex virus types 1 and 2. *J. Gen. Virol.* **55**, 315-331

Davison AJ, Walters DJ, Edson CM (1985). Identification of the products of a varicella-zoster virus glycoprotein gene. *J. Gen. Virol.* **66**, 2237-2242

Dayringer HE, Tramontano A, Sprang SR, Fletterick RJ (1986). Interactive program for visualization and modelling of proteins, nucleic acids and small molecules. *J. Mol. Graphics* **4**, 82-87

de Moragas JM and Kierland RR (1957). The outcome of patients with herpes zoster. *Arch. Dermatol.* **75**, 193-196

Dealty AH, Spivack JG, Lavi E, O'Boyle DR, Fraser NW (1988). Latent herpes simplex virus type 1 transcripts in peripheral and central nervous system tissues of mice map to similar regions of the viral genome. *J. Virol.* **62**, 749-756

Defechereax P, Melen L, Baudoux L, Merville-Louis M-P, Rentier B, Piette J (1993). Characterization of the regulatory functions of varicella-zoster virus open reading frame 4 gene product. *J. Virol.* **67**, 4379-4385

- Dev IK**, Yates BB-Leong J, Dallas WS (1988). Functional role of cysteine-146 in *Escherichia coli* thymidylate synthase. *Proc. Natl. Acad. Sci. USA.* **85**, 1472-1476
- Disney GH**, McKee TA, Preston CM, Everett RD (1990). The product of varicella-zoster virus gene 62 autoregulates its own promoter. *J. Gen. Virol.* **71**, 2999-3003
- Donato H Jr**, Aull JL, Lyon JA, Reinsch JW, Dunlap RB (1976). Formation of ternary complex of thymidylate synthetase as followed by absorbance, fluorescence and circular dichroism spectra and gel electrophoresis. *J. Biol. Chem.* **251**, 1303-1310
- Dumas AM**, Geelen JLMC, Maris W and van der Noordaa J (1980). Infectivity and molecular weight of varicella-zoster virus DNA. *J. Gen. Virol.* **47**, 233-235.
- Dumas AM**, Geelen JLMC, Weststrate MW, Wertheim P, and van der Noordaa J (1981). *XbaI*, *PstI* and *BglIII* restriction enzyme maps of the two orientations of the varicella-zoster virus genome. *J. Virol.* **39**, 390-400.
- Dutia BM**, Frame MC, Subak-Sharpe JH, Clark WN, Marsden, HS (1986). Specific inhibition of herpesvirus ribonucleotide reductase by synthetic peptides. *Nature* **321**, 439-441
- Ecker JR** and Hyman RW (1982). Varicella-zoster virus DNA exists as two isomers. *Proc. Natl. Acad. Sci. USA* **79**, 156-160
- Ellis RW**, Keller PM, Lowe RS, Zivin RA (1985). Use of a bacterial expression vector to map the varicella-zoster virus major glycoprotein gene, gC. *J. Virol.* **53**, 81-88
- Evans RM**, Laskin JD, Hakala MT (1981). Effect of excess folates and deoxyinosine on the activity and site of action of 5-fluorouracil. *Cancer Res.* **41**, 3288-3295
- Everett RD** (1984) *Trans* activation of transcription by herpes virus products: requirement for two HSV-1 immediate early polypeptides for maximum activity. *EMBO J.* **3**, 3135-3141
- Everett RD** and Orr A (1991). The Vmw175 binding site in the IE-1 promoter has no apparent role in the expression of Vmw110 during herpes simplex virus type 1 infection. *Virology* **180**, 509-517.

- Fauman** EB, Rutenber EE, Maley F, Stroud RM (1994). Water-mediated substrate/product discrimination: the product complex of thymidylate synthase at 1.83Å. *Biochemistry* 1502-1511
- Feldman** S, Hughes WT, Daniel CB (1975). Varicella in children with cancer: seventy-five cases. *Pediatrics* **56**, 388-397
- Felser** JM, Straus SE, Ostrove JM (1987). Varicella-zoster virus complements herpes simplex virus type 1 temperature-sensitive mutants. *J. Virol.* **61**, 225-228.
- Fenwick** ML and Everett RD (1990). Inactivation of the shutoff gene (UL41) of herpes simplex virus types 1 and 2. *J. Gen. Virol.* **71**, 2961-2967
- Finer-Moore** JS, Fauman EB, Foster PC, Perry KM, Stroud RM (1993). Refined structures of substrate-bound and phosphate-bound thymidylate synthase from *Lactobacillus casei*. *J. Mol. Biol.*
- Finer-Moore** JS, Montfort WR, Stroud RM (1990). Pairwise specificity and sequential binding in enzyme catalysis: thymidylate synthase. *Biochemistry* **29**, 6977-6986
- Frenkel** N, Schirmer EC, Wyatt LS, Katsafanas G, Roffman E, Danovich RM, June CH. (1990). Isolation of a new herpesvirus from human CD4⁺ T cells. *Proc. Natl. Acad. Sci. USA* **87**, 748-752
- Friedkin** M, Crawford E, Humphreys SR, Goldin A (1962). The association of increased dihydrofolate reductase with amethopterin resistance in mouse leukemia. *Cancer Res.* **22**, 600-606
- Galivin** JH, Maley GF, Maley F (1975). The effect of substrate analogues on the circular dichroic spectra of thymidylate synthetase from *L. casei*. *Biochemistry* **14**, 3338-3344
- Garret** C, Wayata Y, Santi DV (1979). Thymidylate synthetase. Catalysis of dehalogenation of 5-bromo- and 5-iodo-2'-deoxyuridylate. *Biochemistry* **18**, 2798-2804

- Geiser** CF, Bishop Y, Myers M, Jaffe N, Yankee R (1975). Prophylaxis of varicella in children with neoplastic disease: comparative results with zoster immune plasma and gamma globulin. *Cancer* **35**, 1027-1030
- Gelb** LD (1993). Varicella-zoster virus. In *The Human Herpesviruses* 257-308. B Roizman, RJ Whitley and C Lopez (eds). Raven Press, New York
- Gershon** AA, LaRussa, Steinberg SP (1993). In *The Human Herpesviruses* 357-366. B Roizman, RJ Whitley and C Lopez (eds). Raven Press, New York
- Gershon** AA, Steinberg S, Brunell PA (1974). Zoster immune globulin: a further assessment. *N. Engl. J. Med.* **290**, 243-245
- Ghose** C, Oleinick R, Mathews RG, Dunlap RB (1990). Kinetic studies on thymidylate synthase from *Lactobacillus casei*. In *Chemistry and Biology of Pteridines* 1989, 860-865. Curtius H-CH, Chisla S, Blau N (eds). Walter de Gruyter and Company, Berlin
- Gilden** DH, Rozenman Y, Murray R, Devlin M, Vafai A (1987). Detection of varicella-zoster nucleic acid in neurons of normal human thoracic ganglia. *Ann. Neurol.* **22**, 377-380
- Goodrich** JA, Hoey T, Thut CJ, Admon A, Tjian R (1993). Drosophila TAF_{II}40 interacts with both a VP16 activation domain and the basal transcription factor TFIIB. *Cell* **75**, 519-530
- Greaves** RF and O'Hare P (1990). Structural requirements in the herpes simplex virus type 1 transactivator Vmw65 for interaction with the cellular octamer-binding protein and target TAATGARAT sequences. *J. Virol.* **64**, 2716-2724
- Guess** HA (1986). Population-based studies of varicella complications. *Pediatrics* **78**, 723-727
- Haigh** A, Greaves R, O'Hare P (1990). Interference with the assembly of a virus-host interaction complex by peptide competition. *Nature* **344**, 257-259
- Hardy** LW, Finer-Moore JS, Montfort WR, Jones MO, Santi DV, Stroud RM (1987). Atomic structure of thymidylate synthase: target for rational drug design. *Science* **235**, 448-455

- Harrap** KR, Jackman AL, Newell DR, Taylor GA, Hughes LR, Calvert AH (1989). Thymidylate synthase: A target for anticancer drug design. *Adv. Enz. Reg.* **29**, 161-179
- Harrison** PT (1992). Mutagenic studies of the varicella-zoster virus thymidylate synthase. PhD Thesis, University of Glasgow.
- Harrison** PT, Scott JE, Hutchinson MJ, Thompson R (1995). Site-directed mutagenesis of varicella-zoster virus thymidylate synthase- Analysis of 2 highly conserved regions of the enzyme. *European J. Biochem.* **230**, 511-516
- Hattori** M and Sakaki Y (1986). Dideoxy sequencing method using denatured plasmid templates. *Analytical Biochem.* **152**, 232-238
- Hayakawa** Y and Hyman R (1987). Isomerisation of the U_L region of varicella-zoster virus DNA. *Virus Res.* **8**, 25-31
- Hayes** S and O'Hare P (1993). Mapping of a major surface-exposed site in herpes simplex virus protein Vme65 to a region of direct interaction in a transcription complex assembly. *J. Virol.* **67**, 852-862
- Hélène** C and Toulmé J-J (1990). Specific regulation of gene expression by antisense, sense and antigene nucleic acids. *Biochimie et Biophysica Acta* **1049**, 99-125
- Hidaka** Y, Okada K, Kusuhara K, Miyazaki C, Tokugawa K and Ueda K (1994). Exanthem subitum and human herpesvirus 7 infection. *The Pediatric Infectious Disease J* **13**, 1010-1011
- Honess** RW (1984). Herpes simplex and 'the herpes complex': diverse observations and a unifying hypothesis. *J. Gen. Virol.* **65**, 2077-2107
- Honess** RW and Roizman B (1974). Regulation of herpesvirus macromolecular synthesis I. Cascade regulation of the synthesis of three groups of viral proteins. *J. Virol.*, **14**, 8-19.
- Honess** RW and Roizman B (1975). Regulation of herpesvirus macromolecular synthesis: sequential transition of polypeptide synthesis requires functional viral polypeptides. *Proc. Natl. Acad. Sci. USA* **72**, 1276-1280.

Honess RW, Bodemer W, Cameron KR, Niller HH, Fleckenstein B, Randall RE (1986). The A+T-rich genome of herpesvirus saimiri contains a highly conserved gene for thymidylate synthase. *Proc. Natl. Acad. Sci. USA* **83**, 3604-3608

Hope-Simpson RE (1965). The nature of herpes zoster: a long-term study and a new hypothesis. *Proc. R. Soc. Med* **58**, 9-20

Houghton JA, Maroda SJ, Philips JO, Houghton PJ (1981). Biochemical determinants of responsiveness to 5-fluorouracil and its derivatives in human colorectal adenocarcinoma xenografts. *Cancer Res.* **41**, 144-149

Hyman RW, Ecker JR, Tenser RB (1983). Varicella-zoster virus RNA in human trigeminal ganglia. *Lancet* **2**, 814-816

Inchauspe G and Ostrove JM (1989). Differential regulation by varicella-zoster virus (VZV) and herpes simplex virus type-1 *trans*-activating genes. *Virology* **173**, 710-714

Inchauspe G, Nagpal S, Ostrove JM (1989). Mapping of two varicella-zoster virus-encoded genes that activate the expression of viral early and late genes. *Virology* **173**, 700-709

Ivanetich KM and Santi DV (1990). Thymidylate synthase-dihydrofolate reductase in protozoa. *Exp. Parasitol.* **70**, 367-371

Jackers P, Defechereux P, Baudoux L, Lambert C, Massaer M, Merville-Louis M - P, Rentier B, Piette J (1992). Characterization of regulatory functions of the varicella-zoster virus gene 63-encoded protein. *J. Virol.* **66**, 3899-3903

Jackson RC, Jackman AL, Calvert AH (1983). Biochemical effects of a quinazoline inhibitor of thymidylate synthase, N-(4-(N-((2-amino-4-hydroxy-6-quinazoliny)l)methyl)prop-2-ynylamino)benzoyl)L-glutamic acid (CB3717) on human lymphoblastoid cells. *Biochemical Pharmacology* **32**, 3783-3790

Jacob RJ, Morse LS, Roizman B (1979). Anatomy of herpes simplex virus DNA. XII. Accumulation of head-to-tail concatamers in nuclei of infected cells and their role in the generation of the four isomeric arrangements of viral DNA. *J. Virol.* **29**, 448-457

Jazwinski SM and Edelman GM (1984). Evidence for participation of a multiprotein complex in yeast DNA replication *in vitro*. *J. Biol. Chem.* **259**, 6852-6857

Jenh CH, Geyer PK, Johnson LF (1985). Control of thymidylate synthase messenger RNA content and gene transcription in an overproducing mouse cell line. *Mol. Cell. Biol.* **5**, 2527-2532

Johnson DC and Feenstra V (1987). Identification of a novel herpes simplex virus type 1-induced glycoprotein which complexes with gE and binds immunoglobulin. *J. Virol.* **61**, 2208-2216

Johnson DC, Frame MC, Ligas MW, Cross, Stow ND (1988). Herpes simplex virus immunoglobulin G Fc receptor activity depends on a complex of two viral glycoproteins, gE and gI. *J. Virol.* **62**, 1347-1354

Jones TR, Calvert AH, Jackman AL, Brown SJ, Jones M, Harrap KR (1981). A potent antitumour quinazoline inhibitor of thymidylate synthetase: synthesis, biological properties and therapeutic results in mice. *European J. Cancer* **17**, 11-19

Kamb A, Finer-Moore JS, Calvert AH, Stroud RM (1992b). Structural basis for recognition of polyglutamyl folates by thymidylate synthase. *Biochemistry* **31**, 9883-9890

Kamb A, Finer-Moore JS, Stroud RM (1992a). Cofactor triggers the conformational change in thymidylate synthase: implications for an ordered binding mechanism. *Biochemistry* **31**, 12876-12884

Keller PM, Davison AJ, Lowe RS, Bennett CD, Ellis RW (1986). Identification and structure of the gene encoding gpII, a major glycoprotein of varicella-zoster virus. *Virology* **152**, 181-191

Keyomarsi K and Moran RG (1988). Mechanism of the cytotoxic synergism of fluoropyrimidines and folinic acid in mouse leukemic cells. *J. Biol. Chem.* **263**, 14402-14409

Keyomarsi K and Moran RG (1990). Quinazoline folate analogues inhibit the catalytic activity of thymidylate synthase but allow binding of 5-fluorodeoxyuridylate. *J. Biol. Chem.* **265**, 19163-19169

- Kieff ED**, Bachenheimer SL, Roiznam B (1971). Size, composition and structure of the DNA of subtypes 1 and 2 herpes simplex virus. *J. Virol.* **8**, 125-129
- Kinchington PR**, Hougland JK, Arvin AM, Ruyechan WT, Hay J (1992). The varicella-zoster virus immediate-early protein IE62 is a major component of virus particles. *J. Virol.* **66**, 359-366
- Kinchinton PR**, Reinhold WC, Casey TA, Straus SE, Hay J, Ruyechan WT (1985). Inversion and circularisation of the varicella-zoster virus genome. *J. Virol.* **56**, 194-200
- Kisliuk RL**, Gaumont Y, Baugh CM (1974). Polyglutamyl derivatives of folate as substrates and inhibitors of thymidylate synthetase. *J. Biol. Chem.* **249**, 4100-4103
- Kost RG**, Kupinsky H, Straus S (1995). Varicella-zoster virus gene 63- Transcript mapping and regulatory activity. *Virology* **209**, 218-224
- Krugman S**, Ward R, Katz SL (1977). Varicella-zoster infections. In *Infectious diseases of children* (6th ed) 451-471. St. Louis: Mosby
- Künkel TA** (1985). Rapid and efficient site-specific mutagenesis without phenotypic selection. *Proc. Natl. Acad. Sci. USA* **82**, 488-492
- Künkel TA**, Roberts JD and Zakour RA (1987). Rapid and efficient site-specific mutagenesis without phenotypic selection. *Methods in Enzymology* **54**, 367-382
- Kuntz ID** (1992). Structure-based strategies for drug design and discovery. *Science* **257**, 1078-1082
- Kwong AD**, Kruper AJ, Frenkel N (1988). Herpes simplex virus virion host shutoff function. *J. Virol.* **62**, 912-921
- Lagosky PA**, Taylor GR, Haynes GR (1987). Molecular characterisation of the *saccharomyces cerevisiae* dihydrofolate-reductase gene (DFR1). *Nucl. Acids Res.* **15**, 10355-10371
- LaPat-Polasko L**, Maley GF, Maley F (1990). properties of T4-phage thymidylate synthase following mutagenic changes in the active site region. *Biochemistry* **29**, 9561-9572

Lawrence GL, Chee MS, Craxton MA, Gompels UA, Honess RW, Barrell BG (1990). Human herpes virus 6 is closely related to human cytomegalovirus. *J. Virol.* **64**, 287-299

Lazar G, Hong Z, Goodman HM (1993). The origin of the bifunctional dihydrofolate reductase thymidylate isogenes of *Arabidopsis thaliana*. *Plant Journal* **3**, 657-668

Leary RP, Beaudette, Kisliuk RL (1975). Interaction of deoxyuridylate with thymidylate synthetase. *J. Biol. Chem.* **250**, 4864-4878

Lewis CA and Dunlap RB (1981). Thymidylate synthase and its interaction with 5-fluoro-2'-deoxyuridylate. In *Topics in Molecular Pharmacology*, 170-219. Burgen ASV and Roberts GCK (eds). Elsevier/North Holland Biomedical Press

Lim WA and Sauer RY (1991). The role of internal packing interactions in determining the structure and stability of a protein. *J. Molec. Biol.* **219**, 359-376

Ling P, Kinchington PR, Ruyechan WT, Hay J (1991). A detailed analysis of transcripts mapping to varicella-zoster virus gene 14 (glycoprotein V). *Virology* **184**, 625-635

Ling P, Kinchington PR, Sadeghi-Zadeh M, Ruyechan WT, Hay J (1992). Transcription from varicella-zoster virus gene 67 (glycoprotein IV). *J. Virol.* **66**, 3690-3698

Lockshin A and Danenberg PV (1980). Hydrodynamic behaviour of human and bacterial thymidylate synthetases and thymidylate synthetase-5-fluoro-2'-deoxyuridylate-5, 10-methylenetetrahydrofolate complex. Evidence for large conformational changes during catalysis. *Biochemistry* **19**, 4244-4251

Lopez C (1993). Human herpesviruses 6 and 7: Molecular biology and clinical aspects. In *The Human Herpesviruses* 309-316. B Roizman, RJ Whitley and C Lopez (eds). Raven Press, New York

Lorenson MY, Maley GF, Maley F (1967). The purification and properties of thymidylate synthetase from chick embryo extracts. *J. Biol. Chem.* **242**, 3332-3344

- Lu Y-Z, Aiello PD, Mathews RG (1984).** Studies on the polyglutamate specificity of thymidylate synthase from fetal pig liver. *Biochemistry* **23**, 6870-6876
- Maguire HF and Hyman RW (1986).** Polyadenylated cytoplasmic transcripts of varicella-zoster virus. *Intervirology* **26**, 181-191
- Maley GF, Maley F, Baugh CM (1979).** Differential inhibition of host and viral thymidylate synthase by folyl-polyglutamates. *J. Biol. Chem.* **254**, 7485-7487
- Maley, G and Maley F (1988).** Properties of a defined mutant of *Escherichia coli* thymidylate synthase. *J. Biol. Chem.* **263**, 7620-7627
- Manavalan P, Mittelstaedt DM, Schimerlink MI, Johnson WC (1986).** Conformational analysis of thymidylate synthase from amino acid sequence by circular dichroism. *Biochemistry* **25**, 6650-6655
- Marsden HS (1987).** Herpes simplex virus glycoproteins and pathogenesis. In *Molecular Basis of Virus Disease*. SGM **40**, 259-288. Cambridge University Press.
- Marsden HS (1992).** Disruption of protein-subunit interactions. *Seminars in Virol.* **3**, 67-75
- Mathews CK, Moen LK, Wang Y, Sargent RG (1988).** Intracellular organisation of precursor biosynthetic enzymes. *Trends in Biochem. Sci.* **13**, 394-397
- Mathews CK, North TW, Reddy GPV (1978).** Multienzyme complexes in DNA precursor biosynthesis. *Adv. Enz. Regulation* **17**, 133-156
- Mathews DA, Appelt K, Oatley SJ, Xuong NH (1990b).** Crystal structure of *Escherichia coli* thymidylate synthase containing bound 5-fluoro-2'-deoxyuridylate and 10-propargyl-5,8-dideazafolate. *J. Mol. Biol.* **214**, 923-936
- Mathews DA, Villafranca JE, Janson CA, Smith WW, Welsh K, Freer S (1990a).** Stereochemical mechanism of action for thymidylate synthase based on the x-ray structure of the covalent inhibitory ternary complex with 5-fluoro-2'-deoxyuridylate and 5, 10-methylenetetrahydrofolate. *J. Mol. Biol.* **214**, 937-948

McGeoch DJ and Davison AJ (1986). Alphaherpesviruses possess a gene homologous to the protein kinase gene family of eukaryotes and retroviruses. *Nucl. Acids Res.* **14**, 1765-1777

McGeoch DJ, Barnett BC, MacLean CA (1993). Emerging functions of alphaherpesvirus genes. *Seminars in Virology* **4**, 125-134

McGeoch DJ, Dalrymple MA, Davison AJ, Dolan A, Frame MC, McNab D, Perry LJ, Scott JE, Taylor P (1988). The complete DNA sequence of the long unique region in the genome of herpes simplex virus type 1. *J. Gen. Virol.* **69**, 1531-1574

McGeoch DJ, Dolan A, Donald S, Brauer DHK (1986). Complete DNA sequence of the short repeat region in the genome of herpes simplex virus type 1. *Nucl. Acids Res.* **14**, 1727-1745

McGeoch DJ, Dolan A, Donald S, Rixon FJ (1985). Sequence determination and genetic content of the short unique region in the genome of herpes simplex virus type 1. *J. Mol. Biol.* **181**, 1-13

McLauchlan J, Addison C, Craigie MC and Rixon FJ (1992). Noninfectious L-particles supply functions which can facilitate infection by HSV-1. *Virology* **190**, 682-688

McNeil JB and Smith M (1985). *Saccharomyces cerevisiae* CYC1 mRNA 5'-end positioning by *in vitro* mutagenesis, using synthetic duplexes with random mismatch base pairs. *Mol. Cel. Biol.* **5**, 3545-3551

McPherson MJ (1991). Directed mutagenesis. Oxford University Press, New York.

Meek TD, Garvey EP, Santi DV (1985). Purification and characterisation of the bifunctional thymidylate synthase-dihydrofolate reductase from methotrexate-resistant *Leishmania tropica*. *Biochemistry* **24**, 678-686

Meier JL and Straus SE (1992). Comparative biology of latent varicella-zoster virus and herpes simplex virus infections. *J. Infect. Dis.* **166** (Suppl. 1), 13-23.

Michaels ML, Mathews DA, Miller JH (1990). *Escherichia coli* thymidylate synthase: amino acid substitutions by suppression of amber nonsense mutations. *Proc. Natl. Acad. Sci. USA.* **87**, 3957-3961

- Miller** FA, Dixon GJ, Arnett G, Dice JR, Rightsel WA, Schabel FM, McLean JW (1968). Antiviral activity of carbobenzyoxy di and tripeptides on measles virus. *Appl. Microbiol.* **16**, 1489-1496
- Miller** G (1990). Epstein-Barr Virus: Biology, pathogenesis and medical aspects. In *Virology* (2nd ed) 2, 1921-1958. BN Fields, DM Knipe *et al* (eds). Raven Press, New York
- Montfort** WR, Perry KM, Fauman EB, Finer-Moore JS, Maley GF, Hardy L, Maley F, Stroud RM (1990). Structure, multiple site binding, and segmental accommodation in thymidylate synthase on binding dUMP and an anti-folate. *Biochemistry* **29**, 6964-6977
- Morgan** C, Rose HM, Mednis B (1968). Electron microscopy of herpes simplex virus. I. Entry. *J. Virol.* **2**, 507-516
- Moriuchi** H, Moriuchi M, Smith HM, CohenJI (1994). Varicella-zoster virus open reading frame 4 protein is functionally distinct from and does not complement its herpes simplex virus type 1 homolog, ICP27. *J. Virol.* **68**, 1987-1992.
- Myers** CE, Young RC, Johns DG, Chabner BA (1974). Assay of 5-fluorodeoxyuridylate and deoxyuridylate pools following 5-fluorouracil. *Cancer Res.* **34**, 2682-2688
- Myers** MG and Connelly BL (1992). Animal models of varicella. *J. Infect. Dis.* **166** (Suppl. 1), 48-50
- Myers** MG, Kramer LW, Stanbery LR (1987). Varicella in a gorilla. *J. Med. Virol.* **23**, 317-322
- Nagpal** S and Ostrove JM (1991). Characterization of a potent varicella-zoster virus-encoded *trans*-repressor. *J. Virol.* **65**, 5289-5296
- Navalgund** LG, Rossana C, Muench AJ, Johnson LF (1980). Cell cycle regulation of thymidylate synthetase gene expression in cultured mouse fibroblasts. *J. Biol. Chem.* **255**, 7386-7390

- Neipel F**, Ellinger K, Fleckenstein B (1991). The unique region of the human herpesvirus 6 genome is essentially colinear with the U_L segment of human cytomegalovirus. *J. Gen. Virol.* **72**, 2293-2297
- Ner SS**, Goodin DB, Smith M (1988). A simple and efficient procedure for generating random point mutations and for codon replacements using mixed oligonucleotides. *DNA* **7**, 127-134
- Nicolaides E**, deWald H, Westland R, Lipnik M, Posler J (1968). Potential antiviral agents. Carbbenzoxy di and tripeptides active against measles and herpes viruses. *J. Medicinal Chem.* **11**, 74-79
- Nielson E** and Cella R (1988). Thymidylate synthase in plant cells: kinetic and molecular properties of the enzyme from *Daucus carota* L. cell cultures. *Plant and Cell Physiol.* **29**, 503-508
- O'Hare P** (1993). The virion transactivator of herpes simplex virus. *Semin. Virol.* **4**, 145-155
- Ohyama K** (1976). A basis for bromodeoxyuridine resistance in plant cells. *Env. Exp. Botany* **16**, 209-216
- Ostrove JM** (1990). Molecular biology of varicella zoster virus. *Advan. Virus Res.* **38**, 45-98
- Ostrove JM**, Reinhold W, Fan CH, Zorn S, Hay J, Straus SE (1985). Transcription mapping of the varicella-zoster virus genome. *J. Virol.* **56**, 600-606
- Para MF**, Bauckle RB, Spear PG (1980). Immunoglobulin G (Fc)-binding receptors on virions of herpes simplex virus type 1 and transfer of these receptors to the cell surface by infection. *J. Virol.* **34**, 512-520
- Park JS**, Cheng CT-C, Mertes MP (1979). 5-[(4-methyl-1, 2, 3, 4-tetrahydroquinoxalyl)methyl]-2'-deoxyuridine-5'-phosphate: an analogue of a proposed intermediate in thymidylate synthetase catalysis. *J. Medicinal Chem.* **22**, 1134-1137
- Paryani SG** and Arvin AM (1986). Intrauterine infection with varicella-zoster virus after maternal varicella. *N. Engl. J. Med.* **314**, 1542-1546

- Perera LP, Mosca JD, Ruyechan WT, Hay J (1992a).** Regulation of varicella-zoster virus gene expression in human T lymphocytes. *J. Virol.* **66**, 5298-5304
- Perera LP, Mosca JD, Sadeghi-Zadeh M, Ruyechan WT, Hay J (1992b).** The varicella-zoster virus immediate early protein, IE62, can positively regulate its cognate promoter. *Virology* **191**, 346-354
- Perry KM, Fauman EB, Finer-Moore JS, Montfort WR, Maley GF, Maley F, Stroud RM (1990).** Plastic adaptation toward mutations in proteins: structural comparison of thymidylate synthases. *Proteins: Struct. Funct. Genet.* **8**, 315-333
- Perry KM, Fauman EB, Finer-Moore JS, Montfort WR, Maley GF, Maley F, Stroud RM (1990).** Plastic adaptation toward mutations in proteins- Structural comparisons of thymidylate synthases. *Proteins: Struct. Funct. and Genet.* **8**, 315-333
- Perry LJ, McGeoch DJ (1988).** The DNA sequences of the long repeat region and Adjoining parts of the long unique region in the genome of herpes simplex virus type 1. *J. Gen. Virol.* **69**, 2831-2846
- Piggot PJ and Hoch JA (1985).** Revised linkage map of *Bacillus subtilis*. *Microbiological Reviews* **49**, 158-179
- Pogolotti AL Jnr, Danenberg PV, Santi DV (1986).** Kinetics and mechanism of interaction of 10-propargyl-5, 8-dideazafolate with thymidylate synthase. *J. Medicinal Chem.* **29**, 478-482
- Pogolotti ALJ, Danenberg PV, Santi DV (1986).** Kinetics and mechanism of interaction of 10-propargyl-5, 8-dideazafolate with thymidylate synthase. *J. Med. Chem.* **29**, 478-482
- Preston CM (1979).** Control of herpes simplex virus type 1 mRNA synthesis in cells infected with wild-type virus or the temperature-sensitive mutant *tsK*. *J. Virol.* **29**, 275-285.
- Prober CG, Kirk LE, Keeney RE (1982).** Acyclovir therapy of chickenpox in immunosuppressed children: a collaborative study. *J. Pediatr.* **101**, 622-625
- Reinhold W, Straus SE, Ostrove JM (1988).** Directionality and further mapping of varicella-zoster virus transcripts. *Virus Res.* **9**, 249-261

- Reyes P** and Heidelberg C (1965). Fluorinated pyrimidines. *Mol. Pharmacol.* **1**, 14-30
- Richardson CD** and Choppin PW (1983). Oligopeptides that specifically inhibit membrane fusion by paramyxoviruses: studies on the site of action. *Virology* **131**, 518-532
- Richardson CD**, Scheid A, Choppin PW (1980). Specific inhibition of paramyxovirus replication by oligopeptides with amino acid sequences similar to those at the N-termini of the F₁ or HA₂ viral polypeptides. *Virology* **105**, 205-222
- Richter J**, Puchtler I, Fleckenstein B (1988). Thymidylate synthase gene of herpesvirus ateles. *J. Virol.* **62**, 3530-3535
- Rickinson AB**, Kieff E (1996). Epstein-Barr Virus: In *Fields Virology* (3rd ed) 2, 2397-2446. BN Fields, DM Knipe *et al* (eds). Raven Press, New York
- Rixon FJ**, Campbell ME, Clements JB (1984). A tandemly reiterated DNA sequence in the long repeat region of herpes simplex virus type 1 found in close proximity to immediate early mRNA-1. *J. Virol.* **52**, 715-718
- Roizman B** (1979). The structure and isomerization of herpes simplex virus genomes. *Cell* **16**, 481-494
- Roizman B** (1993). The family herpesviridae: A brief introduction. In *The Human Herpesviruses 1-9*. B Roizman, RJ Whitley and C Lopez (eds). Raven Press, New York
- Roizman B** (1996). Herpesviridae. In *Fields Virology* (3rd ed) 2, 2221-2230. BN Fields, DM Knipe *et al* (eds). Raven Press, New York
- Ross AH** (1962). Modification of chicken pox in family contacts by administration of gamma globulin. *N. Engl. J. Med.* **267**, 369-376
- Ross P**, O'Gara F, Condon S (1990). Cloning and characterisation of the thymidylate synthase gene from *Lactococcus lactis* subsp. *lactis*. *Applied and Env. Microbiol.* **56**, 2156-2163

Sani BP, Vaid A, Cory JG, Brockman RW, Elliot RD, Montgomery JA (1986). 5'-haloacetamido-2'-deoxythymidines: novel inhibitors of thymidylate synthase. *Biochimie et Biophysica Acta* **881**, 175-184

Santi DV and Danenberg PV (1984). Folates in pyrimidine nucleotide biosynthesis. In *Folates and Pterins Vol 1- Chemistry and Biochemistry of Folates* 345-398. RL Blakley and SJ Benkovic (eds). John Wiley and Sons, New York

Sartorius C and Franklin RM (1991a). Hybridisation arrest of cell-free translation of the malarial dihydrofolate reductase/thymidylate synthase mRNA by anti-sense oligodeoxyribonucleotides. *Nucl. Acids Res.* **19**, 1613-1618

Sartorius C and Franklin RM (1991b). The use of anti-sense oligonucleotides as chemotherapeutic agents for parasites. *Parasitology Today* **7**, 90-93

Schalling M, Ekman M, Kaaya E, Linde A, Biberfeld P (1995). A role for a new herpes virus (KHSV) in different forms of Kaposi's sarcoma. *Nature Medicine* **1**, 707-708

Schiffer, CA, Davisson VJ, Santi DV, Stroud R (1991). Crystallisation of human thymidylate synthase. *J. Mol. Biol.* **219**, 161-163

Seither RL, Trent DF, Mikulecky DC, Rape TJ, Goldman ID (1991). Effect of direct suppression of thymidylate synthase at the 5, 10-methylene-tetrahydrofolate binding site on the interconversion of tetrahydrofolate cofactors to dihydrofolate by antifolates: influence of degree of dihydrofolate reductase inhibition. *J. Biol. Chem.* **266**, 4112-4118

Shoichet BK, Stroud RM, Santi DV, Kuntz ID, Perry KM (1993). Structure-based discovery of inhibitors of thymidylate synthase. *Science* **259**, 1445-1450

Smibert CA and Smiley JR (1990). Differential regulation of endogenous and transduced β -globin genes during infection of erythroid cells with herpes simplex virus type 1 recombinant. *J. Virol.* **64**, 3882-3894

Smith RF and Smith TF (1989). Identification of new protein kinase-related genes in three herpesviruses, herpes simplex virus, varicella-zoster virus, and Epstein-Barr virus. *J. Virol.* **63**, 450-455

- Spear** PG (1992). Membrane fusion induced by herpes simplex virus. In *Viral fusion mechanisms*. J Bentz (ed). CRC press, Boca Raton, USA
- Stevens** JG, Wagner EK, Devi-Rao GB, Cook ML, Feldman LT (1987). RNA complementary to a herpesvirus alpha gene mRNA is prominent in latently infected neurons. *Science* **235**, 1056-1059
- Stevenson** D, Colman KL, Davison AJ (1992). Characterization of the varicella-zoster virus gene 61 protein. *J. Gen. Virol.* **73**, 521-530
- Storms** RK, Ord RW, Greenwood MT, Mirdamadi B, Chu FK, Belfort M (1984). Cell cycle-dependant expression of thymidylate synthase in *Saccharomyces cerevisiae*. *Mol. Cell. Biol.* **4**, 2858-2864
- Stow** ND and Davison AJ (1986). Identification of a varicella-zoster virus origin of DNA replication and its activation by herpes simplex virus type 1 gene products. *J. Gen. Virol.* **67**, 1613-1623.
- Straus** SE, Aulakh HS, Ruyechan WT (1981). Structures of varicella-zoster virus DNA. *J. Virol.* **40**, 515-525
- Straus** SE, Owens J, Ruyechan WT (1982). Molecular cloning and physical mapping of varicella-zoster virus DNA. *Proc. Natl. Acad. Sci. USA* **79**, 993-997
- Stroop** WG, Rock DL, Fraser NW (1984). Localization of herpes simplex virus in the trigeminal and olfactory systems of the mouse central nervous system during acute and latent infections by in situ hybridisation. *Lab Invest.* **51**, 27-38
- Stroud** RM and Finer-Moore JS (1993). Stereochemistry of a multistep/bipartite methyl transfer reaction: thymidylate synthase. *The FASEB Journal* **7**, 671-677
- Stroud** RM and Finer-Moore JS (1993). Stereochemistry of a multistep/bipartite methyl transfer reaction: thymidylate synthase. *The FASEB J.* **7**, 671-677
- Takahashi** M, Okuno Y, Otsuka T *et al* (1975). Development of a live attenuated varicella vaccine. *Biken J.* **18**, 25-33

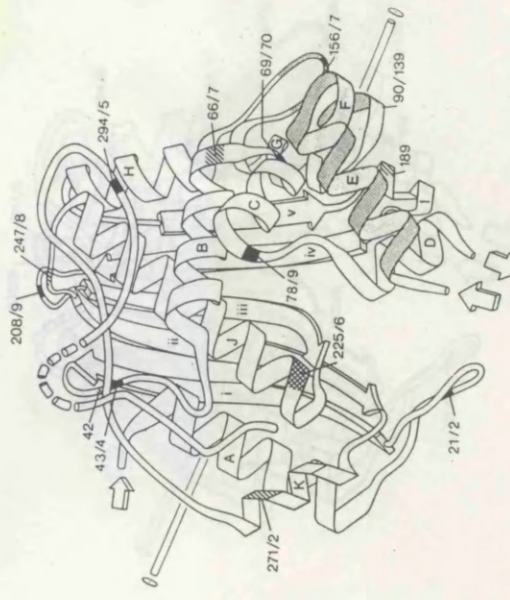
- Takahashi M**, Otsuka T, Okuno Y, Assano Y, Yazaki T, Isomura S (1974). Live vaccine used to prevent the spread of varicella in children in hospital. *Lancet* **2**, 1288-1290
- Tanaka K**, Kondo T, Torigoe S, Okada S, Mukai T, Yamanishi K (1994). human herpesvirus 7: another causal agent for roseola (exanthem subitum). *The journal of pediatrics* **125**, 1-5
- Tatman JD**, Preston VG, Nicholson P, Elliot RM, Rixon FJ (1994). Assembly of herpes simplex virus type 1 capsids using a panel of recombinant baculoviruses. *J. Gen. Virol.* **75**, 1101-1113
- Telford EAR**, Watson MS, Aird HC, Perry J, Davison AJ (1995). The DNA sequence of Equine herpesvirus-2. *J. Molec. Biol.* **249**, 520-528
- Thompson R**, Honess RW, Taylor L, Morran J, Davison AJ (1987). Varicella-zoster virus specifies a thymidylate synthetase. *J. Gen. Virol.* **68**, 1449-1455
- Toth I**, Lazar G, Goodman HM (1987). Purification and immunochemical characterisation of a dihydrofolate reductase-thymidylate synthase enzyme complex from wild-carrot cells. *The EMBO Journal* **6**, 1853-1858
- Ueda K**, Kusuhara K, Okada K, Miyazaki C, Hidaka Y, Tokugawa K Yamanishi K (1994). Primary human herpesvirus 7 infection and exanthem subitum. *The Pediatric Infectious Disease J* **13**, 167-168
- Vafai A**, Murray RS, Wellish M, Delvin M, Gilden D (1988). Expression of varicella-zoster virus and herpes simplex virus in normal trigeminal ganglia. *Proc. Natl. Acad. Sci. USA* **85**, 2362-2366
- Veda T**, Dutschman GE, Broom AD, Cheng Y-C (1986). Interactions of human thymidylate synthetase (TS) with bisubstrate analogues. *Proc. American. Assoc. Cancer Res.* **27**, 998
- Voeller DM**, Changchien L-M, Maley GF, Maley F, Takechi T, Turner R, Montfort WR, Allegra CJ, Chu E (1995). Characterization of a specific interaction between *Escherichia coli* thymidylate synthase and *Escherichia coli* thymidylate synthase mRNA. *Nucl. Acids Res.* **23**, 869-875

- Wagner EK** (1985). Individual HSV transcripts: characterization of specific genes. In *The Herpesviruses*. **3**, 45-104. B. Roizman (ed). Plenum press, New York/London
- Ward RL** and **Stevens JG** (1975). Effect of cytosine arabinoside on viral-specific protein synthesis in cells infected with herpes simplex virus. *J. Virol.* **15**, 71-80.
- Watson RJ** and **Clements JB** (1980). A herpes simplex virus type 1 function continuously required for early and late virus RNA synthesis. *Nature* **285**, 329-330.
- Wayata Y**, **Matsuda A**, **Santi DV** (1980). Interaction of thymidylate synthetase with 5-nitro-2'-deoxyuridylate. *J. Biol. Chem.* **255**, 5538-5544
- Weller TH** and **Witton HM** (1958). The etiologic agents of varicella and herpes zoster. Serologic studies with the viruses as propagated in vitro. *J. Exp. Med.* **108**, 869-890.
- Whitley R**, **Hilty M**, **Haynes R**, **Bryson Y**, **Conner JD**, **Soong SJ**, **Alford CA Jr** (1982). NIAID Collaborative antiviral study group. Vidarabine therapy of varicella in immunosuppressed patients. *J. Pediatr.* **101**, 125-131
- Whitley RJ** and **Alford CA** (1981). Parenteral antiviral chemotherapy of human herpes viruses. In *The Human Herpesviruses : an interdisciplinary perspective*. 478-490. **Nahmias AJ**, **Dowdle WR**, **Schinazi RF** (eds). Elsevier, New York
- Whitley RJ** and **Gnann JW Jr** (1993). The epidemiology and clinical manifestations of herpes simplex virus infections. In *The Human Herpesviruses* 69-105. **B Roizman**, **RJ Whitley** and **C Lopez** (eds). Raven Press, New York
- Wittels M** and **Spear PG** (1991). Penetration of cells by herpes simplex virus does not require a low pH-independent endocytic pathway. *Virus Res.* **18**, 271-290
- Yang F-D**, **Spanevello RA**, **Celiker I**, **Hirschmann R**, **Rubin H**, **Cooperman BS** (1990). The carboxyl terminus heptapeptide of the R2 subunit of mammalian ribonucleotide reductase inhibits enzyme activity and can be used to purify the R1 subunit. *FEBS Lett.* **272**, 61-64
- Zaia J**, **Levin M**, **preblud S**, **Leszczynski J**, **Wright G**, **Ellis r**, **Curtis A**, **Valerio MA**, **LeGore J** (1983). Evaluation of varicella-zoster immune globulin: protection of

immunosuppressed children after house-hold exposure to varicella. *J. Infect. Dis.*
147, 737-43



	17	A	31	-1	37	42	1	54
VZV	mgdlscwtkvpqf	ltgEIQYLkqvddllryGvrkr	DRTGiGTlSVFG	mqarynLrne			
HHV-8	mtvgaetp	heEIQYLrqlreilrcsdrl	DRTGiGTlSVFG	mqarysLrdh			
EHV-2	mvthcEhQYLNt	vreillanGvrrg	DRTGvGTlSVFG	dqakysLrgg			
HVS	msthteeghgEhQYLS	qvqhllyGsfkn	DRTGtGTlSVFG	tgqsrfsLene			
HVA	meelhaEhQYLS	qvkhllncGnfkh	DRTGvGTlSVFG	mqsrysLekd			
Human	mpvagselprp	lppaaqerdaerpphgEIQYLGq	qhllrcGvrkd	DRTGtGTlSVFG	mqarysLrde		
Mouse	mlvvgse	l.....qsdagqlsaeaprhgEIQYLR	qvvehllrcGfkke	DRTGtGTlSVFG	mqarysLrde		
Rat	mlvegse	l.....qsgagqprteaprhgEIQYLR	qvvehlmcGfkke	DRTGtGTlSVFG	mqarysLrde		
S.cerevisiae	mtmdgknkeEeQYLD	lckrIideefrp	DRTGtGTlSVFG	appqlrfsLrdd			
C.albicans	mtvspntaEqaYLD	lckrIideehrp	DRTGtGTkSVFG	appqlrfdLsnd			
P.carinii	mvnaeEgQYLN	lvqvIinhGedrp	DRTGtGTlSVFG	papsplkfsLrnk			
C.neofornans	mtatiddqekn	grnpdheEYQYLD	lirrIinvGevrp	DRTGtGTvalF	papsfrfsLadn		
A.thalianaX	NH2-233	-heEflYlmmvedI	isnGvkn	DRTGtGtlSkFG	cgmknfLrrs		
A.thalianaY	NH2-232	-heEYlYlnlvke	lIsnGnlkd	DRTGtGtlSkFG	cgmknfLrnn		
D.carota	NH2-241	-heEYlYlglvenI	isnGvtkn	DRTtGtVsiFG	cqmrfnLrks		
C.fasiculata	NH2-230	-aeEYQYLe	lIdrImktGlvke	DRTGvGTlSVFG	aqmfsLrdnq		
L.major	NH2-231	-heErQYLe	lIdrImktGivke	DRTGvGTlSVFG	aqmfsLrdn		
L.amazonensis	NH2-231	-heErQYLe	lIdrImktGiak	DRTGvGTlSVFG	aqmfsLrdn		
L.tropica	NH2-231	-heErQYLe	lIdrImktGivke	DRTGvGTlSVFG	aqmfsLrdn		
P.chabaudi	NH2-287	-hpEYQYLN	iIyDIImhGnkqd	DRTGvGvlskFG	ymnkfLlsey		
P.falciptarum	NH2-322	-hpEYQYLN	iIyDIImrnGnkqs	DRTGvGvlskFG	yimkfdLsqy		
T.gondii	NH2-321	-heEYQYLD	lIadIInnGrtmd	DRTGvGvlskFG	ctmrysLdqa		
T.cruzi	NH2-234	-reEYQYLS	lvdrIireGnvkh	DRTGvGTlSVFG	aqmfsLrnn		
E.coli		mkQYLe	lmqkvIdetGtqn	DRTGtGTlSVFG	hqmrfnlqdg		
B.subtilisB		mkQYkdf	crhvlhEgkkg	DRTGtGTlSVFG	yqmrfnlreg		
B.amyloliquefaciens		mi fycvtllkdyf	krmkmkQYkdlcrhvlengEkkq	DRTGtGTlSVFG	yqmrfnlqgg		
S.flexneri		mkQYLe	lmqkvIdetGtqn	DRTGtGTlSVFG	hqmrfnlqdg		
H.influenzae		mkQYLe	lcrriIvseGevwan	eRTGkhc	lvtinadleydvannq		
M.genitalium		mkQYLD	lasyvIlanGkkrk	nRTdtGtlSVFG	yqmKfdLtns		
L.lactis		mtvadqvf	kniqnlIdnGvfsenarpkyk	DgmnaskyvtG	sfvtydlqkg		
L.casei		mlEqpYLD	lakkvIdEgHfkp	DRThtGTlSVFG	hqmrfdLskg		
S.aureus		mynpfdeaYngl	ceeIleIGnrrd	DRThtGTlSVFG	hqlrfdLtkg		
B.subtilisA		mtqfdkQYns	iikdIInnGisdeefdvrtkwsDgT	pahTlSvis	kqmrfdnse		
Phageφ3T		mtqfdkQYns	iikdIInnGisdeefdvrtkwsDgT	pahTlSvms	kqmrfdnse		
Phage T4		mkQYqdl	ikdIfenGyeta	DRTGtGTlSVFG	sklrwdLtkg		
Consensus		-----E-QYL-----I--G-----			-----DRTG-GT-S-FG-----			



VZV FPLLTTKRVfwravveELLWfirGStD.skelaakd.ihIWDiygsskflnringfhkrht.

HHV-8 FPLLTTKRVfwrvgvqELLWflkGStD.sreLertg.vkIWDkngsreflagrglahrre.

EHV-2 FPLLTTKRVfwrvgveELLWfirGStD.snelsarg.vkIWDangsrdf laraglgghrep.

HVS FPLLTTKRVfwrvgveELLWfirGStD.skelsaag.vhIWDangsrdfldklgfydrde.

HVA FPLLTTKRVfwrvgvveELLWfirGStD.skelaasg.vhIWDangsrdfldklgfdree.

Human FPLLTTKRVfwkgvleELLWfirGStn.akelsskg.vkIWDangsrdfldslgfsarce.

Mouse FPLLTTKRVfwkgvleELLWfirGStn.akelsskg.vrIWDangsrdfldslgfsarce.

Rat FPLLTTKRVfwkgvleELLWfirGStn.akelsskg.vrIWDangsrdfldslgfsarce.

S. cerevisiae tFPLLTTKkVftrgiileELLWflaGdtd.anllsegg.vkIWDngsreyl dkmgrfdrkv.

C. albicans tFPLLTTKkVfsgkiihELLWflvaGStD.akilsekg.vkIWDngsrefldklglthrrre.

P. carinii tFPLLTTKRVftrvgiieELLWfirGStD.slkLrekn.ihIWDangsrdfldslgltkrqe.

C. neoformans tLPLLTTKRVftrvgiiaELLWflvsGStD.aknlssgg.vgIWDngskflekvglgghrre.

A. thalianaX FPLLTTKRVfwrvgvveELLWfisGStn.akvlqekg.ihIWDngnasreyl dgigitereee.

A. thalianay FPLLTTKRVfwrvgvveELLWfisGStn.akvlqekg.irIWDngnasrayl dgigitereee.

D. carota FPLLTTKkVfwrvgvveELLWfisGStn.akilkekg.vnIWDngsreyl dsiglt dree.

C. fasciculata lPPLLTTKRVfwrvgvceELLWflrGStn.ahvLadkd.ihIWDngsrefldsrgltenke.

L. major rLPLLTTKRVfwrvgvceELLWflrGSts.aqilLadkd.ihIWDngsrefldsrgltenke.

L. amazonensis rLPLLTTKRVfwrvgvceELLWflrGStn.aqilLadkd.ihIWDngsrefldsrgltenke.

L. tropica rLPLLTTKRVfwrvgvceELLWflrGSts.aqilLadkd.ihIWDngsrefldsrgltenke.

P. chabaudi FPLLTTKklfvrvgiieELLWfirGStn.gntLlekn.vrIWeangtrfldrnlkflhrev.

P. falciparum FPLLTTKklfvrvgiieELLWfirGStn.gntLlnkn.vrIWeangtrfldrnlkflhrev.

T. gondii FPLLTTKRVfwkgvleELLWfirGStn.anhLsekg.vkIWDknvtrfldrnlphrev.

T. cruzi rLPLLTTKRVfwrvgvceELLWflrGSty.akLsdkg.vhIWDddngsrfl dsrglt eyee.

E. coli FPLvTTKrchlrssiHELLWflqGStn.iayLbhenn.vtIWDewaden.

B. subtilisB FPMlTTKklhfksiahELLWflkGStn.vryLqeng.vrIWDewaden.

B. amyloliquefaciens FPMlTTKklhfksiahELLWflkGStn.vryLqeng.vrIWDewaden.

S. flexneri FPLvTTKrchlrssiHELLWflqGStn.igyLhenn.vtIWDdwaden.

H. influenzae FPLiTTkswykaaiaEflgyirGydn.aadfralg.tkTWdananaawlanphrrgv.

M. genitalium FPLLTTKkVnkaivhELLWflkGStn.ikyLvvdng.vnIWDnewyfnkkspsfqmetlqefilkvkt dnefak

L. lactis eFPiLTLripiksaikELWiyvqdGSts.elsvLeeky.gvkyWgewgig.

L. casei FPLLTTKkVpfglikseLLWflhGStn.irfllqhr.nhIWDewa fekwvksdeyhgpdmtdfghrsgkdp efaa

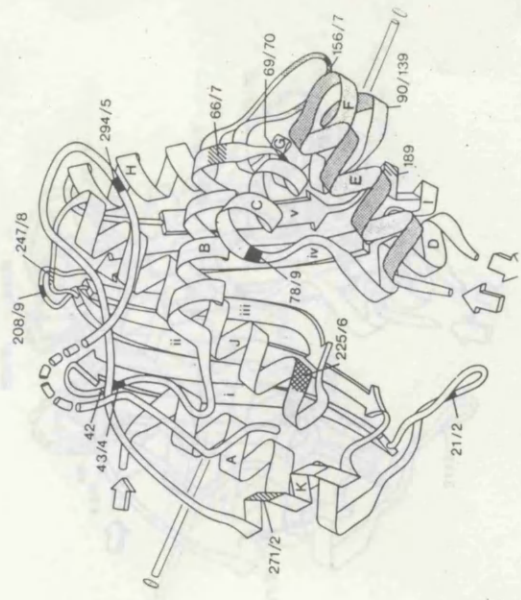
S. aureus FPLLTTKkVsfklvatELLWflkGStn.igyLlkyn.mniIWDewa fenyvgsddyhgpdmtdfghrsgqdp efn

B. subtilisA VPLLTTKkVawktaikELLWiwqiksn.dvndLnmg.v. IWDqwkged.

Phage 3T vPILTTKkVawktaikELLWiwqiksn.dvteLnkmg.vhIWDqwkged.

Phage T4 FPAvTTKklawkaciaEliWflsGStnvdnlrllqhdsligqktvwdenyengakdlgyhs.

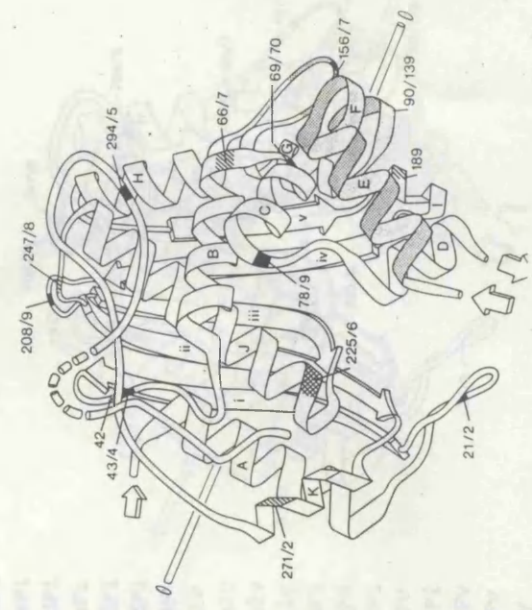
Consensus -----E~~LLW~~F-G-T-----L-----I~~W~~-----



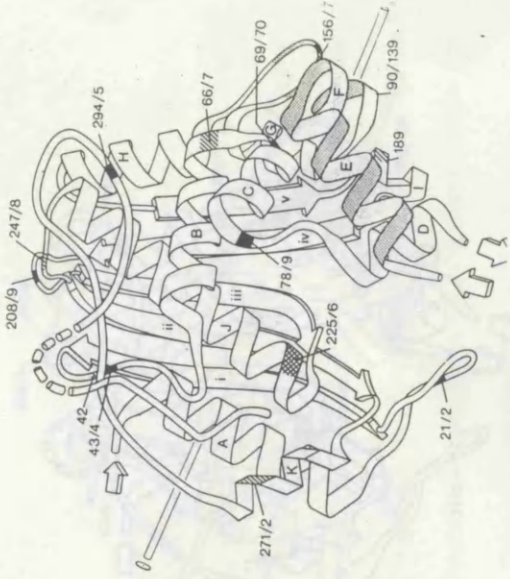
* * * * *

GDLPiYGFQWRhfgaeykdcqsnylqggiDQLqtVIdtIKtnPesRRRmiissWNPkD
 GDLPvYGFQWRhfgaayvdadadytgggfdQLsyivdliKnnPhdRRriimcaWNPcad
 GDLPvYGFQWRhfgaayvdsdktdyrggvdQLrdlIgeiKnnPesRRRlvtawNPad
 GDLPvYGFQWRhfgaeykvgvrdykgvDQLkqIIdtIKtnPtDRRmImcaWNPvsD
 GDLPvYGFQWRhfgaeyqglkhnyggvDQLkqiIntihtnPtDRRmImcaWNPvID
 GDLPvYGFQWRhfgaeyrdmsdysggvDQLqrVIdtIKtnPddRRriimcaWNPpRD
 GDLPvYGFQWRhfgaeykdmsdysggvDQLqkvIIdtIKtnPddRRriimcaWNPkD
 GDLPvYGFQWRhfgadykdmsdysggvDQLqkvIIdtIKtnPddRRriimcaWNPkD
 GDLPvYGFQWRhfgakytcdsdytgggiDQLkqvIhkIKtnFydRRriimsaWNPad
 GDLPvYGFQWRhfgaeykdcdsdytgggfdQLkqvIkkIKtnFydRRriimsaWNPpD
 GDLPiYGFQWRhfgaeyidcktnyigggvDQLaniIqkirtsFydRRlilsaWNPad
 GdLPvYGFQWRhfgaeytdadgdykgvDQLqrVIdtIKnnPtDRRriilsaWNPkD
 GDLPvYGFQWRhfgakyt dmhadytgggfdQLvdvIdkiKnnPddRRriimsaWNPsd
 GDLPvYGFQWRhfgakyt dmhadytgggfdQLldvInkiKnnPddRRriimsaWNPsd
 GDLPiYGFQWRhfgarytdmhadytgggfdQLldvIskiKnnPddRRriiqsaWNPsd
 mDLGPvYGFQWRhfgadykgfdany. degvDQikIivetIKtn. .dRRllvtaWNPca
 mDLGPvYGFQWRhfgadykgfeanydggvDQikIivetIKtnPndRRllvtaWNPca
 mDLGPvYGFQWRhfgaeyrgleanydggvDQikIivetIKannPndRRllftaWNPca
 mDLGPvYGFQWRhfgadykgfeanydggvDQikIivetIKtnPndRRllvtaWNPca
 nDLGPiYGFQWRhfgaeytdmhadykdkvDQLkniInliKndPtRRiilcaWNPvkd
 nDLGPiYGFQWRhfgaeytnmydnykvgvDQLkniInliKndPtRRiilcaWNPvkd
 GDIPGYGFQWRhfgaaykdmhtdytggvDQLknyfqlrtnPtDRRmlmtaWNPaa
 mDLGPvYGFQWRhfgaaythhdanydggvDQikaivetIKtnPddRRmlftaWNPsa
 GDLPvYGFQWRawp.tpdgrhiDQittvlnqlKndPdsRRriivsaWNPge
 GeLGPvYGSQWRswr. gadgetiDQisrIIdiKtnPnsRRliivsaWNPge
 GeLGPvYGSQWRswr. gadgetiDQisrIIdiKtnPnsRRliivsaWNPge
 GDLPvYGFQWRawp.tpdgrhiDQittvlnqlKndPdsRRriivsaWNPge
 dMgGrvYGFQWRawr.kpngetiDQLrkiivmltkgidrgeilftfnpge
 qfaDLG.vYGFQWRnfn.gvDQLkviIgeiKenPnsRRliivsaWNPse
 GtiGrvYGFQWRawr.niigklleglaktPwnRRriinlwqyed
 vyheemakfddrvlhdda faakyGDLPvYGSQWRawh.tskgdtiDQLgavIeqiKthPysRRliivsaWNPed
 qykeemkkfkerilndda fakkyGnLQvYGFQWRdwd.kngnyvDQLksvIggiKtnPnsRRriivsaWNPte
 GtiGhaYGFQlgkn.rslngekvDQvdyllhgIKnnPssRRhiitmlWNPde
 GtiGhaYGFQlgkn.rslngekvDQvdyllhgIKnnPssRRhiitmlWNPpdD
 GeLGPiYGFQWRdfg.gvDQiiievIdriKKlPndRRgqvivsaWNPpae
 -----GDLP-YG-QWR-----DQL---I---K---P---RR-----WN---D

- VZV
- HHV-8
- EHV-2
- HVS
- HVA
- Human
- Mouse
- Rat
- S.cerevisiae
- C.albicans
- P.carinii
- C.neoformans
- A.thalianax
- A.thalianay
- D.carota
- C.fasiculata
- L.major
- L.amazonensis
- L.tropica
- P.chabaudi
- P.falciptarum
- T.gondii
- T.cruzi
- E.coli
- B.subtilisB
- B.amyloliquefaciens
- S.flexneri
- H.influenzae
- M.genitalium
- L.lactis
- L.casei
- S.aureus
- B.subtilisA
- Phageφ3t
- Phage T4
- Consensus



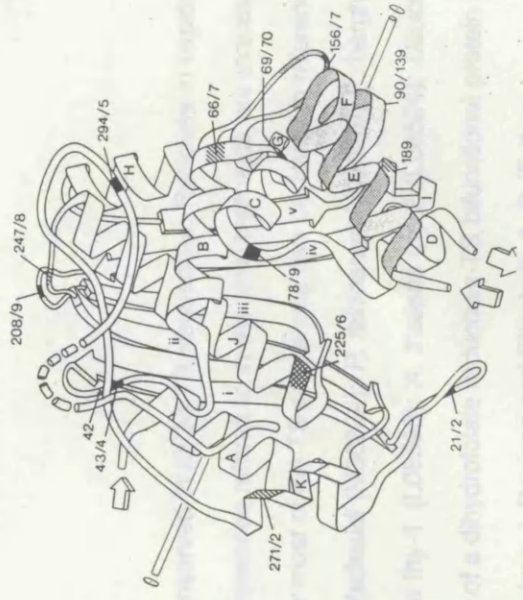
	I	183	iv	192	195	111	207	J	229	235
VZV										
HHV-8										
EHV-2										
HVS										
HVA										
Human										
Mouse										
Rat										
S.cerevisiae										
C.albicans										
P.carinii										
C.neoformans										
A.thalianax										
A.thalianay										
D.carota										
C.fasiculata										
L.major										
L.amazonensis										
L.tropica										
P.chabaudi										
P.falciparum										
T.gondii										
E.coli										
B.subtilisB										
B.amyloliquefaciens										
S.flexneri										
H.influenzae										
M.genitalium										
L.lactis										
L.casei										
S.aureus										
B.subtilisa										
Phageφ3t										
Phage T4										
Consensus										



ip.lMvLPPCHtlcQFVvng.....eLScqYQRSGDMgLGVPFNIAgYaLLTYiVAhvtglktGdli
 ls.lMALPPCHllcQFVvadg.....eLScqlYQRSdMgLGVPFNIAySLLTYmIAhvtglrpGeFi
 lp.aMALPPCHllcQFVvagg.....eLScqlYQRSdMgLGVPFNIAySLLTYmVAhltglpGdFi
 ip.kMvLPPCHvlsQFVvcdg.....kLScqlYQRsAdMgLGVPFNIAySLLTcmIAhvtnlvpGeFi
 vp.kMALPPCHvlsQFVvcdg.....kLScqlYQRsAdMgLGVPFNIAySLLTcmIAhvtldvpGeFi
 lp.lMALPPCHalcQFVvns.....eLScqlYQRSdMgLGVPFNIAySLLTYmIAhitglkpGdFi
 lp.lMALPPCHalcQFVvng.....eLScqlYQRSdMgLGVPFNIAySLLTYmIAhitglpGdFv
 lp.lMALPPCHalcQFVvng.....eLScqlYQRSdMgLGVPFNIAySLLTYmIAhitglpGdFv
 fd.kMALPPCHlfsQFVvfpkge.....egsgkprLScLlYQRScDMgLGVPFNIAySLLTcmIAkvvdmePGeFi
 fa.kMALPPCHvfcQFVvnfptspqnpnkqaktakpLScLlYQRScDMgLGVPFNIAySLLTcmIAhvvdmcdGeFi
 le.kMALPPCHmfcQFVvnhips.....nnhrpelScqlYQRScDMgLGVPFNIAySLLTcmIAhvcldpGdFi
 lp.lMALPPCHmfcQFVvlpadspgskp.....kLScLmYQRScDlglGVFPFNIAySLLTcmIAIIdtdepheFi
 lk.lMALPPCHmfaQFVvaeg.....eLScqmYQRsAdMgLGVPFNIAySLLTcmIAhvcldvpGdFi
 lk.lMALPPCHmfaQFVvaeg.....eLScqmYQRsAdMgLGVPFNIAySLLTcmIAhvcldvpGdFi
 lr.lMALPPCHmfaQFVvaeg.....eLScqmYQRsAdMgLGVPFNIAySLLTcmIAhvcldvpGdFv
 lh.kMavRPCHllgQFVvntqtk.....eLScmlYQRccDMgLGVPFNIAySLLTcmIAkatglrpGely
 lq.kMALPPCHllaQFVvntdts.....eLScmlYQRScDMgLGVPFNIAySLLTcmIAkatglrpGely
 lh.kMALPPCHllaQFVvnteks.....eLScmlYQRScDMgLGVPFNIAySLLTcmIAkatglrpGely
 lq.kMavPPCHllaQFVvntdts.....eLScmlYQRScDMgLGVPFNIAySLLTcmIAkatglrpGely
 ld.qMALPPCHllcQFVvfdg.....kLScimYQRScDlglGVFPFNIAySifTYmiAqvcnlqpaefi
 qMALPPCHllcQFVvfdg.....kLScimYQRScDlglGVFPFNIAySifTYmiAqvcnlqpaefi
 ld.eMALPPCHllcQFVvndqk.....eLScimYQRScDvlgLVFPFNIAySLLTlmvAhvcnlkpkeFi
 ld.kMALaPCHaffQFVvadg.....kLScqlYQRScDvfiGLVPFNIAySLLTlmvAhvmAqqcdlevGdFv
 id.kMALPPCHclfQFVvsdg.....kLScqlYQRsAdvfiGLVPFNIAySLLTcmIAhvtglpGeFi
 id.rMALPPCHclfQFVvadg.....kLScqlYQRsAdvfiGLVPFNIAySLLTcmIAhvtglpGeFv
 ld.kMALaPCHaffQFVvadg.....kLScqlYQRScDvfiGLVPFNIAySLLTlmvAhvmAqqcdlevGdFv
 fd.lgcRrPcmthtFslgd.....tLhltSQRScDvPGLInFNFIqivftflaImAqitgkkaGkay
 le.kMALaPCHslfQFVveed.....kLslqlYQRSGdiFLGVFPFNIAySLLvYlVAhethklpGyFi
 feetegLLPCafqtmfdvrrkdgqi.....yLdaatliQRsDmIvahhiNamqYvaLqmmiAkhfswkvckFf
 vp.tMALPPCHtlYQFVvndg.....kLslqlYQRsAdiFLGVFPFNIAySLLThlVAhceglvGeFi
 id.sMALPPCHtmfQFVvqeg.....kLncqlYQRsAdiFLGVFPFNIAySLLThlVAhceglvGeFi
 ld.aMAltPCvvyetQvVvkgg.....kLhlevrarsDmALGnPFNVfQYnVlQrmiAqvtgylGeyi
 ld.aMAltPCvvyetQvVvkgg.....kLhlevrarsDmALGnPFNVfQYnVlQrmiAqvtgylGeyi
 lk.yMALPPCHmfYQFVvring.....yLdlqYQRsvdVfLGLPFNIAySLLThlVAhvmAkmcnllpGdli
 -----MALPPCH---QFVv-----LS---YQRS-DM-LGVFPFNIA-Y-LLT---A-----G-F-

**

~~~~~| |~~~~~|  
 HtmGDaHiYlnHidalkv.QLaRsPkpF.PcLkiirrvt.....dIndFkwDfqlgDyNp.hppIkmemal  
 HtlGDaHiYktHieplrl.QLrRtPrpf.PrLeilrsvs.....smeEtpdDfrlvdYcp.hptIrmemav  
 HvlGDaHvYlnHveplkl.QLrRsPrpf.PrLrllrrve.....dIdFraeDfalegYnP.haaIpmemav  
 HtiGDaHiYvdHidalkm.QLrRtPrpf.PtLrFarnvs.....cIddFkadDiilenYnP.hpiIkmbmav  
 HtlGDaHvYmHvdalte.QLrRtPrpf.PtLkFarkva.....sIddFkanDiilenYnP.ypsIkmgmav  
 HtlGDaHiYlnHieplki.QLrRePrpf.PkLrllrkve.....kIddFkaeDfiegYnP.hptIkmemav  
 HtlGDaHiYlnHieplki.QLrRePrpf.PkLkllrkve.....tIddFkveDfiegYnP.hptIkmemav  
 HtlGDaHiYlnHieplki.QLrRePrpf.PkLrllrkve.....tIddFkveDfiegYnP.hptIkmemav  
 HtlGDaHvYkdhidalkk.QiLrNPrpf.PkLkikrdvk.....dIddFklDfFeiedYnP.hprIqmbmsv  
 HtlGDaHvYldhidalkk.QfEriPkpF.PkLkivkeerK.....neiksiddFkfeDfeivgYp.yppIkmbmsv  
 HvmGDChIYkdhiealqq.QLrRsPrpf.PtLsInrsit.....dIedFtldDfniqnYnP.yetiKmbmsi  
 lqmGDaHvYrdHveplkt.QLeRePrdf.PkLkWarske.....eigdlDgFkveDfveggYp.wgkIdmksa  
 HvlGDaHvYktHvrvplqe.QLlNpPkpF.PvLkinpekk.....qidsFvasDflltgYdP.hkKiEmkmav  
 HviGDaHvYknHvrvplqe.QLenpPkpF.PvLkinpekk.....didsFvaDfeligYdP.hkKiEmkmav  
 HsiGDaHvYsnHisdLsfetsfmlPktF.PvLkingsgek.....didsFaaDfkligYdP.hqKiEmkmav  
 HtlGtaHvYsnHvealke.QLqRvPvaf.PvLvfkKere.....fIedyestDmevvdYp.yppIkmemav  
 HtlGDaHvYrnHvdalka.QLeRvPhaf.PtLiFkeerq.....yIedyeltDmevidYp.hpaIkmemav  
 HtlGDaHvYrsHidalka.QLeRvPhaf.PtLvFkeerq.....fIedyelmDmevidYp.hppIkmemav  
 HtlGDaHvYrnHvdalka.QLeRvPhaf.PtLiFkeerq.....yIedyeltDmevidYp.hpaIkmemav  
 HvlGnaHvYnnHveslkv.QLnrRtPyPf.PtLklnpeik.....nIedFtisDftvqnYh.hkIsmDMAA  
 HvlGnaHvYnnHidslki.QLnrRiPyPf.PtLklnpdik.....nIedFtisDftiqnYvh.hekIsmDMAA  
 HfmGnHvYtnHvealke.QLrRePrpf.Pivnilnker.....iKeiddFtaeDfveggYp.hgrIqmemav  
 HtlGDaHvYsnHvepcne.QLkRvPraF.PyLvFrrere.....fIedyeegDmevidYaP.yppIsmkmav  
 wtGDtHlYsnHmdqthl.QLsRePrpl.PkLiikrKpe.....sIdyrfedfeiegYdP.hpgIkapvai  
 HtfGDvHiYqnHieqvnL.QLerdvpl.PqLrfarkvd.....sInFafedfiedYdP.hphIkagvsv  
 HtfGDvHiYqnHveqvnL.QLtrdvrpl.PkLrfarnvd.....sIdFafedfiedYdP.hphIkagvsv  
 wtGDtHlYtnHmdqthl.QLsRePrpl.PkLiikrKpe.....sIdyrfedfeiegYdP.hpgIkapvai  
 HkivmaHiYedqielmrdvLkRePpl.PkLeinpdik.....tledletwtmdDfkvvgYqs.hepIkypfsv  
 HtlGDaHiYenHieqikl.QLtrrtldp.PqvvLksdks.....IfaysdDielvgYny.hpfIygrvav  
 yfvnllHiYdnqfegane.lmkRtasekePrLvlNvpDg.....tnffdlkpeDfelvdYePvkpqlkfdLai  
 HtlGDaHiYvnHidake.QLsRtPrpa.PtLqInpdkh.....dIdFdmDiklInYdP.ypaIkapvav  
 HtlGDaHiYsnHmdaiht.QLsRdsYlp.PqLkintdks.....lfdInydelelinYes.hpaIkapiav  
 fniGDChvYtrHidnlki.QmeReqfea.Pelwinpevk.....dfyDfTidDfklInYkh.gdkllfevav  
 fniGDChvYtrHidnlki.QmeReqfea.Pelwinpevk.....dfynFtvDfklInYkh.gdkllfevav  
 fsgGnHlYmHvegcke.iLrRePkel.celvisglpYkfrYlStkeqYkVklrPkdFvlnnVvs.hppIkGkmav  
 H--GD-H-Y-H-----P-L-----I-F-----D-----Y-P-----I-----  
 \* \* \* \* \*



Consensus  
 H--GD-H-Y-H-----P-L-----I-F-----D-----Y-P-----I-----  
 \* \* \* \* \*

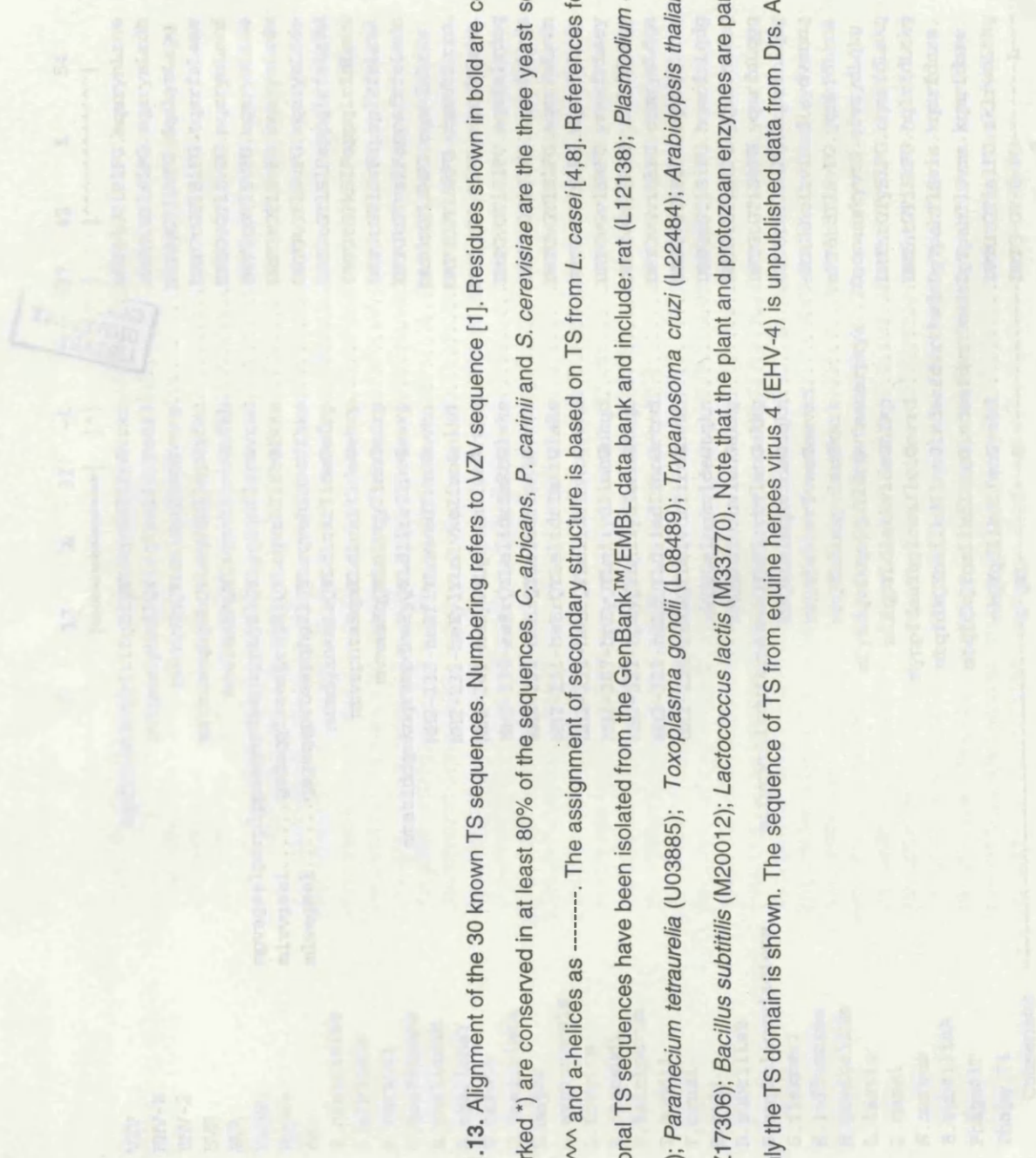


**Figure 1.13.** Alignment of the 30 known TS sequences. Numbering refers to VZV sequence [1]. Residues shown in bold are conserved in all 30 TS sequences. Residues in capitals (and marked \*) are conserved in at least 80% of the sequences. *C. albicans*, *P. carinii* and *S. cerevisiae* are the three yeast sequences referred to in the text. b-strands are indicated as ~~~~~ and a-helices as -----. The assignment of secondary structure is based on TS from *L. casei* [4,8]. References for most of the TS sequences can be found in reference 8. Additional TS sequences have been isolated from the GenBank™/EMBL data bank and include: rat (L12138); *Plasmodium chabaudi* (M30834); *P. falciparum* (J03028); *P. berghei* (U12275); *Paramecium tetraurelia* (U03885); *Toxoplasma gondii* (L08489); *Trypanosoma cruzi* (L22484); *Arabidopsis thaliana thy-1* (L08593); *A. thaliana thy-2* (L08594); *Daucus carota* (Z17306); *Bacillus subtilis* (M20012); *Lactococcus lactis* (M33770). Note that the plant and protozoan enzymes are part of a dihydrofolate reductase-TS bifunctional protein of which only the TS domain is shown. The sequence of TS from equine herpes virus 4 (EHV-4) is unpublished data from Drs. Andrew J. Davison and Elizabeth A. R. Telford.